Time series analysis of long-term vegetation trends, phenology, and ecosystem service valuation for grasslands in the U.S. Great Plains

by

Hilda Uloma Onuoha

B.Tech., Federal University of Technology Owerri, 2008

M.S., Southern Illinois University Edwardsville, 2016

AN ABSTRACT OF A DISSERTATION

submitted in partial fulfillment of the requirements for the degree

DOCTOR OF PHILOSOPHY

Department of Geography and Geospatial Sciences.

College of Arts and Sciences

KANSAS STATE UNIVERSITY

Manhattan, Kansas

2022

Abstract

Grasslands are one of the largest, most biodiverse, and productive terrestrial biomes but they receive very low levels of protection. The temperate grasslands in the United States are one of the most threatened grassland ecosystems. Every year, a significant portion of grasslands in the Great Plains are converted to agricultural use, with almost 96% of the historical extent lost. Other factors that affect existing grassland health include significant climatic changes, invasion of woody, non-native species, fragmentation, lack or inadequate burning, and excessive grazing. The impact of the combination of these factors on grasslands in the US Great Plains is still unknown. The goal of this research is to investigate the long-term grassland vegetation conditions using a well-known indicator (greenness) and assesses its impact on the provision of select grassland ecosystem services within the US Great Plains from 2001 to 2017.

The above goal was achieved with three objectives addressed in three chapters. In Chapter 3, a time-series analysis of Moderate Resolution Imaging Spectrometer (MODIS) 16-day maximum value composite Normalized Difference Vegetation Index (NDVI) and Enhanced Vegetation Index (EVI) data (MOD13Q1 Collection 6) was performed to assess long-term trends in vegetation greenness across the Great Plains ecoregion of the United States. The Breaks for Additive Season and Trend (BFAST) decomposition method was applied to a time series of images from 2001 to 2017 to derive spatially explicit estimates of gradual interannual change. Results show more 'greening' trends than 'browning' and 'no change' trends during the study period. Comparing the trend results from both vegetation indices suggests that EVI is more suitable for this analysis in the study area, especially in areas with high biomass.

In Chapter 4, a time-series analysis of Moderate Resolution Imaging Spectrometer (MODIS) 16-day maximum value composite Enhanced Vegetation Index (EVI) data (MOD13Q1 Collection 5) is used to explore spatial patterns of vegetation phenology and to assess long-term phenology trends across the region. The program TIMESAT was used to extract key measures of vegetation phenological development from 2001 to 2017, including the phenometrics (1) season length, (2) start of growing season, (3) end of growing season, (4) middle of the growing season, (5) maximum NDVI value, (6) small integral, (7) left derivative, and (8) right derivative. Results show important variation in phenological patterns across the region such as a shift to a later start, earlier end, and shorter the growing season length, especially in the southern parts of the region. As shown in the small integral

and maximum EVI, vegetation productivity appears to have increased over many areas in the Great Plains ecoregion.

Finally, Chapter 5 focuses on developing a methodological improvement to the widely used Invest ecosystem services model that uses remotely sensed inputs to capture the interannual spatio-temporal dynamics of grassland vegetation on the provision of grassland ecosystem services across the US Great Plains. A selected set of grassland ecosystem services was quantified (economic and biophysical values) for the period between 2001 and 2017. This exploratory study will be a basis for highlighting the role grasslands play in providing essential ecosystem services and how improved long-term vegetation monitoring can benefit land-use decisions locally and regionally.

Time series analysis of long-term vegetation trends, phenology, and ecosystem service valuation for grasslands in the U.S. Great Plains

by

Hilda Uloma Onuoha

B.Tech., Federal University of Technology Owerri, Nigeria, 2008

M.S., Southern Illinois University Edwardsville, 2016

A DISSERTATION

submitted in partial fulfillment of the requirements for the degree

DOCTOR OF PHILOSOPHY

Department of Geography and Geospatial Sciences.

College of Arts and Sciences

KANSAS STATE UNIVERSITY

Manhattan, Kansas

2022

Approved by:
Major Professor
Dr. J. M. Shawn Hutchinson

Copyright

© Hilda Onuoha 2022.

Abstract

Grasslands are one of the largest, most biodiverse, and productive terrestrial biomes but they receive very low levels of protection. The temperate grasslands in the United States are one of the most threatened grassland ecosystems. Every year, a significant portion of grasslands in the Great Plains are converted to agricultural use, with almost 96% of the historical extent lost. Other factors that affect existing grassland health include significant climatic changes, invasion of woody, non-native species, fragmentation, lack or inadequate burning, and excessive grazing. The impact of the combination of these factors on grasslands in the US Great Plains is still unknown. The goal of this research is to investigate the long-term grassland vegetation conditions using a well-known indicator (greenness) and assesses its impact on the provision of select grassland ecosystem services within the US Great Plains from 2001 to 2017.

The above goal was achieved with three objectives addressed in three chapters. In Chapter 3, a time-series analysis of Moderate Resolution Imaging Spectrometer (MODIS) 16-day maximum value composite Normalized Difference Vegetation Index (NDVI) and Enhanced Vegetation Index (EVI) data (MOD13Q1 Collection 6) was performed to assess long-term trends in vegetation greenness across the Great Plains ecoregion of the United States. The Breaks for Additive Season and Trend (BFAST) decomposition method was applied to a time series of images from 2001 to 2017 to derive spatially explicit estimates of gradual interannual change. Results show more 'greening' trends than 'browning' and 'no change' trends during the study period. Comparing the trend results from both vegetation indices suggests that EVI is more suitable for this analysis in the study area, especially in areas with high biomass.

In Chapter 4, a time-series analysis of Moderate Resolution Imaging Spectrometer (MODIS) 16-day maximum value composite Enhanced Vegetation Index (EVI) data (MOD13Q1 Collection 5) is used to explore spatial patterns of vegetation phenology and to assess long-term phenology trends across the region. The program TIMESAT was used to extract key measures of vegetation phenological development from 2001 to 2017, including the phenometrics (1) season length, (2) start of growing season, (3) end of growing season, (4) middle of the growing season, (5) maximum NDVI value, (6) small integral, (7) left derivative, and (8) right derivative. Results show important variation in phenological patterns across the region such as a shift to a later start, earlier end, and shorter the growing season length, especially in the southern parts of the region. As shown in the small integral

and maximum EVI, vegetation productivity appears to have increased over many areas in the Great Plains ecoregion.

Finally, Chapter 5 focuses on developing a methodological improvement to the widely used Invest ecosystem services model that uses remotely sensed inputs to capture the interannual spatio-temporal dynamics of grassland vegetation on the provision of grassland ecosystem services across the US Great Plains. A selected set of grassland ecosystem services was quantified (economic and biophysical values) for the period between 2001 and 2017. This exploratory study will be a basis for highlighting the role grasslands play in providing essential ecosystem services and how improved long-term vegetation monitoring can benefit land-use decisions locally and regionally.

Table of Contents

Table of Contents viii
List of Figures xii
List of Tables xv
Acknowledgments xvii
Chapter 1 – General introduction 1
1.1 Overview 1
1.2 Research question and objectives 5
1.3 Dissertation structure 6
1.4 References 7
Chapter 2 - Literature review 11
2.1 Grasslands 11
2.1.1 Definition 11
2.1.2 Global extent 14
2.1.3 Importance of grasslands 16
2.1.4 Current management challenges for grasslands 19
2.1.5 The Great Plains ecoregion 23
2.2 Remote sensing of vegetation 25
2.2.1 Land surface phenology 28
2.2.2 Methods for assessing phenological development 29
2.2.3 Long-term trend analysis of satellite time-series data 31
2.3 Ecosystem services 33
2.3.1 Evolution of ecosystem services 34
2.3.2 Ecosystem services classification 35
2.3.3 Ecosystem service valuation and valuation methods 40
2.3.4 Survey of grassland ecosystem service research 46
2.4 Implications of the literature review on the current study 51
2.5 References 52
Chapter 3 - Detection of long-term grassland vegetation trends for the Great Plains ecoregion using temporal decomposition and satellite-derived vegetation indices. 72

3.1 Introduction: 73
3.1.1 Background and purpose 73
3.2 Study area 76
3.3 Data and methods 79
3. 3. 1 Data and data preparation 79
3.3.2 Methods 79
3.3.3 Validation of the time series trend analyses 83
3.3.4 Comparison of NDVI and EVI for trend analysis 87
3.4 Results 90
3.4.1 Gradual interannual trend 90
3.4.2 Validation 95
3.4.3 Comparison of NDVI and EVI trend results 97
3.5 Discussion and conclusions 104
3.5.1 Discussion 104
3.5.2 Conclusions 108
3.6 References 111
Chapter 4 -Time series analysis of phenometrics for the US Great Plains ecoregion using satellite-derived vegetation indices 117
4.1 Introduction 118
4.1.1 Background and purpose 118
4.2 Study area 121
4.3 Methodology 124
4.3.1 Data and data preparation 124
4.3.2 Calculation of phenometrics 125
4.3.3 Phenology trend analysis 130
4.3 Results 131
4.3.1 Spatial patterns of phenology 131
4.3.2. Phenology trends 133
4.4 Discussion 136
4.5 Conclusions 142
4.6 References 145

Chapter 5 - Spatio-temporal valuation of grassland ecosystem services in the U.S. Great Plains .. 152
5.1 Introduction 153
5.1.1 Background and purpose 153
5.2. Study area 155
5.3. Data and methods 158
5.3.1 Modeling important ecosystem services 158
5.3.2 Carbon model 159
5.3.3 Sediment delivery model 162
5.4 Results 166
5.3.1 Carbon model 166
5.3.2 Sediment delivery model 172
5.3.3 Validation 177
5.4. Discussion 177
5.4.1 Carbon model 178
5.4.2 Sediment delivery model 180
5.5. Conclusions 187
5.6 References 190
Chapter 6 – Summary and conclusions 199
6.1 Introduction 199
6.2 Summary of results and key findings 200
6.3 Conclusions 203
6.3.1 Detection of long-term grassland vegetation trends for the Great Plains Ecoregion using temporal decomposition and satellite-derived vegetation indices 203
6.3.2 Time series analysis of phenometrics for the U.S. Great Plains Ecoregion using satellite-derived vegetation indices 205
6.3.3 Spatio-temporal valuation of grassland ecosystem services in the U.S. Great Plains 206
6.4 Contributions and future research 207
6.5 References: 209
Appendices 211
Appendix A: Additional materials for Chapter 3 211
Appendix B: Additional materials for Chapter 4 213

Appendix C: Additional materials for Chapter 5 219

List of Figures

Figure 2.1: Desertification process of grassland over a 100-year period. (Reprinted from Karl et al. 2009). 22

Figure 2.2: Typical temperate North American grassland phenology curve and some associated phenometrics generated in TIMESAT (Concept from Reed et al., 2003). 30

Figure 2.3: Ecosystem services classification by TEEB (Source: TEEB, 2010) 37

Figure 2.4: Illustration of the hierarchical structure of CICES V5.1 using cereals. (Source: Haines-Young & Potschin-Young, 2018). 38

Figure 2.5: IPBES NCP and categories. (Source: Díaz et al., 2018). 39

Figure 3.1: U.S. Great Plains study area showing Omernik level III ecoregions and grassland pixels extracted from the 2011 NLCD. 78

Figure 3.2: The BFAST output showing the raw NDVI time series (Yt), seasonal (St), trend (Tt), and residual components(et). Image (a) Pixel (in southwestern TX) with an overall negative trend over time and significant five breaks (b) Pixel (in northeastern KS) with an overall positive trend over time and three significant breaks (c) Pixel (in northeastern KS) with an overall null trend over time and one significant break. 82

Figure 3.3: Map of the study area location of Landsat image pairs (sample sites) used for validation. 85

Figure 3.4: Four comparisons of trends results produced using NDVI and EVI that illustrate three measures of disagreement: quantity, exchange, and shift (after Pontius and Santacruz, 2014). 89

Figure 3.5: Gradual interannual NDVI trend classes for the 2001- 2017 period in the U.S. Great Plains as determined by BFAST analysis. No Data = non-grassland areas. 91

Figure 3.6: Gradual interannual EVI trend classes for the 2001-2017 study period in the U.S. Great Plains as determined by BFAST analysis. No Data = non-grassland areas. 92

Figure 3.7: Summary of results for gradual interannual trend classes for the 2001-2017 study period for level III ecoregions in the U.S. Great Plains based on BFAST analysis of MODIS NDVI imagery. 94

Figure 3.8: Summary of results for gradual interannual trend classes for the 2001-2017 study period for level III ecoregions in the U.S. Great Plains based on BFAST analysis of MODIS EVI imagery. 95

Figure 3.9: Differences in MODIS NDVI and EVI interannual trend classes for the Great Plains ecoregion (2001-2017). 99

Figure 3.10: Sources of disagreement in NDVI and EVI interannual trend classes (2001 to 2017) for the (a) Southwestern Tablelands and b) Flint Hills ecoregions. 101

Figure 3.11: Visualizing pixel difference in MODIS NDVI and EVI trend class results in the Great Plains. The difference indicated is from NDVI to EVI. 103

Figure 4.1: Typical temperate North American grassland phenology curve and some associated phenometrics generated in TIMESAT (Concept from Reed et al., 2003). 120

Figure 4.2: U.S. Great Plains study area showing Omernik level III ecoregions and grassland pixels extracted from the 2011 NLCD. 123

Figure 4.3: The median values of grassland phenometrics derived from MODIS (MOD13Q1) EVI data from 2001 to 2017 for the Great Plains ecoregion. Start, middle. and end of growing are in day of year. The growing season length is in days. The left/right derivatives, Maximum EVI and small integral are in VI values; they are unitless. 133

Figure 4.4: Trends in grassland phenometrics derived from MODIS (MOD13Q1) EVI data from 2001 to 2017 for the Great Plains ecoregion using the Mann Kendall trend test. Green pixels indicate a positive trend, red a negative trend, and grey pixels indicate no trend. 134

Figure 4.5: Observed regions of distinct spatial patterns for the 2001 to 2017 phenometrics in the Great Plains 138

Figure 5.1: U.S. Great Plains study area showing Omernik level III ecoregions and grassland pixels extracted from the 2011 NLCD. 157

Figure 5.2: Average annual carbon stock (in Mg C/pixel) for the grasslands in the U.S. Great Plains 167

Figure 5.3: Total annual carbon stock (in MgC) for the grasslands in the U.S. Great Plains..... 168

Figure 5.4: Spatial distribution of total carbon stock (in MgC) of grassland in the U.S. Great Plains for 2012 and 2015. 169

Figure 5.5: Total net economic values of carbon sequestered by grasslands in the U.S. Great Plains. 171

Figure 5.6: Spatial distribution of the net economic value of sequestered grassland carbon in the U.S. Great Plains in 2007 U.S. dollars per pixel (2006-2007, 2001-2012). 172

Figure 5.7: Average soil loss values (in tons per hectare) for the grassland area in the U.S. Great Plains 173

Figure 5.8: Total annual soil loss and sediment retention for the grassland areas in the U.S. Great Plains for 2001 to 2017. 174

Figure 5.9: Spatial distribution of soil loss for the grassland areas in the U.S. Great Plains for the years 2010 and 2012. 175

Figure 5.10: Spatial distribution of sediment retention for the grassland areas in the U.S. Great Plains for the years 2012 and 2016 176

Figure 5.11: A comparison of the spatial distribution of total carbon stock of grassland in the U.S. Great Plains for 2015 using the generalized and modified InVEST methods. 180

Figure 5.12: A comparison of the spatial distribution of the average annual soil loss in the grassland areas of the U.S. Great Plains for 2011 using the generalized and modified InVEST methods..... 183

Figure 5.13: Top: Precipitation and earth surface temperature anomalies in the Contiguous 48 States, 2001-2017. Source: EPA's Climate Change Indicators in the United States. Bottom: The combined economic values of carbon sequestration and soil erosion ES for grasslands in the Great Plains ecoregion from 2001 to 2017. 186

List of Tables

Table 2.2: Summary of economic valuation methods 43

Table 2.3: Summary of services, valuation methods, and outputs used in existing grassland ES valuation research. 48

Table 3.1: Parameters used in the BFAST routine analysis..... 80

Table 3.2: Definition and interpretation of gradual interannual trend classes (source: Hutchinson et al., 2015). 83

Table 3.3: Details of Landsat image pairs used for validation 86

Table 3.4: Landsat NDVI difference class threshold..... 87

Table 3.5: Summary of results for gradual interannual trend classes for the 2001-2017 study period in the U.S. Great Plains as determined by BFAST analysis of MODIS NDVI and EVI imagery. ... 93

Table 3.6: Landsat NDVI and EVI change classes compared to MODIS NDVI and EVI change classes. The Landsat NDVI and EVI change classes were considered the reference of the comparison. 96

Table 3.7: Error matrix of NDVI and EVI interannual trend class results for grasslands of the Great Plains ecoregion (2001-2017). The NDVI change classes are considered the reference, and the EVI change classes are considered the comparison map. The number of pixels in an agreement between the NDVI and EVI change classes are in bold. The grey cells contain the higher number of 'misclassified' pixels. 98

Table 3.8: Error matrix with the NDVI and EVI trend results for the Southwestern Tablelands ecoregion interannual trend classes. The NDVI and EVI trend classes are considered the reference and comparison maps, respectively. The number of pixels in an agreement between NDVI and EVI trend classes are in bold. The grey cells contain the higher number of 'misclassified' pixels. 99

Table 3.9: Error matrix with the NDVI and EVI trend results for the Flint Hills ecoregion interannual trend classes. The NDVI and EVI trend classes are considered the reference and comparison maps, respectively. The number of pixels in an agreement between the NDVI and EVI change classes are in bold. The grey cells contain the higher number of 'misclassified' pixels. 100

Table 4.1: MODIS MOD13Q1 pixel reliability values and weights applied within TIMESAT for the extraction of phenometrics. 125

Table 4.2: TIMESAT input parameters 126

Table 4.3: Description of selected TIMESAT Phenometrics. Source: (Eklundh & Jönsson, 2017). 129

Table 4.4: Summary of results for trends in phenometrics derived from MODIS (MOD13Q1) EVI data from 2001 to 2017 for the Great Plains ecoregion using the Mann Kendall trend test. 136

Table 5.1: The details of datasets used for the carbon model. 161

Table 5.2: The details of datasets used for the sediment delivery model. 163

Table 5.3: Total annual net economic values of carbon sequestered by grasslands in the U.S. Great Plains 170

Table 5.4: A comparison of approximate carbon stock estimates (2001-2005) produced for grasslands in the Great Plains ecoregion. 177

Table 5.5: The combined economic values of carbon sequestration and soil erosion ESs for grasslands in the Great Plains ecoregion from 2001 to 2017 185

Acknowledgments

For the success of my doctoral journey and research, I would like to thank my advisor, Dr. J.M. Shawn Hutchison, for his guidance, support, and encouragement throughout the period of working on this research. He, through his wonderful mentorship, taught me many concepts, techniques, persistence, assertiveness, but most importantly, how to be an independent researcher. I am also grateful to my research committee, Dr. Doug Goodin, Dr. Jida Wang, and Dr. Trisha Moore, for their timely and valuable suggestions. Specifically, Dr. Doug Goodin, for his help with several interjected life lessons in and outside his classes. Dr. Jida Wang, for always offering a helping hand and his enthusiasm in my research process. Dr. Trisha Moore, for her unmatched support and working with me even in unfavorable conditions.

I also appreciate the support of other K-State faculty members, to name a few, Drs. Bimal Paul, Chuck Martin, Arnaud Temme, Jeffrey Smith, Max Lu, Vera Smirnova, and Audrey Joslin. I am grateful to the Geography and Geospatial Sciences Department of Kansas State University and faculty for the financial support through assistantships. I remain indebted to the National Space Research and Development Agency, Abuja, for granting me study leave and providing financial support while I made great strides in my research career.

This journey would not have been possible without my husband, Emeka, and children, Ziva and Zani; their support, encouragement, and patience kept me sane. I am grateful to my sisters and friends Chinwe, Chioma, Uche, Kosi, Chineneye, Avantika, Surbana, Hafeez, Kachi, Demilade, Meng, Abiola, Anisah for their constant motivation and encouragement till the end.

Finally, I am grateful for all the financial support I received, including a KansasView Student Research Grant from the USGS-sponsored KansasView Consortium, the Phi Kappa Phi's 2020 Love of Learning Award, Kansas State University Department of Geography and Geospatial Sciences' Graduate Research Grant (2020/2021 academic year), 2020 Steven Kale fellowship and the American Geographical Society's 2021 fellowship.

Note: Specific chapter acknowledgments are included at the end of each chapter.

Chapter 1 – General introduction

1.1 Overview

Grasslands are one of the largest terrestrial ecosystems globally, covering about 40 percent of the Earth's surface (Briggs et al., 2005). Grasslands occur naturally on every continent except Antarctica, although a few grass species occur on the Antarctic Peninsula and surrounding islands due to recent warming (White et al., 2000; Suttie et al., 2005; Blair et al., 2014). They are one of the most biodiverse and productive terrestrial biomes but receive low levels of protection (Mark & McLennan, 2005; Pendall et al., 2018).

Vast grassland areas are converted each year for agricultural production or urban development. In the last decade, more than 8,100 square kilometers of grasslands were converted to croplands in the entire Great Plains (Plowprint report, 2021). In 2019 alone, approximately 10,500 square kilometers of grasslands in the Great Plains were lost to crop cultivation (Plowprint report, 2021). The temperate grasslands in the United States are among the most threatened grassland ecosystems, with almost 62% of the historical extent lost (Comer et al., 2018; Oakleaf et al., 2015).

In addition to conversion to other land-use, threats to grassland include the invasion of non-native species (woody species), fragmentation, overgrazing, desertification, and fire suppression (Gibson, 2009; Jacquin et al., 2016; Ratajczak et al., 2016). Based on the NatureServe landscape condition model for the Great Plains, approximately 20% of shortgrass prairie, 15% of mixed-grass prairie, and 60% of tallgrass prairie are in poor to worst conditions (Comer et al., 2018).

Shafer and colleagues' (2014) assessment of the climate in the Great Plains of the U.S. includes increasing temperatures alongside hazardous event events like flooding, drought, and tornadoes. The changing climate has had several impacts, including water stress and agricultural practices, but most importantly, the variation in vegetation structure and growth cycles (Shafer et al., 2014). The projection of climate in the region is continued rising temperature, increased winter and spring precipitation in the northern Great Plains and increased dry spells in the southern Great Plains (Shafer et al., 2014). Little is known on how the changing climate and other aforementioned anthropogenic activities impact the grasslands in the Great Plains ecoregion. In the Northern hemisphere, phenology

studies have shown changes in seasonality with shifts in time-dependent phenometrics; there are longer growing seasons and delayed end of growing season (Jeong et al., 2011; Wang et al., 2016; Cui et al., 2017).

Declining quality in grasslands can alter the structure and function of grassland ecosystems, and they also likely affects the provision of the many grassland-related ecosystem services. Grassland-related ecosystem services include but are not limited to carbon sequestration, erosion control, water storage, recreation, nutrient cycling, very high biodiversity, and grazing productivity (Briggs et al., 2005; MEA, 2005; TEEB, 2010; Ratajczak et al., 2016). The value of these and other ecosystem services provided by native grasslands in the United States Great Plains is estimated to be more than $5,000 (in 2004 U.S. dollars) per hectare annually (Dodds et al., 2008).

The current declining trends in grasslands have generated considerable interest in the quality and quantity assessments of grasslands (Henebry, 1993; Wang et al., 2013; Ratajczak et al., 2016; Chakraborty, 2018). These studies help comprehend the changes in the environment as climatic patterns change, including the impact on plant growth, carbon balance, and food productivity. The findings, in turn, will help estimate market values of ecosystem services to assess and easily portray the current benefits of an area's natural capital and the potential costs of human impact.

Remotely-sensed images are popular for monitoring grasslands because of the cost-effectiveness of extensive area coverage coupled with advances in data properties (better spatial, spectral, and temporal qualities of data). Analysis of a time series of remotely sensed imagery to evaluate temporal trends in grasslands may be used to inform management practices. NDVI is the most applied vegetation index (VI) used as a proxy to provide an approximate measure of relative vegetation amount (Wang et al., 2018). NDVI has shown a consistent correlation with vegetation dynamics in various scales of land area, and the ratio concept reduces many sources of noise, but it has the limitation of saturation of value over high biomass areas (Huete, 1988; Wang et al. 2018). The enhanced vegetation index (EVI) was developed to improve sensitivity in high-biomass areas and further reduce atmospheric influences. The EVI uses additional wavelength bands and a soil adjustment factor to adjust NDVI for atmospheric and soil noises as well as mitigating the saturation in dense vegetation areas. However, the soil adjustment factor used in calculating the EVI makes it more sensitive to the variation in the radiance that accompanies a change in the topography of a

surface in response to a change in the light source and sensor position (Matsushita et al., 2007). Therefore, making it difficult in areas with rough terrains or mountainous areas (Matsushita et al., 2007).

Long-term studies on a major terrestrial biome like grasslands are critical to achieving an integrated understanding of ecosystems' response to climate change. Understanding the impact of climate change and ecosystems is necessary because these changes impact the provision of various essential ecosystem services provided by grasslands. Therefore, long-term analysis of grassland is needed for monitoring and evaluating long-term changes in biomes like grasslands is also key environmental policy and decision making and evaluating the impact of some implemented policies on the environment.

Some existing studies have highlighted the changing spatial extent of grasslands in the Great Plains (Comer et al., 2018), the phenological trends in the northern hemisphere (Jeong et al., 2011), and greening/browning trends globally (De Jong et al., 2012). Comer et al. (2018) analyzed long-term spatial trends in grassland types across the Great Plains, including identifying species of concern, protected areas, intactness, and connectivity among grassland areas and identifying Grassland Potential Conservation Areas (GPCAs). Results of the long-term spatial trends showed that the tallgrass prairies had the most severe declines in extent, followed by mixed-grass, shortgrass, and semi-desert grasslands. Results from the time-series analyses of long-term phenological trends in the northern hemisphere by Jeong et al. (2011) showed a general earlier start of the growing season and later end of the growing season, which resulted in an increased growing season length. Also, Jong et al. (2012) carried out an analysis on global vegetation greening and browning trends between 1982 and 2008. Although a net greening was detected across all biomes, the trend for grasslands and shrublands showed abrupt greening followed by gradual browning. The southern hemisphere showed the most browning, and the temporal analysis indicates more browning than greening in the time studied.

Despite these past studies, relatively little is known about the long-term conditions of grasslands in the interior of the United States. The objective of this study is to assess long-term trends and spatial patterns in grasslands within the U.S. Great Plains based on vegetation greenness as measured by the

Normalized Difference Vegetation Index (NDVI) and Enhanced Vegetation Index (EVI) over the period 2001 to 2017.

A time series of vegetation indices can be used to determine trends and seasonal variation in vegetation properties (Heumann et al., 2007). One approach used to accomplish this is temporal decomposition, which separates time-series image data into three components, including seasonality (annual), trend (interannual and could be linear or nonlinear), and residuals (remainder of data signal after removing seasonality and trend) (Verbesselt et al., 2010). Phenology metrics or phenometrics such as the start and end of season or duration of the growing season can be extracted from time series of fitted VIs using statistical methods too (Jonsson et al., 2004; Jonsson & Eklundh, 2004).

In North America and the northern hemisphere, phenology studies have shown changes in seasonality with shifts in time-dependent phenometrics like the longer length of the growing season and delayed end of the season (Jeong et al., 2011; McManus et al., 2012; Cui et al., 2017). Jeong et al.'s (2011) study was on the entire northern hemisphere and focused on the broad vegetation categories. Results from the time-series analyses of long-term phenological trends in the northern hemisphere show a general earlier start of the growing season, later end of the growing season, and increased length of the growing season. In North America, existing studies focusing on grasslands are in Canada (McManus et al., 2012; Cui et al., 2017;). Cui et al. (2017) examine the long-term drought-related variability of grassland phenology in relation to drought in the southwestern part of Canadian prairies in Alberta and Saskatchewan (part of the Great Plains) from 1982 to 2014. Results show that droughts do impact the timing of the start and of the growing cycle, with a shorter growing cycle with decreased precipitation.

The U.S. Great Plains ecoregion is the largest grassland reserve in the U.S. The aforementioned drastic decline of this highly biodiverse, agriculturally-dependent ecoregion coupled with the spatial variability in environmental and socioeconomic characteristics makes it essential to understand the health status and dynamics of the ecoregion. Therefore, the overall purpose of this research is to investigate long-term grassland vegetation conditions using a well-known indicator (greenness based on VI values) within the U.S. Great Plains for the period 2001-2017 (based on data availability) and assess the impact on the provision of related grasslands benefits.

1.2 Research question and objectives

As a reflection of the purpose of this dissertation, the comprehensive research question is: *what are the long-term grassland vegetation conditions within the U.S. Great Plains, and what impact might change in these conditions have on the provision of grassland-related ecosystem services?*
This research has three objectives to answer the research question. The objectives of this study are to:

1. **Assess the long-term trends in grassland based on vegetation greenness within the U.S. Great Plains grasslands over the period 2001-2017.**

The temporal decomposition of a time series of vegetation indices (NDVI and EVI) data and the statistical analysis of the trend within the period 2001-2017.

2. **Assess the spatial patterns and trends of grassland phenology in the U.S. Great Plains over the period 2001-2017.**

Filtering of a time series of vegetation indices (NDVI and EVI) data, the extraction of phenology metrics, and the use of summary statistics to assess temporal and spatial patterns over the period 2001-2017. Also, determine the significance of phenometrics across the study area using statistical tests.

3. **Estimate the spatio-temporal changes in grassland-related ecosystem services within the U.S. Great Plains.**

Improve existing spatially-explicit ecosystem valuation methods by highlighting the temporal component in the provision of ecosystem services and estimating the economic value of a subset of grassland-related ecosystem services to assess the impact of changing grassland conditions on the provision of these ecosystem services.

From these objectives, this research primarily seeks to answer one of the National Research Council's (NRC) 2010 grand challenges for Geographic Information Science: "How are we changing the physical environment of earth's surface?" (Gould, 2010). This research also advances our understanding of North American grassland vegetation dynamics as it relates to the global decline in ecosystem services (MEA, 2005) and grasslands in the ecoregion (Comer et al., 2018; Plowprint report, 2018). Finally, this research highlights the importance of the need for the best practices for

grasslands conservation and restoration by showing the potential impact on important benefits grasslands provide.

1.3 Dissertation structure

This dissertation is divided into six independent chapters. Chapter one presents a general introduction of the research-the background of the study, research need, research questions, and objectives. The second chapter discusses the literature that is pertinent to the research, including definitions, classification, importance, and current management challenges for grasslands. The chapter covers a broad view of remote sensing of vegetation, including land surface phenology and long-term trend analysis, highlighting the need for research in the Great Plains. The literature review also covers the evolution of the ecosystem services concept, ecosystem services classification and valuation methods, a survey of grassland ecosystem service research, and concludes with the implication of the review, which provides a further justification for the study.

The third chapter to the sixth chapters are manuscript-format chapters, each focusing on each objective of this dissertation. Chapter three provides the detection and of long-term grassland vegetation trends for the Great Plain's ecoregion using temporal decomposition and satellite-derived vegetation indices. Chapter four provides a time series analysis of phenometrics for the U.S. Great Plains ecoregion using satellite-derived vegetation indices. The fifth chapter provides a spatio-temporal valuation of grassland ecosystem services in the U.S. Great Plains while presenting improved methods of ecosystems services valuation for vegetation. Chapter six presents the conclusion and summary of findings based on the research question and objectives. The chapter also discusses the future direction for this research.

1.4 References

Blair, J., Nippert, J., & Briggs, J. (2014). Grassland Ecology. In R. K. Monson (Ed.), Ecology and the environment (pp. 389–423). Springer New York. https://doi.org/10.1007/978-1-4614-7501-9_14

Briggs, J. M., Knapp, A. K., Blair, J. M., Heisler, J. L., Hoch, G. A., Lett, M. S., & McCarron, J. K. (2005). An Ecosystem in Transition: Causes and Consequences of the Conversion of Mesic Grassland to Shrubland. BioScience, 55(3), 243–254.

Comer, P. J., Hak, J. C., Kindscher, K., Muldavin, E., & Singhurst, J. (2018). Continent-Scale Landscape Conservation Design for Temperate Grasslands of the Great Plains and Chihuahuan Desert. *Natural Areas Journal*, 38(2), 196–211. https://doi.org/10.3375/043.038.0209

Cui, T., Martz, L., & Guo, X. (2017). Grassland phenology response to drought in the Canadian prairies. *Remote Sensing*, 9(12), 1258. https://doi.org/10.3390/rs9121258

Dodds, W. K., Wilson, K. C., Rehmeier, R. L., Knight, G. L., Wiggam, S., Falke, J. A., Dalgleish, H. J., & Bertrand, K. N. (2008). Comparing ecosystem goods and services provided by restored and native lands. *Bioscience*, 58(9), 837–845. https://doi.org/10.1641/B580909

Gibson, D. J. (2009). *Grasses and grassland ecology* (1st ed.). Oxford University Press.

Gould, M. (2010). GIScience Grand Challenges: How can research and technology in this field address big-picture problems? Esri. https://www.esri.com/news/arcuser/1010/files/geochallenges.pdf

Henebry, G. M. (1993). Detecting change in grasslands using measures of spatial dependence with Landsat TM data. Remote Sensing of Environment, 46(2), 223–234. https://doi.org/10.1016/0034-4257(93)90097-H

Huete, A. R. (1988). A soil-adjusted vegetation index (SAVI). *Remote Sensing of Environment*, 25(3), 295–309. https://doi.org/10.1016/0034-4257(88)90106-X

Hutchinson, J. M. S., Jacquin, A., Hutchinson, S. L., & Verbesselt, J. (2015). Monitoring vegetation change and dynamics on US Army training lands using satellite image time series analysis. *Journal of Environmental Management,* 150, 355–366. https://doi.org/10.1016/j.jenvman.2014.08.002

Jacquin, A., Goulard, M., Hutchinson, J. M. S., Devienne, T., & Hutchinson, S. L. (2016). A Statistical Approach for Predicting Grassland Degradation in Disturbance-Driven Landscapes. Journal of Environmental Protection, 07(06), 912–925. https://doi.org/10.4236/jep.2016.76081

Jeong, S. J., Ho, C. H., Gim, H. J., & Brown, M. E. (2011). Phenology shifts at start vs. end of growing season in temperate vegetation over the Northern Hemisphere for the period 1982-2008. Global Change Biology, Feb 17, Early View. https://doi.org/10.1111/j.1365-2486.2011.02397.x

Johnson, L., Cooke, B., Ramos, V. H., & Easson, G. (2008). Use of NASA Satellite Assets for Predicting Wildfire Potential for Forest Environments in Guatemala [Preliminary report]. University of Mississippi Geoinformatics Center (UMGC), Mississippi State University, and National Council for Protected Areas, Guatemala. https://www.gri. msstate.edu/research/nasa_rpc/2005/Wildfire%20REPORT%20SUBMISSION_MSU_RPC05.pdf

Jönsson, P., & Eklundh, L. (2004). TIMESAT—a program for analyzing time-series of satellite sensor data. Computers & Geosciences, 30(8), 833–845. https://doi.org/10.1016/j.cageo.2004.05.006

Mark, A. F., & McLennan, B. (2005). The conservation status of New Zealand's indigenous grasslands. *New Zealand Journal of Botany, 43*(1), 245–270. https://doi.org/10.1080/0028825X.2005.9512953

Matsushita, B., Yang, W., Chen, J., Onda, Y., & Qiu, G. (2007). Sensitivity of the Enhanced Vegetation Index (EVI) and Normalized Difference Vegetation Index (NDVI) to Topographic Effects: A Case Study in High-density Cypress Forest. Sensors (Basel, Switzerland), 7(11), 2636–2651. https://doi.org/10.3390/s7112636

McManus, K. M., Morton, D. C., Masek, J. G., Wang, D., Sexton, J. O., Nagol, J. R., Ropars, P., & Boudreau, S. (2012). Satellite-based evidence for shrub and graminoid tundra expansion in northern Quebec from 1986 to 2010. *Glob Change Biol*, 18(7), 2313–2323. https://doi.org/10.1111/j.1365-2486.2012.02708.x

Millennium Ecosystem Assessment [MEA]. (2005*). Ecosystems and human well-being: Synthesis* (2nd ed., p. 160). Island Press.

Oakleaf, J. R., Kennedy, C. M., Baruch-Mordo, S., West, P. C., Gerber, J. S., Jarvis, L., & Kiesecker, J. (2015). A world at risk: aggregating development trends to forecast global habitat conversion. *Plos One, 10*(10). https://doi.org/10.1371/journal.pone.013833

Pendall, E., Bachelet, D., Conant, R. T., El Masri, B., Flanagan, L. B., Knapp, A. K., Liu, J., Liu, S. & Schaeffer, S. M. (2018). Chapter 10: Grasslands. In Cavallaro, N., G. Shrestha, R. Birdsey, M. A. Mayes, R. G. Najjar, S. C. Reed, P. Romero-Lankao, & Z. Zhu (eds.). *Second State of the Carbon Cycle Report (SOCCR2): A Sustained Assessment Report.(*pp. 399-427). US Global Change Research Program. https://doi.org/10.7930/SOCCR2.2018.Ch10.

Plowprint annual report (2018). World Wildlife Fund. Retrieved from https://c402277.ssl.cf1.rackcdn.com/publications/1171/files/original/PlowprintReport_2018_FINAL_082318LowRes.pdf?1535470091.

Plowprint annual report (2021). World Wildlife Fund. Retrieved from https://files.worldwildlife.org/wwfcmsprod/files/Publication/file/5yrd3g00ig_PlowprintReport_2021_Final_HiRes_b.pdf?_ga=2.206397267.119456530.1640946732-1705276999.1640946731

Ratajczak, Z., Briggs, J. M., Goodin, D. G., Luo, L., Mohler, R. L., Nippert, J. B., & Obermeyer, B. (2016). Assessing the Potential for Transitions from Tallgrass Prairie to Woodlands: Are We Operating Beyond Critical Fire Thresholds? *Rangeland Ecology & Management*, 69(4), 280–287. https://doi.org/10.1016/j.rama.2016.03.004

Shafer, M., Ojima, D., Antle, J. M., Kluck, D., McPherson, R. A., Petersen, S., Scanlon, B., & Sherman, K. (2014). *Ch. 19: Great Plains*. Climate change impacts in the United States: the third national climate assessment. U.S. Global Change Research Program. https://doi.org/10.7930/J0D798BC

Suttie, J. M., Reynolds, S. G., Batello, C., & Food and Agriculture Organization of the United Nations (2005). *Grasslands of the world* (Series No. 34 ed.). Rome, Italy: p.536.

TEEB. (2010). The Economics of Ecosystems and Biodiversity: Mainstreaming the Economics of Nature: A synthesis of the approach, conclusions and recommendations of TEEB. Progress Press

Verbesselt, J., Hyndman, R., Newnham, G., & Culvenor, D. (2010). Detecting trend and seasonal changes in satellite image time series. *Remote Sensing of Environment*, 114(1), 106–115. https://doi.org/10.1016/j.rse.2009.08.014

Wang, C., Hunt, E. R., Zhang, L., & Guo, H. (2013). Phenology-assisted classification of C3 and C4 grasses in the U.S. Great Plains and their climate dependency with MODIS time series. *Remote Sensing of Environment*, 138, 90–101. https://doi.org/10.1016/j.rse.2013.07.025

Wang, S., Yang, B., Yang, Q., Lu, L., Wang, X., & Peng, Y. (2016). Temporal Trends and Spatial Variability of Vegetation Phenology over the Northern Hemisphere during 1982-2012. *Plos One*, 11(6), e0157134. https://doi.org/10.1371/journal.pone.0157134

Wang, S., Lu, X., Cheng, X., Li, X., Peichl, M., & Mammarella, I. (2018). Limitations and challenges of MODIS-Derived phenological metrics across different landscapes in Pan-Arctic regions. *Remote Sensing*, 10(11), 1784. https://doi.org/10.3390/rs10111784

White, R., Murray, S., Rohweder, M., & Prince, S. D. (2000*). Pilot analysis of global ecosystems: grassland ecosystems* (Illustrated, p. 94). World ResourcesBaghi, N. G. & Oldeland, J. (2015). *BFAST: A replacement of climate indicators for monitoring time-series using MODIS.* The XXIII International Grassland Congress (Sustainable use of Grassland Resources for Forage Production, Biodiversity and Environmental Protection). New Delhi, India. https://uknowledge.uky.edu/igc/23/1-2-1/2

Chapter 2 - Literature review

2.1 Grasslands

Grasslands are one of the largest terrestrial ecosystems and major biomes. They cover roughly 20 to 40 percent of the entire earth's surface (Blair et al., 2014; Briggs et al., 2005). The variation in extent is because of the varying definitions and classification of grasslands. In the following sections, we discuss the variations in the definition and classification of grasslands along with the spatial distribution of grassland globally. We also discuss why grasslands are important and the several management challenges of managing grasslands.

2.1.1 Definition

The International Union for Conservation of Nature (IUCN) and UNESCO describes the definition and usage of the term “grassland” as ecological as opposed to associated terms like “rangeland” or “grazing land,” which is land-use based and sometimes interchanged. This definition based on ecosystems is a significant factor in the variation of grassland extent as there are several ecosystem classification systems. Ecosystem classification systems are dependent on the investigator(s), scale (local or regional), environmental conditions, including physiography, climate, soils, and hydrology (Singh et al., 1983). The common theme in grassland definition is the vegetation composition, which is linked to ecosystem division based on climate (Bailey, 2009). Vegetation composition, in this case, is the absence or sparse presence of trees and/or shrubs.

Grasslands are generally defined as gramineous vegetation (dominated by grasses) that include variable amounts of other herbaceous plants, small amounts of shrubs, and sparse trees (Barnes & Nelson, 2003; Suttie et al., 2005; White et al., 2000; Xu & Guo, 2015). That means the term ‘grassland’ broadly encompasses non-woody vegetation, savannas, woodlands, shrublands, and even tundra. Therefore, it can be used to describe ecosystems with significant variations in the ratio of relative abundance of grasses to other plants like legumes, sedges, trees, and shrubs (Blair et al., 2014; West & Nelson, 2017). For example, some definitions allow 10 to 40 percent tree or shrub cover in areas covered with grass (UNESCO, 1973; White, 1983). Other definitions allow 15 to 50 percent tree or shrub cover provided the ground layer has a continuous grass layer, and some specify less than one tree per 5 acres (Anderson, 2006; White et al., 2000). In most cases, the term grasslands generally

mean natural and semi-natural grasslands, meaning they have had little improvement and are mostly native species (Bengtsson et al., 2019).

Variation in definitions also comes with differences in grassland terminology. Most of the popular terms relating to grasslands originate from historic grassland management, land use, and geographic location (Gibson, 2009). Several international organizations have developed formal descriptions for grassland-related terms. A popular example is the Forage and Grazing Terminology Committee that several U.S. agencies, with representation from Australia and New Zealand, published the definitions of several grassland-related terms in 1991 (Allen et al., 2011; Gibson, 2009). A more recent edition of definitions was published in 2011 that includes more international participation. The newer edition includes definitions of specific terms that are used synonymously to the term "grasslands" based on varying geographic locations and structures (Table 1.1). From relatively open savannas and woodlands (e.g., the cerrados of South America), treeless rolling grasslands in North America (Prairies), and some deserts and shrub grasslands referred to as steppes.

Table 2.1: Grassland terminology. The definitions are modified from those provided by Allen et al. (2011) for Forage and Grazing Terminology Committee.

Term	**Definition**	**Category***
Grazing land	***All-inclusive of any (vegetated) land that is or can be grazed.***	a
Pastureland	***Vegetation used to produce introduced or indigenous forage for grazing or harvest by cutting.***	a
Rangeland	***Land on which the indigenous vegetation is predominantly grasses, forbs, or shrubs that is or can be grazed and is managed as a natural ecosystem.***	a
Savanna	***Grasslands with variable proportions of trees or large shrubs,***	b

	especially in tropical and subtropical regions. It is often a transition between grassland and forests.	
Steppe	***Semi-arid, sparse to rolling grassland with short to medium-height grasses occurring with other herbaceous vegetation and some shrubs. Common in North America, south-eastern Europe, and Asia.***	b
Tundra	***Arctic and alpine regions without large trees and covered with varying low-lying vegetation to bare ground.***	b
Prairie	***Nearly level or rolling grassland, few or no trees treeless. They are short, intermediate, or tall-grass prairie depending on the variation of climate, fire regimes, and soil depth. Common in North America.***	c
Campos	***Consist of grasses with herbs, small shrubs, and a few trees on an undulating and hilly landscape. Climate is colder than in Cerrados. Common in Uruguay, southern Brazil, and north-eastern Argentina.***	c
Pampa	***Treeless grasslands on low-lying temperate grassland or subtropical steppe. Named after the pampas region and includes grasslands in southern South America.***	c
Cerrados	***Specific to central Brazil. They are savanna with varying amounts of trees and shrubs along rivers and in valley bottoms.***	c
Veld	***Open, indigenous grasslands. The term is of Afrikaans origin; they are found in most southern African countries.***	c

*Category: a = Land use; b = Grassland type; c = Location-specific grassland synonym

Another factor in the variation of grassland extent that is closely related to the definition aredifferences in land cover characterization (Faber-Langendoen & Josse, 2010; White et al., 2000). Because grasslands areas are usually large, estimation of extent, which is extremely important in monitoring temporal alteration in their extent, structure, and composition with modification, is usually done using remotely sensed data. Variations in sensor capabilities and remote sensing data properties might result in slightly different area estimations. For example, the U.S. Geological Survey's Global Land Cover Characterization (GLCC) with the International Geosphere-Biosphere Project (IGBP) classified landcover using a 1-km Advanced Very High-Resolution Radiometer (AVHRR) data, compared to the Chinese 30-m GlobeLand30 land cover classification created using Landsat and Chinese HJ-1 satellite images (Wang et al., 2018b; White et al., 2000). Land cover data have different classification methods and levels of accuracy, but beyond these, and more importantly, the variation in extent is primarily dependent on the choice of land cover classes and what constitutes grassland by an organization, authority, or researcher. The Pilot Analysis of Global Ecosystems (PAGE), a pioneering and popularly accepted estimate of global and regional grassland extent, highlights different authorities' variations in grassland definition. An example is the modification of the IGBP land cover classification to include tundra in grassland extent after separating these areas from classes like barren land and snow; also, the exclusion of urban areas from grassland extent using nighttime lights (Gibson, 2009; Grekousis et al., 2015; White et al., 2000). Other factors in the variation of grassland extent are the difficulty characterizing the limits of grasslands because their canopy structure is less persevering, the frequency of disturbance regimes, and occurrence within a continuum between forests and deserts (Dixon et al., 2014).

2.1.2 Global extent

Grassland occurrence and distribution are linked to climate and land management practices: temperature, precipitation (moisture), soil type, fire regimes, and grazing (Mucina et al., 2006; Singh et al., 1983). Globally, natural grasslands occurrence is extensive because they encompass a wide range of ecological communities and have a wide range of climatic tolerance (Belesky & Malinowski, 2016; Blair et al., 2014). They generally exist in areas with a fair amount of dry season (semiarid to sub-humid areas). That is, a variation from temperate to tropical regions with annual precipitation ranging from 250 to 1020 mm and mean annual temperature from temperature 0^0C to around 26^0C (Blair et al., 2014; Watkinson & Ormerod, 2001; Woodward et al., 2004). A fair amount of grasslands

still exist in Cold and arid zones (Squires & Feng, 2018). The climatic variation correlates to grassland net primary productivity, and they are sensitive to climate variability and change (Woodward et al., 2004). Even though the climate is a significant factor in the occurrence of grasslands, it is ill-advised to use this sole factor to define the distribution of biomes as it could lead to circularity (Woodward et al., 2004). Other factors that are also key in determining the distribution of grasslands include grazing intensity and fire regimes that prevent tree regeneration or soil properties that support the existence of natural grasslands in areas with relatively high precipitation (Watkinson & Ormerod, 2001; West & Nelson, 2017).

Grasslands occupy between 41 to 56 million square kilometers and occur naturally in every continent except Antarctica; although a few native grass species do occur on the Antarctic Peninsula and surrounding islands due to recent warming (Archibold, 1995; Blair et al., 2014; O'Mara, 2012; Suttie et al., 2005; White et al., 2000). Sub-Saharan Africa has the most substantial portion of its total land area as grassland, with approximately 30% of the global grassland area (White et al., 2000; Squires & Feng, 2018). However, on a country level, Australia, Russia, China, the United States of America, Canada, and Brazil hold the largest grassland areas (White et al., 2000; Gibson, 2009; Blair et al., 2014).

Based on Bailey's (2009) ecosystem divisions using the Köppen–Trewartha climate zones, natural grassland occurs in five major conditions or habitats *savanna*, *steppes*, *Mediterranean*, *tundra,* and *prairie** (*updated from Borchert's (1950) recognition as a climate type). Savanna is found in humid tropical areas without frost, and other conditions like soil properties and large herbivores prevent the growth of trees. Savannas, which includes the Llanos of the Orinoco Valley in Colombia and Venezuela, the veld of South Africa, and the Campos and Cerrados of Brazil (Watkinson & Ormerod 2001; Blair et al. 2014). *Steppes* are found in dry, tropical, and temperate regions where evaporation is higher than precipitation, and therefore, forest growth is limited. Steppes are typical in eastern Europe and Asia (Russia, Mongolia, and China). *Prairies* are found in humid temperate with eight months or less below 10^0C, and major examples are the tallgrass, mixed-grass, and shortgrass prairies of North America. Mediterranean grassland is like prairies (in temperate regions), but they have dry summers with short, wet, and relatively warm winters. Examples include the grasses found in the California area of the US (Blair et al., 2014; Bailey, 2009). *Tundra* is found in polar regions where most months are too cold for forest growth (Squires & Feng, 2018). Grasslands can also be found in

marine and montane regions (White et al., 2000; Blair et al., 2014). The Pilot Analysis of Global Ecosystems (PAGE) report's calculation of grassland area shows there are more savannas and shrublands (66%) globally compared to non-woody grasslands or steppes (about 20%) and tundra grasslands has the least area covering approximately 14% (White et al., 2000).

2.1.3 Importance of grasslands

Grasslands have significant importance globally, both for human well-being as well as ecosystem function.. They provide a range of goods and services necessary for the livelihood and well-being of people, and it also plays a massive role in maintaining the structure, functions, and processes of ecosystems (Briggs et al., 2005; Dodds et al., 2008; Nelson et al., 2009). White et al. (2000) estimates that approximately 800 million people (many are low-income) globally, whose livelihoods depend directly on grasslands.

Of all the many important functions of grasslands, their provision of food is the most popular. Grasslands provide food for both livestock, wildlife, and humans equally (O'Mara, 2012). With the exponential population growth rates since the 18th century and continuous growth to date (from approximately 3 billion in 1950 to 7.8 billion in 2018), the concern for food security has heightened (The United Nations, 2019). Besides population growth, growing incomes and shift towards high protein repackaged foods have also been linked to increased food demand (O'Mara, 2012). Grasslands constitute a major feed supply ruminant, including domestic herbivores like cattle, sheep, and goats (Gibson, 2009; O'Mara, 2012). A range of 20 to 60% (up to 70% in temperate regions) of the net primary production of grasslands is consumed by herbivores (West & Nelson, 2017). Although livestock densities (head per square kilometers) are higher in developed countries because of high-intensity production, the total number of livestock in developing countries with extensive natural grassland is more (White et al. 2000). Livestock production, in turn, provides a large percentage of protein-based food for humans: milk and meat and other relevant products like wool and leather (White et al., 2000; Carlier et al., 2009; O'Mara 2012; Hönigová et al., 2012). Demand for livestock-generated food is higher in developed countries; Europe, North and Latin America, and Asia are the main regions of livestock meat and milk production (O'Mara, 2011). In general, grasslands indirectly contribute to the global food supply (O'Mara, 2012).

Recently, the roles and functions of grasslands that are perceived to be very important with the current changing climate are carbon sequestration. Grasslands act as carbon sinks by reducing greenhouse gas (GHG) emissions (Peeters, 2010; Boval & Dixon, 2012). The global stock of carbon (SOC) stored by grasslands is 50% more than other agroecosystems (West & Nelson, 2017). The World Resources Institute PAGE analysis on grasslands reported that grassland carbon storage potential ranges from 1 to 3 metric tonnes per square kilometer. There is more SOC in the upper soil layer than in the grasslands because of the concentration of biomass production in grass roots; therefore, there is more carbon storage in grassland soils than in forest soils (White et al., 2000, Blair et al., 2014). Grassland soil holds up to 20% of the world's carbon stock (Rumpel, 2011). The downside to high carbon storage in grasslands soils is that it could become a carbon source when converted to other land uses (De Vliegher & Van Gils, 2010). In addition to carbon, grasslands are also known for the retention of nutrients like Nitrogen, Calcium, Magnesium, Sodium, and other micronutrients that are not only essential for plant/animal production but act as a sink for excessive availability of compounds like nitrogen in the atmosphere (Dubeux et al., 2007).

Another great thing about grasslands that is related to their soils is the high soil organic matter. High soil organic matter is tied to more root biomass, and organic material steadies soil aggregates to resist erosion and retain water and nutrients (West & Nelson, 2017). Many soil erosion models show that land cover influences short to long-term erosion rates (Wischmeier & Smith, 1978). Grasslands and forests provide a permanent vegetation cover that mitigates soil erosion compared to arable lands and other non-vegetated land covers (Cerdan et al., 2010).

Grasslands are also known to be one of the most biodiverse ecosystems that provide habitat for both plants and micro to megafauna (White et al., 2000). The IUCN's summary analyses of species richness for grasslands around the world for plot-level studies indicate all grassland types have high levels of richness with temperate grasslands and shrubland being distinctively very rich (Faber-Langendoen & Josse, 2010). Ricketts et al. (1999) carried out a broader analysis of biodiversity in the North American region using the term biological distinctiveness index (BDI). BDI is a broader (than species richness) definition of diversity that is inclusive of species richness, endemism, rare ecological and evolutionary phenomena, and rare habitat types. So, incorporating these measures not only represent biodiversity but the ecological processes that sustain ecological biodiversity (Ricketts et al., 1999). The authors grouped BDI assessments into scale-dependent categories, and the

Mediterranean/flooded grasslands and savanna ranked high as globally outstanding. Temperate grasslands also ranked the highest as regionally outstanding (Ricketts et al., 1999).

With the growing demand/cost of fossil fuels and the increasing concerns on environmental pollution and sustainability, agro-fuel production amongst many other "cleaner" and more sustainable fuel sources have become popular (De Vliegher & Van Gils, 2010). Even though arable lands are the go-to for agro-fuel production (like ethanol from sugarcane and corn), grasslands have an advantage because they give 50 percent more energy per hectare than corn ethanol and they do not need additional help like fertilizer or biofuels to grow (Machovina & Feeley, 2017; Patel, 2017). There have been concerns about the ability of sustainably growing or using the "low-input" grasslands for biofuel related to arable lands having the necessary nutrient input for biofuel biomass (Russelle et al., 2007). Tilman et al. 's (2007) experiment results show that low input biofuels could provide similar or higher net energy gains per land area than biofuels produced from crops grown on fertile soil with high inputs. Ceotto's (2008) review to highlight the downsides of using grassland for biofuel; he presented issues like the displacement of grasslands from their essential role of providing highly demanded foods and the release of reactive nitrogen during biofuel processing. On the other hand, urged that the use of grassland for biofuels should still be considered as arable lands do provide food for people just like grasslands (Ceotto, 2008).

The trending use of grasslands is a destination for tourists and recreational activities. These activities include hiking, biking, horse rides, camping, picnics, spiritual needs, and aesthetic views (Gibson, 2009). Generally, the tourism industry supports millions of jobs and contributes significantly to the Gross National Product (GDP). According to the World Tourism Organization (2017), international tourism accounts for 10% of world GDP, and one in every eleven jobs globally is in tourism (World Tourism Organization, 2017). In Japan, the Aso region grasslands have an estimated 19 million tourists visits annually (Inoue, 2017). The added perk with ecotourism is that it encourages the conservation of some native ecosystems. The trend of eco-friendly tourism is becoming popular with increasing awareness of how environmental alteration can change the climate. In the U.S., nature-based tourism, as reported by the National Park Service, had about 331 million visits and an estimated $18.2 billion was spent by visitors in areas within 60 miles of a park in 2017 (Cullinane et al., 2018). Grasslands are also important for other cultural, spiritual, and aesthetic benefits (Hönigová et al., 2012). Some native to semi-native grasslands in northeastern Europe are located on ancient sacred

sites; this is common with ethnic religions that tie sacred sites to the physical environment (Lindborg et al., 2008). Estimating the value of grasslands for tourism and recreation can be tricky because the level of enjoyment or recreational satisfaction derived from grasslands is subjective (White et al., 2000). Some proxies have been used to estimate these values; popular examples include the willingness to pay for a service or distance traveled to the site (Van Berkel & Verburg, 2014).

2.1.4 Current management challenges for grasslands

Despite all the many benefits of grasslands discussed in the last section, they are one of the most unprotected terrestrial ecosystems (Mark & McLennan, 2005). Significant proportions of the earth's grasslands have been modified or converted to other land uses (Finch & Dahms, 2004). Generally, approximately 54 percent of grasslands worldwide are degraded (White et al., 2000). The factors driving grassland degradation are intricate and sometimes contested, but they are generally a give-and-take between climatic factors and land use.

The major threats to grasslands are conversion to croplands and invasion of non-native species; others include fragmentation, overgrazing, desertification, and lack of fires (Gibson, 2009). Globally, the temperate grassland ecosystems are the most altered, with over 48% lost or degraded (Gibson, 2009; Henwood, 2010). Of all temperate grasslands, the prairie or plains of North America is the most altered (Finch & Dahms, 2004). Even though policies like the 2018 Farm Bill have been put in place to reduce the conversion of grassland to cropland, there is still rapid decline. In the Great Plains, a total of 62% of the historical extent of grassland has been lost, and in the years 2016 and 2017 alone, approximately 17,400 square kilometers of grassland was lost to cropland (Comer et al., 2018; Plowprint report, 2018). Also, with the growing crop production for biofuel, the source of new cropland in the contiguous U.S. from 2008 to 2012 was 77 % from grasslands (Lark et al., 2015).

Fragmentation of grasslands into smaller units or patches from a more heterogeneous landscape is mostly driven by disturbances that can be more subtle than the conversion to other land uses but can also affect grassland structure and function (Gibson, 2009). White et al. (2000) report a high fragmentation of grasslands in the Great Plains due to road networks with 70 percent of grasslands in this region with patches that are less than 1,000 square kilometers. Wang et al. (2009) analysis in grasslands in the Northeastern region of China using time series of geospatial data and results show the number of patches increased from 865 to 2035, and the mean patch size decreased from 16.4km^2

to 2.5 km^2 between the years 1954 and 2000. This study also links the increased fragmentation to socioeconomic factors and climate change. The greatest concern with grassland fragmentation is the loss of biodiversity as habitat loss and isolation can lead to decreased species population, richness, and in some cases, complete extinction (Debinski & Holt, 2000; Krause et al., 2015).

The invasion of non-native species can also lead to degradation of grasslands. Gibson (2009) summarized the IUCN Species Survival Commission (SSC) invasion of non-native or exotic species that invade and sometimes dominate native grasslands. The invasion of non-native species can lower soil quality and alter the structure and dynamics of grassland ecosystems. Invasion of nonnative species is linked to other stressing factors like overgrazing, lack of or infrequent burning, fragmentation, drought, increased available nitrogen from fertilization of crops, and the increasing carbon dioxide concentration (Gibson, 2009; Karl et al., 2009). An example is the invasion of the herbaceous Japanese knotweed (*Fallopia japonica (Houtt.) Ronse Decraene*) and the *salt cedar* into North American, European, and Australian grasslands (Gibson, 2009).

Fires are an essential component of grasslands globally. Grasslands are derived and maintained by fires (Gibson, 2009). Unintentional and commonly intentional annual burning is a common maintenance practice, especially in tropical and subtropical grasslands (Pathak et al., 2017; Squires & Feng, 2018). The fundamental uses of fires in grasslands are for the prevention of woody encroachment in grass-dominated ecosystems (Ratajczak et al., 2014). Woody encroachment is also a threat to grasslands globally (Eldridge et al., 2011; Archer et al., 2017). The process of shrubland and woodland encroachment in grasslands is complex and is attributed to a hierarchy of drivers operating at varying spatial and temporal scales- climate change, geomorphology, soils, and topography fire, grazing frequency, and land use (Archer et al., 2017). Fires eliminate woody species encroachment, although they might have some difficulty eliminating fire-resistant woody species from grasslands (Gibson, 2009). The frequency and intensity of fires in maintaining grasslands has been a contentious subject; plot experiments conducted in the Flint Hills region of the Great Plains in the United States show that fire frequency less than three years return can lead to transitions to shrublands and greater than ten years can lead to transition to woodlands (Ratajczak et al., 2016). There is, therefore, trends of increased frequency (annual or biannual) in burning in areas with broad grassland coverage to improve or maintain grasslands in most of the North American grasslands (Mohler & Goodin, 2012; Ratajczak et al., 2014). Fires also maximize grassland productivity, which

in turn increases livestock production and preserves native biota (Towne & Kemp, 2003; Pathak et al., 2017). There has been an evident increase in warm-season grasses after burning; the aboveground biomass of annually burned prairie was found to be almost double that of the infrequently burned prairie (Benson & Hartnett, 2006; Towne & Kemp, 2003). Pathak et al. 's (2017) field experiment also showed increased aboveground and belowground biomass production in burned sites compared to unburned sites. Also, herbicide application has been used as a method of preventing woody encroachment in North American grasslands, but the process is short-lived and, in most cases, requires a follow-up prescribed burning (Scholtz et al., 2018). There are some downsides to prescribed burning, air pollution with chemicals and particulates, increased danger of wildfire, reduction of nutrient cycling, and possible harm to native biota (Blair et al., 2014; KDHE, 2010; Mohler & Goodin, 2012). The benefits, as mentioned earlier of the prescribed burning of grasslands, demonstrate that the lack of fires can present management and conservation issues for grasslands.

One of the many uses of grasslands, as discussed previously, is livestock grazing. It is considered one of the fundamental uses of grasslands worldwide (Asner et al., 2004). Livestock grazing of grasslands has few perks; they create opportunities for lease hunting, which provides ecotourism revenue; they can also prevent woody plant encroachment (Archer et al., 2017). Livestock grazing can also maintain the quality (tillering rate and density) of grasses (Cao et al., 2013). Just like fire, grazing frequency and intensity for grassland conservation are highly contested and vary with spatial and temporal scale. Some studies have shown that grazing can increase species diversity and net carbon storage (Gomez-Casanovas et al., 2018; Isbell & Wilsey, 2009), but high-intensity grazing is attributed to vegetation decline which ultimately leads to the lowering of species diversity particularly in xeric grasslands (Isbell & Wilsey, 2009; Hilker et al., 2014; Blair et al., 2014; West & Nelson, 2018). There is vagueness in a global continuum of low to high-intensity grazing, as represented as grazing pressure (Zhang et al., 2015). Overgrazing is also attributed to biomass reduction, which decreases productivity and reduces the frequency and intensity of fires, thereby enhancing woodland and non-native species encroachment (Archer et al., 2017). The interaction between grazing and fires can lead to selective grazing of burned areas by livestock, increasing the grazing intensity of the areas, and leading removal of aboveground biomass (Blair et al., 2014). Even though grasslands in certain parts of the world (Africa and the Americas) are resilient to grazing, degradation, woodland, and non-native plant invasion, nutrient loss by overgrazing is common in many areas of the world without moderation and optimizing the exploitation of grassland for (Blair et al., 2014; Zhang et al., 2015).

Desertification in this context is the large-scale transition of native, productive, tasty-for-livestock grassland to unproductive non-grazable invasive species, woodland, or bare ground (Peters et al., 2013). The impacts of desertification on grassland ecosystems is complicated because the threat is a cumulative both climatic and land-use drivers working in varying time and spatial scales (Peters et al., 2013; Weber & Horst, 2011). Figure 2.1 shows an example of the process of desertification of grassland in Arizona over a century attributed to a combination of overgrazing and reduced rainfall in the southwest region of the United States (Karl et al., 2009).

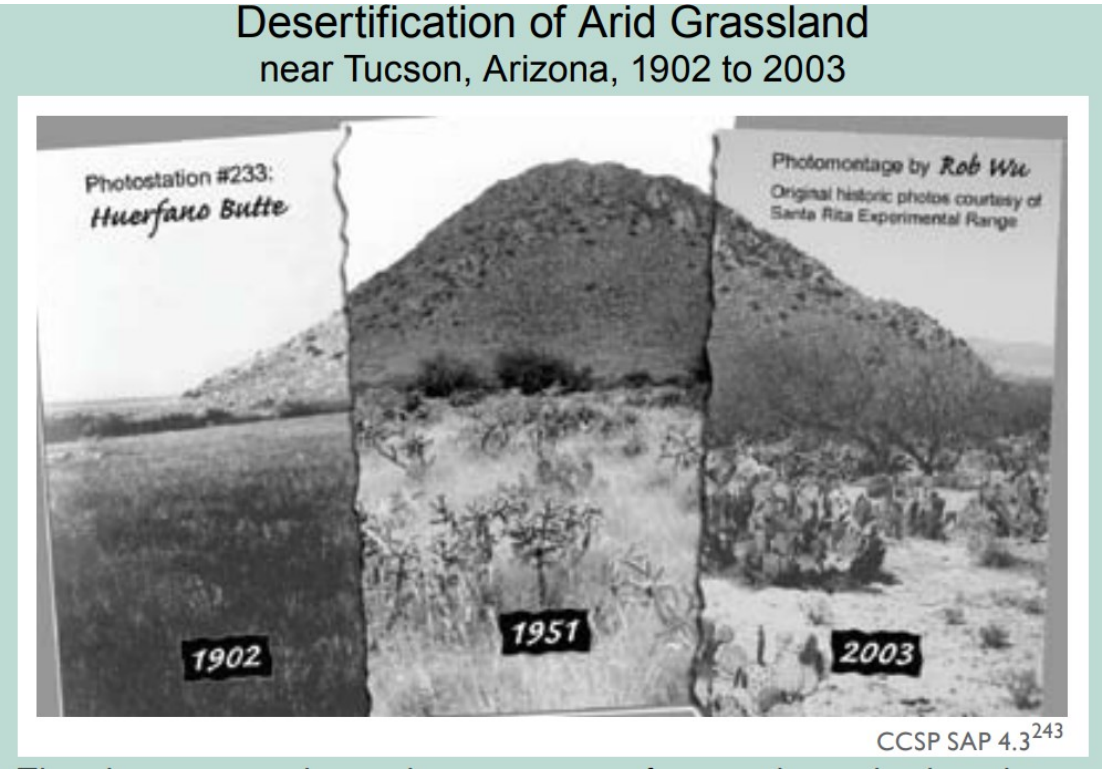

Figure 2.1: Desertification process of grassland over a 100-year period. (Reprinted from Karl et al. 2009).

These factors include those discussed earlier (overgrazing, fire, drought, invasive species, and more). In essence, it could be large-scale extreme weather events like floods to large-scale changes in climate; on the other hand, it could be small-scale grazing pressure that can lead to large-scale changes in ecosystem dynamics (Peters et al., 2013). In summary, grasslands are threatened mostly by conversion to cropland and urban development and an interplay of grazing pressure, fire intensity/pressure, and encroachment of woody plants and invasive species.

2.1.5 The Great Plains ecoregion

In North America, the expansion of the grass-dominated ecosystem and the expense of forests was prominent in the late Cenozoic (mid to late Miocene) era (Squires & Feng, 2018). A large portion of grassland ecosystems in North America is found in the Great Plains. The extent of the Great Plains varies with definitions and classifications of ecosystem components. A popular example of the definition of the ecoregion includes Omernik's (1987) definition based on both biotic and abiotic components. Another example is the definition by Bailey (2009) based on Koppen's climatic regions and the variety of vegetation and soils. In general, the ecoregion begins in the Canadian prairie provinces (Alberta, Saskatchewan, and Manitoba), a large portion cutting through the middle of the United States (Montana, Wyoming, North Dakota, South Dakota, Minnesota, Iowa, Missouri, Nebraska, New Mexico, Colorado, Kansas, Oklahoma, Texas, and Louisiana), and ending in grassland areas in the Mexican States (Coahuila, Nuevo Leon, and Tamaulipas) close to the Gulf of Mexico (Wiken et al., 2011; Tollerud et al., 2018).

The Great Plains, predominantly grasslands, have developed and are maintained by a combination of fire, grazing, and climate (Robin-Abbott & Pardo, 2011). There has been a lot of conversion to other land uses and degradation dating back to the 16th-century wave of migration and settlement in the United States. Over 50% of the historical extent of grasslands has been lost with the current coverage of approximately 44% of the ecoregion (Comer et al., 2018; Tollerud et al., 2018). Of the 50% of the historic grasslands lost, 96% of the Tallgrass prairie, 76% of the mixed-grass prairie, and 46% of the shortgrass prairie were lost (Comer et al., 2018). Furthermore, these prairies mostly exist in smaller fragments now compared to the historical state (Tinker & Hild, 2005).

The region is known to be highly biodiverse and one of the significant agricultural centers of the world (Gauthier et al., 2003). In the U.S., agriculture in this region (alongside related industries) contributed 1.053 trillion dollars to the U.S. GDP and 21.6 million jobs in 2017 (USDA, 2019). With mostly fertile soils (mollisols), it is one of the productive areas in the world for the cultivation of the most corn, sorghum, soybean, wheat, alfalfa, cotton, hay, and some fruit farming like peaches in the south (Wiken et al., 2011). The region is also known for ranging and dairying livestock for consumption and export in the U.S., Canada, and Mexico. They include the reintroduced bison, cattle, sheep, goats, and (Robin-Abbott & Pardo, 2011; Wiken et al., 2011). The region is significant to meeting regional and global food demands (USDA, 2019).

There is also tourism and recreation through wildlife, hiking, and scenic views. Wildlife and other grassland-adapted animals in the ecoregion include but are not limited to prairie dogs, coyotes, white-tailed deer, and the snowshoe hare (Wiken et al., 2011). The region is also home to a variety of bird species like prairie chickens, sharp-tailed grouse, ducks and geese, and native plants like the tobosagrass, grama grass, switchgrass, wheatgrass, bluestem, and Indiangrass (Robin-Abbott & Pardo, 2011; Wiken et al., 2011). With the loss of grasslands and climate change in the region in the last two decades, the population of indigenous bird species in the region are continually declining (Comer et al., 2018; Wesley et al., 2019), and so are prairie dogs (Martínez-Estévez et al., 2013). The declining biodiversity is a major concern regarding the future of the ecoregion in general.

The Great Plains is also rich in oil and gas (mostly in the south), coal mining, and vast tar sands reserves in the north (Canada). It is also one of the major water systems in the U.S. and southern Canada, draining the Missouri and Saskatchewan River systems (Robin-Abbott & Pardo, 2011). There is also a lot of surface water in the form of temporary pools or playa lakes (prairie potholes) that replenishes the very important Ogallala Aquifer (Wiken et al., 2011).

The region is very complex, with variations in rainfall, soils, management practices, temperature, and elevation (Tollerud et al., 2018). There is a wide range of temperatures (higher in the south and reducing toward the north) and precipitation (higher in the east and reducing toward the west) in the Great Plains region. The climate in the region, including hazards like floods, droughts, tornadoes, and hurricanes, profoundly impacts the energy-water-food nexus (Shafer et al., 2014). According to Shafer et al. (2014), there have been increasing temperatures in the Great Plains generally, and the increasing average temperature is projected to occur more frequently in the future. There is also a projection of increased winter and spring precipitation in the northern Great Plains and more dry spells in the southern Great Plains (Shafer et al., 2014). These diverse climatic patterns also impact the composition and conditions of grasses in the region. Climate-impacting factors on grasslands include increasing landscape fragmentation, water stress, and changes in vegetation growth cycles that may need change(s) in management practices (Shafer et al., 2014).

Manier and colleagues (2019) modeled four climate scenarios (warm-dry, warm-wet, hot-dry, and hot-wet) to weigh the vulnerability of grassland to future climate change in the southern Great Plains using grass species indicators for the grass communities in the region. The results show relatively low vulnerability for semi-desert grasslands and shortgrass prairie, higher vulnerability for mixed-

grass, and a very high vulnerability for tallgrass prairie. The high vulnerability of the tallgrass prairie was linked to the potential sensitivity of indicator species (indiangrass and the big bluestem grass) to the climate scenarios used and lower adaptivity due to long-term conversion to croplands (Manier et al., 2019).

Private-lands conservation programs, such as the Conservation Reserve Program, may play an important role in managing and conserving mixed-grass and tallgrass prairies by addressing potential changes in productivity of some species and addressing the landscape distribution of plants communities. The results of our analysis could help prioritize locations and species composition for habitat management on private lands, for example, through the CRP and public lands that could enhance the connectivity of prairie grasslands and supplement current conservation areas.

The loss and degradation of grasslands due to climate change and land use is a big issue. Even though lands in the Great Plains are mostly privately-owned, conservation strategies like the 2018 Farm Bill, the U.S. Department of Agriculture's Northern Great Plains Grasslands Strategic Plan, the U.S. Department of the Interior's BLM Grasslands Strategic Plan, the Saskatchewan/Manitoba Prairie Conservation Action Plans and other tri-national collaboration and financial incentives were implemented to encourage conservation (Gauthier et al., 2003; Drummond & Auch, 2015). Despite these, there is still a need for improvement in regulations, policies, and programs that favor grasslands conservation, better inter-agency coordination, and across-the-board technique for long-term monitoring and terminology (Gauthier et al., 2003).

2.2 Remote sensing of vegetation

Remote sensing of vegetation involves the interpretation of satellite images to measure and monitor vegetation status through their biophysical character (Xu & Guo, 2015). The use of remote sensing techniques and data for vegetation monitoring and grassland dates explicitly back to four decades ago (Xu & Guo, 2015). The use of remote sensing techniques is popular for monitoring grasslands because of the cost-effectiveness of extensive area coverage coupled with advances in techniques (better spatial, spectral, and temporal qualities of data) and methods. Ali et al. (2016) reviewed the use of several remote sensing data and methods for deriving grassland information. They found that high temporal optical satellite data is popularly used to generate time series because of the generation, and particularly to overcome cloud interruptions. However, popularly used data are usually low

spatial resolution data because of the limited availability high-resolution data and the required technology for processing.

For landscape analysis, low to moderate spatial resolution data like the National Oceanic and Atmospheric Administration (NOAA) agency's 250m to 1km Moderate Resolution Imaging Spectrometer (MODIS), and the Advanced Very High-Resolution Radiometer (AVHRR) have been sufficient (Reed et al., 1994; Zhang et al., 2003; Tan et al., 2011). With consistent, repeatable measurements of vegetation condition, they are adequate to capture phenological events in sufficient detail (Reed et al., 1994; Kennedy et al., 2009). An example is the MODIS 16-day composite NDVI data is accessible; it has sufficient and consistent temporal coverage for most long-term vegetation trend analyses (Reed et al., 1994; Wang et al., 2018).

Vegetation mapping with remote sensing uses the measurement of reflectance at visible and infrared wavelengths to discern the status of vegetation using distinct spectral signatures from chlorophyll in plants (Ali et al., 2016). Alongside these measures is the prevalent use of vegetation indices (VI). They used the surface reflectance at two or more wavelength bands that emphasize vegetation properties. Examples include the normalized difference vegetation index (NDVI) (Reed et al., 2003; Zhang et al., 2003), enhanced vegetation index (EVI) (Zhang et al., 2007), the soil-adjusted vegetation index (SAVI) (Huete, 1988) and several others. These VI have shown a considerable correlation to and used as proxies for vegetation amount or condition (Wang et al., 2018).

NDVI is the most applied VI; it uses a ratio of the red and near-infrared reflectance values to provide an approximate measure of relative vegetation health or greenness (Wang, 2018). NDVI has shown a consistent correlation with vegetation dynamics in various scales of land area, and the ratio concept reduces many sources of noise, but it has the limitation of saturation of value over high biomass areas (Huete, 1988; Wang et al., 2018). NDVI is the ratio of the difference and sum between near-infrared band reflectance (where most radiation is absorbed by vegetation) and red band reflectance where most radiation is reflected by vegetation (Zhang et al., 2003). Values vary between -1 to 1 (Equation 1); higher values are associated with healthier vegetation, while degraded vegetation is associated with lower NDVI values (Zhang et al., 2003).

$$\text{NDVI} = \frac{\rho nir - \rho red}{\rho nir + \rho red} \quad [1]$$

where:

NDVI = normalized difference vegetation index

ρnir = reflectance in the near-infrared spectrum

ρred = reflectance in the red spectrum

The NDVI does have several limitations that include sensitivity to the effects of soil brightness, soil color, atmosphere, clouds, and shadows; but the most prominent limitation is the saturation of values in areas with high biomass due to the non-linearity of the index (Matsushita et al., 2007; Xue & Su, 2017).

The enhanced vegetation index (EVI) was developed to improve sensitivity in high-biomass areas, reduce soil interference, and to further reduce atmospheric influences (Matsushita et al., 2007). It also uses a coefficient to correct scattering in the red band using the blue band and includes a soil adjustment factor (Equation 2) (Xue & Su, 2017).

$$EVI = \boldsymbol{G} \times \frac{\boldsymbol{\rho nir - \rho red}}{(\boldsymbol{\rho nir + C1 \times \rho red - C2 \times \rho blue + L})} \quad [2]$$

where:

EVI = enhanced vegetation index

ρnir = reflectance in the near-infrared spectrum

ρred = reflectance in the red spectrum

L = soil brightness adjustment factor

C1 = atmospheric scattering red correction coefficient

C2 = atmospheric scattering blue correction coefficient

G = gain factor

Generally, the value for the above coefficients is as follows; G=2.5, C1=6.0, C2=7.5, and L=1, but they may vary depending on the situation or sensor (Huete, 1997).

Very similar to the NDVI, the EVI is also popular in vegetation studies. It also provides an approximate measure of relative vegetation health or greenness, and it was adopted by the MODIS Group as the second global-based vegetation index for monitoring the Earth's terrestrial vegetation

activity (Matsushita et al., 2007). However, the soil adjustment factor used in calculating the EVI makes it more sensitive to the variation in the radiance that accompanies a change in the topography of a surface in response to a change in the light source and sensor position (Matsushita et al., 2007). Therefore, making it difficult in areas with rough terrains or mountainous areas (Matsushita et al., 2007).

Other vegetation indices have been developed recently to minimize the limitations mentioned above of using those VIs as a monitoring tool. Wang et al. (2018) reviewed and compared the performances of different VI's for extracting phenological metrics across different landscapes; they all show uncertainties in varying landscapes against eddy covariance estimates from flux sites. Xue and Su (2017) also reviewed over 100 vegetation indices, summarizing their developments, abilities, and limitations. Conclusions were that VI's are suitable for specific applications, and choice should be made based on capabilities or a combination of VI's. This study uses both NDVI and EVI because they correlate the most to vegetation vigor and biomass, which have been proven by many studies to show high correlation ground measurements during validations.

2.2.1 Land surface phenology

Phenology is the variation in seasonal patterns of natural phenomena on land surfaces in relation to climate (Cleland et al., 2007; Tan et al., 2011). Vegetation structure and production are tied to climate, and they respond to even small climatic variations; hence, phenological records have been used to monitor climate change (Schwartz, 1994; Bailey, 2009; Tan et al., 2011). Land surface phenology is the term for using remote sensing data to study the timing of seasonal patterns of variation in vegetated land surfaces (Tan et al., 2011; Wang et al., 2018).

Historically, specific plant species were used as indicator plants to study seasonal plant development with many data collection, observers, and network stations for regional studies (Schwartz, 1994). However, remote sensing is now widely used for monitoring vegetation because of the relatively cost-effective data acquisition, improving spatial, spectral, and temporal sensors' capacity and data quality resulting in advancing techniques and methods (Reed et al., 1994).

Since the dawn of remote sensing, phenological studies have used several methods to study the seasonal patterns and trends in vegetation. Methods have gone from the use of less accurate analog models in the early 20th century to algorithms that automatically retrieve land surface phenology metrics from satellite data (Schwartz, 1994; Tan et al., 2011). It is challenging to retrieve land surface

phenology metrics from satellite data directly because of atmospheric and radiometric noise, and data is a measurement of reflectance in different bands of wavelengths in the electromagnetic spectrum. Therefore, parameters like leaf area index (LAI), the fraction of photosynthetically active radiation (FPAR), green aboveground biomass, and vegetation indices have been used to determine vegetation structure (Pasolli et al., 2015). Changes in phenology are part of a complex system; they are influenced by forces other than long-term climate change, forces such as fire or conversion to urban areas (Willis, 2015). Coupled with the complexity that comes with variation in community composition, micro and regional climate, soils, and land practice at a regional scale (Zhang et al., 2003). In some cases, some vegetation types can show multiple modes of growth within one annual cycle. Therefore, both seasonality and trend components are crucial.

2.2.2 Methods for assessing phenological development

Phenological parameters or metrics (phenometrics as commonly referred to) such as the start of the season (SOS) and end of the season (EOS) can be extracted from remotely sensed vegetation index time series using linear or non-linear fitting functions and models (Jonsson & Eklundh, 2004). Before raw remote sensing data can be used for phenology analysis, it is put through a series of filtering, compositing, and smoothing procedures to isolate the signal from the noise. (Cai et al., 2017). Many smoothing methods exist; asymmetric Gaussian (AG), double logistic (DL), Savitzky–Golay filtering (SG), locally weighted regression scatterplot smoothing (LO), and spline smoothing (SP) (Tan et al., 2011; Cai et al., 2017). There is no conclusive evidence that one method is better than the many existing others. Cai et al. (2017) investigated several smoothing methods using MODIS NDVI, comparing them to ground NDVI measurements. Results indicate that the local filtering methods (SG and LO) can generate accurate results if smoothing parameters are optimally calibrated with function fitting methods (AG and DL) when calibration is impossible.

The conventional method is the derivation of the phenological parameters from a fitted curve identified by examining curve characteristics where VI data exhibit a rapid, sustained increase, decrease, and dormancy of increased value (Reed et al., 2003). The vegetation curve depicting the seasonal cycle of vegetation growth has varying definitions and terms for parameters or metrics used to measure the temporal changes in vegetation growth patterns (Figure 2.2). For example, Reed et al. (2003) defined the start of the growing season as to where the left time derivative transitions from

zero to a positive number and the end of the growing season as to the point where the right derivative transitions from a negative number to zero. Some limitations with this method are the difficulty of extracting these parameters in vegetation that is evergreen, snow-covered, or has a slow senescence rate (Reed et al., 2003). Also, Moulin et al. (1997) defined SOS and EOS as the timing of the highest positive and lowest negative derivative in VI, respectively. The limitation with this method is the difficulty in determining these parameters if the VI values do not follow an abrupt increase or decrease (De Beurs & Henebry, 2010).

Threshold-based phenology has become an effective technique to curb several limitations in hardline methods for the extraction of phenological parameters. The threshold-based method uses a relative reference value for defining the parameters (Reed et al., 2003). It could be the day of the year the VI value reached a certain threshold in an upward or downward direction. The threshold could be based on long-term average VI values, baseline year, NDVI ratios, NDWI (the Normalized Difference Water Index), or reference value (from an area with similar variables) (De Beurs & Henebry, 2010).

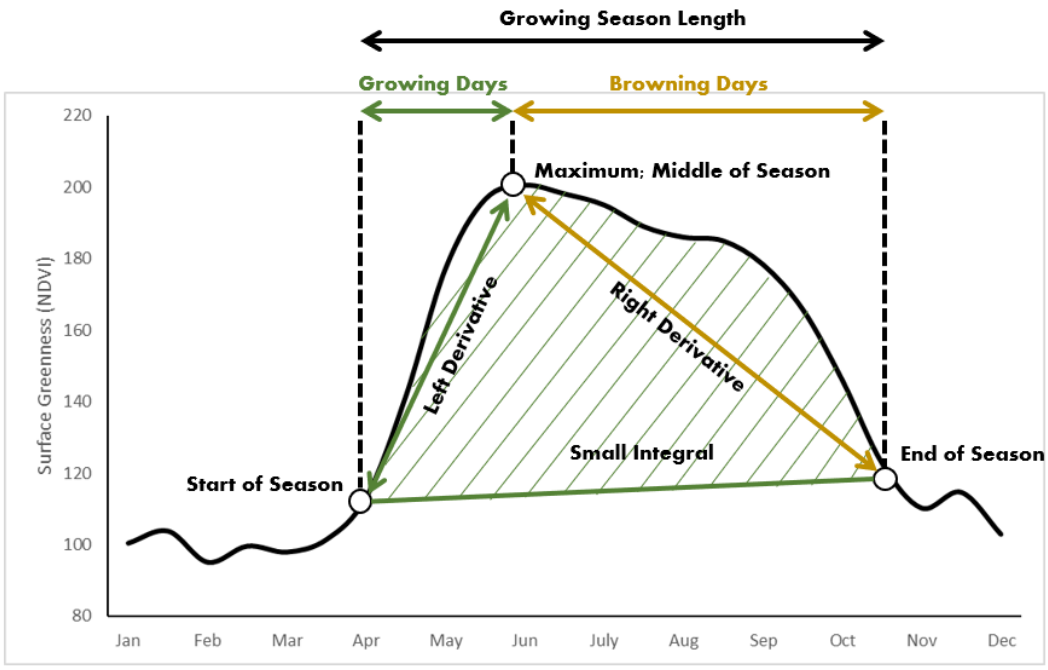

Figure 2.2: Typical temperate North American grassland phenology curve and some associated phenometrics generated in TIMESAT (Concept from Reed et al., 2003).

This study uses threshold method based on relative reference values for North America to define parameters (Reed et al., 2003). The software with this method is a widely used method of analyzing time-series satellite sensor data: TIMESAT (3.3) (Jonsson & Eklundh, 2004). It provides five smoothing functions to fit time series data and extracts (up to 13) phenometrics from smoothed data; then, it uses an analytical indicator to define the start and end of the growing season (Zhang et al., 2003; Eklundh & Jonsson, 2010). In North America, phenology studies have shown changes in seasonality with shifts in time-dependent phenometrics; there is the longer length of growing season and delayed end of growing season (Jeong et al., 2011; Wang et al., 2016; Cui et al., 2017). Cui et al. (2017) used the double logistic smoothing function in TIMESAT to smooth and extract long-term grassland phenology in the northern (Canadian) area of the Great Plains ecoregion. Results show a significant correlation to variation in precipitation. These findings are like Jeong et al. (2011) in the northern hemisphere. These findings are similar to other vegetation studies conducted in Canada (McManus et al., 2012; Ju & Masek, 2016), North America (Jong et al., 2012), and my preliminary results in the Great Plains ecoregion.

2.2.3 Long-term trend analysis of satellite time-series data

A time series of remote sensing data (usually vegetation indices) can be used to determine trends, seasonal variation in vegetation properties, and dynamics (Heumann et al., 2007; Eklundh & Jonsson, 2010). A temporal decomposition of time series data results in three elements: the trend, seasonality, and remainder. The time series decomposition is used to extract relevant information in the time series data. For this study, the trend component was used for the analysis. A popular method for decomposing trends in time series data is the use of the Breaks for Additive Seasonal and Trend (BFAST) (Verbesselt et al., 2010).

The BFAST routine is based on a LOESS-driven STL temporal decomposition, one of the many statistical methods used to extract the trends from time-series data. BFAST uses the least-squares regression to model the trend component within a time series, which detects gradual (interannual) and abrupt (intraannual) changes (Verbesselt et al., 2010). A newer method developed for detecting both abrupt and non-abrupt changes, named DBEST (Detecting Breakpoints and Estimating Segments in Trend), and can quickly accurately estimate change time and magnitude just like BFAST (Jamali et al., 2012). Nevertheless, DBEST cannot detect changes in the seasonal component (Fang

et al., 2018). Forkel et al. (2013) did a performance test on several methods used to detect trends and trend changes in the long-term VI time series, season-trend method (BFAST) had an overall excellent performance in both gradual and abrupt interannual variability. Fang et al. (2018) used BFAST to decompose grassland phenology trends in Canada; results show a general increased positive trend (greening).

Several (statistical) methods exist to extract and analyze trends from time-series data, and the choice falls on the characteristic of the data. Characteristics include seasonality, autocorrelation between observations, and whether it is stationary (properties not changing with time). Various trend detection methods include the ordinary linear regression, moving least squares regression smoother (LOESS), Nonparametric correlation coefficient (Man-Kendall's test), test using first derivatives, likelihood ratio test, autoregressive-moving average (Gray, 2007; Tan et al., 2011). The prevalent method of trend analyses in a time-series, especially for ecological data, is a linear regression model using the least-squares approach. The ordinary linear regression model (OLS) implemented with the primary assumption of linear and gradual changes in image time-series, making it suitable for analyzing linear changes in time-series data (De Beurs & Henebry, 2005; Jamali et al., 2012). The OLS regression, in this case, time is the independent variable and VI values (or summarized measure) the dependent variable and trend are expressed as the slope of the regression curve (De Beurs & Henebry, 2005). The simple regression method does have its limitations as the character of vegetation is dynamic and presents a variation in seasons and temporal trends. Besides the overall error for the OLS, there is also associated error with the parameter estimated because the parameters are not always significant from zero, and the slope parameter does not report this error (De Beurs & Henebry, 2005). The method is also susceptible to outliers alongside some assumptions with the OLS method. The assumptions are that the estimation error or residual must be normally distributed, be independent of the explanatory variable (time in this case), have a mean value of zero, and have a constant variance (De Beurs & Henebry, 2005; Qin, 2011).

Unlike the OLS regression, the non-parametric Mann-Kendall trend test (MK) does not depend on the normality of residuals for the validity of significant tests and is not sensitive to outliers and can work with missing values in the data (Helsel & Hirsch, 2002; Yue et al., 2002). The MK is also useful for analyzing linear changes, and it uses the same slope estimation format as the OLS

regression, but the estimation of the intercept and slope are non-parametric (Helsel & Hirsch, 2002). The slope is computed by comparing the data in a pairwise manner and ranking them in chronological order, that is a data set of an (X, Y) pairs will result in n(n-1)/2; the slope for each of these comparisons computed, and the median of all possible pairwise slopes estimated. The test determines the significance of any changes (decrease or increase) according to the differences between observation pairs (yearly observations in this case). So, the differences between observations of a given year and those of a previous year result in positive or negative values as a reflection of positive or negative change (Suepa et al., 2016). The Man-Kendall statistical test is popularly used in hydrological studies (Helsel & Hirsch, 2002; Yue et al., 2002) but recently being applied to vegetation studies for both general and phenological trends from VI time-series data (Cui et al., 2012; Suepa et al., 2016; Wang et al., 2016).

The OLS and MK methods are both useful in the analysis of linear, gradual, long-term trends. Even though the OLS methods involve some assumptions, Jamali et al., (2012) compared the performance of parametric vs. nonparametric techniques for trend analysis in different sites using these aforementioned methods as examples and the results show that slopes and statistical significance were comparable for the two methods in sites with linear and monotonic trends, but the OLS method performed better in sites with abrupt changes in slopes.

2.3 Ecosystem services

The concept of ecosystem services was developed as a bridge between nature and humans, specifically, the environmental functions of ecosystems and their value to human beings (De Groot, 1987). Although there are other terms used to describe ecosystem benefits to humans like “nature services,” “nature’s contribution to people,” “environmental services,” or “ecological services,” ecosystem services (ES) remain the most common and used term (Chaudhary et al., 2015; Díaz et al., 2018). The concept has ecological, socio-cultural, and economic roots (De Groot et al., 2017). The ecosystem services concept was not just developed to draw attention to the benefits we derive from ecosystems but also to promote biodiversity conservation and environmental sustainability.

There are several definitions of ecosystem services, but the general idea or theme is that they are benefits people obtain from ecosystems either directly or indirectly (Daily, 1997; MEA, 2005; TEEB, 2010). A lot of working terms and conditions have been interwoven into the general definition of

ecosystem services to enable a more consistent way of quantification and mapping of ES. Examples include Costanza et al.'s (1997, 2017) distinction between ecosystem process and function from ES and TEEB's (2010) identification of intermediate versus final services. Crossman et al. (2013) and La Notte et al. (2017) provide a detailed set of examples of ecosystem services terminology and definitions compiled from selected literature. The ecosystem services-related terminologies are a bid to avoid double-counting arising from linkages, stock, and flows of function and the need to break down the very complex ecosystem functions into discrete services (Birkhofer et al., 2015).

2.3.1 Evolution of ecosystem services

The concept dates to five decades ago (1960's: Marsh, 1965; Westman, 1977), and the term was coined in the 1980s by Ehrlich and Ehrlich (De Groot et al., 2012; 2017). But the concept garnered full attention with the invention of publications that presented innovative and collaborative definitions, classification, and valuation methods like those of Constanza and Daily both in 1997 then the UN's Millennium Ecosystem Assessment in 2005 (De Groot et al., 2012; Chaudhary et al., 2015; De Groot et al., 2017). Ecosystem service reached an even broader audience after the publication of the UN's second initiative, the Economics of Ecosystems and Biodiversity (TEEB), in 2010 (Costanza et al., 2014). Another huge milestone in the evolution of ecosystem service is the creation of the Intergovernmental Platform on Biodiversity and Ecosystem Services (IPBES) in 2012. This platform placed the concept on a political table, igniting the inception and improvement of national-level involvement in using the concept to ignite conservation and sustainability (De Groot et al., 2017). More recently (in 2018), (Díaz et al., 2018) described nature benefits as "nature's contribution to people" (NCP) instead of ecosystem services. This idea, an extension of the existing ecosystem services concept, recognizes the role of culture as central to the link between people and nature; the NCP concept also includes both positive and negative contributions to people. The view of culture being central in NCP is to widen the viewpoints of the concept to involve more people, especially stakeholders (Díaz et al., 2018). This generalized perspective is evident in the categorization of these benefits different from the popular classifications (I will discuss more details in the next section).

Several reviews of the literature on the evolution and trends of research in "ecosystem services" exist (Seppelt et al., 2011; De Groot et al., 2012; Chaudhary et al., 2015; McDonough et al., 2017). Chaudhary et al. 's (2015) findings show that before the 1997 popularity of ecosystem services, there

were only 166 studies with that term, and there has been an exponential increase to (over 5000 in 2015) thousands in this field since then. These findings are like those of De Groot et al.'s (2017) review, and a more recent review by McDonough et al. (2017) shows the same trend in the last decade.

Beyond the number of professional publications in the field, there is also an increase in subject areas, applications, contributions from different countries, the number of outlets (scientific journals and publications) focused on reporting ecosystems services trends (Chaudhary et al., 2015). Subject areas have grown from mostly environmental sciences and economics to health sciences, medicine, political ecology, and Engineering. The top subject areas are environmental sciences, agriculture, and biological sciences (Chaudhary et al., 2015; McDonough et al., 2017). Also, the top-ranking countries with a contribution to the ecosystem services field are the United States, the United Kingdom, China, Australia, and Germany. The U.S. and U.K. are top of this list, while sub-Saharan African and middle eastern countries are still lacking in this research area (Chaudhary et al., 2015; McDonough et al., 2017). The MEA in 2005 reports a declining global trend in ecosystem services despite the advances made in this regard, possibly due to the long list of countries or regions not making adequate contributions to this field to encourage biodiversity, conservation, and sustainability. In summary, this concept has gone from increased economic and policy interest, global and regional research, collaboration in the form of intergovernmental bodies on biodiversity and ecosystem services, and several national organizations and agencies (Chaudhary et al., 2015). There is still a need to expand the views of this concept and address some specific issues like consensual definition, classification, and valuation methods.

2.3.2 Ecosystem services classification

One of the significant challenges with ecosystem services research alongside variation in terminology is the variation in classification systems. Since the 1997 popularity milestone, there has been an emergence of several methods to classify ecosystem services. The central theme of all classifications of ecosystem services is the variety of ways in which ecosystems support human needs (La Notte et al., 2017). There is also the need to consider the following: variation in spatial scales, beneficiaries, direct or indirect use, short-term or long-term benefits, perspectives, approaches (service flow) and terminologies, and mostly level of detail (hierarchies) have evolved with time (USEPA, 2015). Popular classification systems for ecosystem services include the following: Daily (1997),

Millennium Ecosystem Assessment (2005), Haines-Young and Potschin-Young (2013, 2018), Common International Classification of Ecosystem Services (CICES) in 2017, U.S. Environmental Protection Agency (2015), and the IPBES adopted NCPs in 2018.

A form of categorization of ecosystem service is required to adequately map, measure, value, and communicate findings (De Groot et al., 2017). The initial studies of ES were in the form of a list of ecosystem services with the expectation of expanding those lists with time (Daily, 1997; Costanza et al., 1997). Daily (1997) included a list of 13 services, and Costanza et al. (1997) used a list of 17 ecosystem services to estimate the value of global ecosystem services and functions. The UN's MEA (2005) classification system groups existing ES into ways that benefit humans. These categories include provisioning, regulating, supporting, and cultural services, as described below (MEA, 2005).

- **Provisioning services** are materials and energy directly used by humans; examples include food and fiber, water, medicine from natural sources.
- **Regulating services** are services that regulate ecosystems or other environmental processes; examples include water regulation, flood control, and erosion control.
- **Cultural services** are nonmaterial value services. They include recreation, aesthetics, reflection, place identity, and other derived cultural or spiritual benefits.
- **Supporting services** – services that support other types of services. They include soil formation and nutrient cycling. They are different from other types of services because their impacts on humans are either indirect or occur over a very long period.

The TEEB (2010) classification system further expands on the MEA system adding a more economical aspect (Figure 2.3). It includes provisioning, regulating, and cultural services, but the fourth category is "habitat services" (USEPA, 2015; Costanza et al., 2017). The new category includes two new services: 'maintenance of life cycles of migratory birds' and 'maintenance of genetic diversity' (TEEB, 2010; La Notte et al., 2017).

	Main service types
	PROVISIONING SERVICES
1	**Food** (e.g. fish, game, fruit)
2	**Water** (e.g. for drinking, irrigation, cooling)
3	**Raw Materials** (e.g. fiber, timber, fuel wood, fodder, fertilizer)
4	**Genetic resources** (e.g. for crop-improvement and medicinal purposes)
5	**Medicinal resources** (e.g. biochemical products, models & test-organisms)
6	**Ornamental resources** (e.g. artisan work, décorative plants, pet animals, fashion)
	REGULATING SERVICES
7	**Air quality regulation** (e.g. capturing (fine)dust, chemicals, etc)
8	**Climate regulation** (incl. C-sequestration, influence of vegetation on rainfall, etc.)
9	**Moderation of extreme events** (eg. storm protection and flood prevention)
10	**Regulation of water flows** (e.g. natural drainage, irrigation and drought prevention)
11	**Waste treatment** (especially water purification)
12	**Erosion prevention**
13	**Maintenance of soil fertility** (incl. soil formation)
14	**Pollination**
15	**Biological control** (e.g. seed dispersal, pest and disease control)
	HABITAT SERVICES
16	**Maintenance of life cycles of migratory species** (incl. nursery service)
17	**Maintenance of genetic diversity** (especially in gene pool protection)
	CULTURAL & AMENITY SERVICES
18	**Aesthetic information**
19	**Opportunities for recreation & tourism**
20	**Inspiration for culture, art and design**
21	**Spiritual experience**
22	**Information for cognitive development**

Figure 2.3: Ecosystem services classification by TEEB (Source: TEEB, 2010)

The Common International Classification of Ecosystem Services (CICES) was initially developed in 2013 (4.3), the latest version (5.1), which is an extension of the 2013 version, was released in 2018 (Haines-Young & Potschin-Young, 2018). The CICES uses three functional groups of the MEA and TEEB classification (provisioning, regulating, and cultural services) but describes the ES groups in a five-level hierarchy with a more scientific approach (Figure 2.4). Each level in the hierarchy has more detail and specificity. This classification system considers only 'final services'; that is, only the end-product of nature that has a direct contribution to human well-being (Fisher et al., 2009; Costanza et al., 2017). For the reason of not being considered a 'final service,' the supporting services from the MEA and TEEB categories are not included in this system (Costanza et al., 2017; Ruskule et al., 2018). The supporting services are considered a 'function' rather than a 'service' (La Notte et al., 2017). The CICES also category called 'regulating and maintenance services,' which is a merge of

the TEEB's (2010) 'habitat services' and 'regulating services' (Haines-Young & Potschin-Young, 2018). The difference between the current version (V5.1) and the older version (V4.3) clarification of the definition of ecosystem services, the extension of the scope of the classification, provision of more straightforward ES names and numeric codes of each ES to aid easy referencing (Haines-Young & Potschin-Young, 2018).

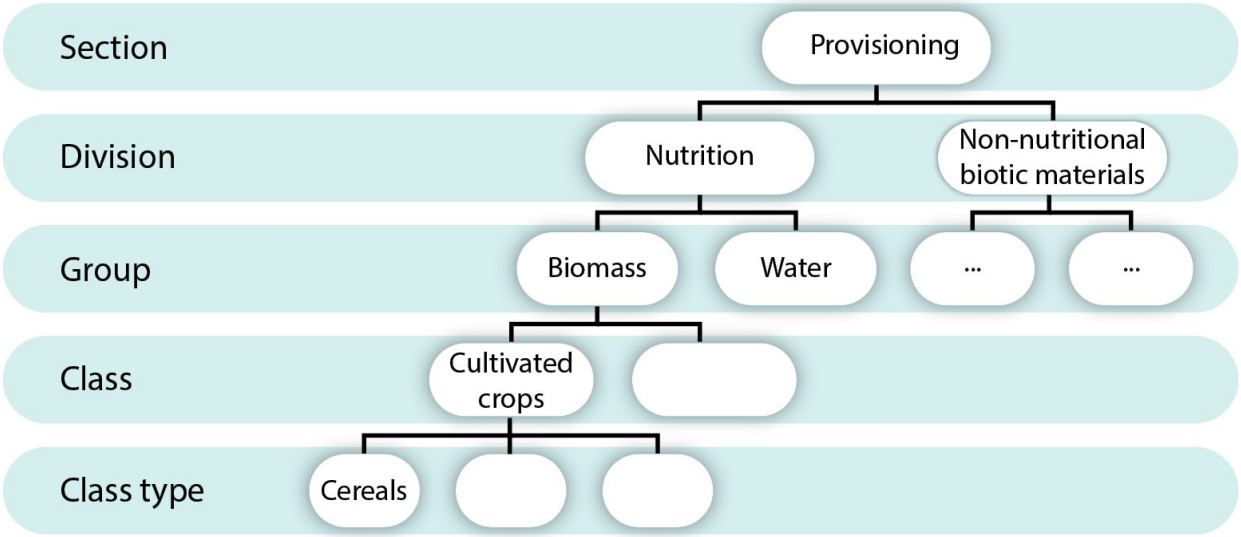

Figure 2.4: Illustration of the hierarchical structure of CICES V5.1 using cereals. (Source: Haines-Young & Potschin-Young, 2018).

The U.S. Environmental Protection Agency also developed two classification systems; the Final Ecosystem Goods and Services Classification System (FEGS-CS) and the National Ecosystem Services Classification System (NESCS) (Landers & Nahlik, 2013; USEPA, 2015). They are like the CICES in the sense that they only consider final ecosystem services to avoid double counting, and it has a hierarchical order with numeric codes for each category (USEPA, 2015; Costanza et al., 2017). The NCP concept as adopted by the IPBES has developed its own classification framework. This system is not very popular because it is relatively new, but it is gaining recognition with varying views from researchers in their fields. Pascual et al. (2017) describe these benefits and steps to their valuation which include both popular valuation techniques like modeling and narrative analysis to capture people's views. Categories in this classification system include three broad groups; regulating NCPs (similar to the MEA's regulating services), non-material NCPs, and material NCPs (Díaz et

al., 2018). All NCP's have a cultural context, so cultural benefits are not a separate category like the popular MEA classes. Figure 2.5 shows an example of NCPs and their categories.

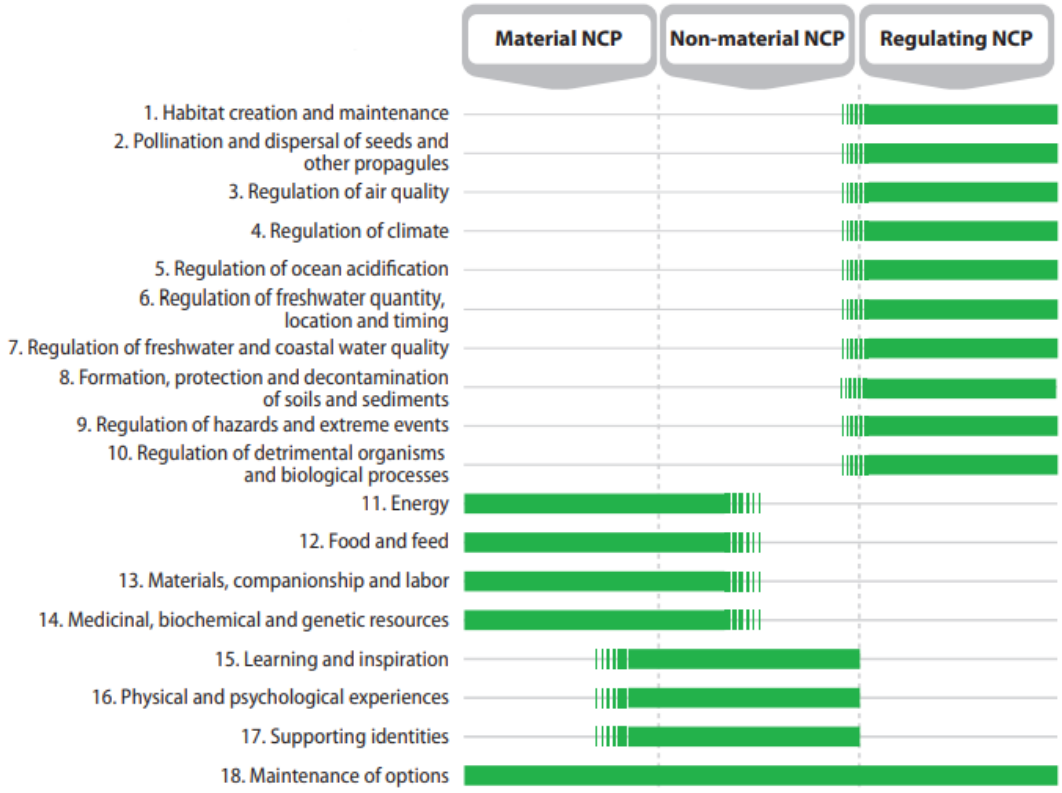

Figure 2.5: IPBES NCP and categories. (Source: Díaz et al., 2018).

The U.S. Environmental Protection Agency (2015), Costanza et al. (2017), and Ruskule et al. (2018) reviewed in extreme detail major ecosystem services classification systems. They discussed various challenges related to the categorization of ecosystem services. One of the major issues, especially with the earlier typologies (Daily, Costanza, and MEA), is the possibility of double counting in valuation from overlapping services (La Notte et al., 2017). An example of possible overlapping is the explicit Millennium Ecosystem Assessment (2005) supporting ecosystem services that are dependent on underlying ecosystem functions of other ecosystem services (i.e., provisioning, regulating, and cultural). Also, the impacts of supporting services on humans are either indirect or occur over a very long period compared to changes in the other categories being direct with short-term impacts on people (MEA, 2005; TEEB, 2010). The double-counting issue is the main reason more recent classification systems (CICES, FEGS-CS, NESCS) consider only final services.

However, there is a problem with determining what is considered "final services" as they vary with application, the reason CICES lists potential services (La Notte et al., 2017). There is also the issue of differentiating ecosystem services, goods, or benefits for proper valuation (La Notte et al., 2017). Although there are widely used classifications of ecosystem services (MEA and TEEB), the choice of an appropriate classification system to use should be based on the application area while considering their strengths and limitations (La Notte et al., 2017).

2.3.3 Ecosystem service valuation and valuation methods

The valuation of ES is as old as the concept (four decades ago). There are specific reasons why estimating the value of these services is essential. They include helping supranational, national, and local policymakers/environmental managers in urban and land use planning, raising awareness to the general population, estimating payments and incentives for ecosystem services, and more (Costanza et al., 2014). With the growing fields and applications of the ecosystem services concept, chances are there might be other needs for valuation arising in the future.

The valuation of ecosystem services has several challenges. First, the varying definitions and classifications for ecosystem services based on views on how they are generated and linked to their benefits to the well-being of humans (Birkhofer et al., 2015; Boerema et al., 2017; Seppelt et al., 2011). The ambiguousness in the definition makes the research on ecosystem services concept fluid across disciplines, but on the other hand, it makes it difficult to draw a generally accepted line for quantification (Seppelt et al., 2011). The variation in classification schemes has brought up the notion of double counting in economic valuation arising from linkages, stock, and flows of function and the need to break down the very complex ecosystem functions into discrete services (Birkhofer et al., 2015). Also, there is confusion between the quantification of stocks and flows, for example, measuring carbon stocks instead of carbon sequestration for climate regulation ecosystem service (Boerema et al., 2017).

Second, the diversity of beneficiaries of this contributes to complexity and plurality to the idea of quantifying ecosystem services. This can be an issue of both spatial and temporal scales. A plant considered food in a specific region might not be very useful in a different location and temporally, some plants currently considered as medicinal could be realized to be toxic or invasive in the future (Small et al., 2017). The third is the challenge for quantifying intangible ecosystem services, most

notably cultural services like aesthetic, spiritual, and religious values as defined by the Millennium Ecosystem Assessment. Since culture is individualistic, it is difficult to determine the interaction of an individual vs. community with their environment. It is making quantification of services very subjective and widely dependent on scale and time. Also, cultural services are prevalent within other services (i.e., provisioning, regulating, and cultural); Fishes or snails can be considered as a cultural service from the angle of recreation and also a provisioning service as a source of food (Small et al., 2017).

Fourth, it is difficult to distinguish between anthropogenically-created, potential, and actual supply of ecosystem services by an ecosystem (Millennium Ecosystem Assessment, 2005). This differs at spatial scales, and with the increasing presence of modified landscapes, it is hard to draw a line or get an accurate measure of an ecosystem's productivity. Finally, there is a wide variation in methods used to measure ecosystem services, ranging from simple scoring systems to complex field-specific surveys, measurements, and modeling. Also, the use of indicators as a proxy (Yu et al. 2005), making services values sometimes a proxy of a proxy as the case of using remotely sensed data for indicators. With all these challenges, several methods of valuation of ES used (especially recently) have yielded substantial values enough for policy and legal decisions (Costanza et al., 2014; Kallis et al., 2013).

The methods used in the valuation of ecosystem services are based on the type of service, data available, and researcher. Around the explosion of the ES concept, the well-known Daily (1997) had three categories of valuation methods: avoided cost for provisioning services, direct (consumptive) and indirect (non-consumptive) values for other services. Currently, broad categories of valuation methods include economic, sociocultural, and ecological or biophysical valuation methods (TEEB, 2010, Castro et al., 2014; Gómez-Baggethun et al., 2016; Burkhard & Maes, 2017; Ruskule et al., 2018). These methods incorporate the well-known ecosystem cascade that ties a biophysical structure from ecosystems and biodiversity to human well-being; going from and biophysical processes through functions, services, benefits, and finally values (Costanza et al., 2017; De Groot et al., 2017).

Biophysical valuation methods measure in biophysical units, that is, a measure of the physical costs of producing a service (Pascual et al., 2010; Ruskule et al., 2018). Therefore, these methods use indicators, proxies, or models for quantification (Gómez-Baggethun et al., 2016; Ruskule et al., 2018; Vihervaara et al., 2017). An example is the quantification of the amount of soil carbon or forest stock in biomass units. The focus of this method is the assessment of structures or health, processes, and

functions of services. In other words, these methods are suitable for measuring both stocks and flows of ecosystem services (Vihervaara et al., 2017). Ruskule et al. (2018) grouped these methods into direct and indirect methods. The former being the use of directly measured indicators (surveys or field measurements like vegetation biomass), and the latter uses some assumptions alongside secondary (for vegetation indices from remote sensing data). Lang (2018) used the biophysical method for urban green mapping in city planning. He utilized a proxy for land cover (high-resolution satellite image) to delineate areas with uniform vegetation and generate units of "geons" of urban green space in Salzburg, Austria.

Sociocultural valuation methods also involve the quantification of ES in non-monetary units. These methods are focused on perceptions of demand and supply of society regarding social needs. The contribution of nature in this sense includes but is not limited to cultural, inspirational spiritual, emotional, or aesthetic needs (Gómez-Baggethun et al., 2016; Santos-Martin et al., 2017). It is common to use primary data in socio-cultural methods. Due to the difficulty (time and cost) of collecting primary data, coupled with the lack of formality of a common methodological approach, these methods were the least popular. But the use of the methods has grown in the last decade and incorporates better social and cultural valuation techniques (Gómez-Baggethun et al., 2016; Santos-Martin et al., 2017). Examples of methodologies under this category include the use of narrative methods, participatory mapping, preference assessment, photo-elicitation surveys, scenario planning, and time-use assessment (Ruskule et al., 2018; Santos-Martin et al., 2017).

The economic valuation methods measure the value of goods and services in monetary values. These methods are popular because it promotes awareness of the importance of nature as most people can relate to or understand monetary terms (Boerema et al., 2017; Gómez-Baggethun et al., 2016). It is often used to measure ES demands which are also known as the cascades of value and benefits (Boerema et al., 2017; Vihervaara et al., 2017). A lot of economic valuation methods have been developed over the last four decades with refinement as time goes by (Gómez-Baggethun et al., 2016). Brander and Crossman (2017) classified economic valuation methods into two broad categories; the first is *primary valuation methods.* Primary valuation methods use primary data that is related directly to ecosystem services if available (Brander & Crossman, 2017; Gómez-Baggethun et al., 2016). The process of primary valuation is usually costly and time consuming the reason for the other category, the value transfer methods. The methods in this category include market prices, public pricing,

hedonic pricing, contingent valuation, restoration cost, replacement cost, choice modeling, etc. The second category is the *value transfer methods*, they are for a quick and low-cost valuation. The methods include the use of existing primary values for decision making or for extrapolation values to a larger spatial scale (Brander & Crossman, 2017). A valuation (TEEB) database exists for this purpose with estimates of economic values of ecosystem services (Van der Ploeg et al., 2010). Examples of value transfer methods include the unit value transfer (using existing primary values for similar ecosystems), value function transfer, and the use of estimation from many primary values (Brander & Crossman, 2017; De Groot et al., 2012). Pascual et al. (2010) further classified the primary economic valuation methods into three subcategories. They include (1) direct market value, (2) revealed preference approaches, and (3) revealed preference approaches. Table 2.2 summarizes the difference between these classification systems.

Table 2.1: Summary of economic valuation methods

Brander and Crossman (2017)	**Pascual et al. (2010)**	**Methods**
Primary valuation methods	Direct market value methods	Market price, Restoration cost, Replacement cost, Avoided cost, Public pricing, Production function, Damage cost avoidance

	Revealed preference methods	Hedonic Pricing, Travel Cost
	Stated preference methods	Contingent valuation, Choice modelling, Group valuation, Factor income
Value transfer methods	Benefit transfer	Unit value transfer, Value function transfer, Meta-analytic function transfer

A detailed review of economic valuation methods is beyond the scope of this study, a complete description including the strengths and limitations of these methods are available in the cited publications (Brander & Crossman, 2017; Pascual et al., 2010; TEEB, 2010). The authors also discuss the concept of total economic value (TEV), which describes the comprehensive value derived from an ecosystem and not just from one service (Brander & Crossman, 2017).

With the long list of valuation methods as presented in the last three paragraphs, a pressing and important question in the ecosystem services valuation process is "what method to use." Beyond the strengths and weaknesses of the existing methods, factors like data availability, cost of data acquisition, the purpose of valuation, spatial scale, technical certainty of the method, and type of service. Even though there are these categories of valuation methods, most ecosystem services studies combine, compare, or attempt to link the categories of methods in the valuation process (Castro et al., 2014; Kragt et al., 2010; Nelson et al., 2009; Whitham et al., 2015). Castro et al. (2014), in other to assess the relation between supply and demand of scarce ecosystem services by analyzing trade-offs on several landscape units in Spain, used biophysical values to measure supply and socio-cultural and economic values to measure demand.

A common characteristic with the varying ecosystem services valuation methods is the use of statistical methods and models to extract values. A detailed review of ecosystem services models was carried out by Dunford et al. (2017) and Kienast and Helfenstein (2016); they include process-based models, Empirical models, Landscape models, Statistical models, Conceptual models, etc. But for ES

services, integrated models are more effective in modeling the natural environment, they include biophysical models and LULC models. In the last two decades, ES modeling frameworks with consistent methods were created specifically for the biophysical and economic quantification and valuation of ecosystem services (Dunford et al., 2017). These modeling frameworks use a mix of several modeling components (process-based, conceptual, agent-based, etc.) and they are commonly used in regional scale studies where input data are not as detailed as local or site scale studies (Kienast & Helfenstein, 2016). These frameworks have become popular too because of the high use frequency in policy and decision making as most policies for large-scale areas. Widely used and well-tested examples of the modeling software packages include InVEST (models 18 ES for supply and demand yielding both biophysical and economic values); Artificial Intelligence for ES (ARIES) (uses AI to assess the best model to map and quantify the ES using the driver-response correlation; Multiscale Integrated Model of ES (MIMES) (models ES by linking them to the earth systems); Social Values for ES (SoLVE) (more for social-cultural methods, using data from surveys or value transfer. It alleviates the challenges of quantifying cultural services); ESTIMAP (developed by the European Union to assess the supply, demand, stock and flows of ES) (Bagstad et al., 2013; Dunford et al., 2017; Kienast & Helfenstein, 2016; Turner et al., 2016). Other modeling packages include GLOBIO-ES, EcoServ, EcoAIM, ESValue, LUCI (polyscape), etc.

Bagstad et al. (2013) reviewed and carried out a performance rating for seventeen modeling tools against criteria that include data requirement, level of development, scale application, and capacity of the independent application. Seven of the seventeen tools (included InVEST, ARIES, and EcoAIM) were tested on the San Pedro watershed in Arizona, U.S.A. InVEST, ARIES, SoLVE, and MIMES include tools that are generalizable, independently applicable, and suitable for landscape-scale areas, while LUCI was more site-specific. InVEST has been the top choice tool for most ES valuation studies not because it is open source and has standalone tools (like ARIES, MIMES) but because it has high generalizability, unlike ARIES that has a model for specific geographic areas; InVEST is also well documented and readily available without contacting for the required software like MIMES (Bagstad et al., 2013).

The choice of model to use is like that listed for the choice of methods: spatial and temporal scale, available data, output expected, involved stakeholders, and type of ES (Kienast & Helfenstein, 2016). This study uses both biophysical and economic valuation methods to assess the impact of grassland

trends in the Great Plains ecoregion between 2001 and 2017. The modeling tools used is the InVEST model suite because it has been well tested, opensource, generalizable, suitable for the spatial scale of the study area and the availability of required data (Bagstad et al., 2013; Dunford et al., 2017; Kienast & Helfenstein, 2016; Nelson et al., 2009).

2.3.4 Survey of grassland ecosystem service research

The importance of grasslands, as discussed in the previous section (2.1.3), include but are not limited to the use for livestock food and, in turn, food production, the use of biofuels, sequestering carbon in vegetation and soil, water regulation, soil erosion control, high biodiversity, and nutrient cycling (White et al., 2000). These, in turn, translate to the supply and demand of ecosystem services for humans. Even with the popularity of provision and valuation ecosystem services from other biomes like forests and water bodies, the grasslands biome, which is one of the largest and important biomes are, yet to receive the attention it needs in highlighting how the ever-changing, very little protected biome affects the supply of ecosystem services. Costanza et al. (1997) published the estimated individual and total economic values of ES from major biomes in the world based on the estimated value for each biome, and grasslands did not come off as very valuable as other biomes as importance was mainly for food provision and waste treatment. Grasslands have therefore been overlooked in global and regional policy discussions relating to ES (Bengtsson et al., 2019; Pascual et al., 2017).

Focus on the ES provided by grasslands was brought to the limelight by Sala and Paruelo in the same year (1997). In the last decade, more attention is being drawn to grassland ES as global declination in grasslands is still ongoing. There is an increasing number of studies focusing on grasslands, with the inclusion of previously overlooked services, ES that require indirect methods of valuation and those ES that have non-use values (Bengtsson et al., 2019; Hendrickson et al., 2019; Hönigová et al., 2012; Sala et al., 2017; Sollenberger et al., 2019; Yu et al., 2005). The current ecosystem services provided by grasslands include but are not limited to the provision of food both for livestock and agriculturally for humans; regulation of erosion, pest, water flow, soil fertility, and climate; Cultural services such as tourism, recreation, and the use in scientific studies (Havstad et al., 2007; Hönigová et al., 2012; Inoue, 2017; Sala et al., 2017; Sollenberger et al., 2019). There is also further study into the role of synergies and tradeoffs in ecosystem services with the conversion of land use and how it impacts policy decisions and management practices (Bengtsson et al., 2019); like will the conversion

from grassland to forests yield more ecosystem services? But the multifunctionality of grasslands is undisputed and requires more attention (Bengtsson et al., 2019).

With the growing focus on grassland ES and growing environmental concerns, there are several policies that have been put in place to either protect grasslands or restore natural grasslands that have been converted to other land covers. Though grasslands are resilient and highly adaptable to various environmental conditions, recovery may be difficult, and restoration yields much lower quality than natural grasses (Roch & Jaeger, 2014). A study shows reduced total value in restored grasslands compared to natural or semi-natural grasslands in the Great Plains region of the U.S., and conservation is therefore recommended for grasslands (Dodds et al., 2008).

Due to the vast coverage of grasslands, remote sensing is a popular method of data acquisition for mapping and valuation of grasslands ES. Remotely sensed data is used to produce spatially explicit assessments and quantification of ecosystem services (De Araujo Barbosa, et al., 2015; Liquete et al., 2016). They also provide adequate temporal scale data or even real-time data for monitoring of ES (Ayanu et al., 2012). A detailed review of remote sensing data, techniques suitability was described by several studies (Ayanu et al., 2012; De Araujo Barbosa, et al., 2015; Liquete et al., 2016). Ayanu et al. (2012) provide details of commonly used remotely sensed data (which include the Landsat, SPOT, and MODIS series), their key attributes, and their suitability in mapping and quantifying several ES. De Araujo Barbosa, et al. (2015) presents a summary of trends in remote sensing for ecosystem services research and what can be improved upon in the future in this research area by addressing methodological challenges and suggesting solutions. Even though remote sensing for ES mapping and quantification is cost-effective and relatively accurate, there are several limitations associated with the techniques; they include spatial data resolution, temporal scale, sensor type, and data uncertainties (Ayanu et al., 2012). These factors also determine the suitability of any available remotely sensed data for a study.

Remotely sensed data are usually used as a proxy for a variable or indicator, which is then used as a proxy for an ES; that is, a proxy of a proxy (Ayanu et al., 2012). In this case, vegetation greenness (indices) is a proxy for a service like carbon sequestration. There is either the direct use of remote sensing data using the radiative transfer or statistical models or the indirect use of generating land use/land cover data or vegetation indices. The direct methods will be problematic in this study because of the large spatial scale of the Great Plains ecoregion and the unavailability or high-

acquisition-cost of site measurement required for the model. So, the land use/land cover or VI is the best bet for this study.

Valuation of grassland ecosystem services is similar to the valuation of the ecosystem services of other biomes (e.g., forests). Values could be biophysical, socio-cultural, or economic and valuation methods cut across a broad range and discussed in the last section. The biophysical and economic valuation methods are most common for grassland ecosystem services (Table 2.3). Economic values range from contingent valuation-the willingness to pay (Costanza et al., 1997; Costanza et al., 2014) to unit value transfer (Yu et al., 2005). Table 2.3 summarizes valuation methods used (alongside other aspects) for grassland ecosystem research.

Table 2.2: Summary of services, valuation methods, and outputs used in existing grassland ES valuation research.

ES group (TEEB)	**Ecosystem service (TEEB)**	**Scale of/ and study area**	**Valuation Method**	**Valuation Output (unit)**	**References**
Provisioning	Food provision	1. Regional (Mongolian Plateau) 2. Country (Czech Republic) 3. Municipality (Shenzhen, China)	1.Preference assessment (socio-cultural) 2. Market price 3. Benefit transfer	1. Kg/capita 2. Euro/yr 3. USD/ha/yr 4. Kg per capita/yr	1. Zhen et al., 2010 2. Hönigová et al. 2012 3. Li et al. 2010 4. Du et al. 2018

		4. Landscape (inner Mongolia China)	4. Biophysical		
	Water (drinking)	1. Landscape (Te Papanui Conservation Park, New Zealand) 2. Municipality (Shenzhen, China)	1. Market price 2. Benefit transfer	1. NZD/ha/yr 2. USD/ha/yr	1. Butcher Partners Limited 2006 2. Li et al. 2010
Regulating	Climate regulation (Carbon sequestration)	1.Landscape (Tibetan- Plateau China) 2. Landscape (Paramo grasslands, Ecuador) 3. Landscape (Northern Chihuahuan desert) 4. Country (Czech Republic) 5.Landscape (Eastern Colorado USA)	1. Public pricing 2. Biophysical 3. Biophysical 4. Damage cost 5. Benefit transfer	1. USD/hm^2 2. Tons/ha 3. C/m^2/yr 4. Euro/ton 5. USD/ha/yr	1. Yu et al. 2005 2. Farley et al., 2013 3. Petrie et al., 2015 4. Hönigová et al. 2012 5. Sala & Paruelo 1997
	Water retention	1.Landscape (Tibetan- Plateau China) 2.Country (Czech Republic) 3. Regional (Catalonia, Spain)	1. Production function 2.Replacement cost 3.Benefit transfer	1. USD 2. Euro/ha/yr 3. USD/ha/yr	1. Yu et al. 2005 2.Hönigová et al. 2012 3. Brenner-Guillermo, 2007
	Water purification	1. Regional (Catalonia, Spain) 2. Municipality (Shenzhen, China)	1.Benefit transfer 2.Benefit transfer	1. USD/ha/yr 2.Yuan/ha/yr	1. Brenner-Guillermo, 2007 2. Li et al. 2010
	Soil conservation	1.Landscape (Tibetan- Plateau China) 2. Landscape (inner Mongolia China)	1. Production function 2. Biophysical	1. USD/month 2. g/kg	1. Yu et al. 2005 2. Du et al. 2018
	Soil nutrient	Landscape (inner Mongolia China)	Biophysical	mg/kg	Du et al. 2018
	Erosion Prevention	1. Country (Czech Republic) 2. Landscape (Central grasslands, USA) 3. Country (USA) 4. Regional (Catalonia, Spain)	1. Damage cost 2. Market price 3. Benefit transfer 4. Benefit transfer	1. Euro/ha/yr 2. USD/ha/yr 3. USD/ha/yr 4. USD/ha/yr	1. Hönigová et al. 2012 2. Barrow 1991 3. Sala & Paruelo 1997 4. Brenner-Guillermo, 2007

	Air quality	Municipality (Shenzhen, China)	Benefit Transfer	Yuan/ha/yr	Li et al. 2010
Cultural	Ecotourism	1. Country (Czech Republic) 2. Country (Botswana)	1. Contingent valuation (WTP) 2. Market price	1. Euro/ha/yr 2. Botswana Pula/ha	1. Hönigová et al. 2012 2. Barnes 2002
	Aesthetic	1. Landscape (Los Angeles, California, USA) 2. Landscape (Drakenberg Hill & Harz Mountain Villages, Germany)	1. Hedonic pricing 2. Contingent valuation (WTP)	1. USD/month 2. Euro/month	1. Brookshire et al. 1982 2. Barkmann & Zschiegner 2010
	Recreation	1. Country (Czech Republic) 2. Municipality (Shenzhen, China)	1. Contingent valuation (WTP) 2.Benefit transfer	1. Euro/ha/yr 2. Yuan/ha/yr	1. Hönigová et al., 2012 2. Li et al. 2010
Habitat	Genepool (Biodiversity) Protection	1.Landscape (Tibetan- Plateau China) 2. Municipality (Shenzhen, China) 3. Country (South Africa)	1. Value transfer 2.Benefit transfer 3. Contingent valuation (WTP)	1. USD/hm^2 2. Yuan/ha/yr 3. USD/ha/yr	1. Yu et al. 2005 2. Li et al. 2010 3. Turpie 2003
	TEV	1. Global 2. Global 3. Country (Australia)	Total Economic Value	1. USD/ha/yr 2. USD/ha/yr 3. AUD/ha/yr	1. Costanza et al. 1997 2. Costanza et al. 2014 3. Blackwell 2006

USD=U.S. dollars; AUD=Australian dollars; NZD=New Zealand dollars; hm^2=square hectometer; ha=hectares; yr=year; WTP=willingness to pay

Some existing modeling suites that incorporate the methods listed in table 2.3 can be used to value grasslands ecosystem services as well as other ES. Although there are some conceptual models for the monitoring of grasslands and vegetation-properties-based models to map grassland ecosystem services (Tinker & Hild, 2005; Lavorel et al., 2011), there is no modeling suite built specifically for grassland ecosystem services valuation. Other limitations with grassland ES valuation in the variation in definition and categorization of grasslands coupled with the varied categorization of ecosystem services. With this growing list of ecosystem services grasslands provide, it can be challenging to decide which ES to map and value that will best impact policy decisions. Yu et al. (2005) highlight

the need to choose related ecosystem services based on the varying structure of the grassland ecosystem.

2.4 Implications of the literature review on the current study

Having reviewed several related works of literature in the previous sections, the implication for the current study is that despite several definitions and classification of grasslands, they occur largely globally, and they are very important to humans and the environment. The review also shed some light on major methods used in mapping and monitoring grasslands, including their pros and cons. The temporal condition and spatial coverage are important in the mapping and monitoring effort. Specifically important in the time series analysis of remote sensing data to analyze grassland vegetation trends and highlight the impact of climate change and other factors influencing the dynamics of grasslands.

The most important implication of the review of literature is the dearth of studies assessing the condition of the Great Plains ecoregion as a whole. The Great Plains is one of the very important ecoregions in the U.S. and the world with its impact on climate regulation, livestock production, and biodiversity, to name a few. Second, is also a scarcity of studies in the valuation of grassland ecosystem services. The TEEB database shows only 56 out of 1310 entries for grassland, and most of the studies entered do not specifically focus on grassland. Even in the past decade, highlighting the services provided by grasslands and how they are impacted by the changing state of grasslands (declination and degradation) still needs more work.

2.5 References

Allen, V. G., Batello, C., Berretta, E. J., Hodgson, J., Kothmann, M., Li, X., McIvor, J., Milne, J., Morris, C., Peeters, A., & Sanderson, M. (2011). The Forage and Grazing Terminology Committee. An international terminology for grazing lands and grazing animals. *Grass and Forage Science*, 66(1), 2–28. https://doi.org/10.1111/j.1365-2494.2010.00780.x

Ali, I., Cawkwell, F., Dwyer, E., Barrett, B., & Green, S. (2016). Satellite remote sensing of grasslands: from observation to management, *Journal of Plant Ecology*, 9(6), 649–671, https://doi.org/10.1093/jpe/rtw005

Anderson, R. C. (2006). Evolution and Origin of the Central Grassland of North America: Climate, Fire, and Mammalian Grazers. The Journal of the Torrey Botanical Society, 133(4), 626–647.

Archer, S. R., Andersen, E. M., Predick, K. I., Schwinning, S., Steidl, R. J., & Woods, S. R. (2017). *Woody Plant Encroachment: Causes and Consequences*. In D. D. Briske (Ed.), Rangeland Systems: Processes, Management and Challenges (pp. 25–85). Springer.

Archibold, O. w. (1995). Ecology of World Vegetation (series; 16) (1995th ed., p. 510). Springer.

Asner, G. P., Elmore, A. J., Olander, L. P., Martin, R. E., & Harris, A. T. (2004). Grazing systems, ecosystem responses, and global change. *Annual Review of Environment and Resources*, 29(1), 261–299. https://doi.org/10.1146/annurev.energy.29.062403.102142

Ayanu, Y. Z., Conrad, C., Nauss, T., Wegmann, M., & Koellner, T. (2012). Quantifying and mapping ecosystem services supplies and demands: a review of remote sensing applications. *Environmental Science & Technology*, 46(16), 8529–8541. https://doi.org/10.1021/es300157u

Bagstad, K. J., Semmens, D. J., Waage, S., & Winthrop, R. (2013). A comparative assessment of decision-support tools for ecosystem services quantification and valuation. *Ecosystem Services*, 5, 27–39. https://doi.org/10.1016/j.ecoser.2013.07.004

Bailey, R. G. (2009). Ecosystem Geography: From Ecoregions to Sites (2nd ed. 2009). Springer-Verlag.

Barkmann, J., & Zschiegner, A. K. (2010). Grasslands as a sustainable tourism resource in Germany: environmental knowledge effects on resource conservation preferences. *International Journal of Services Technology and Management*, 13(3/4), 174. https://doi.org/10.1504/IJSTM.2010.032076

Barrow, C. J. (1991). *Land degradation: development and breakdown of terrestrial environments* (1st ed., p. 316). Cambridge University Press.

Belesky, D. P., & Malinowski, D. P. (2016). Grassland communities in the USA and expected trends associated with climate change. *Acta Agrobotanica*, 69(2). https://doi.org/10.5586/aa.1673

Bengtsson, J., Bullock, J. M., Egoh, B., Everson, C., Everson, T., O'Connor, T., O'Farrell, P. J., Smith, H. G., & Lindborg, R. (2019). Grasslands-more important for ecosystem services than you might think. *Ecosphere*, 10(2), e02582. https://doi.org/10.1002/ecs2.2582

Benson, E. J., & Hartnett, D. C. (2006). The role of seed and vegetative reproduction in plant recruitment and demography in tallgrass prairie. *Plant Ecology*, 187(2), 163–178. https://doi.org/10.1007/s11258-005-0975-y

Birkhofer, K., Diehl, E., Andersson, J., Ekroos, J., Früh-Müller, A., Machnikowski, F., Mader, V. L., Nilsson, L., Sasaki, K., Rundlöf, M., Wolters, V., & Smith, H. G. (2015). Ecosystem services-current challenges and opportunities for ecological research. *Frontiers in Ecology and Evolution*, 2. https://doi.org/10.3389/fevo.2014.00087

Blackwell, B. D. (2006). *The economic value of Australia's natural coastal assets: Some preliminary findings.* Australia New Zealand Society for Ecological Economics 2005 Conference, New Zealand.

Blair, J., Nippert, J., & Briggs, J. (2014). *Grassland Ecology*. In R. K. Monson (Ed.), Ecology and the environment (pp. 389–423). Springer New York. https://doi.org/10.1007/978-1-4614-7501-9_14

Boerema, A., Rebelo, A. J., Bodi, M. B., Esler, K. J., & Meire, P. (2017). Are ecosystem services adequately quantified? *The Journal of Applied Ecology*. https://doi.org/10.1111/1365-2664.12696

Borchert, J. F. (1950). The climate of the central North American grassland. *Annals Association of American Geographers.* 40, 1–39.

Boval, M., & Dixon, R. M. (2012). The importance of grasslands for animal production and other functions: a review on management and methodological progress in the tropics. *Animal: An International Journal of Animal Bioscience*, 6(5), 748–762. https://doi.org/10.1017/S1751731112000304

Brander, L. M., & Crossman, N. (2017). *Economic quantification*. In B Burkhard & J. Maes (Eds.), Mapping Ecosystem Services (pp. 113–123). Pensoft Publishers.

Brenner-Guillermo, J. (2007). Valuation of ecosystem services in the Catalan coastal zone [Doctoral Dissertation].

Briggs, J. M., Knapp, A. K., Blair, J. M., Heisler, J. L., Hoch, G. A., Lett, M. S., & McCarron, J. K. (2005). An Ecosystem in Transition: Causes and Consequences of the Conversion of Mesic Grassland to Shrubland. *BioScience*, 55(3), 243–254.

Brookshire, D. S., Thayer, M. A., Schulze, W. D., & D'Arge, R. C. (1982). Valuing public goods: A comparison of survey and hedonic approaches. *The American Economic Review*, 72(1), 165–177.

Burkhard, B., & Maes, J. (Eds.). (2017). *Mapping Ecosystem Services*. Pensoft Publishers. https://doi.org/10.3897/ab.e12837

Butcher Partners Limited [BPL]. (2006). *The Economic benefits of water in Te Papanui Conservation Park* (pp. 13–13). The New Zealand Department of Conservation.

Cai, Z., Jönsson, P., Jin, H., & Eklundh, L. (2017). Performance of Smoothing Methods for Reconstructing NDVI Time-Series and Estimating Vegetation Phenology from MODIS Data. *Remote Sensing*, 9(12), 1271. https://doi.org/10.3390/rs9121271

Cao, J., Yeh, E. T., Holden, N. M., Qin, Y., & Ren, Z. (2013). The roles of overgrazing, climate change and policy as drivers of degradation of China's grasslands. *Nomadic Peoples*, 17(2), 82–101. https://doi.org/10.3167/np.2013.170207

Carlier, L., Rotar, L., Vlahova, M., & Vidican, R. (2009). Importance and Functions of Grasslands. *Notulae Botanicae Horti Agrobotanici Cluj-Napoca*, 37(1), 25–30.

Castro, A. J., Verburg, P. H., Martín-López, B., Garcia-Llorente, M., Cabello, J., Vaughn, C. C., & López, E. (2014). Ecosystem service trade-offs from supply to social demand: A landscape-scale spatial analysis. *Landscape and Urban Planning*, 132, 102–110. https://doi.org/10.1016/j.landurbplan.2014.08.009

Ceotto, E. (2008). Grasslands for bioenergy production. A review. *Agronomy for Sustainable Development*, 28(1), 47–55. https://doi.org/10.1051/agro:2007034

Cerdan, O., Govers, G., Le Bissonnais, Y., Van Oost, K., Poesen, J., Saby, N., Gobin, A., Vacca, A., Quinton, J., Auerswald, K., Klik, A., Kwaad, F. J. P. M., Raclot, D., Ionita, I., Rejman, J., Rousseva, S., Muxart, T., Roxo, M. J., & Dostal, T. (2010). Rates and spatial variations of soil erosion in Europe: A study based on erosion plot data. *Geomorphology*, 122(1–2), 167–177. https://doi.org/10.1016/j.geomorph.2010.06.011

Chaudhary, S., McGregor, A., Houston, D., & Chettri, N. (2015). The evolution of ecosystem services: A time series and discourse-centered analysis. *Environmental Science & Pol*icy, 54, 25–34. https://doi.org/10.1016/j.envsci.2015.04.025

Cleland, E. E., Chuine, I., Menzel, A., Mooney, H. A., & Schwartz, M. D. (2007). Shifting plant phenology in response to global change. *Trends in Ecology & Evolution*, 22(7), 357–365. https://doi.org/10.1016/j.tree.2007.04.003

Comer, P. J., Hak, J. C., Kindscher, K., Muldavin, E., & Singhurst, J. (2018). Continent-Scale Landscape Conservation Design for Temperate Grasslands of the Great Plains and Chihuahuan Desert. *Natural Areas Journal*, 38(2), 196–211. https://doi.org/10.3375/043.038.0209

Costanza, R., d'Arge, R., de Groot, R., Farber, S., Grasso, M., Hannon, B., Limburg, K., Naeem, S., O'Neill, R. V., Paruelo, J., Raskin, R. G., Sutton, P., & van den Belt, M. (1997). The value of the world's ecosystem services and natural capital. *Nature*, 387(6630), 253–260. https://doi.org/10.1038/387253a0

Costanza, R., de Groot, R., Braat, L., Kubiszewski, I., Fioramonti, L., Sutton, P., Farber, S., & Grasso, M. (2017). Twenty years of ecosystem services: How far have we come and how far do we still need to go? *Ecosystem Services*, 28, 1–16. https://doi.org/10.1016/j.ecoser.2017.09.008

Costanza, R., de Groot, R., Sutton, P., van der Ploeg, S., Anderson, S. J., Kubiszewski, I., Farber, S., & Turner, R. K. (2014). Changes in the global value of ecosystem services. *Global Environmental Change*, 26, 152–158. https://doi.org/10.1016/j.gloenvcha.2014.04.002

Crossman, N. D., Burkhard, B., Nedkov, S., Willemen, L., Petz, K., Palomo, I., Drakou, E. G., Martín-Lopez, B., McPhearson, T., Boyanova, K., Alkemade, R., Egoh, B., Dunbar, M. B., & Maes, J. (2013). A blueprint for mapping and modelling ecosystem services. *Ecosystem Services*, 4, 4–14. https://doi.org/10.1016/j.ecoser.2013.02.001

Cui, T., Martz, L., & Guo, X. (2017). Grassland phenology response to drought in the Canadian prairies. *Remote Sensing*, 9(12), 1258. https://doi.org/10.3390/rs9121258

Cui, Y. P., Liu, J. Y., Hu, Y. F., Kuang, W. H., & Xie, Z. L. (2012). An analysis of temporal evolution of NDVI in various vegetation-climate regions in inner Mongolia, China. Procedia *Environmental Sciences*, 13, 1989–1996.

Cullinane, K. L. & Cornachione, E. T. C. (2018). *2017 National Park visitor spending effects: Economic contributions to local communities, states, and the nation*. Natural Resource Report NPS/NRSS/EQD/NRR—2018/1616. The National Park Service, Fort Collins, Colorado.

Daily, G. C. (1997). *Nature's services: Societal dependence on natural ecosystems* (2nd ed., p. 412). Island Press.

De Araujo Barbosa, C. C., Atkinson, P. M., & Dearing, J. A. (2015). Remote sensing of ecosystem services: A systematic review. *Ecological Indicators*, 52(52), 430–443. https://doi.org/10.1016/j.ecolind.2015.01.007

De Beurs, K. M., & Henebry, G. M. (2005). A statistical framework for the analysis of long image time series. *International Journal of Remote Sensing*, 26(8), 1551–1573. https://doi.org/10.1080/01431160512331326657

De Beurs, K. M., & Henebry, G. M. (2010). Spatio-temporal statistical methods for modelling land surface phenology. In I. L. Hudson & M. R. Keatley (Eds.), Phenological Research (pp. 177–208). Springer Netherlands. https://doi.org/10.1007/978-90-481-3335-2_9

De Groot, R., Braat, L., & Costanza, R. (2017). *A short history of the ecosystem services concept*. In B. Burkhard & J. Maes (Eds.), Mapping Ecosystem Services (p. 375). Pensoft Publishers.

De Groot, R., Brander, L., van der Ploeg, S., Costanza, R., Bernard, F., Braat, L., Christie, M., Crossman, N., Ghermandi, A., Hein, L., Hussain, S., Kumar, P., McVittie, A., Portela, R., Rodriguez, L. C., ten Brink, P., & van Beukering, P. (2012). Global estimates of the value of ecosystems and their services in monetary units. *Ecosystem Services*, 1(1), 50–61. https://doi.org/10.1016/j.ecoser.2012.07.005

De Groot, R. S. (1987). Environmental functions as a unifying concept for ecology and economics. *The Environmentalist*, 7(2), 105–109. https://doi.org/10.1007/BF02240292

De Vliegher, A., & Van Gils, B. (2010). Roles and utility of grasslands in Europe. D1.1. Multisward, Collaborative Project Seventh Framework Programme.

Debinski, D. M., & Holt, R. D. (2000). A survey and overview of habitat fragmentation experiments. *Conservation Biology*, 14(2), 342–355. https://doi.org/10.1046/j.1523-1739.2000.98081.x

Díaz, S., Pascual, U., Stenseke, M., Martín-López, B., Watson, R. T., Molnár, Z., Hill, R., Chan, K. M. A., Baste, I. A., Brauman, K. A., Polasky, S., Church, A., Lonsdale, M., Larigauderie, A., Leadley, P. W., van Oudenhoven, A. P. E., van der Plaat, F., Schröter, M., Lavorel, S., … Shirayama, Y. (2018). Assessing nature's contributions to people. *Science*, 359(6373), 270–272. https://doi.org/10.1126/science.aap8826

Dixon, A. P., Faber-Langendoen, D., Josse, C., Morrison, J., & Loucks, C. J. (2014). Distribution mapping of world grassland types. *Journal of Biogeography*, 41(11), 2003–2019. https://doi.org/10.1111/jbi.12381

Dodds, W. K., Wilson, K. C., Rehmeier, R. L., Knight, G. L., Wiggam, S., Falke, J. A., Dalgleish, H. J., & Bertrand, K. N. (2008). Comparing ecosystem goods and services provided by restored and native lands. *Bioscience*, 58(9), 837–845. https://doi.org/10.1641/B580909

Drummond, M. A., & Auch, R. F. (2015). *Land-cover trends in the Great Plains of the United States—1973 to 2000*. In J. L. Taylor, W. Acevedo, R. F. Auch, & M. A. Drummond (Eds.), Status and trends of land change in the Great Plains of the United States—1973 to 2000 (pp. 3–19). U.S. Geological Survey.

Du, B., Zhen, L., Hu, Y., Yan, H., De Groot, R., & Leemans, R. (2018). Comparison of ecosystem services provided by grasslands with different utilization patterns in China's Inner Mongolia Autonomous Region. *Journal of Geographical Sciences*, 28(10), 1399–1414. https://doi.org/10.1007/s11442-018-1552-3

Dubeux, J. C. B., Sollenberger, L. E., Mathews, B. W., Scholberg, J. M., & Santos, H. Q. (2007). Nutrient Cycling in Warm-Climate Grasslands. *Crop Science*, 47(3), 915–928. https://doi.org/10.2135/cropsci2006.09.0581

Dunford, R. W., Harrison, P. A., & Bagstad, K. J. (2017). Computer modelling for ecosystem service assessment-4.4. In B. Burkhard, & J. Maes, J (Eds). *Mapping Ecosystem Services*. Advanced Books. https://doi.org/10.3897/ab.e12837

Ehrlich, P., & Ehrlich, A. (1981). *Extinction: the causes and consequences of the disappearance of species.* Random House, New York.

Eklundh, L., & Jonsson, P. (2010). *Timesat 3.0 Software Manual*. Timesat 3.0 Software Manual.

Eldridge, D. J., Bowker, M. A., Maestre, F. T., Roger, E., Reynolds, J. F., & Whitford, W. G. (2011). Impacts of shrub encroachment on ecosystem structure and functioning: towards a global synthesis. *Ecology Letters*, 14(7), 709–722. https://doi.org/10.1111/j.1461-0248.2011.01630.x

Faber-Langendoen, D., & Josse, C. (2010). *World grasslands and biodiversity patterns*. NatureServe.

Fang, X., Zhu, Q., Ren, L., Chen, H., Wang, K., & Peng, C. (2018). Large-scale detection of vegetation dynamics and their potential drivers using MODIS images and BFAST: A case study

in Quebec, Canada. *Remote Sensing of Environment*, 206, 391–402. https://doi.org/10.1016/j.rse.2017.11.017

Farley, K. A., Bremer, L. L., Harden, C. P., & Hartsig, J. (2013). Changes in carbon storage under alternative land uses in biodiverse Andean grasslands: implications for payment for ecosystem services. *Conservation Letters*, 6(1), 21–27. https://doi.org/10.1111/j.1755-263X.2012.00267.x

Finch, D. M., & Dahms, C. W. (2004). Purpose and Need for a Grassland Assessment. In D. M. Finch (Ed.), Assessment of grassland ecosystem conditions in the southwestern United States: Vol. GTR-135 (pp. 1–11). U.S. Dept. of Agriculture, Forest Service, Rocky Mountain Research Station.

Fisher, B., Turner, R. K., & Morling, P. (2009). Defining and classifying ecosystem services for decision making. Ecological Economics: The Journal of the International Society for Ecological Economics, 68(3), 643–653. https://doi.org/10.1016/j.ecolecon.2008.09.014

Forkel, M., Carvalhais, N., Verbesselt, J., Mahecha, M., Neigh, C., & Reichstein, M. (2013). Trend Change Detection in NDVI Time Series: Effects of Inter-Annual Variability and Methodology. Remote Sensing, 5(5), 2113–2144. https://doi.org/10.3390/rs5052113

Gauthier, D. A., Lafon, A., Toombs, T., & Wiken, E. (2003). Grasslands: Towards a North American conservation strategy (p. 127). Commission for Environmental Cooperation University of Regina. Canadian Plains Research Center.

Gibson, D. J. (2009). Grasses and grassland ecology (1st ed., p. 320). Oxford University Press.

Gómez-Baggethun, E., Barton, D. N., Berry, P., Dunford, R., & Harrison, P. A. (2016). Concepts and methods in ecosystem services valuation. In M. Potschin, R. Haines-Young, R. Fish, & R. K. Turner (Eds.), Routledge handbook of ecosystem services (pp. 99–111). Routledge. https://doi.org/10.4324/9781315775302-9

Gomez-Casanovas, N., DeLucia, N. J., Bernacchi, C. J., Boughton, E. H., Sparks, J. P., Chamberlain, S. D., & DeLucia, E. H. (2018). Grazing alters net ecosystem C fluxes and the global warming potential of a subtropical pasture. Ecological Applications, 28(2), 557–572. https://doi.org/10.1002/eap.1670

Gray, K. L. (2007). Comparison of Trend Detection Methods [Doctoral Dissertation]. https://scholarworks.umt.edu/etd/228

Grekousis, G., Mountrakis, G., & Kavouras, M. (2015). An overview of 21 global and 43 regional land-cover mapping products. International Journal of Remote Sensing, 36(21), 5309–5335. https://doi.org/10.1080/01431161.2015.1093195

Haines-Young, R., & Potschin-Young, M. (2018). Revision of the common international classification for ecosystem services (CICES V5.1): A policy brief. *One Ecosystem*, 3, e27108. https://doi.org/10.3897/oneeco.3.e27108

Havstad, K. M., Peters, D. P. C., Skaggs, R., Brown, J., Bestelmeyer, B., Fredrickson, E., Herrick, J., & Wright, J. (2007). Ecological services to and from rangelands of the United States. Ecological Economics, 64(2), 261–268. https://doi.org/10.1016/j.ecolecon.2007.08.005

Helsel, D., & Hirsch, R. (2002). Statistical Methods in Water Resources Techniques of Water Resources Investigations, Book 4, chapter A3 (first (eBook), p. 522). United States Geological Survey.

Hendrickson, J. R., Sedivec, K. K., Toledo, D., & Printz, J. (2019). Challenges facing grasslands in the Northern Great Plains and North Central Region. *Rangelands*, 41(1), 23–29. https://doi.org/10.1016/j.rala.2018.11.002

Henwood, W. D. (2010). Toward a strategy for the conservation and protection of the world's temperate grasslands. *Great Plains Research*, 20(1), 121–134.

Heumann, B. W., Seaquist, J. W., Eklundh, L., & Jönsson, P. (2007). AVHRR derived phenological change in the Sahel and Soudan, Africa, 1982-2005. *Remote Sensing of Environment*, 108(4), 385–392. https://doi.org/10.1016/j.rse.2006.11.025

Hilker, T., Natsagdorj, E., Waring, R. H., Lyapustin, A., & Wang, Y. (2014). Satellite observed widespread decline in Mongolian grasslands largely due to overgrazing. Global Change Biology, 20(2), 418–428. https://doi.org/10.1111/gcb.12365

Hönigová, I., Vačkář, D., Lorencová, E., Melichar, J., Götzl, M., Sonderegger, G., Ouškova, V., Hošek, M., & Chobot, K. (2012). Survey on grassland ecosystem services. Report to the EEA – European Topic Centre on Biological Diversity. (p. 78). Nature Conservation Agency of the Czech Republic, Kaplanova 1, 148 00 Prague 11, Czech Republic.

Huete, A. (1997). A comparison of vegetation indices over a global set of TM images for EOS-MODIS. Remote Sensing of Environment, 59(3), 440–451. https://doi.org/10.1016/S0034-4257(96)00112-5

Huete, A. R. (1988). A soil-adjusted vegetation index (SAVI). Remote Sensing of Environment, 25(3), 295–309. https://doi.org/10.1016/0034-4257(88)90106-X

Inoue, M. (2017). Change of Landscape and Ecosystem Services of Semi-natural Grassland in Mt. Sanbe, Shimane Prefecture, Japan. In S. K. Hong & N. Nakagoshi (Eds.), Landscape ecology for sustainable society (pp. 111–122). Springer International Publishing. https://doi.org/10.1007/978-3-319-74328-8_7

Isbell, F. I., & Wilsey, B. J. (2009). Exotic Species and Overgrazing Can Drive Declines in Grassland Biodiversity and Productivity. Iowa State Research Farm Progress Reports. 633.

Jamali, S., Seaquist, J., Eklundh, L., & Ardö, J. (2012). Comparing parametric and non-parametric approaches for estimating trends in multi-year NDVI. First EARSeL Workshop on Temporal Analysis of Satellite Images, Mykonos, Greece.

Jeong, S. J., Ho, C. H., Gim, H. J., & Brown, M. E. (2011). Phenology shifts at start vs. end of growing season in temperate vegetation over the Northern Hemisphere for the period 1982-2008. *Global Change Biology*, Feb 17, Early View. https://doi.org/10.1111/j.1365-2486.2011.02397.x

Jong, R., Verbesselt, J., Schaepman, M. E., & Bruin, S. (2012). Trend changes in global greening and browning: contribution of short-term trends to longer-term change. *Global Change Biology*, 18(2), 642–655. https://doi.org/10.1111/j.1365-2486.2011.02578.x

Jonsson, P., & Eklundh, L. (2004). TIMESAT—a program for analyzing time-series of satellite sensor data. *Computers & Geosciences*, 30(8), 833–845. https://doi.org/10.1016/j.cageo.2004.05.006

Ju, J., & Masek, J. G. (2016). The vegetation greenness trend in Canada and US Alaska from 1984–2012 Landsat data. *Remote Sensing of Environment*, 176, 1–16. https://doi.org/10.1016/j.rse.2016.01.001

Kallis, G., Gómez-Baggethun, E., & Zografos, C. (2013). To value or not to value? That is not the question. *Ecological Economics*, 94, 97–105. https://doi.org/10.1016/j.ecolecon.2013.07.002

Karl, T. R., Melillo, J. M., & Peterson, T. C. (2009). *Global climate change impacts in the United States.* Cambridge University Press.

KDHE (Kansas Department of Health & Environment) (2010). *State of Kansas Flint Hills smoke management plan*. Flint Hills Smoke Management Advisory Committee.

Kennedy, R. E., Townsend, P. A., Gross, J. E., Cohen, W. B., Bolstad, P., Wang, Y. Q., & Adams, P. (2009). Remote sensing change detection tools for natural resource managers: Understanding

concepts and tradeoffs in the design of landscape monitoring projects. *Remote Sensing of Environment*, 113(7), 1382–1396. https://doi.org/10.1016/j.rse.2008.07.018

Kienast, F., & Helfenstein, J. (2016). *Modelling ecosystem services*. In M Potschin, R. Haines-Young, R. Fish, & R. K. Turner (Eds.), Routledge handbook of ecosystem services (pp. 144–156). Routledge.

Kragt, M. E., Bennett, J. W., & Jakeman, A. J. (2010). *An Integrated Assessment approach to linking biophysical modelling and economic valuation tools*. 1011-1022. Proceedings of the International Congress on Environmental Modelling and Software (iEMSs 2010). http://hdl.handle.net/1885/60961

Krause, B., Culmsee, H., Wesche, K., & Leuschner, C. (2015). Historical and recent fragmentation of temperate floodplain grasslands: Do patch size and distance affect the richness of characteristic wet meadow plant species? *Folia Geobotanica*, 50(3), 253–266. https://doi.org/10.1007/s12224-015-9220-1

La Notte, A., D'Amato, D., Mäkinen, H., Paracchini, M. L., Liquete, C., Egoh, B., Geneletti, D., & Crossman, N. D. (2017). Ecosystem services classification: A systems ecology perspective of the cascade framework. *Ecological Indicators*, 74, 392–402. https://doi.org/10.1016/j.ecolind.2016.11.030

Landers, D. H., & Nahlik, A. M. (2013). *Final Ecosystem Goods and Services Classification System (FEGS-CS)*. EPA/600/R-13/ORD-004914 (p. 108). U.S. Environmental Protection Agency, Office of Research and Development.

Lang, S. (2018). Urban green valuation integrating biophysical and qualitative aspects. European Journal of Remote Sensing, 51(1), 116–131. https://doi.org/10.1080/22797254.2017.1409083

Lark, T. J., Meghan Salmon, J., & Gibbs, H. K. (2015). Cropland expansion outpaces agricultural and biofuel policies in the United States. *Environmental Research Letters*, 10(4), 044003. https://doi.org/10.1088/1748-9326/10/4/044003

Lavorel, S., Grigulis, K., Lamarque, P., Colace, M. P., Garden, D., Girel, J., Pellet, G., & Douzet, R. (2011). Using plant functional traits to understand the landscape distribution of multiple ecosystem services. *The Journal of Ecology*, 99(1), 135–147. https://doi.org/10.1111/j.1365-2745.2010.01753.x

Li, T. H., Li, W. K., & Qian, Z. H. (2010). Variations in ecosystem service value in response to land use changes in Shenzhen. *Ecological Economics,* 69(7), 1427–1435. https://doi.org/10.1016/j.ecolecon.2008.05.018

Lindborg, R., J., Bengtsson, Å., Berg, S. A. O., Cousins, O. Eriksson, T., Gustafsson, K. P., Hasund, L. Lenoir, A. Pihlgren, E. Sjödin, & Stenseke, M. (2008). A landscape perspective on conservation of semi-natural grasslands. *Agriculture, Ecosystems and Environment* 125, 213-222. https://doi.org/10.1016/j.agee.2008.01.006

Liquete, C., Haas, E., Bondo, T., Hirzinger, C., Schnelle, M., Reisinger, D., Lyon, D., Finisdore, J., & Ledwith, M. (2016). *A practical approach to mapping of ecosystems and ecosystem services using remote sensing.* In Marion Potschin, R. Haines-Young, R. Fish, & R. K. Turner (Eds.), Routledge handbook of ecosystem services (pp. 205–212). Routledge. https://doi.org/10.4324/9781315775302-18

Machovina, B., & Feeley, K. J. (2017). Restoring low-input high-diversity grasslands as a potential global resource for biofuels. *The Science of the Total Environment*, 609, 205–214. https://doi.org/10.1016/j.scitotenv.2017.07.109

Manier, D. J., Carr, N. B., Reese, G. C., & Burris, L., (2019). *Using scenarios to evaluate vulnerability of grassland communities to climate change in the Southern Great Plains of the United States*: U.S. Geological Survey, Open-File Report 2019–1046, 48 p., https://doi.org/10.3133/ofr20191046.

Mark, A. F., & McLennan, B. (2005). The conservation status of New Zealand's indigenous grasslands. *New Zealand Journal of Botany*, 43(1), 245–270. https://doi.org/10.1080/0028825X.2005.9512953

Marsh, G. P. (1965). *Man and Nature* (D. Lowenthal, Ed.; Reprint of 1864 Edition, p. 472). Harvard University Press.

Martínez-Estévez, L., Balvanera, P., Pacheco, J., & Ceballos, G. (2013). Prairie dog decline reduces the supply of ecosystem services and leads to desertification of semiarid grasslands. *Plos One*, 8(10), e75229. https://doi.org/10.1371/journal.pone.0075229

Matsushita, B., Yang, W., Chen, J., Onda, Y., & Qiu, G. (2007). Sensitivity of the Enhanced Vegetation Index (EVI) and Normalized Difference Vegetation Index (NDVI) to Topographic Effects: A Case Study in High-density Cypress Forest. *Sensors (Basel, Switzerland),* 7(11), 2636–2651. https://doi.org/10.3390/s7112636

McDonough, K., Hutchinson, S., Moore, T., & Hutchinson, J. M. S. (2017). Analysis of publication trends in ecosystem services research. *Ecosystem Services*, 25, 82–88. https://doi.org/10.1016/j.ecoser.2017.03.022

McManus, K. M., Morton, D. C., Masek, J. G., Wang, D., Sexton, J. O., Nagol, J. R., Ropars, P., & Boudreau, S. (2012). Satellite-based evidence for shrub and graminoid tundra expansion in northern Quebec from 1986 to 2010. *Glob Change Biol*, 18(7), 2313–2323. https://doi.org/10.1111/j.1365-2486.2012.02708.x

MEA (Millennium Ecosystem Assessment). (2005). *Ecosystems and Human Well-being: Synthesis* (2nd ed., p. 160). Island Press.

Mohler, R. L., & Goodin, D. G. (2012). Mapping burned areas in the Flint Hills of Kansas and Oklahoma, 2000—2010. *Great Plains Research*, 22(1), 15–25.

Moulin, S., Kergoat, L., Viovy, N., & Dedieu, G. (1997). Global-scale assessment of vegetation phenology using NOAA/AVHRR satellite measurements. *Journal of Climate*, 10(6), 1154–1170. https://doi.org/10.1175/1520-0442(1997)010<1154:GSAOVP>2.0.CO;2

Mucina, L., Hoare, D. B., Lotter, M. C., Du Preez, P. J., Rutherford, M. C., & Scott-Shaw, C. R. (2006). *Grassland Biome*. In L. Mucina & M. C. Rutherford (Eds.), The vegetation of South Africa, Lesotho, and Swaziland (pp. 348–437). South African National Biodiversity Institute.

Nelson, E., Mendoza, G., Regetz, J., Polasky, S., Tallis, H., Cameron, D., Chan, K. M., Daily, G. C., Goldstein, J., Kareiva, P. M., Lonsdorf, E., Naidoo, R., Ricketts, T. H., & Shaw, M. (2009). Modeling multiple ecosystem services, biodiversity conservation, commodity production, and tradeoffs at landscape scales. *Frontiers in Ecology and the Environment*, 7(1), 4–11. https://doi.org/10.1890/080023

O'Mara, F. P. (2011). The significance of livestock as a contributor to global greenhouse gas emissions today and in the near future. *Animal Feed Science and Technology*, 166–167, 7–15. https://doi.org/10.1016/j.anifeedsci.2011.04.074

O'Mara, F. P. (2012). The role of grasslands in food security and climate change. *Annals of Botany*, 110(6), 1263–1270. https://doi.org/10.1093/aob/mcs209

Omernik, J. M. (1987). Ecoregions of the Conterminous United States. *Annals of the Association of American Geographers*, 77(1), 118–125. https://doi.org/10.1111/j.1467-8306.1987.tb00149.x

Pascual, U., Balvanera, P., Díaz, S., Pataki, G., Roth, E., Stenseke, M., Watson, R. T., Başak Dessane, E., Islar, M., Kelemen, E., Maris, V., Quaas, M., Subramanian, S. M., Wittmer, H.,

Adlan, A., Ahn, S., Al-Hafedh, Y. S., Amankwah, E., Asah, S. T., … Yagi, N. (2017). Valuing nature's contributions to people: the IPBES approach. *Current Opinion in Environmental Sustainability,* 26–27, 7–16. https://doi.org/10.1016/j.cosust.2016.12.006

Pascual, U., Muradian, R., Brander, L., Gómez-Baggethun, E., Martín-López, B., Verma, M., Armsworth, P., Christie, M., Cornelissen, H., Eppink, F., Farley, J., Loomis, J., Pearson, L., Perrings, C., Polasky, S., Mcneely, J. A., Norgaard, R., Siddiqui, R., David Simpson, R., … Simpson, R. D. (2010). *The economics of valuing ecosystem services and biodiversity*. In P. Kumar (Ed.), The Economics of Ecosystems and Biodiversity: The Ecological and Economic Foundations (pp. 1–117). Routledge.

Pasolli, L., Asam, S., Castelli, M., Bruzzone, L., Wohlfahrt, G., Zebisch, M., & Notarnicola, C. (2015). Retrieval of Leaf Area Index in mountain grasslands in the Alps from MODIS satellite imagery. *Remote Sensing of Environment*, 165, 159–174. https://doi.org/10.1016/j.rse.2015.04.027

Patel, P. (2017). Converting Pastures to Grasslands Could Yield Staggering Amounts of Energy. http://www.anthropocenemagazine.org/2017/08/switching-pastures-to-grasslands-for-biofuels-could-give-staggering-amounts-of-energy/

Pathak, K., Nath, A. J., Sileshi, G. W., Lal, R., & Das, A. K. (2017). Annual burning enhances biomass production and nutrient cycling in degraded Imperata grasslands. *Land Degradation & Development,* 28(5), 1763–1771. https://doi.org/10.1002/ldr.2707

Peeters, A. (2010). *Socio-economic and political driving forces of these evolutions: Importance and evolutions of grasslands and grassland-based farming systems in Europe* (p. 64). Multisward deliverable D5.1.

Peters, D. P. C., Bestelmeyer, B. T., Havstad, K. M., Rango, A., Archer, S. R., Comrie, A. C., Gimblett, H. R., López-Hoffman, L., Sala, O. E., Vivoni, E. R., Brooks, M. L., Brown, J., Monger, H. C., Goldstein, J. H., Okin, G. S., & Tweedie, C. E. (2013). *Desertification of Rangelands.* In Climate Vulnerability (pp. 239–258). Elsevier. https://doi.org/10.1016/B978-0-12-384703-4.00426-3

Petrie, M. D., Collins, S. L., Swann, A. M., Ford, P. L., & Litvak, M. E. (2015). Grassland to shrubland state transitions enhance carbon sequestration in the northern Chihuahuan Desert. *Global Change Biology*, 21(3), 1226–1235. https://doi.org/10.1111/gcb.12743

Plowprint report (2016). World Wildlife Fund. Retrieved from https://c402277.ssl.cf1.rackcdn.com/publications/946/files/original/plowprint_AnnualReport_2016_GenInfo_FINAL_112016.pdf?1479923301.

Plowprint report (2018). World Wildlife Fund. Retrieved from https://c402277.ssl.cf1.rackcdn.com/publications/1171/files/original/PlowprintReport_2018_FINAL_082318LowRes.pdf?1535470091.

Qin, C. (2011). *Assessing Phenological Changes and Drivers in East Africa from 1982 to 2006* [Doctoral Dissertation].

Ratajczak, Z., Briggs, J. M., Goodin, D. G., Luo, L., Mohler, R. L., Nippert, J. B., & Obermeyer, B. (2016). Assessing the Potential for Transitions from Tallgrass Prairie to Woodlands: Are We Operating Beyond Critical Fire Thresholds? *Rangeland Ecology & Management*, 69(4), 280–287. https://doi.org/10.1016/j.rama.2016.03.004

Ratajczak, Z., Nippert, J. B., Briggs, J. M., & Blair, J. M. (2014). Fire dynamics distinguish grasslands, shrublands and woodlands as alternative attractors in the Central Great Plains of North America. *The Journal of Ecology*, 102(6), 1374–1385. https://doi.org/10.1111/1365-2745.12311

Reed, B. C., Brown, J. F., VanderZee, D., Loveland, T. R., Merchant, J. W., & Ohlen, D. O. (1994). Measuring phenological variability from satellite imagery. *Journal of Vegetation Science*, *5*, 703–714.

Reed, B. C., White, M., & Brown, J. F. (2003). *Remote Sensing Phenology*. In M. D. Schwartz (Ed.), Phenology: an integrative environmental science (Vol. 39, pp. 365–381). Springer Netherlands. https://doi.org/10.1007/978-94-007-0632-3_23

Robin-Abbott, M. J., & Pardo, L. H. (2011). *Ecosystem Classification*. In L. H. Pardo, M. J. Robin-Abbott, & C. T. Driscoll (Eds.), Assessment of nitrogen deposition effects and empirical critical loads of nitrogen for ecoregions of the United States (pp. 9–15). U.S. Dept. of Agriculture, Forest Service, Northern Research Station.

Roch, L., & Jaeger, J. A. G. (2014). Monitoring an ecosystem at risk: what is the degree of grassland fragmentation in the Canadian Prairies? *Environmental Monitoring and Assessment*, 186(4), 2505–2534. https://doi.org/10.1007/s10661-013-3557-9

Rumpel, C. (2011). Carbon storage and organic matter. In G. Lemaire, J. Hodgson, & A. Chabbi (Eds.), Grassland Productivity and Ecosystem Services (pp. 65–72). CABI Publishing.

Ruskule, A., Vinogradovs, I., & Pecina, M. V. (2018). *The guidebook on ecosystem service framework in integrated planning* (R. Kasparinskis, Ed.; V28 ed.). The University of Latvia, Estonian University of Life Sciences, and Baltic Environmental Forum.

Russelle, M. P., Morey, R. V., Baker, J. M., Porter, P. M., & Jung, H.-J. G. (2007). Comment on "Carbon-negative biofuels from low-input high-diversity grassland biomass". Science, 316(5831), 1567; author reply 1567. https://doi.org/10.1126/science.1139388

Sala, O. E., & Paruelo, J. M. (1997). *Ecosystem Services in Grasslands*. In G C Daily (Ed.), Nature's Services: Societal Dependence on Natural Ecosystems (pp. 237–252). Island Press.

Sala, O. E., Yahdjian, L., Havstad, K., & Aguiar, M. R. (2017). *Rangeland ecosystem services: nature's supply and humans' demand.* In D. D. Briske (Ed.), Rangeland Systems (pp. 467–489). Springer International Publishing. https://doi.org/10.1007/978-3-319-46709-2_14

Santos-Martin, F., Kelemen, E., Garcia-Llorente, M., Jacobs, S., Oteros-Rozas, E., Barton, D., Palomo, I., Hevia, V., & Martín-López, B. (2017). *Socio-cultural valuation approaches*. In B Burkhard & J. Maes (Eds.), Mapping Ecosystem Services (pp. 104–113). Pensoft Publishers.

Scholtz, R., Polo, J. A., Fuhlendorf, S. D., Engle, D. M., & Weir, J. R. (2018). Woody plant encroachment mitigated differentially by fire and herbicide. *Rangeland Ecology & Management*, 71(2), 239–244. https://doi.org/10.1016/j.rama.2017.10.001

Schwartz, M. D. (1994). Monitoring global change with phenology: The case of the spring green wave. *International Journal of Biometeorology*, 38(1), 18–22. https://doi.org/10.1007/BF01241799

Seppelt, R., Dormann, C. F., Eppink, F. V., Lautenbach, S., & Schmidt, S. (2011). A quantitative review of ecosystem service studies: approaches, shortcomings and the road ahead. *Journal of Applied Ecology*, 48(3), 630–636. https://doi.org/10.1111/j.1365-2664.2010.01952.x

Shafer, M., Ojima, D., Antle, J. M., Kluck, D., McPherson, R. A., Petersen, S., Scanlon, B., & Sherman, K. (2014). *Ch. 19: Great Plains*. Climate change impacts in the United States: the third national climate assessment. U.S. Global Change Research Program. https://doi.org/10.7930/J0D798BC

Singh, J. S., Lauenroth, W. K., & Milchunas, D. G. (1983). Geography of grassland ecosystems. Progress in Physical Geography: Earth and Environment, 7(1), 46–80. https://doi.org/10.1177/030913338300700102

Small, N., Munday, M., & Durance, I. (2017). The challenge of valuing ecosystem services that have no material benefits. *Global Environmental Change*, 44, 57–67. https://doi.org/10.1016/j.gloenvcha.2017.03.005

Sollenberger, L. E., Kohmann, M. M., Dubeux, J. C. B., & Silveira, M. L. (2019). Grassland management affects delivery of regulating and supporting ecosystem services. *Crop Science*, 59(2), 441-459. https://doi.org/10.2135/cropsci2018.09.0594

Squires, V. R., & Feng, H. (2018). *Brief history of grassland utilization and its significance to humans.* In V. R. Squires, J. Dengler, H. Feng, & L. Hua (Eds.), Grasslands of the world : diversity, management and conservation (pp. 3–15). CRC Press.

Suepa, T., Qi, J., Lawawirojwong, S., & Messina, J. P. (2016). Understanding spatio-temporal variation of vegetation phenology and rainfall seasonality in the monsoon Southeast Asia. *Environmental Research*, 147, 621–629. https://doi.org/10.1016/j.envres.2016.02.005

Suttie, J. M., Reynolds, S. G., Batello, C., & Food and Agriculture Organization of the United Nations (2005). Grasslands of the world (Series No. 34 ed.). Rome, Italy: p.536.

Tan, B., Morisette, J. T., Wolfe, R. E., Gao, F., Ederer, G. A., Nightingale, J., & Pedelty, J. A. (2011). An Enhanced TIMESAT Algorithm for Estimating Vegetation Phenology Metrics from MODIS Data. *IEEE Journal of Selected Topics in Applied Earth Observations and Remote Sensing*, 4(2), 361–371. https://doi.org/10.1109/JSTARS.2010.2075916

TEEB. (2010). *The Economics of Ecosystems and Biodiversity: Mainstreaming the Economics of Nature: A synthesis of the approach, conclusions and recommendations of TEEB*. Progress Press.

Tilman, D., Hill, J., & Lehman, C. (2007). Response to Comment on "Carbon-Negative Biofuels from Low-Input High-Diversity Grassland Biomass." *Science*, 316(5831), 1567–1567. https://doi.org/10.1126/science.1140365

Tinker, D., & Hild, A. (2005). Short-grass and Mixed-grass Ecosystems in the Southern Plains, U.S.A.: Conceptual Ecosystem Models (pp. 1–18). The Great Plains Cooperative Ecosystem Studies Unit, the National Park Service and Southern Plains Inventory and Monitoring Program.

Tollerud, H., Brown, J., Loveland, T., Mahmood, R., & Bliss, N. (2018). Drought and Land-Cover Conditions in the Great Plains. *Earth Interactions*, 22(17), 1–25. https://doi.org/10.1175/ EI-D-17-0025.1

Towne, E., & Kemp, K. (2003). Vegetation dynamics from annually burning tallgrass prairie in different seasons. *Jurnal Rekayasa Mesin*, 56(2). https://doi.org/10.2458/azu_jrm_v56i2_towne

Turner, K. G., Anderson, S., Gonzales-Chang, M., Costanza, R., Courville, S., Dalgaard, T., Dominati, E., Kubiszewski, I., Ogilvy, S., Porfirio, L., Ratna, N., Sandhu, H., Sutton, P. C., Svenning, J.-C., Turner, G. M., Varennes, Y.-D., Voinov, A., & Wratten, S. (2016). A review of methods, data, and models to assess changes in the value of ecosystem services from land degradation and restoration. *Ecological Modelling*, 319, 190–207. https://doi.org/10.1016/j.ecolmodel.2015.07.017

Turpie, J. K. (2003). The existence value of biodiversity in South Africa: how interest, experience, knowledge, income and perceived level of threat influence local willingness to pay. *Ecological Economics,* 46(2), 199–216. https://doi.org/10.1016/S0921-8009(03)00122-8

UNESCO (United Nations Educational and Cultural Organization). (1973). International Classification and Mapping of Vegetation. United Nations Educational, Scientific, and Cultural Organization.

United Nations. (2019). World Population Prospects 2019 highlights. https://www.un.org/development/desa/en/news/population/world-population-prospects-2019.html

United States Environmental Protection Agency, (USEPA). (2015). National Ecosystem Services Classification System (NESCS): Framework Design and Policy Application. EPA-800-R-15-002. The United States Environmental Protection Agency.

U.S. Global Change Research Program. (2009). Global climate change impacts in the United States (1st ed., p. 192). Cambridge University Press.

USDA (United States Department ofAgriculture). (2019). Ag and Food Sectors and the Economy. https://www.ers.usda.gov/data-products/ag-and-food-statistics-charting-the-essentials/ag-and-food-sectors-and-the-economy/

Van Berkel, D. B., & Verburg, P. H. (2014). Spatial quantification and valuation of cultural ecosystem services in an agricultural landscape. *Ecological Indicators*, 37, 163–174. https://doi.org/10.1016/j.ecolind.2012.06.025

Van der Ploeg, S., De Groot, R. S., & Wang, Y. (2010). The TEEB Valuation Database: overview of structure, data and resultss. Foundation for Sustainable Development, Wageningen, the Netherlands. . Foundation for Sustainable Development.

Verbesselt, J., Hyndman, R., Newnham, G., & Culvenor, D. (2010). Detecting trend and seasonal changes in satellite image time series. *Remote Sensing of Environment*, 114(1), 106–115. https://doi.org/10.1016/j.rse.2009.08.014

Vihervaara, P., Mononen, L., Santos, F., Adamescu, M., Cazacu, C., Luque, S., Geneletti, D., & Maes, J. (2017). *Biophysical quantification*. In B Burkhard & J. Maes (Eds.), Mapping Ecosystem Services (pp. 95–104). Pensoft Publishers.

Wang, S., Lu, X., Cheng, X., Li, X., Peichl, M., & Mammarella, I. (2018). Limitations and Challenges of MODIS-Derived Phenological Metrics Across Different Landscapes in Pan-Arctic Regions. *Remote Sensing*, 10(11), 1784. https://doi.org/10.3390/rs10111784

Wang, S., Yang, B., Yang, Q., Lu, L., Wang, X., & Peng, Y. (2016). Temporal Trends and Spatial Variability of Vegetation Phenology over the Northern Hemisphere during 1982-2012. *Plos One*, 11(6), e0157134. https://doi.org/10.1371/journal.pone.0157134

Wang, Y., Zhang, J., Liu, D., Yang, W., & Zhang, W. (2018). Accuracy Assessment of GlobeLand30 2010 Land Cover over China Based on Geographically and Categorically Stratified Validation Sample Data. *Remote Sensing*, 10(8), 1213. https://doi.org/10.3390/ rs10081213

Wang, Z., Song, K., Zhang, B., Liu, D., Ren, C., Luo, L., Yang, T., Huang, N., Hu, L., Yang, H., & Liu, Z. (2009). Shrinkage and fragmentation of grasslands in the West Songnen Plain, China. *Agriculture, Ecosystems & Environment*, 129(1–3), 315–324. https://doi.org/10.1016/ j.agee.2008.10.009

Watkinson, A. R., & Ormerod, S. J. (2001). Grasslands, grazing and biodiversity: editors' introduction. *Journal of Applied Ecology*, 38(2), 233–237. https://doi.org/ 10.1046/j.1365-2664.2001.00621.x

Weber, K. T., & Horst, S. (2011). Desertification and livestock grazing: The roles of sedentarization, mobility and rest. *Pastoralism: Research, Policy and Practice*, 1(1), 19. https://doi.org/10.1186/2041-7136-1-19

Wesley, C. B., Grand, J., Wu, J., Michel, N., Grogan-Brown, J., & Trusty, B. (2019). North American Grasslands (pp. 14–15). National Audubon Society.

West, P. C., & Nelson, C. J. (2017). Managing Grassland Ecosystems. In R. F. Barnes, C. J. Nelson, M. Collins, & K. J. Moore (Eds.), Forages, Volume 1: An Introduction to Grassland Agriculture (7th ed., pp. 357–373). Wiley-Blackwell.

Westman, W. E. (1977). How much are nature's services worth? *Science*, 197(4307), 960–964. https://doi.org/10.1126/science.197.4307.960

White, F. (1983). *The vegetation of Africa: A descriptive memoir to accompany the UNESCO/AETFAT/UNSO vegetation map of Africa*. United Nations Educational. https://unesdoc.unesco.org/ark:/48223/pf0000058054

White, R., Murray, S., Rohweder, M., & Prince, S. D. (2000). *Pilot Analysis of Global Ecosystems: Grassland Ecosystems* (Illustrated, p. 94). World Resources Institute.

Whitham, C. E. L., Shi, K., & Riordan, P. (2015). Ecosystem service valuation assessments for protected area management: A case study comparing methods using different land cover classification and valuation approaches. *Plos One*, 10(6), e0129748. https://doi.org/10.1371/journal.pone.0129748

Wiken, E., Nava, F. J., & Glenn, G. E. (2011). North American Terrestrial Ecoregions—Level III (pp. 76–86). Commission for Environmental Cooperation.

Wischmeier, W. H., & Smith, D. D. (1978). *Predicting rainfall erosion losses* (Vol. 537). US Dep. of Agriculture.

Woodward, F. I., Lomas, M. R., & Kelly, C. K. (2004). Global climate and the distribution of plant biomes. Philosophical Transactions of the Royal Society of London. Series B, Biological Sciences, 359(1450), 1465–1476. https://doi.org/10.1098/rstb.2004.1525

World Tourism Organization. (2017). World Tourism Organization. "Why Tourism." http://www.tourism4development2017.org/why-tourism/

Xu, D., & Guo, X. (2015). Some insights on grassland health assessment based on remote sensing. *Sensors (Basel, Switzerland),* 15(2), 3070–3089. https://doi.org/10.3390/s150203070

Xue, J., & Su, B. (2017). Significant remote sensing vegetation indices: A review of developments and applications. *Journal of Sensors*, 2017, 1–17. https://doi.org/10.1155/2017/1353691

Yu, G., Lu, C., Xie, G., Luo, J., & Yang, L. (2005). Grassland ecosystem services and their economic evaluation in Qinghai-Tibetan plateau based on RS and GIS. Proceedings. 2005 IEEE International Geoscience and Remote Sensing Symposium, 2005. IGARSS '05., 2961–2964. https://doi.org/10.1109/IGARSS.2005.1525690

Yue, S., Pilon, P., & Cavadias, G. (2002). Power of the Mann–Kendall and Spearman's rho tests for detecting monotonic trends in hydrological series. *Journal of Hydrology*, 259(1), 254–271.

Zhang, X., Friedl, M. A., Schaaf, C. B., Strahler, A. H., Hodges, J. C. F., Gao, F., Reed, B. C., & Huete, A. (2003). Monitoring vegetation phenology using MODIS. *Remote Sensing of Environment*, 84(3), 471–475. https://doi.org/10.1016/S0034-4257(02)00135-9

Zhang, X., Tarpley, D., & Sullivan, J. T. (2007). Diverse responses of vegetation phenology to a warming climate. *Geophysical Research Letters*, 34(19). https://doi.org/10.1029/2007GL031447

Zhang, Y., Huang, D., Badgery, W. B., Kemp, D. R., Chen, W., Wang, X., & Liu, N. (2015). Reduced grazing pressure delivers production and environmental benefits for the typical steppe of North China. *Scientific Reports*, 5, 16434. https://doi.org/10.1038/srep16434

Zhen, L., Ochirbat, B., Lv, Y., Wei, Y. J., Liu, X. L., Chen, J. Q., Yao, Z. J., & Li, F. (2010). Comparing patterns of ecosystem service consumption and perceptions of range management between ethnic herders in Inner Mongolia and Mongolia. *Environmental Research Letters*, 5(1), 015001. https://doi.org/10.1088/1748-9326/5/1/015001

Chapter 3 - Detection of long-term grassland vegetation trends for the Great Plains ecoregion using temporal decomposition and satellite-derived vegetation indices.

Abstract

Grasslands cover approximately half of the terrestrial earth surface and provide a plethora of environmental benefits and ecosystem services. They have become one of the most changed biomes in the world, and therefore, proper monitoring and management of grasslands cannot be overemphasized. Remotely sensed, vegetation indices timeseries dataset is an effective tool to investigate large-scale vegetation change dynamics. A time-series analysis of Moderate Resolution Imaging Spectrometer (MODIS) 16-day maximum value composite Normalized Difference Vegetation Index (NDVI) and Enhanced Vegetation Index (EVI) data (MOD13Q1 Collection 5) was performed to assess long-term trends in vegetation greenness across the Great Plains ecoregion of the United States. The Breaks for Additive Season and Trend (BFAST) decomposition method was applied to a time series of images from 2001 to 2017 to derive spatially-explicit estimates of gradual interannual change. Results show more 'greening' trends than 'browning' and 'no change' trends in the study area during the study period. Comparing the trend results from both vegetation indices implies that the EVI is more suitable for this analysis in the study area, especially in areas with high biomass. The findings of this study suggest the need for additional analyses to quantify the influence of climate and soils, along with critical regional anthropogenic factors such as fire, on shaping long-term vegetation dynamics and estimate the impact on the values or services we acquire from grasslands in the ecoregion.

KEYWORDS: Grasslands, Trends, NDVI, EVI, Great Plains Ecoregion, and BFAST.

3.1 Introduction:

3.1.1 Background and purpose

Grasslands are one of the most biodiverse and productive terrestrial biomes that provide many benefits or ecosystem services (ES) (Millennium Ecosystem Assessment [MEA], 2005; TEEB, 2010). Despite grasslands providing for a number of ES, including supporting services (e.g., nutrient cycling and soil formation), regulating service (carbon sequestration, erosion control, and water storage), provisioning services (e.g., food, freshwater, wood, and fiber), and cultural services (e.g., recreation and aesthetics), they receive very low levels of protection (Mark & McLennan, 2005; Pendall et al., 2018). In the last decade, more than 8,100 square kilometers of grasslands were converted to croplands in the entire Great Plains (Plowprint report, 2021). In 2019 alone, approximately 10,500 square kilometers of grasslands in the Great Plains were lost to crop cultivation (Plowprint report, 2021). The temperate grasslands in the United States are among the most threatened grassland ecosystems, with almost 62% of the historical extent lost (Comer et al., 2018; Oakleaf et al., 2015). Many factors have, and continue, to contribute to this, including fire frequency, invasion of non-native species (usually woody species), fragmentation, and conversion to other land use (Gibson, 2009; Jacquin et al., 2016; Ratajczak et al., 2016).

Long-term studies on a major terrestrial biome like grasslands are critical to achieving an integrated understanding of ecosystems' response to climate change. Understanding the impact of climate change and ecosystems is necessary because these changes impact the provision of various essential ecosystem services provided by grasslands. Therefore, long-term analysis of grassland is needed for monitoring and evaluating long-term changes in biomes like grasslands is also key environmental policy and decision making and evaluating the impact of some implemented policies on the environment.

Some existing studies have highlighted the changing spatial extent of grasslands in the Great Plains (Comer et al., 2018), the phenological trends in the northern hemisphere (Jeong et al., 2011), and greening/browning trends globally (De Jong et al., 2012). Comer et al. (2018) analyzed long-term spatial trends in grassland types across the Great Plains, including identifying species of concern, protected areas, intactness, and connectivity among grassland areas and identifying Grassland Potential Conservation Areas (GPCAs). Results of the long-term spatial trends showed that the

tallgrass prairies had the most severe declines in extent, followed by mixed-grass, shortgrass, and semi-desert grasslands. Results from the time-series analyses of long-term phenological trends in the northern hemisphere by Jeong et al. (2011) showed a general earlier start of the growing season and later end of the growing season, which resulted in an increased growing season length. Also, Jong et al. (2012) carried out an analysis on global vegetation greening and browning trends between 1982 and 2008. Although a net greening was detected across all biomes, the trend for grasslands and shrublands showed abrupt greening followed by gradual browning. The southern hemisphere showed the most browning, and the temporal analysis indicates more browning than greening in the time studied.

Despite these past studies, relatively little is known about the long-term conditions of grasslands in the interior of the United States. The objective of this study is to assess long-term trends and spatial patterns in grasslands within the U.S. Great Plains based on vegetation greenness as measured by the Normalized Difference Vegetation Index (NDVI) and Enhanced Vegetation Index (EVI) over the period 2001 to 2017.

Time-series analyses of remotely-sensed imagery have been used to monitor vegetation conditions to inform management practices (Hutchinson et al., 2015; Jeong et al., 2011). The most commonly used vegetation index for this purpose is NDVI which serves as a proxy for important biophysical measures such as aboveground biomass and leaf area index (Wang et al., 2018). NDVI has shown to have reliable correlations with several vegetation properties at varying spatial scales, with the ratio-based value reducing many sources of noise. However, a key limitation of NDVI is saturation over areas with high biomass (Huete, 1988; Wang et al., 2018). An alternative vegetation index, EVI, was developed to improve sensitivity over areas of high biomass and to further reduce atmospheric influences. The EVI uses additional wavelength bands and a soil adjustment factor to adjust NDVI for atmospheric and soil noises as well as mitigating the saturation in dense vegetation areas. However, the soil adjustment factor used in calculating the EVI makes it more sensitive to the variation in the radiance that accompanies a change in the topography of a surface in response to a change in the light source and sensor position (Matsushita et al., 2007). Therefore, making it difficult in areas with rough terrains or mountainous areas (Matsushita et al., 2007). While several other vegetation indices exist, EVI and NDVI remain popular choices among remote sensing researchers (Wang et al., 2018).

A time series of vegetation indices can be used to determine trends and seasonal variation in vegetation properties (Heumann et al., 2007). One approach used to accomplish this is temporal decomposition, which separates time-series image data into three components, including seasonality (annual), trend (interannual and could be linear or nonlinear), and residuals (remainder of data signal after removing seasonality and trend) (Verbesselt et al., 2010).

A popular method for decomposing trends in time series data is using the Breaks for Additive Seasonal and Trend (BFAST) (Verbesselt et al., 2010). The BFAST routine is one of the many statistical methods used to extract the trends from time-series data. BFAST uses least-squares regression to model the trend component within a time series to detect gradual (interannual) and abrupt (intraannual) changes (Verbesselt et al., 2010). A newer method developed for detecting both abrupt and non-abrupt changes, named DBEST (Detecting Breakpoints and Estimating Segments in Trend), can quickly and accurately estimate change time and magnitude just like BFAST (Jamali et al., 2012). However, DBEST cannot detect changes in the seasonal component (Fang et al., 2018). Forkel et al. (2013) did a performance test on several methods used to detect trends and trend changes in long-term VI time series and noted that BFAST showed excellent performance in detecting both gradual and abrupt interannual changes in trend. Fang et al. (2018) used BFAST and the Moderate Resolution Imaging Spectroradiometer (MODIS) 16-day NDVI at a spatial resolution of 250 m to detect abrupt vegetation trends (disturbances) in Southern Quebec, Canada, during the years 2000 to 2011. Results were presented in and discussed in land cover categories, and the results for grasslands in the region show an overall positive trend (greening) for the study period. However, the years 2001, 2002, and 2007 had abrupt vegetation browning (a more negative trend) for grasslands. De Jong et al. (2012) also used BFAST and the Global Inventory for Mapping and Modeling Studies (GIMMS) NDVI data to detect trend changes in NDVI data between 1982 and 2008 at the global scale. Results show more negative than positive gradual change for grasslands in the northern hemisphere during the study period. Baghi and Oldeland (2015) used BFAST and MODIS (MOD13Q1) 16-day EVI at a spatial resolution of 250 m to detect the abrupt and gradual trend of grasslands in Northeast Iran between the years 2000 to 2004 (monthly intervals). Results showed a more stable than positive or negative trends and an average of 3 breaks per study period.

This study uses BFAST and a time series of MODIS NDVI/EVI images to quantify long-term interannual trends across the entire U.S. Great Plains. The Great Plains ecoregion is the largest

grassland reserve in the U.S. Given the dramatic decline of grasslands in this highly biodiverse, agriculturally-dependent ecoregion, coupled with the spatial variability in environmental and socioeconomic characteristics, improving our understanding of long-term changes in the dominant grassland vegetation will provide useful insight into the future provision of ecosystem services.

3.2 Study area

The Great Plains region is situated in the vast interior of North America, running from Canada in the North to Mexico in the south and lies east of the Rocky Mountains and west of the eastern temperate forests and the Appalachian Mountains (Rossum & Lavin, 2000). The region experiences extreme weather with periodic floods, droughts, and tornado events (Drummond & Auch, 2015). Climate is also diverse across this large region and is influenced by latitude (north to south) and elevation (increasing from east to west) (Tollerud et al., 2018). The Koeppen-Geiger climate classifications within the Great Plains show the range from the cold (snow) climate in northwestern North Dakota with warm, humid summers and long, cold, snowy winters to the arid climate of Texas in the south (Beck et al., 2018). Precipitation in the Great Plains is highly variable from year to year and, based on 30-year normal (1981-2010), ranges from a high of 1500 mm in the southeast to a low of 250 mm in the west. Annual mean temperatures range from 0^0C in the north to 22^0C in the south (PRISM Climate Group, 2019). Elevations in the region are similarly varied but generally decrease from a maximum of 3610 meters above sea level in Colorado to an average of 200 meters in eastern Oklahoma to central Texas (U.S. Geological Survey, 2017).

The boundary for the Great Plains region used for this study is that defined by the United States Environmental Protection Agency (EPA) based on Omernik (1987) and Omernik and Griffith's (2014) ecoregion classifications. These classifications are based on patterns of phenomena, including geology, physiography, vegetation, climate, soils, land use, wildlife, and hydrology (Omernik, 1987). The U.S. EPA categorizes the Great Plains as a Level I ecoregion. one of the 15 coarsest ecosystems in North America. In this ecosystem classification, the Great Plains has four level-II divisions and 16 Level III subdivisions (Omernik, 2014).

The Great Plains in the U.S. spans over 2.2 million square kilometers, with more than 40 percent of this land area in grassland, followed by agricultural land uses (Drummond & Auch, 2015). This study

focuses only on grassland areas as defined by the grassland/herbaceous class of the United States Geological Survey's National Land Cover Dataset (NLCD) for 2011 (Homer et al., 2015). The grassland area, as defined for this study, is approximately 826,000 square kilometers and covers 13 U.S. states (Figure 3.1). It contains a mixture of tallgrass prairie (east), mixed-grass prairie (north central), and short grass prairie (west).

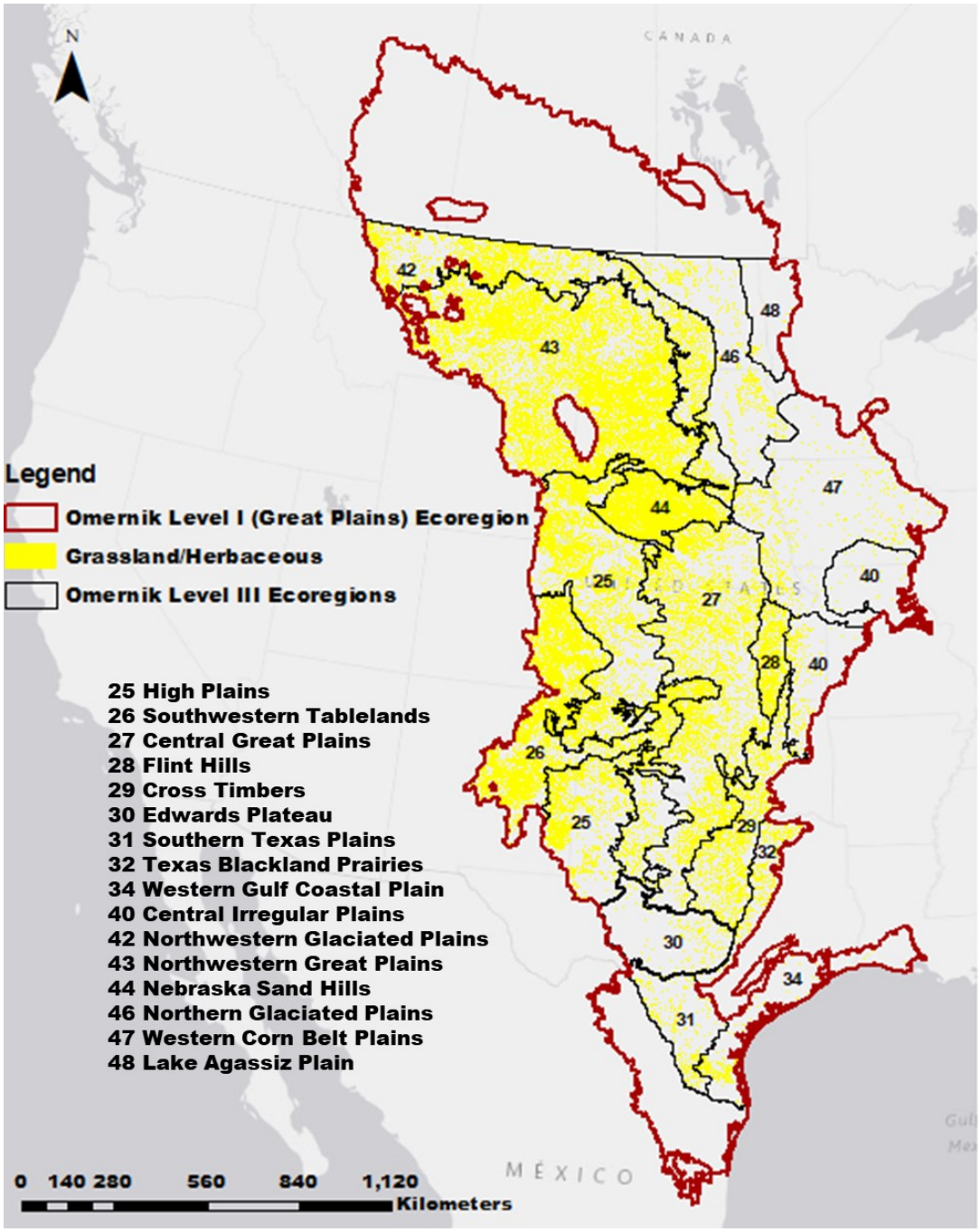

Figure 3.1: U.S. Great Plains study area showing Omernik level III ecoregions and grassland pixels extracted from the 2011 NLCD.

3.3 Data and methods

3. 3. 1 Data and data preparation

For this analysis, MODIS (MOD13Q1 Collection 6) 16-day maximum composite normalized difference vegetation index (NDVI), and the enhanced vegetation index (EVI) products for the period of 2001 to 2017 were used. Twenty-three composite images are produced per year, resulting in a total of 391 images for the study period. Images were downloaded from NASA's Earth Observation Data website using the "MODIStsp" package (version 1.3.3) in R as a 16-bit signed integer grid. The MOD13Q1 data has a 250-meter spatial resolution. The various scenes of the downloaded images that make up the EPA Great Plains were mosaiced and reprojected from their native sinusoidal projection to the USA Contiguous Albers Equal Area Conic projection.

To extract the area of interest, pixels belonging to the "grassland/herbaceous" class of the 2011 NLCD data produced from a 30-meter spatial resolution were resampled to match the spatial resolution of the MOD13Q1 imagery. To address the potential for misidentifying a grassland pixel, resampled pixels having at least 80% of their area comprised of the original NLCD grassland/herbaceous class were retained and used as a mask to extract the grassland pixels from the time series MODIS NDVI and EVI images. Due to the size of the study area and the computational effort required to perform the later analyses, the original NDVI and EVI images for the Great Plains (11634 rows and 7629 columns) were subdivided into a total of 423 smaller tiles having a maximum size of 350 rows by 350 columns (or up to 122,500 individual pixels).

3.3.2 Methods

Pixel values for each tile were extracted based on centroids and stored in tables. As a quality control step and to meet the data requirements of later analyses, missing VI data were replaced with the mean of the preceding and succeeding values of the same pixel in the time series. Tables for each tile were exported in CSV format and analyzed using the Breaks for Additive Seasonal and Trend (BFAST version 1.5.7) package for R in parallel using Beocat, the high-performance computing cluster at Kansas State University.

The BFAST routine is based on a LOESS-driven STL temporal decomposition that produces reliable estimations of seasonal and trend components from time-series data (Johnson et al., 2008). BFAST is also capable of modeling the trend component using linear or nonlinear regression to detect breakpoints, identifying when they occur, and quantifying the magnitude of change associated with each abrupt change (Verbesselt et al., 2010).

BFAST method uses an additive model (Equation 1) to decompose each pixel of a time series dataset into three components: Seasonal (St), trend (Ct), and residuals (εt) (Cleveland et al., 1990).

$$Yt = St + Ct + \varepsilon t \quad [1]$$

Performing temporal decomposition using BFAST requires specification of several parameters, including (1) the length of the time series, in this case, the total number of images in the time series, (2) the length of the season or the number of images within one vegetation cycle, (3) the season model, (4) a value (h) which relates to the minimum time interval between potential breaks in the trend component which is given as the fraction of the number of images in one vegetation cycle and the total number of images in the time series, and (5) the maximum number of breaks determined by h (Verbesselt et al., 2010). Table 1 summarizes the parameters used for this analysis.

Table 3.1: Parameters used in the BFAST routine analysis.

BFAST Parameter		**Parameter Value**
1	Length of the time series	391
2	Length of the season time series	23
3	Season model	harmonic
4	h	0.05
5	Maximum number of breakpoints	17 (based on h value)

The BFAST change detection algorithm decomposes the time series into seasonal, trend, and the residual components (Figure 3.2). In the example, BFAST graphical outputs shown in Figure 3.2, the time factor on the horizontal axis represents the year in the study period. The first row is the raw VI value; the second row is the seasonal component, which is a fitted seasonal model of the VI values; the third row is the trend component, which is a fitted (multi-annual linear or nonlinear) trend of the VI values consisting of segments with gradual or abrupt changes. The fourth row is the residual or remainder component after removal of trend and seasonal components. In addition to the graphical output, BFAST generates tabular outputs with raw values for the trend component for each pixel during the study period.

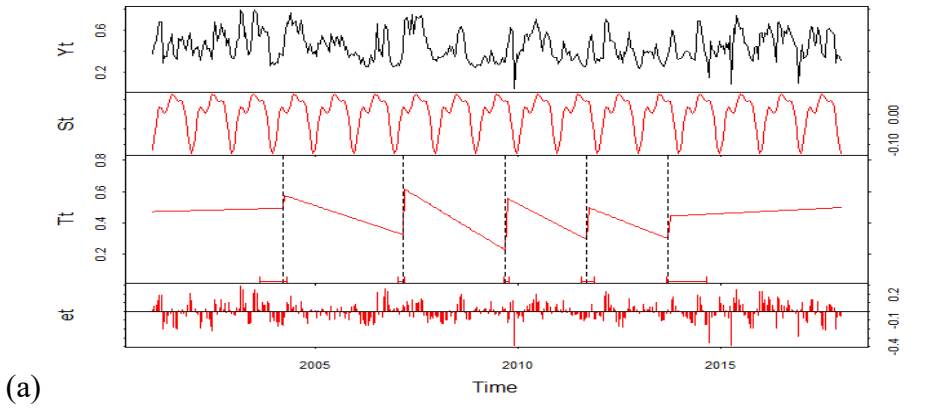

(a)

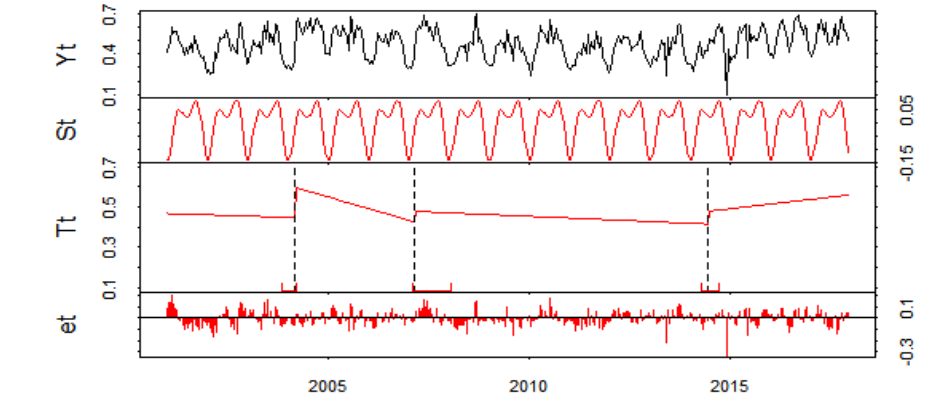

(b)

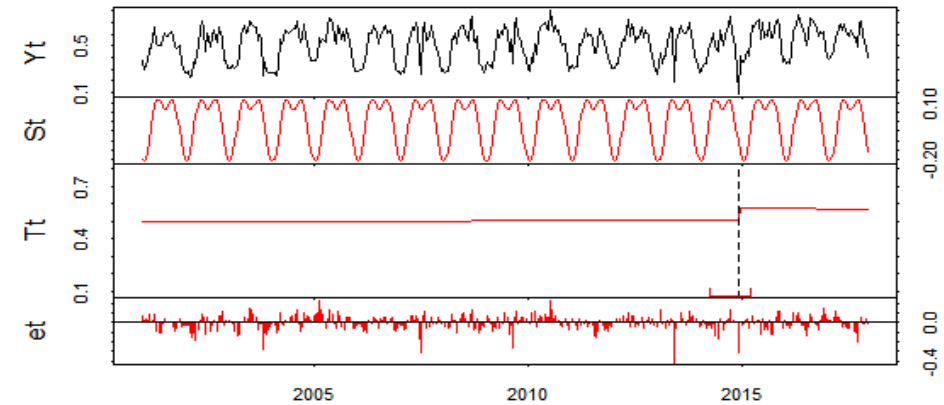

(c)

Figure 3.2: The BFAST output showing the raw NDVI time series (Yt), seasonal (St), trend (Tt), and residual components(et). Image (a) Pixel (in southwestern TX) with an overall negative trend over time and significant five breaks (b) Pixel (in northeastern KS) with an overall positive trend over time and three significant breaks (c) Pixel (in northeastern KS) with an overall null trend over time and one significant break.

The long-term trend in surface greenness, or gradual interannual change, was calculated for each pixel and VI using data returned by BFAST in the trend component. Gradual interannual change corresponds to the linear slope of the trend component across the 17-year study period without considering the presence or magnitude of any intraannual breaks detected in the trend. Ordinary least squares regression was used to calculate the slope of the trend, and its significance against a null slope was assessed using a Student's t-test (Hutchinson et al., 2015). Based on the statistical significance and sign of the slope, all pixels were placed into one of three gradual interannual trend classes (Table 3.2). The percentage of trend classes was calculated for the entire Great Plains Level I ecoregion study area and each of its Level III subdivisions.

Table 3.2: Definition and interpretation of gradual interannual trend classes (source: Hutchinson et al., 2015).

Trend Class	**Significance of trend slope value ($\alpha = 0.05$)**	**Sign of trend slope**	**Interpretation**
Browning	Slope value significantly different from a null slope	Negative	VI-derived trend indicates surface greenness has declined over time.
Greening		Positive	VI-derived trend indicates surface greenness has increased over time.
No Change	Slope value is not significantly different from a null slope	Negative and Positive	VI-derived trend indicates surface greenness has remained stable over time.

3.3.3 Validation of the time series trend analyses

To validate the resulting trend classes calculated using the MODIS VIs during the study period, a change analysis was computed using Landsat-derived NDVI images for the starting year (2001) and

ending year (2017) of the study period. This validation method has been used for change analysis in grasslands (Borak et al., 2000; Tarantino et al., 2016), especially in large study areas that make field validation challenging or that might rely on historical data to calculate. Given the intra-region diversity of grasslands within the Great Plains, sample areas for validation were chosen to include shortgrass, mixed-grass, and tallgrass prairie sites (Figure 3.3). Using a power analysis based upon a 95% confidence level and 0.5 confidence interval, 38,320 pixels were determined to be the minimum required number of pixels to be sampled. Here, a total of 455,600 pixels were used for the validation process. Two cloud- and scan-line free Landsat images for each sample area were acquired from the USGS Earth Explorer website (https://earthexplorer.usgs.gov/). The Landsat sensor and date of acquisition for each sample area are listed in Table 3.3.

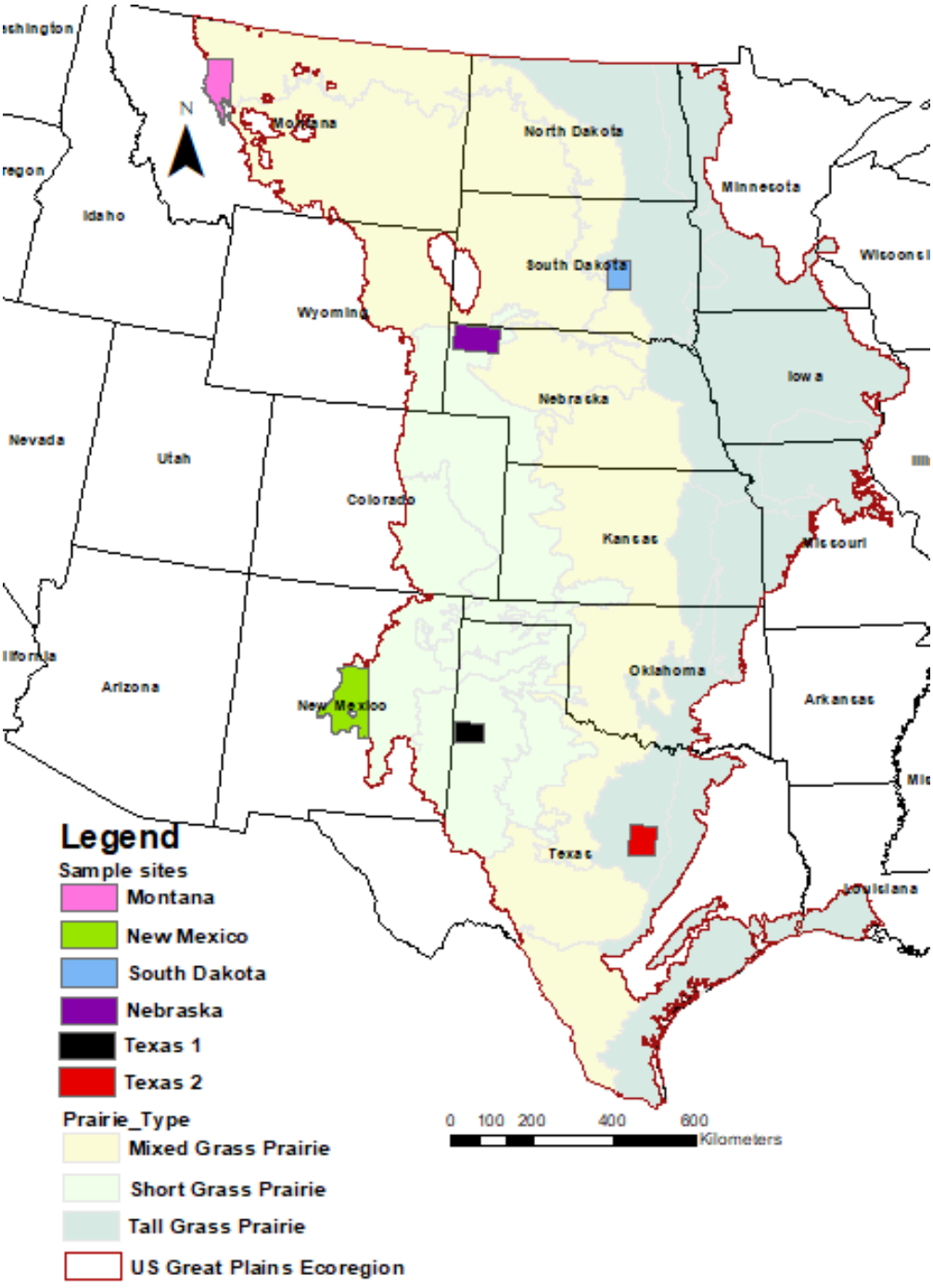

Figure 3.3: Map of the study area location of Landsat image pairs (sample sites) used for validation.

Table 3.3: Details of Landsat image pairs used for validation

Sample Site	**Image and Image dates**	**Area of Sample site (KM^2)**	**No. of Pixels in Sample Sites**
Montana	Landsat-5 TM: 08/25/2001 Landsat-8 OLI: 08/21/2017	7,163	71465
Nebraska	Landsat-5 TM: 08/24/2001 Landsat-8 OLI: 08/20/2017	6,901	99077
New Mexico	Landsat-5 TM: 09/09/2001 Landsat-8 OLI: 06/17/2017	13,757	168356
South Dakota	Landsat-5 TM: 06/16/2001 Landsat-8 OLI: 07/14/2017	4,187	38285
Texas 1	Landsat-7 TM: 07/17/2001 Landsat-8 OLI: 07/21/2017	3,323	27847
Texas 2	Landsat-7 TM: 06/19/2001 Landsat-8 OLI: 06/23/2017	4,924	50570

NDVI was calculated from the multispectral Landsat images and non-grassland pixels masked. The Landsat-derived NDVI images were then resampled and reprojected to match the characteristics of the MODIS NDVI images. The grassland pixels difference (2001 - 2017) in the Landsat NDVI was calculated for each sample area. As with the MODIS NDVI trend classes, three high-resolution trend classes were created (browning, no change, greening) for the Landsat NDVI using thresholds. That threshold was based on upper and lower levels of the mean NDVI difference standard deviations, which vary for each sample area (Table 3.4). Finally, the percentage of the change classes from the

Landsat NDVI validation dataset were compared to those created from MODIS NDVI analysis for the same sites.

Table 3.4: Landsat NDVI difference class threshold

Sample Site	**Threshold (Standard deviation from the mean)**	
	NDVI	**EVI**
Montana	∓ 0.5	∓ 0.25
Nebraska	∓ 0.25	∓ 0.75
New Mexico	∓ 0.25	∓ 0.5
South Dakota	∓ 1.25	∓ 0.5
Texas 1	∓ 1.25	∓ 1.25
Texas 2	∓ 0.5	∓ 0.5

3.3.4 Comparison of NDVI and EVI for trend analysis

To compare the results of trend analysis from the MODIS NDVI and EVI time series, a Chi-square test was first carried out to determine if the gradual interannual trend results were dependent on the VI used. The null hypothesis that the trend is independent if the VI used should be rejected if the test statistic ($p < 0.05$) is significant.

Second, an error matrix was constructed to compare trend results based on the two indexes. The focus of the error matrix was on summarizing the cross-tabulation, rather than reporting the proportion "correct" and a kappa index, to gain more valuable insights into the two trend outcomes. The error matrix includes the user's and producer's accuracy metrics. The user's accuracy represents the proportion of a category in the reference data that have been correctly identified, but, in this case, it represents the number of pixels that are the same in both NDVI and EVI results. The producer's accuracy represents the proportion of a category in the reference data that were classified properly (it does not apply in this situation). Differences between the reference (NDVI) and comparison (EVI) maps were quantified in terms of quantity and allocation disagreement (Pontius & Millones, 2011). Quantity disagreement results from an imperfect match in the number, or proportion, of pixels across categories represented in the reference and comparison maps. Allocation disagreement arises when there is an imperfect match in the spatial allocation of categories caused by pairs of misallocated

pixels. Within such pairs, one pixel represents an error of omission and the other an error of commission. The concepts behind quantity and allocation disagreement have been called by various terms in different fields. For example, in landscape ecology, composition is the "quantity" of each category, and "configuration" describes how categories are arranged spatially (Gerger & Turner, 2002). Allocation disagreement can further be subdivided into two components called exchange and shift, which result in allocation differences due to confusion in pairwise and non-pairwise categorical comparisons with a minimum of three categories, respectively (Pontius and Santacruz, 2014).

Figure 3.4 shows several comparisons of trend results with their corresponding error matrices and values for quantity disagreement, exchange, and shift. The first example illustrates a pure quantity difference where six green pixels (positive trend) exist in the reference, but only three are found in the comparison map. As in this case, quantity differences are indicated when the marginal totals of the reference do not exactly match those for the comparison. The second example is a complete exchange difference given that three pixels that are red (negative trend) on the reference are replaced by green on the comparison, but there are six green and three red pixels on both. The third example presents a complete shift difference and highlights the requisite of having a minimum of three categories present for such differences to exist. The total number of pixels in each of the three categories is the same across both maps, but there are six total pixels that shift values (e.g., red to green, gray (stable) to red, and green to gray). These differences cannot be considered exchanges because there are, for example, three pixels that are red in the reference that become green in the comparison but no green pixels in the reference that are red in the comparison. The fourth and final comparison illustrates all three types of differences.

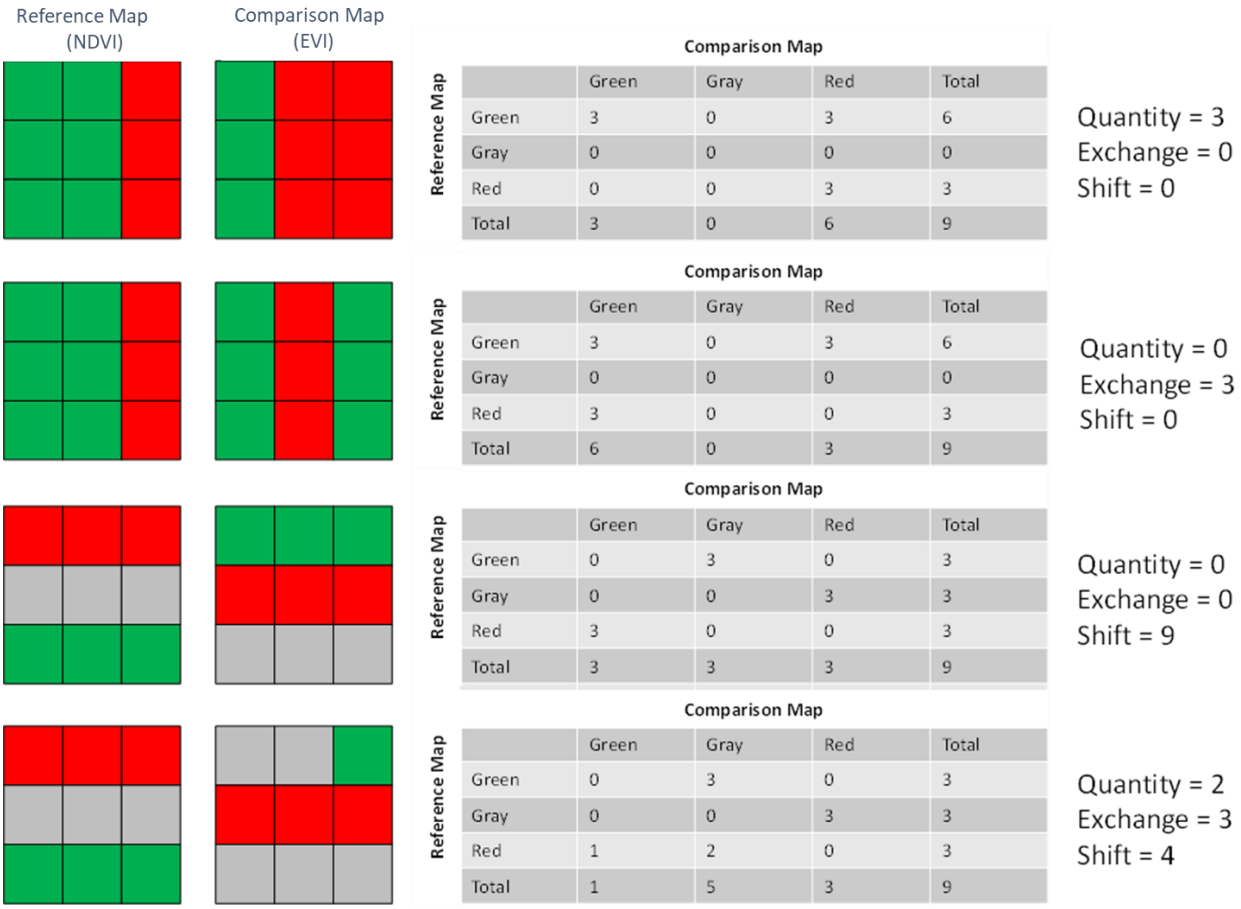

Figure 3.4: Four comparisons of trends results produced using NDVI and EVI that illustrate three measures of disagreement: quantity, exchange, and shift (after Pontius and Santacruz, 2014).

To further assess the impact of using NDVI versus EVI for grassland trend analysis in the Great Plains, trend results from two level III ecoregions within the study region having the lowest and highest average VI values were compared. Based on a zonal analysis, the level III ecoregion with the highest average VI values was the Central Irregular Plains. However, the Flint Hills (the next highest) was used for this analysis because it included significantly more grassland pixels as compared to the Central Irregular Plains, including high-biomass tallgrass prairie. The level III ecoregion with the lowest average VI values in the Great Plains during the study period was the Southwestern Tablelands. To conclude the comparison of the NDVI- and EVI-derived trends, a pixel difference analysis was carried out to illustrate any spatial variation between the two results.

3.4 Results

3.4.1 Gradual interannual trend

The gradual interannual trend classes for 2001 to 2017 from MODIS VI analyses are shown in Figures 3.5 (NDVI) and 3.6 (EVI). Pixels with statistically significant positive (greening) and negative (browning) trends are shown in green and red, respectively. Pixels without a significant trend (null slope) are shown in dark grey. Pixels with a positive trend indicate grasslands are getting greener over time which suggests improvement in condition (e.g., higher aboveground biomass, greater leaf area index, etc.). Conversely, pixels with a negative trend highlight areas where VI values are declining over the study period, which points to degrading vegetation condition (e.g., less aboveground biomass, lower leaf area index, etc.). Finally, pixels with non-significant, or null, slopes are considered to exhibit stable greenness values over time.

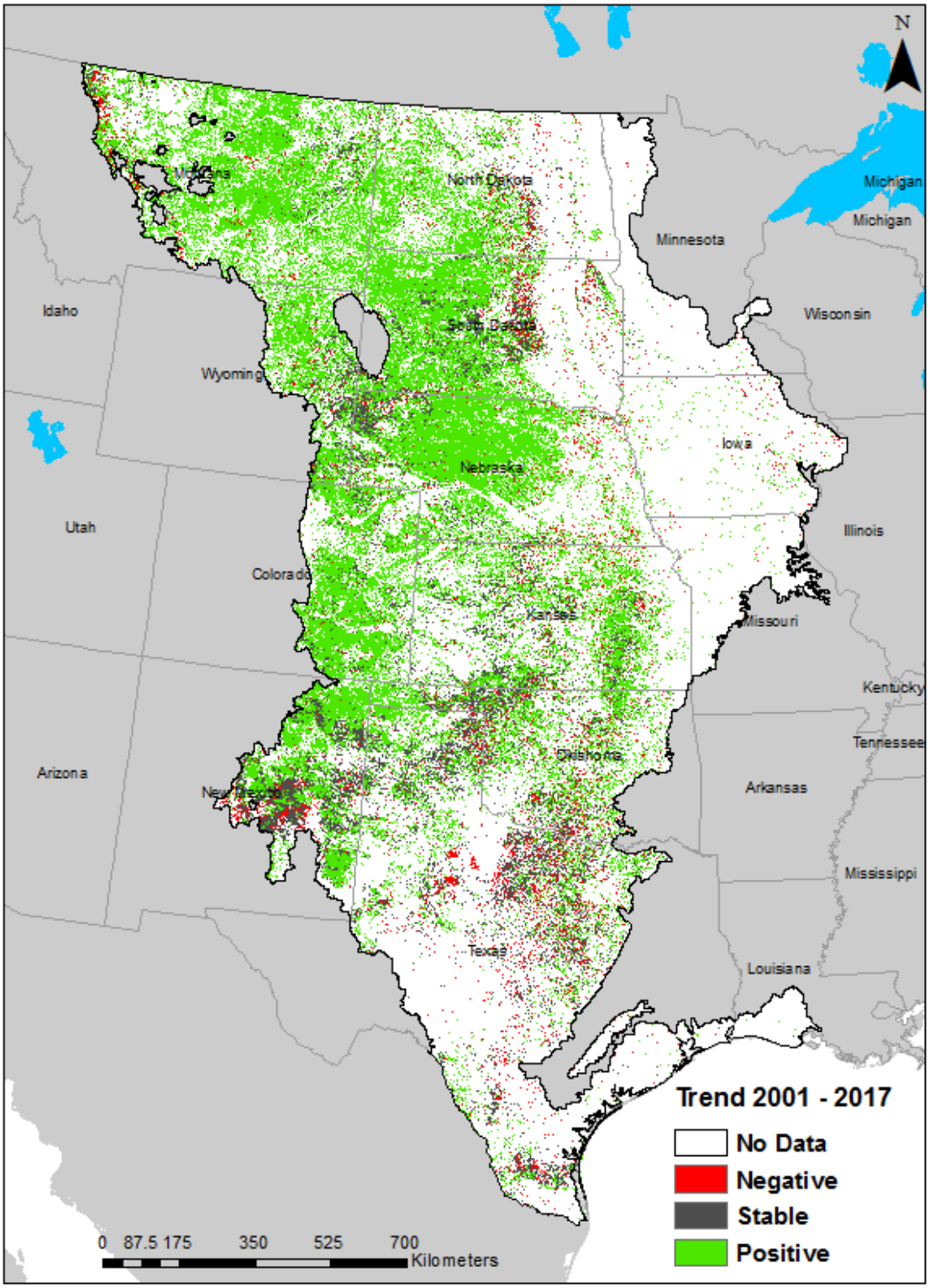

Figure 3.5: Gradual interannual NDVI trend classes for the 2001- 2017 period in the U.S. Great Plains as determined by BFAST analysis. No Data = non-grassland areas.

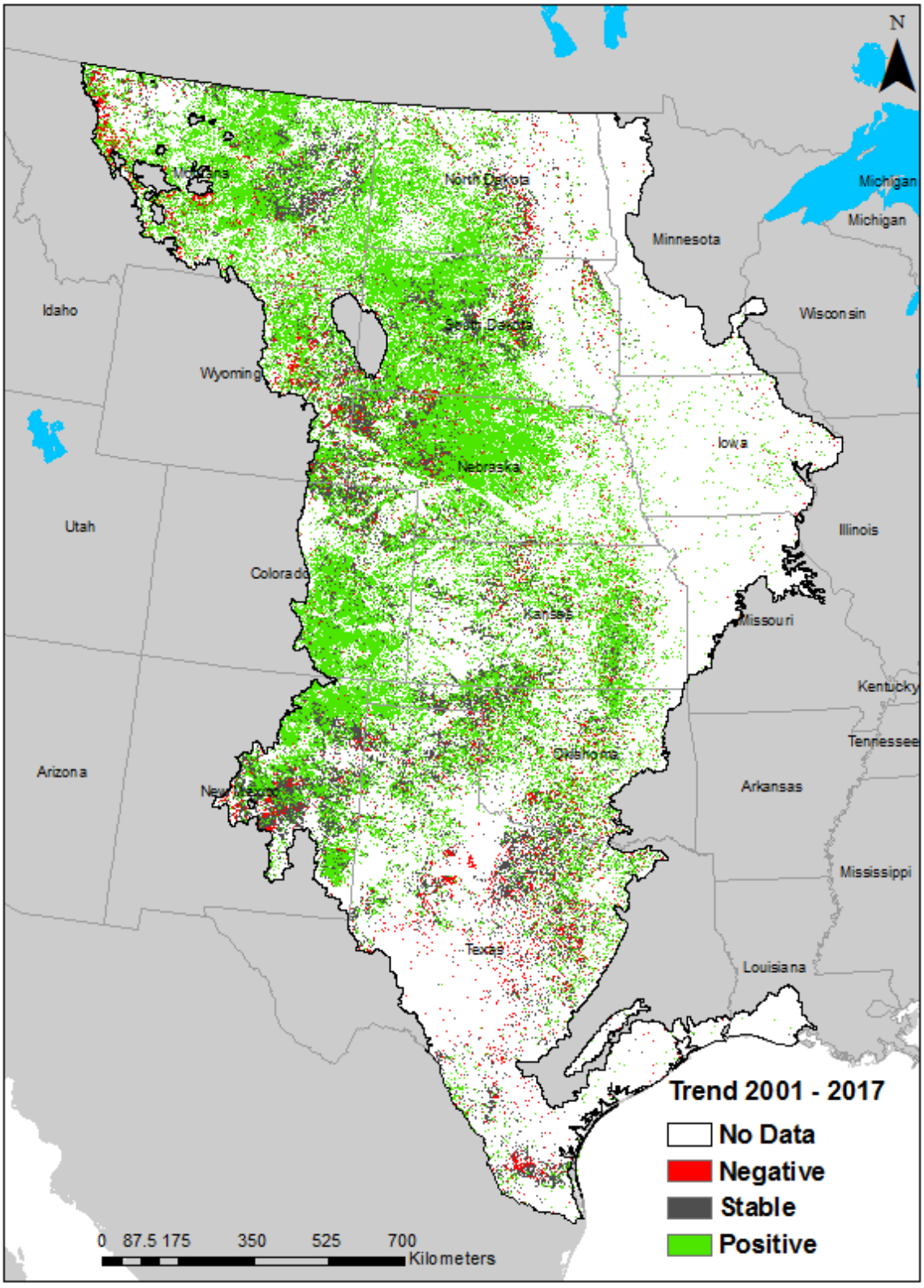

Figure 3.6: Gradual interannual EVI trend classes for the 2001-2017 study period in the U.S. Great Plains as determined by BFAST analysis. No Data = non-grassland areas.

Gradual interannual trend classes are quantified in Table 3.5. Results from the analysis of MODIS NDVI show that 73.3% of the grassland area in the Great Plains experienced significant greening, 6.8% significant browning, and 19.9% stable conditions during the study period. The percentages from the EVI-derived classes were similar, with 68.7% of grasslands experiencing greening, 7.8% browning, and 23.5% stable trends.

Table 3.5: Summary of results for gradual interannual trend classes for the 2001-2017 study period in the U.S. Great Plains as determined by BFAST analysis of MODIS NDVI and EVI imagery.

Grassland Interannual Trend Classes	**Negative Trend (Browning)**		**Positive Trend (Greening)**		**Stable (No Significant Trend)**	
	NDVI	**EVI**	**NDVI**	**EVI**	**NDVI**	**EVI**
Number of pixels	1,048,040	1,200,757	11,281,432	10,572,918	3,057,760	3,613,160
Area (sq. kilometers)	56,242.7	64,438.2	605,414.3	567,392.1	164,093.7	193,899.0
Percent of Total Area	6.8%	7.8%	73.3%	68.7%	19.9%	23.5%

3.4.1.1 Regional gradual interannual trend results

Gradual interannual trend classes were also summarized at the level III ecoregion scale (Figures 3.7 and 3.8). Grasslands in most level III ecoregions experienced a higher percentage of positive VI trends during the study period. The Nebraska Sand Hills had the highest percentage of positive trends, with 95.9% and 85.2% of grasslands greening over time, respectively. This ecoregion has the largest grassland extent in the U.S. and is also the most homogeneous ecoregion in North America (Omerick, 1987; Tollerud et al., 2018). The few areas with a significantly negative trend are generally located in the western part of the ecoregion. The Edwards Plateau had the highest percentage of negative VI trends with 31.6% and 42.6% of grasslands browning over time, respectively. This ecoregion also

had the lowest percentage of grassland pixels having a greening trend. The Edwards Plateau is located entirely in Texas and is hilly and mostly semiarid (Tollerud et al., 2018). Significant differences between the NDVI and EVI derived trends results on the level III ecoregions are in the Western Corn Belt Plains, Northwestern Glaciated Plains, Central Irregular Plains, and the Southern Texas Plains; most of which are tallgrass prairies (Figures 3.7 and 3.8).

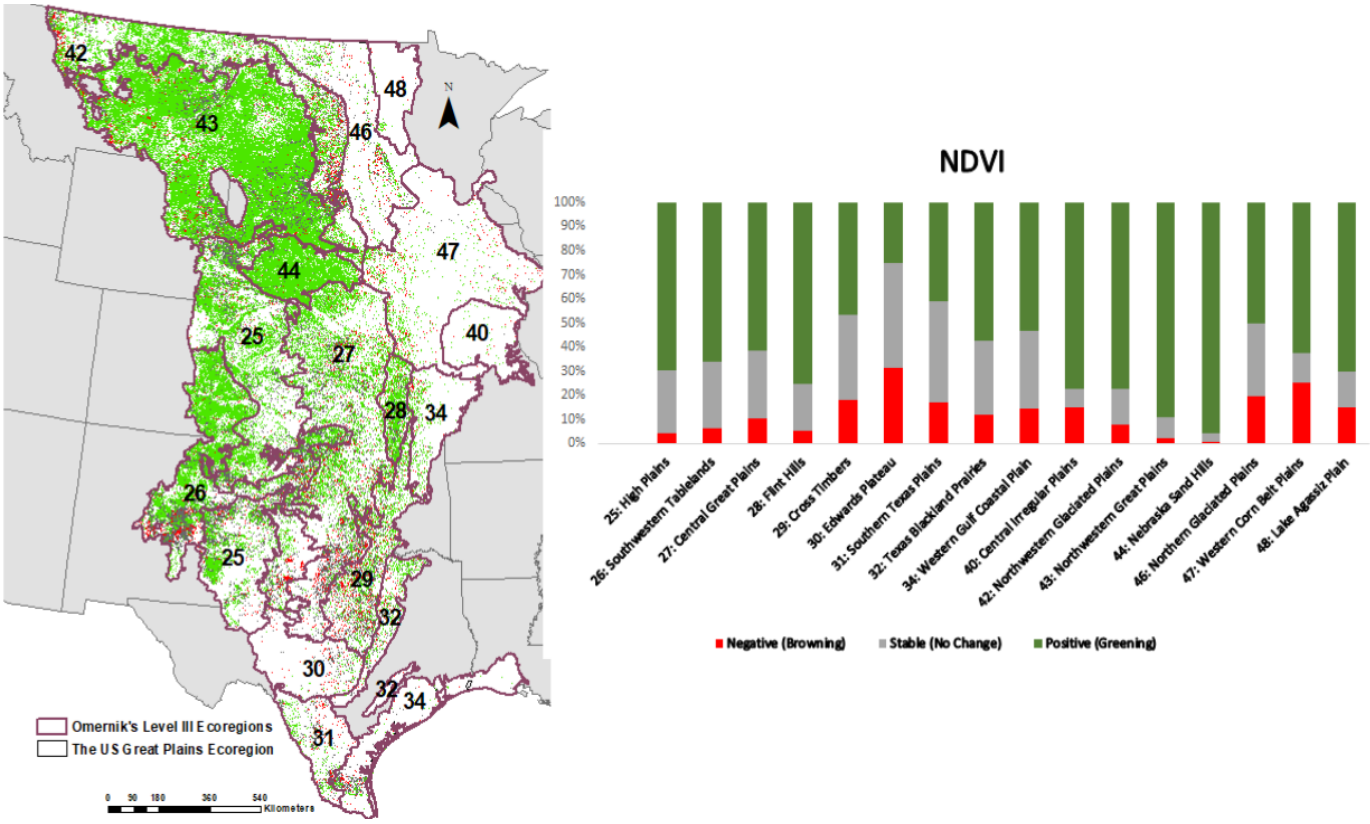

Figure 3.7: Summary of results for gradual interannual trend classes for the 2001-2017 study period for level III ecoregions in the U.S. Great Plains based on BFAST analysis of MODIS NDVI imagery.

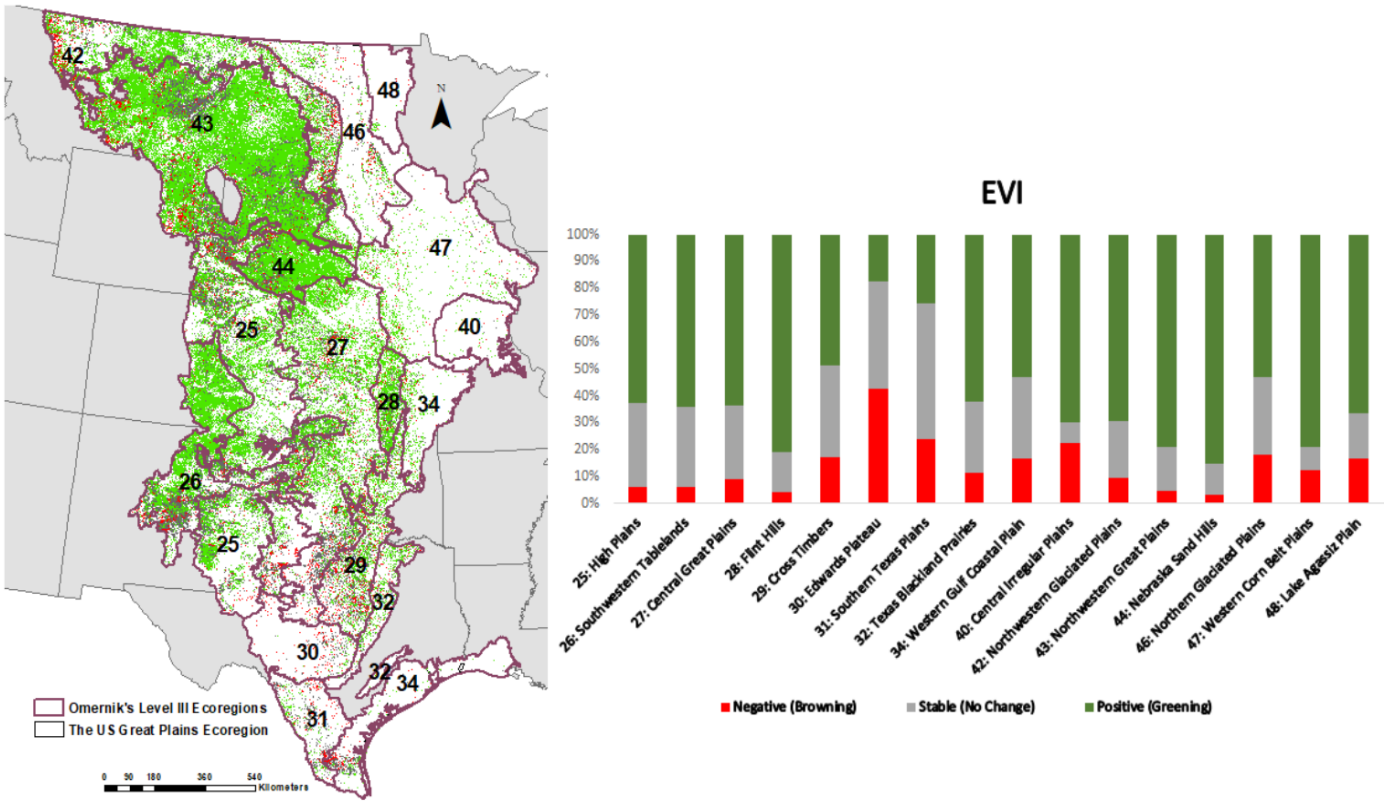

Figure 3.8: Summary of results for gradual interannual trend classes for the 2001-2017 study period for level III ecoregions in the U.S. Great Plains based on BFAST analysis of MODIS EVI imagery.

3.4.2 Validation

The comparison of the percentage of trend classes from the Landsat NDVI analysis (Table 6) shows good agreement across indexes, sensors, and spatial resolutions. This provides additional confidence in the results reported for the MODIS-derived trend classes. The difference calculated for the NDVI and the EVI trend classes in the six samples are as follows (Table 3.6): At the Montana site, the EVI has more stable and fewer negative trend pixels at higher spatial resolution. The EVI has more positive, less stable, and more negative trend pixels at the Nebraska site at higher spatial resolution. At the New Mexico site, the EVI has less positive, less stable, and more negative trend pixels at higher spatial resolution. At the Texas 1 site, the EVI has less positive, less stable, and more negative trend pixels at higher spatial resolution. At the Texas 2 site, the EVI has less positive, more stable, and less negative trend pixels at higher spatial resolution. At the South Dakota site, the EVI has more

positive, less stable, and more negative trend pixels at higher spatial resolution. There are no clear patterns in the variation between the differences calculated for the NDVI and the EVI trend classes.

While the agreement is generally high for each index and trend class, the EVI validation samples have a lower total difference compared to NDVI. The largest differences between the Landsat-derived and MODIS-derived validation data were in the stable class (Montana, South Dakota, and Texas 2 sites). These variations can be attributed to any of the following factors: differences in the method of classification of the change classes, the difference in the spatial resolution of data used for both analyses, and the fact that Landsat-derived classes consist of only two time periods.

Table 3.6: Landsat NDVI and EVI change classes compared to MODIS NDVI and EVI change classes. The Landsat NDVI and EVI change classes were considered the reference of the comparison.

Sample Site	**Interannual Trend Class**	**NDVI (Percent of Total Grassland Area)**			**EVI (Percent of Total Grassland Area)**		
		MODIS	**Landsat**	**Difference**	**MODIS**	**Landsat**	**Difference**
Montana	Positive	69.6	68.8	**-0.8**	52.6	51.8	**-0.8**
	Stable	10.1	14.1	**4**	7.3	14.4	**7.1**
	Negative	20.3	17.1	**-3.2**	40.1	33.8	**-6.3**
Nebraska	Positive	54	51	**-3**	51	51.1	**0.1**
	Stable	37.9	38.6	**0.7**	38.8	39.1	**0.3**
	Negative	8.1	10.4	**2.3**	10.2	9.8	**-0.4**
New Mexico	Positive	45.8	44.9	**-0.9**	40.1	39	**-1.1**
	Stable	39.8	37.7	**-2.1**	46.9	43.9	**-3**
	Negative	14.4	17.3	**2.9**	13	17.1	**4.1**

South Dakota	Positive	31.3	28.1	**-3.2**	53	53.2	**0.2**
	Stable	49.1	54.6	**5.5**	38	39.5	**1.5**
	Negative	19.6	17.3	**-2.3**	9	7.3	**-1.7**
Texas 1	Positive	75.1	73.0	**-2.1**	76.7	75.9	**-0.8**
	Stable	20.3	22.1	**1.8**	19.6	18.5	**-1.1**
	Negative	4.6	4.9	**0.3**	5.6	3.7	**1.9**
Texas 2	Positive	30.9	37.1	**6.2**	29.4	29.8	**-0.4**
	Stable	48.8	40.3	**-8.5**	51.6	47.0	**4.6**
	Negative	20.3	22.6	**2.3**	19	23.2	**-4.2**

3.4.3 Comparison of NDVI and EVI trend results

The Pearson's Chi-squared test of NDVI- and EVI-derived interannual trend classes showed significant differences exist ($X^2 = 8101700$, df = 2, p-value << 0.001). Therefore, the null hypothesis that calculated intraannual trends are independent of VI is rejected, and it can be concluded that trends are highly dependent on the VI used. The trends results are further summarized in a contingency table or error matrix (Table 3.7). The error matrix shows nearly 80% agreement between the interannual trend classes computed from the NDVI and EVI time series. Also evident from the error matrix is that there is a much higher agreement between VIs with the positive trend class, whether considering producer's or user's accuracy metrics. When differences in trend classes happen, the majority of those differences occur between "adjacent" trend classes. For example, when the MODIS NDVI results for negative, stable, and positive trends are stable, positive, and stable in the MODIS EVI outcomes. This suggests that the EVI algorithm may be more sensitive to small magnitude differences in surface greenness that have an important impact on the ultimate trend class into which a pixel is placed.

Table 3.7: Error matrix of NDVI and EVI interannual trend class results for grasslands of the Great Plains ecoregion (2001-2017). The NDVI change classes are considered the reference, and the EVI change classes are considered the comparison map. The number of pixels in an agreement between the NDVI and EVI change classes are in bold. The grey cells contain the higher number of 'misclassified' pixels.

NDVI Trend	EVI Trend					
		Negative	Stable	Positive	Total	User's accuracy (%)
	Negative	**691,127**	247,204	108,261	1,046,592	66.0
	Stable	340,006	**1,925,179**	789,670	3,054,855	63.0
	Positive	169,451	1,440,624	**9,670,715**	11,280,790	85.7
	Total	1,200,584	3,613,007	10,568,646	15,382,237	
	Producer's Accuracy (%)	57.6	53.3	91.5		**79.9**

The differences between MODIS VI trend classes are considered further in terms of quantity and allocation disagreement (Figure 3.9). While quantity disagreement (non-spatial) is important, especially for the positive and stable trend classes, allocation disagreement (spatial) is the dominant type of difference for each trend class. Within the allocation differences, it is exchange that largely explains differences, particularly for the stable and positive classes. It should also be noted that only the stable class experienced any shift. Combining data from Table 3.7 and Figure 8 illustrates that most of the allocation difference that occurs is between MODIS NDVI positive and stable pixels that are classified in the MODIS EVI results as stable and positive, respectively. Exchange between MODIS NDVI negative and MODIS EVI stable is also evident.

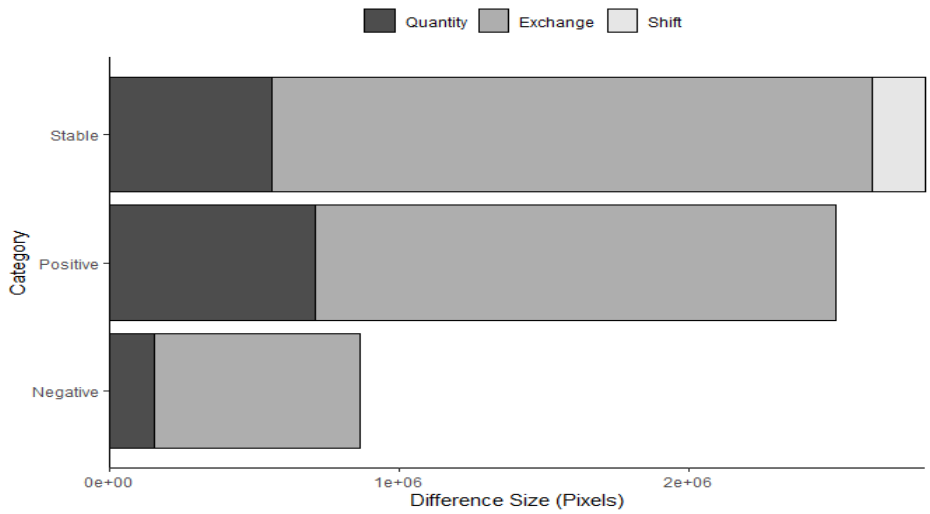

Figure 3.9: Differences in MODIS NDVI and EVI interannual trend classes for the Great Plains ecoregion (2001-2017).

Comparing the difference in NDVI- and EVI-derived interannual trend classes, the level III ecoregion with the lowest average VI value (Southwestern Tablelands) shows 78.6 percent agreement between the interannual change classes of the NDVI and EVI trend results (Table 3.8). While the level III ecoregion chosen to represent the highest average VI (Flint Hills) shows 82.5 percent agreement (Table 3.9).

Table 3.8: Error matrix with the NDVI and EVI trend results for the Southwestern Tablelands ecoregion interannual trend classes. The NDVI and EVI trend classes are considered the reference and comparison maps, respectively. The number of pixels in an agreement between NDVI and EVI trend classes are in bold. The grey cells contain the higher number of 'misclassified' pixels.

NDVI Trend	EVI Trend					
		Negative	Stable	Positive	Total	User's Accuracy (%)
	Negative	**79,691**	49,754	5,704	135,149	59.0
	Stable	48,591	**396,369**	157,428	602,388	65.8
	Positive	8,099	197,328	**1,234,851**	1,440,278	85.7
	Total	136,381	643,451	1,397,983	2,177,815	
	Producer's Accuracy (%)	58.4	61.6	88.3		**78.6**

Table 3.9: Error matrix with the NDVI and EVI trend results for the Flint Hills ecoregion interannual trend classes. The NDVI and EVI trend classes are considered the reference and comparison maps, respectively. The number of pixels in an agreement between the NDVI and EVI change classes are in bold. The grey cells contain the higher number of 'misclassified' pixels.

NDVI Trend	EVI Trend					
		Negative	Stable	Positive	Total	User's Accuracy (%)
	Negative	**9,391**	4,085	4,555	18,031	52.1
	Stable	2,683	**31,410**	31,388	65,481	48.0
	Positive	1,319	15,340	**238,472**	255,131	93.5
	Total	13,393	50,835	274,415	338,643	
	Producer's Accuracy (%)	70.1	61.8	86.9		**82.5**

The Southwestern Tablelands ecoregion cross-tabulation shows that the largest difference between the NDVI and EVI results is within the negative trend class. Thirty-seven percent of pixels that were negative in the NDVI trend results were stable in the EVI trend results. Twenty-six percent of pixels that were stable in the NDVI trend results were positive in the EVI trend results. Finally, only 14 percent of pixels that were positive in the NDVI trend were stable in the EVI trend. Figure 3.10a confirms that the stable class has the largest overall difference and that exchange, or interchanges between the stable and the negative class, are driving that disagreement.

The cross-tabulation for the Flint Hills ecoregion reveals that, like the Southwestern Tablelands, the stable class contains the largest difference between the NDVI and EVI trend results. Forty-eight percent of pixels that were stable in the NDVI trend were positive in the EVI results. There is also a large portion (25 percent) of negative pixels in the NDVI trend that was positive in the EVI comparison map (Table 3.9). Figure 9b shows that most of the difference in the stable class is allocation disagreement comprised largely of exchange with some shift. In the Flint Hills, non-spatial quantity differences are much more prevalent and account for approximately 1/3 of the disagreement in the positive and negative classes.

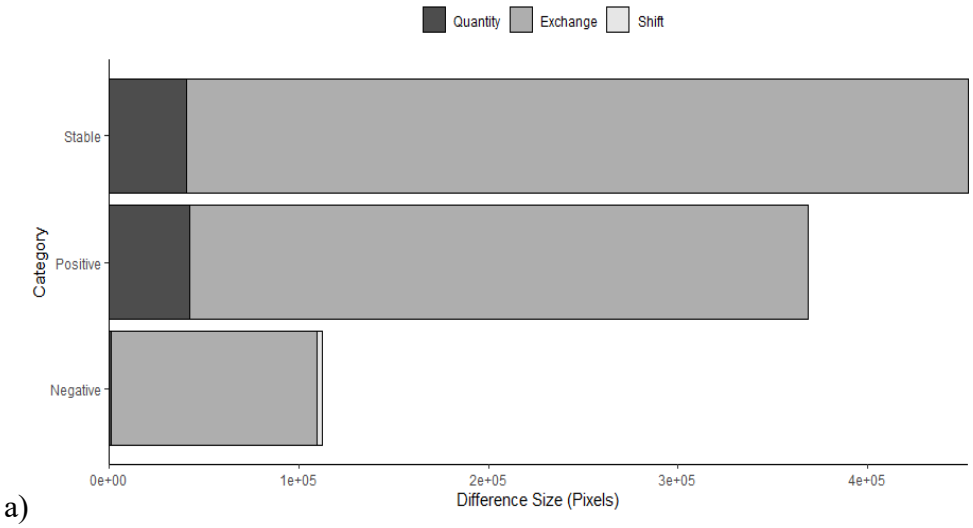

a)

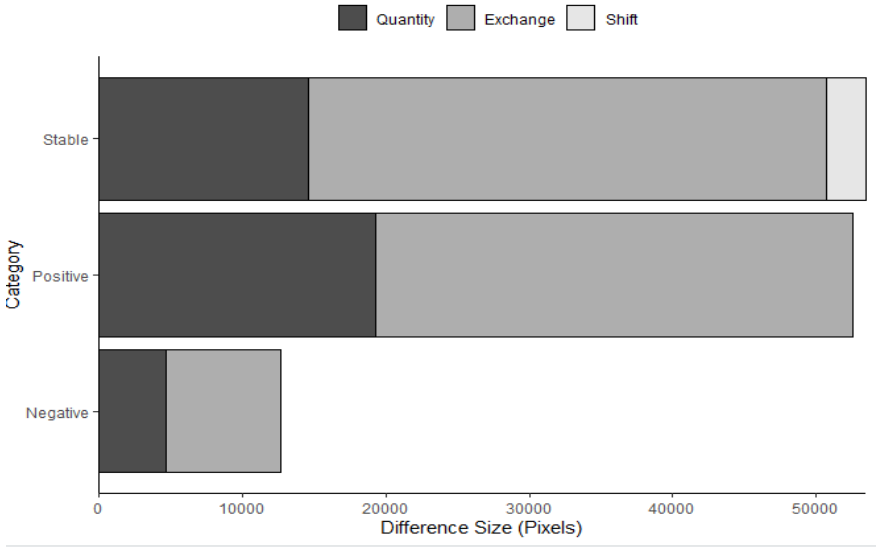

b)

Figure 3.10: Sources of disagreement in NDVI and EVI interannual trend classes (2001 to 2017) for the (a) Southwestern Tablelands and b) Flint Hills ecoregions.

In addition to summarizing quantity and allocation disagreement from the error matrix, differences in trend class results calculated from the NDVI and EVI time series can also be mapped to better visualize the spatial component of the differences. (Figure 3.11). Pixels in blue and red shades indicate a move to a "greener" or "browner" trend result, respectively, in the EVI comparison versus the NDVI reference map. Pixels shown in yellow indicated no change between the maps in terms of computed trend class.

No change pixels dominate Figure 3.11 and are present in large proportions across the entire study area. Generally, much of the movement to browner classes in the EVI trends results occurred in the mixed and shortgrass prairies of the western, and especially the northwestern, part of the Great Plains. However, movement to greener classes is almost exclusively found mixed and tallgrass prairies in the eastern Great Plains.

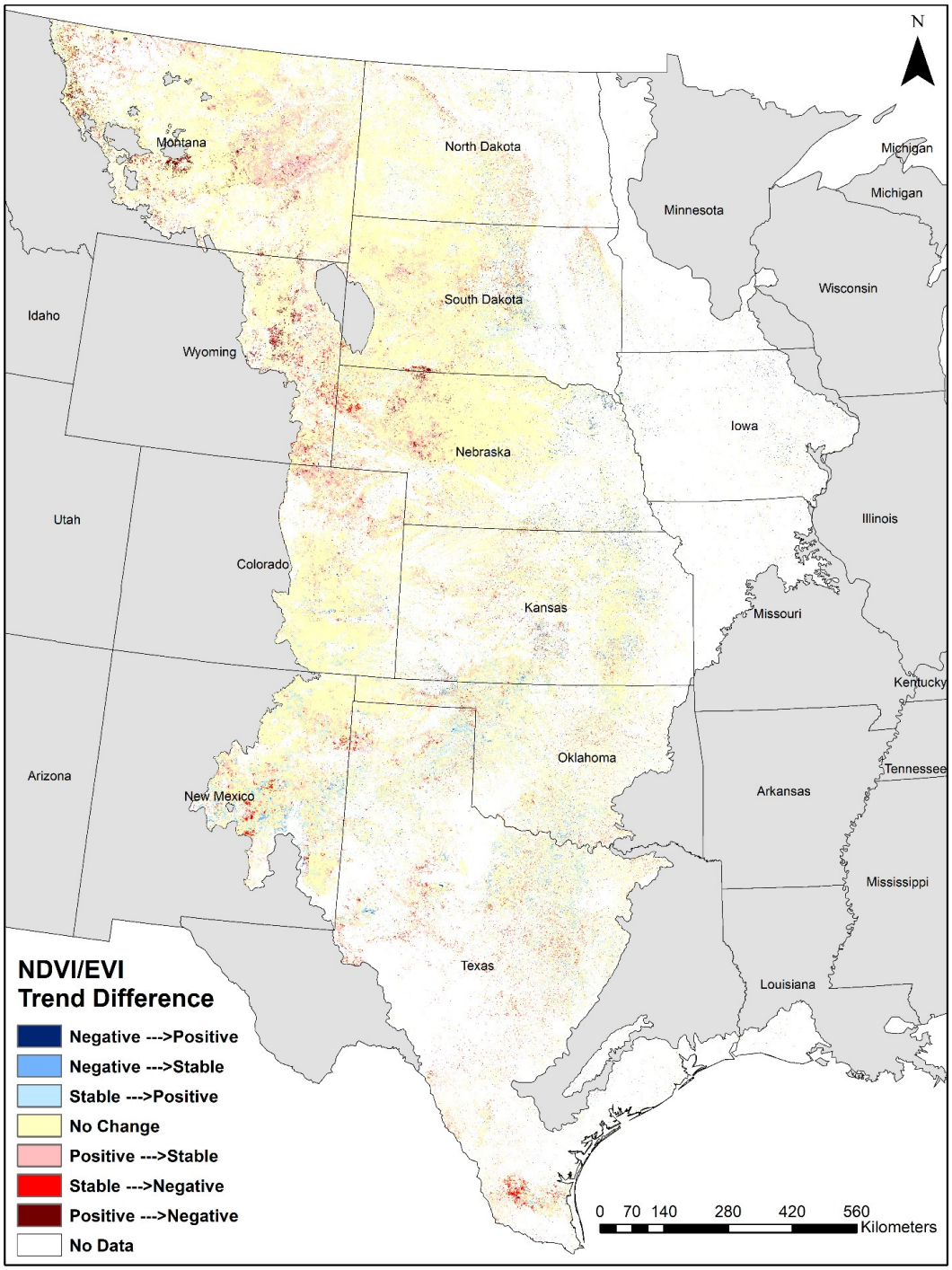

Figure 3.11: Visualizing pixel difference in MODIS NDVI and EVI trend class results in the Great Plains. The difference indicated is from NDVI to EVI.

3.5 Discussion and conclusions

3.5.1 Discussion

Results from the BFAST trend analysis provide a summary of the vegetation dynamics within the Great Plains that should be of interest not only to land managers and owners but also policymakers and other researchers. From 2001 to 2017, most of the Great Plains (68.7-73.3%) experienced significant positive or greening trends suggesting improved or more robust grassland vegetation over time. Positive trends can be found within each ecoregion of the study area but are especially prominent within the Nebraska Sand Hills, Northwestern Great Plains, Northwestern Glaciated Plains, Flint Hills, and the High Plains of Colorado and northern New Mexico. Much of the study area (19.9-23.5%) also experienced no significant change or a stable trend in grassland greenness over the study period. Ecoregions with large proportions of stable trend grasslands were mostly in the southern Great Plains and included the Southern Texas Plains, Edwards Plateau, Cross Timbers, Texas Blackland Prairies, and Western Gulf Coastal Plain. Relatively little of the Great Plains (6.8-7.8%) were found to have a significant negative or browning trend. Despite the relative paucity of negative trends within the region, several ecoregions had relatively high percentages of grassland pixels classified as browning, including many of those listed above for the stable class as well as ecoregions on the northeast corner of the Great Plains such as Northern Glaciated Plains, Western Cornbelt Plains, and Lake Agassiz Plain. Considering the locations of dominant trend "signals", there appears to be a generalizable north to a south gradient where greening is strongest in the northwest and central Great Plains and browning in the south and southeast.

Trend analysis results computed from MODIS NDVI and EVI were compared to simple difference-based trends calculated from higher spatial resolution Landsat imagery for several sample sites throughout the Great Plains. This validation step was similar to those employed by Hutchinson et al., (2015) and Browning et al. (2017), who also examined grassland regions. For this study, a strong agreement was found between MODIS and Landsat VIs, with EVI-based trends having a lower total difference compared to NDVI. These validation findings confirm that trend class results from the coarse resolution MOD13Q1 data product are both valid and reflect the reality on the ground at least as well as higher spatial resolution imagery.

Comparing BFAST-derived NDVI and EVI results via Chi-square analysis showed that the two VIs produced a significantly different number of pixels in the three trend classes. The cross-tabulation and examination of its disagreement components (quantity, exchange, and shift) revealed while quantity (non-spatial) disagreement existed in each of the trend classes, it was a larger component for the positive and stable classes. A more important source of disagreement, however, was allocation and, in particular, exchange differences between the NDVI stable and EVI positive classes and NDVI negative and EVI stable. These results are important for at least two reasons. First, trend results computed from MODIS NDVI and EVI time series yield different results. This outcome corroborates the findings of Zhang et al. (2017), who reported significant differences between trend results based on NDVI and EVI image products acquired from the MODIS MOD13C2 and MYD13C2 satellites.

Comparison of NDVI and EVI-derived trend classes suggest that, overall, EVI results are more conservative in the identification of positive trends and slightly more likely to distinguish negative trends within relatively stable greenness trajectories. However, where important trend differences occur (allocation disagreement) support that the improvements in the EVI calculation that correct for atmospheric conditions, reduce canopy background noise, and saturation over dense vegetation are effective. "Greener" trend classes in the EVI output tend to occur in the east and south, in regions of higher grassland vegetation biomass, while "browner" classes typically are found in the south and west.

The overall grassland trend results reported here compare well to findings reported by similar studies, with some important differences. Zhang et al. (2017) analyzed global vegetation trends from 2001 to 2015 using the MODIS (MOD13C2 and MYD13C2) data products and noted greening was predominant in the Great Plains region. On the other hand, Lamchin et al. (2020) carried out a global vegetation greenness trend analysis from 1982 to 2014 using NDVI. The vegetation greenness trend results within the period of 2003 to 2014 in the Great Plains ecoregion show a negative trend predominantly. This result is unlike our findings. Also, Braget's 2017 study, which is similar to ours, was carried out in the Flint Hills Ecoregion from 2001 to 2015. The results showed a prominent browning compared to our results, with a majority greening trend in the same ecoregion using the same VI but with two additional years to the time series. The dissimilarity in these results compared

to ours demonstrates the impacts of time sensitivity on long-term trend analysis (Liebmann et al., 2010).

The variability of trend classes with different start and end dates is very important and should seriously be considered when carrying out this type of analysis. Since trends are estimated using values of a phenomenon (in this case, vegetation greenness) and time, the variation in the start and end dates could result in a "strong positive/negative" when the connection between the two variables is strong within the study time or a "weak positive/negative" when the connection the two variables is not very strong within the study time. So, if the first or last data used represents an abnormal year, drought, or wet period, this could overly influence the overall trend and skew the trend to be positive or negative. Liebmann et al. (2010) developed a method to determine the appropriate time frame where trend results are robust and representative of a long-term trend using global surface temperature. Based on the results of the study, changes around 20 years ending after about 2000 exceed the 95% significance level (using the student t-test); this indicates that results from this analysis are representative of a real, significant long-term trend.

Considering the expanse or extent of the Great Plains ecoregion, the major influence under greenness as a proxy for productivity is climate. We discussed the trends and patterns of key climate variables: temperature, precipitation, and soil moisture across the region and tied them to other factors that may impact grassland trends in smaller regions of the Great Plains. Climate is varied in this region, but because it is influenced by latitudes from north to south and elevation from east to west, each variable has apparent patterns (Tollerud et al., 2018). the Great Plains has a distinct north-south gradient and average temperature patterns with higher temperatures in the south and lower temperature and the not. On the other hand, the Great Plains has a distinct east-west gradient of average precipitation, with a wetter east and a dryer west (Shafer et al., 2014). The near-surface soil moisture patterns, which is a good proxy for both temperature and precipitation, are different. The region's middle is drier than the east and west ends based on the average annual surface soil moisture values from 1987 to 2016 (McDonough et al., 2020).

Regarding the trends of the climate variables discussed for the past two decades in the Great Plains, Precipitation has varied annually, but there has been overall increasing precipitation with more increase in the north than southern Great Plains (Conant et al., 2018; Kloesel et al., 2018).

Precipitation is also projected to keep increasing in the future. Like precipitation, the temperature has also been rising in the Great Plains with more increase in temperature in the south down the northern Great Plains, and temperature is also projected to keep rising (Kunkel et al., 2013; Conant et al., 2018). The soil moisture trend show and overall north-south gradient with a significant drying trend in the southern parts of the ecoregion (McDonough et al., 2020).

Comparing the trend of climate variables to the MODIS NDVI and EVI trend results, the increased browning trends prominent in the south and southeastern parts of the ecoregion can be attributed to the increasing temperature. Even though precipitation was generally increasing in this region in the time studied, the increasing temperature can lead to increased evapotranspiration reduce water availability for vegetation growth. Precipitation, temperature, and drought frequency are projected to increase in the Great Plains (Walsh et al., 2014). Despite the projected precipitation increase, projected increases in temperature and drought frequency will likely stress moisture availability for vegetation in the Great Plains.

Focusing on regions with distinct trend patterns, one of which is in Nebraska Sandhills ecoregion. The region has a predominantly greening trend and has the largest and most homogenous grassland expanse in North America. It also lies in the part of the region with the close to median temperature and precipitation values in the Great Plains. This region's average near-surface soil moisture is one of the lowest in the Great plains because it is predominantly sandy, but there is usually an abundance of groundwater reservoirs and wetlands that promotes vegetation growth, hence the greening trend (Tollerud et al., 2018; McDonough et al., 2020).

The Northwestern Great Plains ecoregion has similar trend patterns as the Nebraska Sandhills. The ecoregion borders the north of Nebraska cuts through the west of the Dakotas, then covers eastern Montana and northeastern Wyoming. The ecoregion had more areas with a negative trend than the Nebraska Sandhills. The areas with negative trends are close to the boundaries of the ecoregion, which borders the Rocky Mountains front. The region has less precipitation than Nebraska Sandhills and comes to play when considering the interplay of elevation, temperature, and precipitation (McDonough et al., 2020). Even though the region has less precipitation than the Nebraska Sandhills, the soil texture is primarily loamy and clay loam, hence more rainfall retention than the sandy Nebraska Sandhills. The predominant positive trend can be attributed to that. In addition, the areas

with negative trends are mainly close to the region's boundary, and those negative trends can be attributed to the fact that those regions are within the transition zone from the flat Great Plains to the higher-elevation Rocky Mountains. There is also a possibility those pixels are likely not grasslands or mixed.

Another distinct trend pattern in the ecoregion is the southern part of the study area that extends from the northeastern parts of New Mexico. It cuts across Texas, Oklahoma, and the southwestern parts of Louisiana. In the areas close to New Mexico, the temperature is high, but precipitation is very low; a combination of these two is evident in the drying surface soil moisture trend in this region, leading to a significant amount of the area having a negative trend or browning. The areas within Texas, Oklahoma, and Louisiana also have a significant portion with a browning trend. This area generally has high temperatures and precipitation, but the sun moisture trend in this area is also drying. Even though rainfall is high in this area, with high temperatures, it could result in excessive evapotranspiration leading to a general negative trend or browning of grasslands in this region.

3.5.2 Conclusions

Long-term studies on a major ecosystem are critical to achieving an integrated understanding of how components of ecosystems interact. The use of remotely-sensed VI time series for trend analysis using BFAST is a reliable and valuable method to characterize long-term trends in grasslands and other vegetation biomes. This study uses the MOD13Q1(C5) NDVI and EVI data to determine grassland vegetation greenness in the Great Plains over a 17-year interval. The description of both the overall and area-specific trends in the U.S. Great Plains can provide important information to aid decision-making in conservation, biodiversity, and sustainability-related policies.

Overall, our results show a prevalent greening trend within the time studied, indicating that vegetation greenness or productivity, as implied, increased over the study period. Our study also found, by comparing our results to climate patterns in the region, that this period was associated with the increasing precipitation and temperature trends. There is a north-south temperature gradient with higher temperatures and the south and east-west precipitation gradient with higher precipitation in the east after Great Plains. The gradients of these climatic variables influence the distinct trend patterns in various regions after the study area, with more browning trends in the southern and southeastern parts of the study area. This leads us to conclude that even though there was increasing

precipitation, overall high temperatures in the south have more influence on vegetation patterns than precipitation.

Comparing our results to similar studies conducted within the same region and within a similar time, there were some findings that were not similar to ours and a few that were similar to ours too, but the validation using higher resolution images provides confidence in interpreting the interannual trend results confirming the overall greening in the Great Plains (2001-2017). The comparison of our results to other studies with dissimilar findings can be attributed to a difference in the period of the time series that was analyzed. Meaning an additional or excluded couple of years can highly impact our trend results given that the major driver of vegetation trends – climate, is highly variable. This has led us to infer that climate change impacts are unpredictable; therefore, there is a need for continuous trend monitoring analysis (Lamchin et al., 2020).

We also explored the impact of using difference VI data for the trend analysis in this region. The difference between the NDVI and EVI results shows the prominent limitation of the NDVI: the saturation of values in areas with high biomass making pixels to be classified as stable, whereas in the EVI trend, they were classified as positive. The impact of saturation and less variation in high biomass areas can affect the classification into and the overall trend analysis. The EVI is thereby strongly recommended for long-term trend analysis in the Great Plains, especially in the tallgrass prairies.

The findings of this study suggest the need for additional analyses to quantify the influence of climate and soils, along with critical regional anthropogenic factors such as fire, on shaping long-term vegetation dynamics and estimate the impact on the values or services we acquire from grasslands in the ecoregion. To further assess the long-term condition of grassland in the U.S. Great Plains, follow on studies will look at the spatial patterns and trends of grassland phenology and how the trends reported in this work impact the provision of selected grassland-related ecosystem services within the U.S. Great Plains.

Acknowledgment

This work was partially supported by a KansasView Student Research Grant from the USGS-sponsored KansasView Consortium. Data processing capacity and hardware were provided by

Beocat, a high-performance computing cluster, and the Geographic Information Systems Spatial Analysis Laboratory (GISSAL) at Kansas State University.

3.6 References

Baghi, N. G. & Oldeland, J. (2015). *BFAST: A replacement of climate indicators for monitoring time-series using MODIS.* The XXIII International Grassland Congress (Sustainable use of Grassland Resources for Forage Production, Biodiversity and Environmental Protection). New Delhi, India. https://uknowledge.uky.edu/igc/23/1-2-1/2

Beck, H. E., Zimmermann, N. E., McVicar, T. R., Vergopolan, N., Berg, A., & Wood, E. F. (2018). Present and future Köppen-Geiger climate classification maps at 1-km resolution. *Scientific Data*, *5*, 180214. https://doi.org/10.1038/sdata.2018.214

Borak, J. S., Lambin, E. F., & Strahler, A. H. (2000). The use of temporal metrics for land cover change detection at coarse spatial scales. *International Journal of Remote Sensing, 21*(6–7), 1415–1432. https://doi.org/10.1080/014311600210245

Braget, R. B. (2017, Spring). *Time Series Analysis of Phenometrics and Long-Term Vegetation Trends for the Flint Hills Ecoregion using Moderate Resolution Satellite Imagery* [Master's thesis, Kansas State University]. https://krex.k-state.edu/dspace/handle/2097/35553

Browning, D. M., Maynard, J. J., Karl, J. W., & Peters, D. C. (2017). Breaks in MODIS time series portend vegetation change: verification using long-term data in an arid grassland ecosystem. Ecological applications: a publication of the Ecological Society of America, 27(5), 1677–1693. https://doi.org/10.1002/eap.1561

Cleveland, C. R., Cleveland, W. S., McRae, J. E., & Terpenning, I. J. (1990). STL: A seasonal trend decomposition procedure based on LOESS. *Journal of Official Statistics*, *6*(1), 3–33.

Comer, P. J., Hak, J. C., Kindscher, K., Muldavin, E., & Singhurst, J. (2018). Continent-Scale Landscape Conservation Design for Temperate Grasslands of the Great Plains and Chihuahuan Desert. *Natural Areas Journal, 38*(2), 196–211. https://doi.org/10.3375/043.038.0209

Conant, R. T., Kluck, D., Anderson, M., Badger, A., Boustead, B. M., Derner, J. D., Farris, L., Hayes, M. J., Livneh, B., McNeeley, S., Peck, D., Shulski, M. D., & Small, V. A. (2018). *Chapter 22: northern great plains. impacts, risks, and adaptation in the United States:*

the fourth national climate assessment, volume II. U.S. Global Change Research Program. https://doi.org/10.7930/NCA4.2018.CH22

DeAngelis, A., Dominguez, F., Fan, Y., Robock, A., Kustu, M. D., & Robinson, D. (2010). Evidence of enhanced precipitation due to irrigation over the Great Plains of the United States. *Journal of Geophysical Research*, *115*, D15115. https://doi.org/10.1029/2010JD013892

De Jong, R., Verbesselt, J., Schaepman, M. E., De Bruin, S. (2012). Trend changes in global greening and browning: contribution of short-term trends to longer-term change. *Global Change Biology*, 18, 642-655. http://dx.doi.org/10.1111/j.1365-2486.2011.02578.x.

Drummond, M. A., & Auch, R. F. (2015). Land-Cover Trends in the Great Plains of the United States—1973 to 2000. In J. L. Taylor, W. Acevedo, R. F. Auch, & M. A. Drummond (Eds.), *Status and Trends of Land Change in the Great Plains of the United States—1973 to 2000* (pp. 3–19). US Geological Survey.

Fang, X., Zhu, Q., Ren, L., Chen, H., Wang, K., & Peng, C. (2018). Large-scale detection of vegetation dynamics and their potential drivers using MODIS images and BFAST: A case study in Quebec, Canada. *Remote Sensing of Environment, 206*, 391–402. https://doi.org/10.1016/j.rse.2017.11.017

Forkel, M., Carvalhais, N., Verbesselt, J., Mahecha, M., Neigh, C., & Reichstein, M. (2013). Trend Change Detection in NDVI Time Series: Effects of Inter-Annual Variability and Methodology. *Remote Sensing, 5*(5), 2113–2144. https://doi.org/10.3390/rs5052113

Gauthier, D. A., Lafon, A., Toombs, T., & Wiken, E. (2003). *Grasslands: Towards a North American conservation strategy* (p. 127). Commission for Environmental Cooperation University of Regina. Canadian Plains Research Center.

Gergel, S. E. & Tuner, M. G. (1st eds). (2002). Learning landscape ecology: a practical guide to concepts and techniques. Springer-Verlag.

Gibson, D. J. (2009). *Grasses and grassland ecology* (1st ed., p. 320). Oxford University Press.

Heumann, B. W., Seaquist, J. W., Eklundh, L., & Jönsson, P. (2007). AVHRR derived phenological change in the Sahel and Soudan, Africa, 1982-2005. *Remote Sensing of Environment, 108*(4), 385–392. https://doi.org/10.1016/j.rse.2006.11.025

Homer, C., Dewitz, J., Yang, L., Jin, S., Danielson, P., Xian, G., Coulston, J., Herold, N., Wickham, J., & Megown, K. (2015). Completion of the 2011 National Land Cover Database for the

Conterminous United States – Representing a Decade of Land Cover Change Information. *Photogrammetric Engineering & Remote Sensing, 81*(5), 345–354.

Huete, A. R. (1988). A soil-adjusted vegetation index (SAVI). *Remote Sensing of Environment, 25*(3), 295–309. https://doi.org/10.1016/0034-4257(88)90106-X

Hutchinson, J. M. S., Jacquin, A., Hutchinson, S. L., & Verbesselt, J. (2015). Monitoring vegetation change and dynamics on US Army training lands using satellite image time series analysis. *Journal of Environmental Management,* 150, 355–366. https://doi.org/10.1016/j.jenvman.2014.08.002

Jacquin, A., Goulard, M., Hutchinson, J. M. S., Devienne, T., & Hutchinson, S. L. (2016). A Statistical Approach for Predicting Grassland Degradation in Disturbance-Driven Landscapes. *Journal of Environmental Protection, 07*(06), 912–925. https://doi.org/10.4236/jep.2016.76081

Jamali, S., Seaquist, J., Eklundh, L., & Ardö, J. (2012). *Comparing parametric and non-parametric approaches for estimating trends in multi-year NDVI.* First EARSeL Workshop on Temporal Analysis of Satellite Images, Mykonos, Greece.

Jeong, S. J., Ho, C. H., Gim, H. J., & Brown, M. E. (2011). Phenology shifts at start vs. end of growing season in temperate vegetation over the Northern Hemisphere for the period 1982-2008. *Global Change Biology, 17*(7), 2385-2399. https://doi.org/10.1111/j.1365-2486.2011.02397.x

Johnson, L., Cooke, B., Ramos, V. H., & Easson, G. (2008). *Use of NASA satellite assets for predicting wildfire potential for forest environments in Guatemala [preliminary report].* University of Mississippi Geoinformatics Center (UMGC), Mississippi State University, and National Council for Protected Areas, Guatemala. https://www.gri.msstate.edu/research/nasa_rpc/2005/Wildfire%20REPORT%20SUBMISSION_MSU_RPC05.pdf

Kunkel, K. E., Stevens, L. E., Stevens, S. E., Sun, L., Janssen, E., Wuebbles, D., Kruk, M. C., Thomas, D., Shulski, M., Umphlett, N. A., Hubbard, K. G., Robbins, K., Romolo, L., Akyuz, A., Pathak, T. B., Bergantino, T. R., & Dobson, J. G. (2013). *Regional Climate Trends and Scenarios for the US National Climate Assessment Part 4. Climate of the US Great Plains*, NOAA Technical Report NESDIS 142-4, 82 pp.

Lamchin, M., Wang, S. W., Lim, C.-H., Ochir, A., Pavel, U., Gebru, B. M., Choi, Y., Jeon, S. W., & Lee, W.-K. (2020). Understanding global spatio-temporal trends and the relationship between

vegetation greenness and climate factors by land cover during 1982–2014. *Global Ecology and Conservation*, 24, e01299. https://doi.org/10.1016/j.gecco.2020.e01299

Liebmann, B., Dole, R. M., Jones, C., Bladé, I., & Allured, D. (2010) Influence of choice of time period on global surface temperature trend estimates. *Bulletin of the American Meteorological Society*, *91*(11), 1485–1492. https://doi.org/10.1175/2010BAMS3030.1.

Mark, A. F., & McLennan, B. (2005). The conservation status of New Zealand's indigenous grasslands. *New Zealand Journal of Botany, 43*(1), 245–270. https://doi.org/10.1080/0028825X.2005.9512953

Matsushita, B., Yang, W., Chen, J., Onda, Y., & Qiu, G. (2007). Sensitivity of the Enhanced Vegetation Index (EVI) and Normalized Difference Vegetation Index (NDVI) to Topographic Effects: A Case Study in High-density Cypress Forest. *Sensors (Basel, Switzerland), 7*(11), 2636–2651. https://doi.org/10.3390/s7112636

McDonough, K. R., Hutchinson, S. L., & Hutchinson, J.M.S. (2020). Declining soil moisture threatens water availability in the US Great Plains. *Transactions of the ASABE, 63*(5): 1147-1156. https://doi.org/10.13031/trans.13773

Millennium Ecosystem Assessment [MEA]. (2005*). Ecosystems and human well-being: Synthesis* (2nd ed., p. 160). Island Press.

Oakleaf, J. R., Kennedy, C. M., Baruch-Mordo, S., West, P. C., Gerber, J. S., Jarvis, L., & Kiesecker, J. (2015). A world at risk: aggregating development trends to forecast global habitat conversion. *Plos One, 10*(10). https://doi.org/10.1371/journal.pone.013833

Omernik, J. M. (1987). Ecoregions of the Conterminous United States. *Annals of the Association of American Geographers, 77*(1), 118–125. https://doi.org/10.1111/j.1467-8306.1987.tb00149.x

Omernik, J. M., & Griffith, G. E. (2014). Ecoregions of the conterminous United States: evolution of a hierarchical spatial framework. Environmental Management, 54(6), 1249–1266. https://doi.org/10.1007/s00267-014-0364-1

Pendall, E., Bachelet, D., Conant, R. T., El Masri, B., Flanagan, L. B., Knapp, A. K., Liu, J., Liu, S. & Schaeffer, S. M. (2018). Chapter 10: Grasslands. In Cavallaro, N., G. Shrestha, R. Birdsey, M. A. Mayes, R. G. Najjar, S. C. Reed, P. Romero-Lankao, & Z. Zhu (eds.). *Second State of the Carbon Cycle Report (SOCCR2): A Sustained Assessment Report.(*pp. 399-427). US Global Change Research Program. https://doi.org/10.7930/SOCCR2.2018.Ch10.

Plowprint annual report (2021). World Wildlife Fund. Retrieved from https://files.worldwildlife.org/wwfcmsprod/files/Publication/file/5yrd3g00ig_PlowprintReport_2021_Final_HiRes_b.pdf?_ga=2.206397267.119456530.1640946732-1705276999.1640946731

Pontius Jr, R. G., & Millones, M. (2011). Death to Kappa: birth of quantity disagreement and allocation disagreement for accuracy assessment. *International Journal of Remote Sensing*, *32*(15), 4407–4429. https://doi.org/10.1080/01431161.2011.552923

Pontius Jr, R. G., & Santacruz, A. (2014). Quantity, exchange, and shift components of difference in a square contingency table. *International Journal of Remote Sensing*, *35*(21), 7543–7554. https://doi.org/10.1080/2150704X.2014.969814

PRISM Climate Group. (2019). *PRISM Climate Data*. Oregon State University. http://prism.oregonstate.edu

Ratajczak, Z., Briggs, J. M., Goodin, D. G., Luo, L., Mohler, R. L., Nippert, J. B., & Obermeyer, B. (2016). Assessing the Potential for Transitions from Tallgrass Prairie to Woodlands: Are We Operating Beyond Critical Fire Thresholds? *Rangeland Ecology & Management, 69*(4), 280–287. https://doi.org/10.1016/j.rama.2016.03.004

Ricketts, T. H., Dinerstein, E., Olson, D. M., Loucks, C. J., Eichbaum, W., DellaSala, D. A., Kavanagh, K., Hedao, P., Hurley, P., Carney, K., Abell, R. & Walters, S. (1999). *Terrestrial Ecoregions of North America: A Conservation Assessment* (1st ed.). Island Press.

Rossum, S., & Lavin, S. (2000). Where are the great plains? A cartographic analysis. *The Professional Geographer, 52*(3), 543–552. https://doi.org/10.1111/0033-0124.00245

Tarantino, C., Adamo, M., Lucas, R., & Blonda, P. (2016). Detection of changes in semi-natural grasslands by cross correlation analysis with WorldView-2 images and new Landsat 8 data. *Remote Sensing of Environment, 175*, 65–72. https://doi.org/10.1016/j.rse.2015.12.031

Taylor, J. L., Acevedo, W., Auch, R. F., & Drummond, M. A. (2015). *Status and Trends of Land Change in the Great Plains of the United States—1973 to 2000:* US Geological Survey Professional Paper 1794–B. United States: US Geological Survey. http://dx.doi.org/10.3133/pp1794B

The Economics of Ecosystems and Biodiversity [TEEB]. (2010). *The Economics of Ecosystems and Biodiversity: Mainstreaming the Economics of Nature: A synthesis of the approach, conclusions, and recommendations of TEEB*. Progress Press.

Tollerud, H., Brown, J., Loveland, T., Mahmood, R., & Bliss, N. (2018). Drought and Land-Cover Conditions in the Great Plains. *Earth Interactions, 22*(17), 1–25. https://doi.org/10.1175/ei-d-17-0025.1

U.S. Geological Survey. (2017). *1 Arc-second Digital Elevation Models (DEMs) - USGS National Map 3DEP Downloadable Data Collection*. https://www.usgs.gov/core-science-systems/ngp/tnm-delivery/gis-data-download

Verbesselt, J., Hyndman, R., Newnham, G., & Culvenor, D. (2010). Detecting trend and seasonal changes in satellite image time series. *Remote Sensing of Environment, 114*(1), 106–115. https://doi.org/10.1016/j.rse.2009.08.014

Walsh, J., Wuebbles, D., Hayhoe, K., Kossin, J., Kunkel, K., Stephens, G., Thorne, P., Vose, R., Wehner, M., Willis, J., Anderson, D., Doney, S., Feely, R., Hennon, P., Kharin, V., Knutson, T., Landerer, F., Lenton, T., Kennedy, J., & Somerville, R. (2014). *Ch. 2: our changing climate. climate change impacts in the United States: the third national climate assessment*. U.S. Global Change Research Program. https://doi.org/10.7930/J0KW5CXT

Wang, S., Lu, X., Cheng, X., Li, X., Peichl, M., & Mammarella, I. (2018). Limitations and Challenges of MODIS-Derived Phenological Metrics Across Different Landscapes in Pan-Arctic Regions. *Remote Sensing, 10*(11), 1784. https://doi.org/10.3390/rs10111784

Zhang, Y., Song, C., Band, L. E., Sun, G., & Li, J. (2017). Reanalysis of global terrestrial vegetation trends from MODIS products: Browning or greening? *Remote Sensing of Environment*, 191, 145–155. https://doi.org/10.1016/j.rse.2016.12.018

Chapter 4 -Time series analysis of phenometrics for the US Great Plains ecoregion using satellite-derived vegetation indices.

Abstract

Grasslands are one of the largest terrestrial ecosystems in the world. They are one of the most biodiverse and productive terrestrial biomes but receive very low levels of protection. The temperate grasslands in the United States are one of the most threatened grassland ecosystems, with almost 96% of the historical extent lost. In the bid to understand the dynamics of grassland in the Great Plains ecoregion of the United States, a time-series analysis of Moderate Resolution Imaging Spectrometer (MODIS) 16-day maximum value composite Enhanced Vegetation Index (EVI) data (MOD13Q1 Collection 5) to explore patterns of vegetation phenology and was used to assess long-term phenology trends across the region was performed. Using the program TIMESAT to extract key measures of vegetation phenological development from 2001 to 2017. Phenometrics of interest included (1) season length, (2) start of growing season, (3) end of growing season, (4) middle of growing season, (5) maximum NDVI value, (6) small integral, (7) left derivative, and (8) right derivative. The results show variation in phenological patterns across the region. The overall patterns show a shift to a later start, earlier end, and consequently a decrease in the growing season length, especially in the southern parts of the region. As shown in the small integral and maximum EVI, vegetation productivity has increased over many areas in the Great Plains ecoregion. To further assess the long-term condition of grassland in the U.S. Great Plains, follow-on studies will look at how the spatial patterns and trends of grassland phenology reported in this work impact the provision of selected grassland-related ecosystem services within the U.S. Great Plains. Future analyses will also seek to quantify the influence of climate and soils, along with key regional anthropogenic factors such as fire, on shaping long-term vegetation dynamics.

KEYWORDS: Grasslands, Phenometrics, EVI, Great Plains Ecoregion, and TIMESAT.

4.1 Introduction

4.1.1 Background and purpose

Grasslands are one of the largest biomes covering about 20 to 40 percent of the terrestrial earth surface (Blair et al., 2014; Briggs et al., 2005). They are highly biodiverse and productive, yet they are not adequately protected (Mark & McLennan, 2005; Ricketts et al., 1999). The grassland biome is considered the most at-risk natural land (Oakleaf et al., 2015). Generally, approximately 54 percent of grasslands worldwide are degraded (White et al., 2000). North America's temperate grasslands are the most altered grassland ecosystems (Finch & Dahms, 2004). The U.S. temperate grasslands are one of the most threatened, with almost 62% of the historical extent lost (Comer et al., 2018). The factors driving grassland degradation or loss are intricate, but they are generally a give-and-take between climatic factors and land use. They include changing precipitation/temperature patterns, burn frequency, invasion of non-native species (usually woody species), overgrazing, fragmentation, and conversion to other land use (Archer et al., 2017; Gibson, 2009; Ratajczak et al., 2016).

Not tackling these factors individually, it is crucial to know the general condition of grasslands because they are essential for agronomic and, more important ecological purposes (Briggs et al., 2005). They contribute to carbon sequestration through high carbon storage in their high-biomass roots, control erosion, help store groundwater, help with adequate nutrient cycling, are used for agro-fuel, are important for recreation or ecotourism, and are most popularly known to provide food for livestock (Cerdan et al., 2010; Inoue, 2017; Machovina & Feeley, 2017; O'Mara, 2012; Rumpel, 2011; West & Nelson, 2017). Long-term studies on a major biome like grasslands are critical to achieving an integrated understanding of how components of ecosystems interact and how the conditions of grasslands (degradation, restoration, loss, or conversion to other uses) may impact an ecosystem. However, relatively little is known about the long-term conditions of grasslands in the Great Plains ecoregion of the U.S. (which is predominantly grassland).

Vegetation phenology is the variation in seasonal patterns of vegetation growth in relation to climate (Cleland et al., 2007; Tan et al., 2011). Vegetation responds to even small climatic variations; hence, phenological records have been used to monitor climate change (Schwartz, 1994). Land surface phenology is the use of remote sensing data to study the timing of seasonal patterns of variation in vegetated land surfaces (Tan et al., 2011; Wang et al., 2018). The analysis of a time series of remotely

sensed imagery can be used to quantify temporal and spatial phenological changes hence phenological monitoring (Suepa et al., 2016).

In addition to satellite remote sensing, satellite image derived vegetation indices like the normalized difference vegetation index (NDVI) and the enhanced vegetation index (EVI) have been used to assess and monitor vegetation phenology successfully (Cui et al., 2017; Jeong et al., 2011; Reed et al., 2003; Suepa et al., 2016; Wang et al., 2016). The NDVI has shown a reliable correlation with vegetation dynamics in varying spatial scales, and the ratio concept reduces many sources of noise, but it has the limitation of saturation of values over areas with high biomass (Wang et al., 2018). The enhanced vegetation index (EVI) was developed to improve sensitivity in high-biomass areas and to further reduce atmospheric and soil influences (Matsushi et al., 2007). These characteristics, coupled with a recent recommendation from our previous work of a better performance in the Great Plains ecoregion, make it ideal for this study. MODIS-derived indices are suitable for monitoring vegetation phenology because they support a wide variety of phenology-related data products (i.e., NDVI, EVI, Leaf Area Index (LAI), and Albedo). Also, MODIS images are acquired daily, then composited into eight or sixteen-day products (Willis, 2015).

Phenological parameters or metrics (phenometrics from now on) like the start of the growing season (SOS) and end of the growing season (EOS) can be extracted from remotely sensed vegetation index time series using linear or non-linear fitting functions and models (Jönsson & Eklundh, 2004). The conventional method derives the phenometrics from a fitted curve identified by examining curve characteristics where VI data exhibit a rapid, sustained increase, decrease, and dormancy of increased value (Reed et al., 2003). The vegetation curve depicting the seasonal cycle of vegetation growth has varying definitions and terms for parameters or metrics used to measure the temporal changes in vegetation growth patterns (Figure 4.1). This study uses thresholds based on long-term average VI values to define phenometrics (Reed et al., 2003). TIMESAT software is a widely used method for analyzing time-series satellite sensor data (Jönsson & Eklundh, 2004). It provides five smoothing functions to fit time series data and extracts (up to 13) phenometrics from smoothed data; then, it uses an analytical indicator to define the start and end of the growing season (Eklundh & Jönsson, 2017; Zhang et al., 2003).

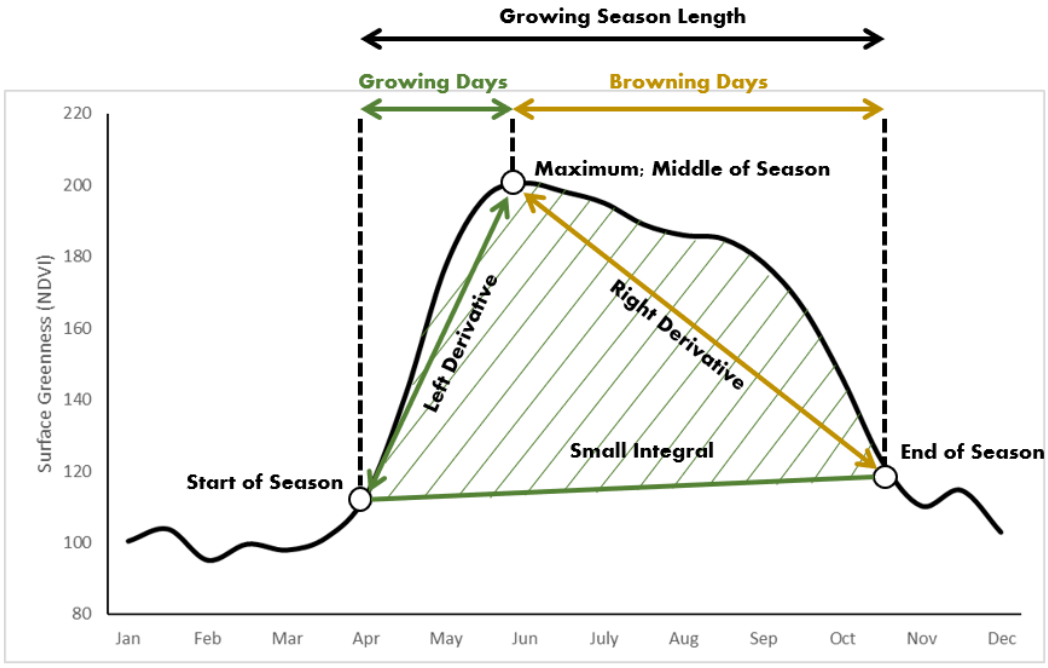

Figure 4.1: Typical temperate North American grassland phenology curve and some associated phenometrics generated in TIMESAT (Concept from Reed et al., 2003).

Some existing studies using satellite-derived time-series data to derive phenometrics include the following: Moulin et al.'s (1997) study on a global scale and focused on the broad category of vegetation, satellite-derived data (NDVI) was used to derive the main phenological stages of the vegetation including the start, the maximum, the end, and the length of the vegetation cycle. Results show that the start of the vegetation cycle was related to temperature sums in temperate deciduous forests and related to precipitation in savannahs. Jeong et al.'s (2011) study of the northern hemisphere also focused on the broad vegetation category. Results from the time-series analyses of long-term phenological trends in the northern hemisphere show a general earlier start of the growing season, later end of the growing season, and increased length of the growing season. In North America, existing studies focusing on grasslands are in Canada (Cui et al., 2017; McManus et al., 2012). Cui et al. (2017) examine the long-term drought-related variability of grassland phenology in relation to drought in the southwestern part of Canadian prairies in Alberta and Saskatchewan (part of the Great Plains) from 1982 to 2014. Results show that droughts do impact the timing of the start and of the growing cycle, with a shorter growing cycle with decreased precipitation. McManus et al.

(2012) used a time series of Landsat data to analyze the contrast in long-term climate-related phenology trend between forests and grasslands in northern Quebec province, Canada, between 1986 to 2010. The trend results, which indicate leaf area, show that the grasslands contributed more to the greening trend, while forested areas show less significant trends in NDVI. In the US, there are existing phenology studies in the forested northeastern US (Zhang et al., 2003), the grasslands of the northern Great Plains (Dunnell & Travers, 2011), and the grasslands of the Flint Hills (Braget, 2017). Zhang et al., 2003 examines vegetation phenology (2000-2001) in the northeastern US and southeastern Canada. Results show the northern parts of the study area had a later start of growing season than the southern parts. The end of growing season did not show significant spatial variations, however. Dunnell and Travers (2011) compared climate-associated phenological shifts of grasslands in the northern US Great Plains for the periods between 1910 to 1961 and 2007 to 2010. Results show and overall lengthened growing season with increasing temperatures. Braget (2017) examined the vegetation development using the phenology metrics of grasslands in the Flint Hills Ecoregion for the period starting from 2001 to 2015. The result shows a significant variation of vegetation development in the area.

This study's objective is to capture the spatiotemporal dynamics of grasslands phenology across the entire U.S. Great Plains. TIMESAT and a time-series of MODIS EVI images were used to extract key vegetation phenological development measures across the same period from 2001 to 2017 (the study period is based on data availability). The ANOVA and Tukey tests are employed to determine the significance of spatiotemporal differences in the phenometrics across the study area, and the Mann–Kendall trend test was utilized to determine the phenological trend of grasslands in the study area from 2001 to 2017.

4.2 Study area

The Great Plains region is the vast interior of North America running from Canada in the North to Mexico in the south and lies between east of the Rocky Mountains and west of the eastern temperate forests and the Appalachian Mountains (Rossum & Lavin, 2000). The Great Plains Ecoregion used for this study is defined by the United States Environmental Protection Agency (EPA) based on Omernik (1987) and Omernik and Griffith's (2014) classifications. The ecoregion classifications are based on patterns of geology, physiography, vegetation, climate, soils, land use, wildlife, and

hydrology affecting ecosystem quality (Omernik, 1987). The US EPA categorizes the area as a Level I ecoregion of the 15 coarsest level ecosystems in North America. In this ecosystem classification, the Great Plains has 4 level II divisions and 16 Level III subdivisions (Omernik & Griffith, 2014). The EPA Great plains cover approximately 2.8 million square kilometers, with more than 80 percent of this area in the US (about 2.2 square kilometers). The ecoregion is dominated by grasslands followed by agricultural lands, then other land uses (Drummond & Auch, 2015). This study, however, focuses only on grasslands in the Great Plains Ecoregion within the United States. The grassland area was defined by the grassland/herbaceous class of the United States Geological Survey's National Land Cover Dataset (NLCD) for 2011 (Homer et al., 2015). As defined for this study, the grassland area is approximately 825,000 square kilometers and covers 13 U.S. states (Figure 4.2). It contains a mixture of tallgrass prairie (east), mixed-grass prairie (north central), and short grass prairie (west).

Climate is also diverse in this region, influenced by latitudes from north to south and elevation from east to west (Tollerud et al., 2018). The Koppen-Geiger climate classifications within the Great Plains show the range from the cold (snow) climate in northwestern North Dakota, with warm, humid summers and long, cold, snowy winters, to the arid climate of Texas (Beck et al., 2018). Precipitation in the Great Plains is highly variable from year to year. Based on 30-year normal (1981-2010), precipitation ranges from 1500 mm in the southeastern portions of the Great Plains to 250 mm in the west, and annual mean temperature ranges from 0^0C in the north to 22^0C in the south (PRISM Climate Group, 2019). The Great Plains elevation is generally described as low lying, but it decreases from the foot of the Rocky Mountains in the west to the east in meters above sea level. The west edge with a maximum of 3610 meters above sea level in Colorado to more than 18230 meters in New Mexico but on the eastern edge, it reduces to an average of 200 meters from east Oklahoma to mid-Texas (U.S. Geological Survey, 2017).

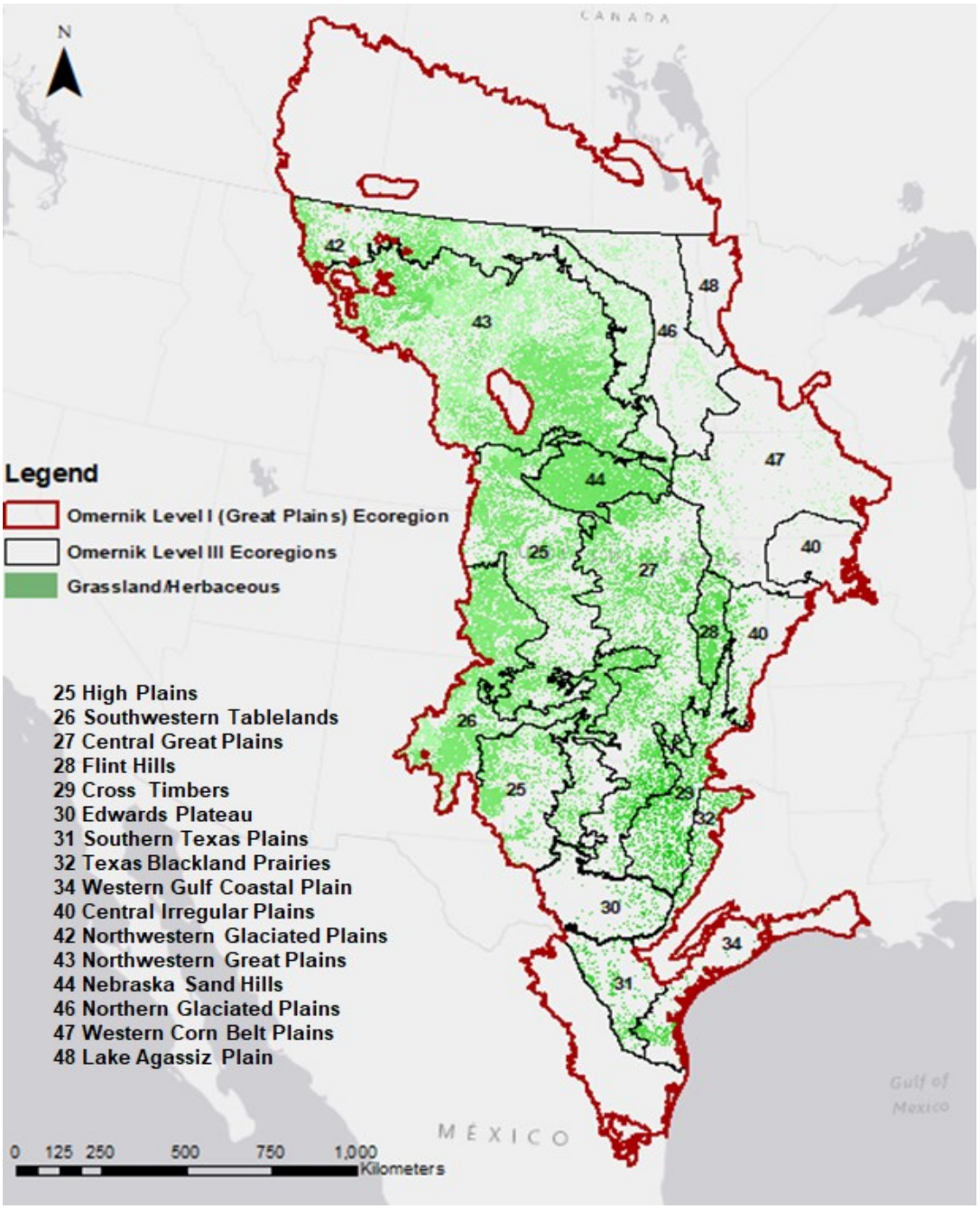

Figure 4.2: U.S. Great Plains study area showing Omernik level III ecoregions and grassland pixels extracted from the 2011 NLCD.

4.3 Methodology

4.3.1 Data and data preparation

The MODIS (MOD13Q1 Collection 6) 16-day maximum composite enhanced vegetation index (EVI) and pixel quality reliability products for the period of 2001 to 2017 were used in this study. Twenty-three composite images are produced per year, resulting in a total of 391 images for the study period. Images were downloaded from NASA's Earth Observation Data website (https://urs.earthdata.nasa.gov/) using the "MODIStsp" package (version 1.3.3) in R. The MODIStsp package is used to download MODIS HDF files automatically. The MOD13Q1 has a 250-meter spatial resolution. The scenes of the downloaded images that make up the study area were mosaiced and reprojected from their original sinusoidal projection to a more useful projection (the US Contiguous Albers Equal Area Conic projection). To extract the area of interest, pixels belonging to the "grassland/herbaceous" class of the 2011 NLCD data produced from a 30-meter spatial resolution were resampled to match the spatial resolution of the MOD13Q1 images. To address the potential for misidentifying a grassland pixel, resampled pixels included an 80% minimum of the original NLCD grassland/herbaceous class. This grassland mask was then used to extract the grassland pixels from the EVI data. After the extraction of the EVI grassland pixels, the resulting images were exported in a binary file format as required for processing in the software TIMESAT (version 3.3) used to extract the phenometrics. The MODIS products, just like all satellite-derived data, encounter some cloud and atmospheric contamination. To further reduce the effects, the pixel reliability data provided by the MOD13Q1 was used to assess the quality of the EVI pixels, and a Savitzky–Golay function was applied within the TIMESAT program to eliminate outliers and spikes. The pixel reliability data were assigned weights for each pixel (Table 1) to ensure the only good quality of pixels were processed. Of the pixels in the study area, 98.8% belong to the good data class, 0.7% belong to the marginal data class, 0.1% belong to the snow/ice class, 0.3% belong to the cloudy class, and no pixel was classified as 'No Data' (Table 4.1).

Table 4.1: MODIS MOD13Q1 pixel reliability values and weights applied within TIMESAT for the extraction of phenometrics.

Pixel Reliability Score	**Summary Quality Assurance Information**	**Description**	**Weight in TIMESAT**	**Percentage of pixels in each category**
-1	Fill/No Data	Not processed	0.0	0
0	Good data	Use with confidence	1.0	98.9
1	Marginal data	Useful, but depend on other QA information	0.5	0.7
2	Snow/Ice	Target covered with snow/ice	0.5	0.1
3	Cloudy	Target not visible, covered with cloud	0.1	0.3

4.3.2 Calculation of phenometrics

The TIMESAT program (Jönsson & Eklundh, 2004) graphical user interface was used to create time-series curves, select a smoothing method, and set associated parameters to estimate phenometrics for one pixel. The settings were then applied to other pixels. The parameters used are described in Table 4.2.

Table 4.2: TIMESAT input parameters

Parameters	**Input Values**	**Description (Eklundh & Jönsson, 2017)**
Job name	EVIWithQuality	Unique file name (identifiable and no spaces)
Image/series mode (1/0)	1	Image mode
Trend (1/0)	0	No
Use quality data (1/0)	1	Yes
Data file list/name	...\EviImagesDat\ file_list_full.txt	Input VI data list file (see appendix B-1 for content)
Quality file list/name	...\QualImagesDa t\file_list_full.txt	Input quality data list file
Image file type	3 = 32-bit real	Image file type representing a wide ranges of values
Byte order (1/0)	0	0 = little endian byte order
Image dimension (nrow ncol)	11634 7629	The number of rows in an image and the number of columns per row
Processing window (row start/stop; col start/stop)	1/11634; 1/ 7629	Window or sample pixels to process
No. of years and points per year	17 23	23 data points per year for 17 years
Data range	-10000 to 10000	Valid lower and upper data values
Quality 1 range and weight	0 0 1	Lower and upper quality data class 1 and its assigned weight (See Table 1)

Quality 1 range and weight	1 2 0.5	See Table 1
Quality 1 range and weight	3 3 0.1	See Table 1
Amplitude cutoff value	0.0	Low amplitude cutoff. Any series with amplitude lower than this values will not be processed
Debug (0-3)	0	Debug flag. 0 =do not print debug data
Output files (1/0 1/0 1/0)	1 1 0	1= create seasonality output, 1= create fitted data output, 0= original data
Use land cover (1/0)	0	None: due to single land-use class
Name of the land cover file	none	None was used
Spike method	1 (median filter)	The median filter method retains all raw data values and classifies significantly different from neighboring values as outliers.
Spike value	2	Weights from STL-decomposition
STL stiffness value	3	Default parameter value for STL trend stiffness.
Seasonality parameter	1 (one season)	Indicates one growing season per year in North America.
Number of envelope iteration	2	A value of 2 was determined to fit the raw data values within the region better.
Adaptation strength	2	A value of 2 was determined to eliminate very low VI values.
Force to minimum (1/0) and	1 and 0.15	1 = points below value of minimum given

value of minimum		minimum value will be forced to the specified minimum value.
Fitting method (3/2/1)	1 (Savitzky–Golay (SG) filter)	The SG sensitive to local variations in VI values, which is useful in regional comparisons.
Window size for SG	4	Half window for SG filtering. A large window value yields a high degree of smoothing
Start/end of season method	1 (seasonal amplitude)	Based on the curve.
Season start values	0.2	The value of 0.2 means a season start was identified when 25% of the maximum growing season amplitude is reached.
Season end values	0.2	Same as above

TIMESAT (3.3) extracts a total of 13 phenometrics for each pixel from a vegetation curve for a maximum of n-1 years in a time series. This study only examines 8 phenometrics (Table 4.3) for 16 seasons (17 years minus 1) because they can illustrate phenology changes in North America.

Table 4.3: Description of selected TIMESAT Phenometrics. Source: (Eklundh & Jönsson, 2017).

Phenometric	**Definition**	**Biological Significance**	**Unit**
Start of Season	Time for which the left edge has increased to a user-defined level measured from the left minimum level	Time of initial vegetation green-up	Day of the year from Jan 1
End of Season	Time for which the right edge has decreased to a user-defined level measured from the right minimum level	Time of initial vegetation senescence	Day of the year from Jan 1
Growing Season Length	Time from the start to the end of the season	Length of the growing season from green-up to senescence	Days
Middle of Season	Mean value of the times for which the left edge has increased to 80% level, and the right edge has decreased to 80% level	Time of the middle of the growing season	Day of the year from Jan 1
Maximum Value	The largest data value for the fitted function during the season	The highest VI value of the season	VI unit (unitless)
Left derivative	The ratio of the difference between the left 20% and 80% levels and the corresponding time difference	Rate of vegetation green-up	VI unit (unitless)

Right derivative	The absolute value of the ratio of the difference between the right 20% and 80% levels and the corresponding time difference	Rate of vegetation senescence	VI unit (unitless)
Small Integral	Integral of the difference between the function describing the season and the base level from season start to season end	Proxy for the relative amount of vegetation biomass while regarding minimum values	VI unit (unitless)

4.3.2.1 Phenometrics Extraction and Spatial Patterns

Seasonality parameters were extracted from the smoothed curves and processed to generate numerical phenometric data and converted to images using the TSF_seas2img program in TIMESAT. The mean values and standard deviation of 8 of the phenometrics of interest (Table 3.2) were calculated in a GIS to analyze and present a general view of the spatial patterns of seasonality in the study area over the period of 2001 to 2017.

4.3.3 Phenology trend analysis

The Mann–Kendall (MK) trend test and Sen's methods (De Beurs & Henebry, 2005; Helsel & Hirsch, 2002; Yue et al., 2002) were used to determine the phenological trends from 2001 to 2017. The test determines the significance of any changes (decrease or increase) according to the differences between observation pairs (annual seasons in this case). So, the differences between observations of a given year and those of a previous year result in positive or negative values as a reflection of positive or negative change, and the sum of these values specifies the strength and direction of a trend (Suepa et al., 2016). The Kendall rank correlation coefficient or score ranges from − 1 to + 1 with a value of + 1, meaning that a trend consistently increased (no decrease) during the time studied and vice versa for a value of – 1; a 0 value means there was no consistent trend (Davis et al., 2017). The statistical significance for phenological trends ($p < 0.05$) was computed using an MK significance test (Helsel

& Hirsch, 2002). So, pixels that had P values that are higher than 0.05 we excluded from the results presented.

4.3 Results

4.3.1 Spatial patterns of phenology

The spatial patterns of the 16-year (2001 to 2016) median values of the eight phenometrics of interest derived from EVI are shown in Figure 4.3 The median values were calculated because of the non-normal phenometrics values. The start of growing season (SOS) usually ranged from late January (day 30) to late July (day 210) (Figure 4.3). The early SOS dates usually occurred in the southern parts of the study area in the eastern parts of Texas. The predominant SOS dates were in May; there are also areas with June to July SOS dates across North Dakota, Nebraska, Colorado, and New Mexico.

The midpoint or middle of the growing season (MOS) usually ranges from late June (day 180) to the end of the year. Generally, the middle date of growing season in this region was between July and October. However, the middle dates in the southernmost edge of Texas and western New Mexico were in December. The later middle dates are close to the EOS dates in those regions, indicating a fast senescence rate. Also, the northwestern area of the study area had middle dates close to the EOS dates in those regions, indicating a fast senescence rate. The growing season's length varied across the ecoregion from north to south, with the growing season length increasing southwards (Figure 4.3).

The end of growing season (EOS) ranged from late June (day 180) to the end of the year (Figure 4.3). The early EOS dates usually occurred mostly in the western parts of the study area (Montana, parts of North Dakota and South Dakota, Wyoming, and Colorado). The rest of the study area has EOS dates that range from late October to the end of December and a few areas in the southernmost edge of Texas with EOS dates that extend into the next season or year. The growing season length usually ranged from 180 to 300 days. There were short growing seasons on the Northeastern axis that ranged from 60 to 120 days. The Mid to western axis had growing season lengths between 180 to 240 days and 240 to 300+ days in the south.

The left derivative is like the maximum EVI values in the ecoregion. Generally, values usually increased going from west to east (Figure 4.3), meaning that the areas in the east with higher grassland biomass usually experienced a longer or rather slower green-up rate than the western parts of the study area. The right derivative signifies the rate of senescence, and it also increases from west to east of the ecoregion (Figure 4.3). This means that the areas in the east with higher grassland biomass usually experienced a longer or rather slower senescence rate than the western parts of the study area. The east-west variation in senescence rates can be implied from the difference in the SOS, MOS, and EOS dates described earlier. The small integral indicates seasonally active vegetation, which is a proxy for vegetation biomass or productivity. The small integral was usually higher in the east than the western parts of the study area (Figure 4.3). The maximum EVI values vary from west to east of the study area, increasing eastwards (Figure 4.3). These showing values are like the prairie-type biomass and rainfall distribution in the ecoregion, also increasing eastward. The spatial pattern of the small integral was similar to the maximum EVI, right derivative, and left derivative phenometrics, which corresponds to vegetation types in the ecoregion.

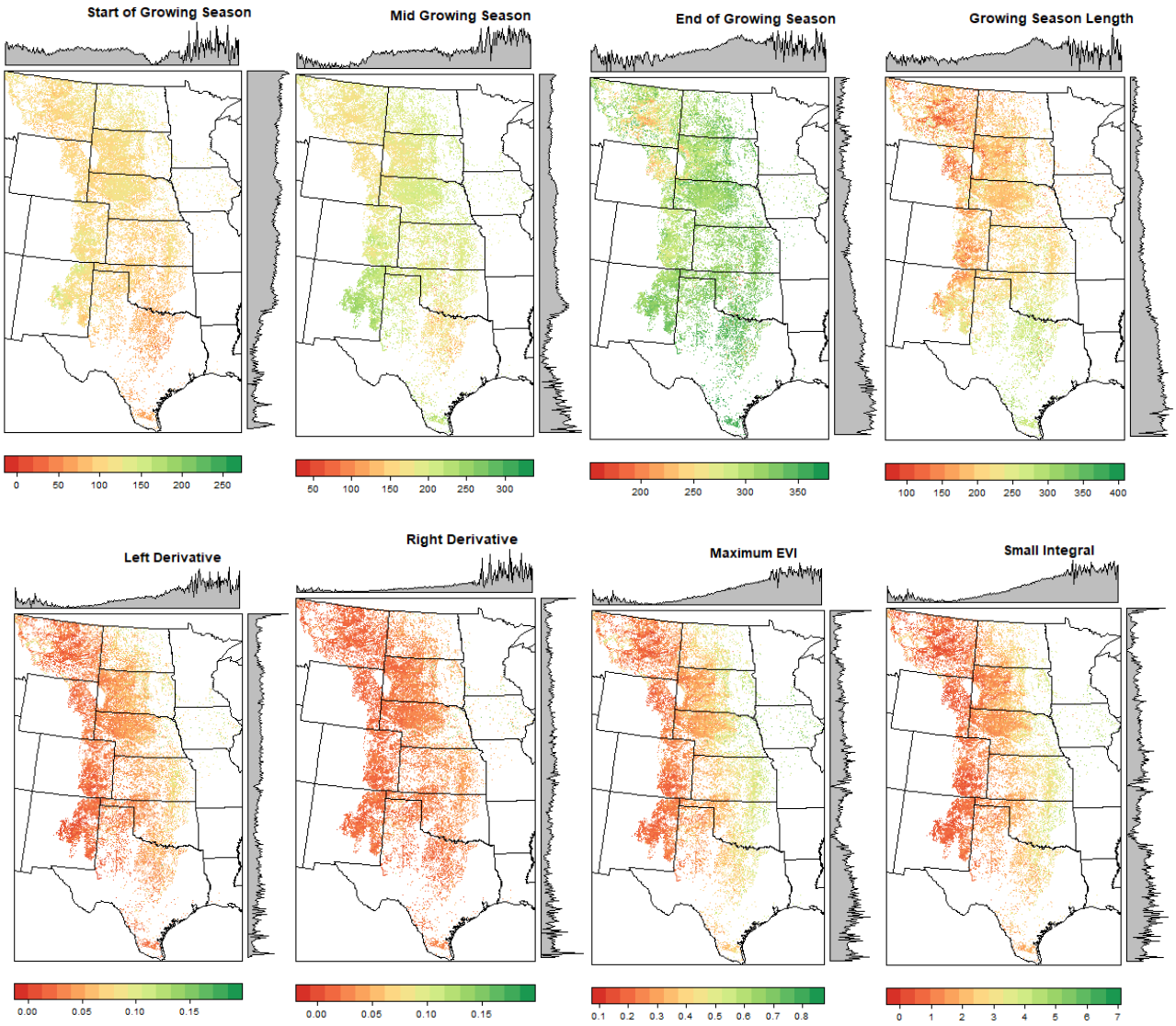

Figure 4.3: The median values of grassland phenometrics derived from MODIS (MOD13Q1) EVI data from 2001 to 2017 for the Great Plains ecoregion. Start, middle. and end of growing are in day of year. The growing season length is in days. The left/right derivatives, Maximum EVI and small integral are in VI values; they are unitless.

4.3.2. Phenology trends

The trends of phenology were processed by using the MK method. Trends in phenometrics were detected for the first 16 growing seasons during the period 2001 to 2017 at a 90% confidence level (α=0.05). Figure 4.4 shows the spatial distribution of significant overall trends, while table 4.4 shows the summary of results for trend analysis for the eight phenometrics of interest. In Figure 4, the pixels

with statistically significant increasing trends are shown in green (positive MK statistic score). The pixels with statistically significant decreasing trends are shown in red (negative MK statistic score), and pixels with a zero score were considered to have no trend are shown in grey. Positive and negative trends refer to later and earlier dates for the time-based phenometrics (SOS, MOS, EOS), longer and shorter lengths of growing seasons, as well as increased and decreased magnitudes for small integral and the rates of green-up/senescence.

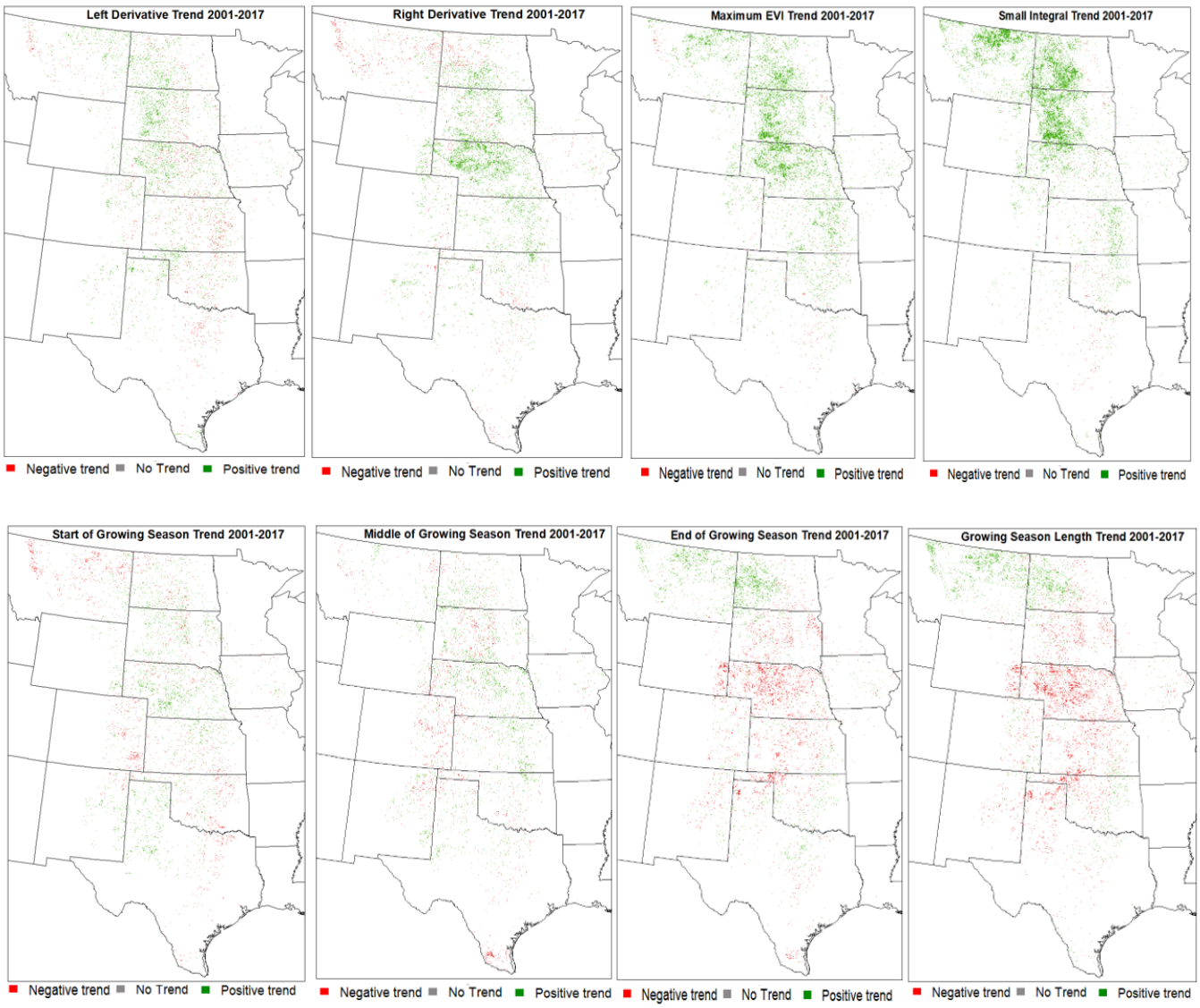

Figure 4.4: Trends in grassland phenometrics derived from MODIS (MOD13Q1) EVI data from 2001 to 2017 for the Great Plains ecoregion using the Mann Kendall trend test. Green pixels indicate a positive trend, red a negative trend, and grey pixels indicate no trend.

Table 4.4 shows a 65% positive trend (shift a later start date) and a 35% negative trend (shift an earlier start date) for the start of growing season. Overall, the portion of the study that has no trend (stable) is not significant (Table 4.4). The shift to a later start of the growing season is spread across the study area but more prominent in the northwestern and southeastern axis of the study area, while the shifts to an earlier start date close across the middle of the study area, specifically in South Dakota, Nebraska, Northern Kansas, and Northern Texas (Figure 4.4). The trends of the middle of growing season are similar to the start of start of the growing trends, in that there is a slightly higher percentage of the area with positive trends than negative trends. Approximately 65% of the area experienced a positive middle-of-season trend, and 35% had a negative trend. The spatial distribution of the MOS Trend is varied across the study area (Figure 4.4).

On the other hand, the end of growing season and growing season lengths had a slightly higher negative trend than positive trends. Table 4 shows 53% and 59% negative trends and 47% and 41% positive trends for EOS and GSL, respectively. This means that more of the area experienced a shift to earlier EOS dates than shifts to a later date, and for the growing season length, it means there is a slightly higher shift to a shorter growing season length than increasing growing season length. The shift to an earlier end of growing season trend is prominent in the middle and southern portion of the study area: South Dakota, Nebraska, Kansas, New Mexico, and Texas (Figure 4.4). In contrast, the North experienced a shift to later EOS dates. The spatial distribution of the GSL trends is similar to the EOS trends. It can be inferred that the shorter EOS dates in those regions led to a shorter growing season length (Figure 4.4).

The LDER and RDER represent the green-up and senescence rates. Table 4 shows a 23.5% and 16% negative trends and 77.5% and 84% positive trends for the LDER and RDER, respectively. This indicates that most of the study area experienced faster green-up and senescence rates within the time studied. Figure 4 shows that there has been a general increasing green-up rate, and this trend is spread across the study area but more prominent in the western axis of the study area. Decreasing increasing green-up rates occur in the Northwestern and southeastern parts of the study area. The decreasing senescence rates are particularly predominant over the northern and southern regions (Montana, North Dakota, New Mexico, and Texas); however, some areas in the central area (Nebraska and Kansas) experienced an increase in the senescence rates (Figure 4.4).

The maximum EVI and Small Integral are proxies for vegetation productivity within the growing season. The two phenometrics trends show similarity, with approximately 95% of the area having a positive trend for both phenometrics (Table 4.4). This trend s means that there was generally increasing productivity or biomass in the time studied. The spatial pattern of both phenometrics trends is similar too (Figure 4). The maximum EVI and small integral have increased significantly over areas in the Great Plains ecoregion extending from the northern to the central region while the southern region shows decreasing trends (Figure 4.4).

Table 4.4: Summary of results for trends in phenometrics derived from MODIS (MOD13Q1) EVI data from 2001 to 2017 for the Great Plains ecoregion using the Mann Kendall trend test.

Phenometric	**Negative trend**		**No trend**		**Positive trend**	
	Number of pixels	Percent of total	Number of pixels	Percent of total	Number of pixels	Percent of total
SOS	280545	34.9	2	0.0	523922	65.1
MOS	291770	35.2	6	0.0	538140	64.8
EOS	649557	52.6	7	0.0	585108	47.4
GSL	782916	58.6	5	0.0	553391	41.4
LDER	226048	22.5	15	0.0	779990	77.5
RDER	193848	15.6	10	0.0	1047024	84.4
MAX EVI	88105	5.0	5	0.0	1676028	95.0
SINT	94307	0.05	3	0.0	1988156	95.5

4.4 Discussion

The results from the time-series analysis of phenometrics provide a summary of the vegetation phenology, productivity patterns, and their trends in the Great Plains Ecoregion for the period 2001 to 2017. Characterizing the long-term vegetation phenology and productivity is important because it provides a spatially explicit summary of grassland vegetation dynamics across the ecoregion,

providing information to efficiently understand change which should be of interest not only to land managers and owners within the ecoregion but policymakers and other researchers. The phenometrics derived from MODIS (MOD13Q1) EVI data and defined by TIMESAT were able to capture the spatial patterns of vegetation dynamics across the Great Plains ecoregion. There are no existing similar field-based studies in the Great Plains, but Suepa et al. (2016) used the same data and method for vegetation in Southeast Asia and found great agreement between the results from satellite-derived phenology and field-based phenology. So, we are confident in our results.

The summary of the grassland phenometrics in the Great Plains ecoregion between 2001 and 2017 are as follows: the average start of growing season was day 105, the average middle of growing season was day 189, the average end of growing season was day 313, and average growing season length was 204 days. Values of these time-based phenometrics do not have much variation across the ecoregion, with the coefficient of variation values ranging from 0.1 to 0.2. For the VI-based phenometrics, the average left derivative value was 0.04, the average right derivative value was 0.03, the average maximum EVI value was 0.34, and the average small integral was 1.75. The values of the VI-based phenometrics vary greatly across the ecoregion, with the coefficient of variation values ranging from 0.3 to 0.6.

The trend of the time-based phenometrics for grasslands in the Great Plains between 2001 and 2017 showed a predominant move to a later start of growing season, a later middle of growing season, an earlier end of growing season, and a shorter growing season. There were also increasing rates of green-up and senescence, including increasing productivity as seen in the maximum EVI and small integral trends.

The observed spatio-temporal patterns and trends of the phenometrics studied varied across the ecoregion. There were several distinct patterns in various regions for the observed spatial patterns of the time-based phenometrics (Figure 4.5). The observed pattern indicates a longitudinal separated regions at the 100°W. In the 19th century, John Wesley Powell, introduced the idea that the 100th meridian divides the North American continent into arid regions in the west and humid regions in the east (Seager et al., 2018). Seager et al. (2018) in their 2018 study confirms an obvious west-east gradient in aridity roughly at the 100°W that is expressed in hydroclimate, soil moisture, and as a result, vegetation.

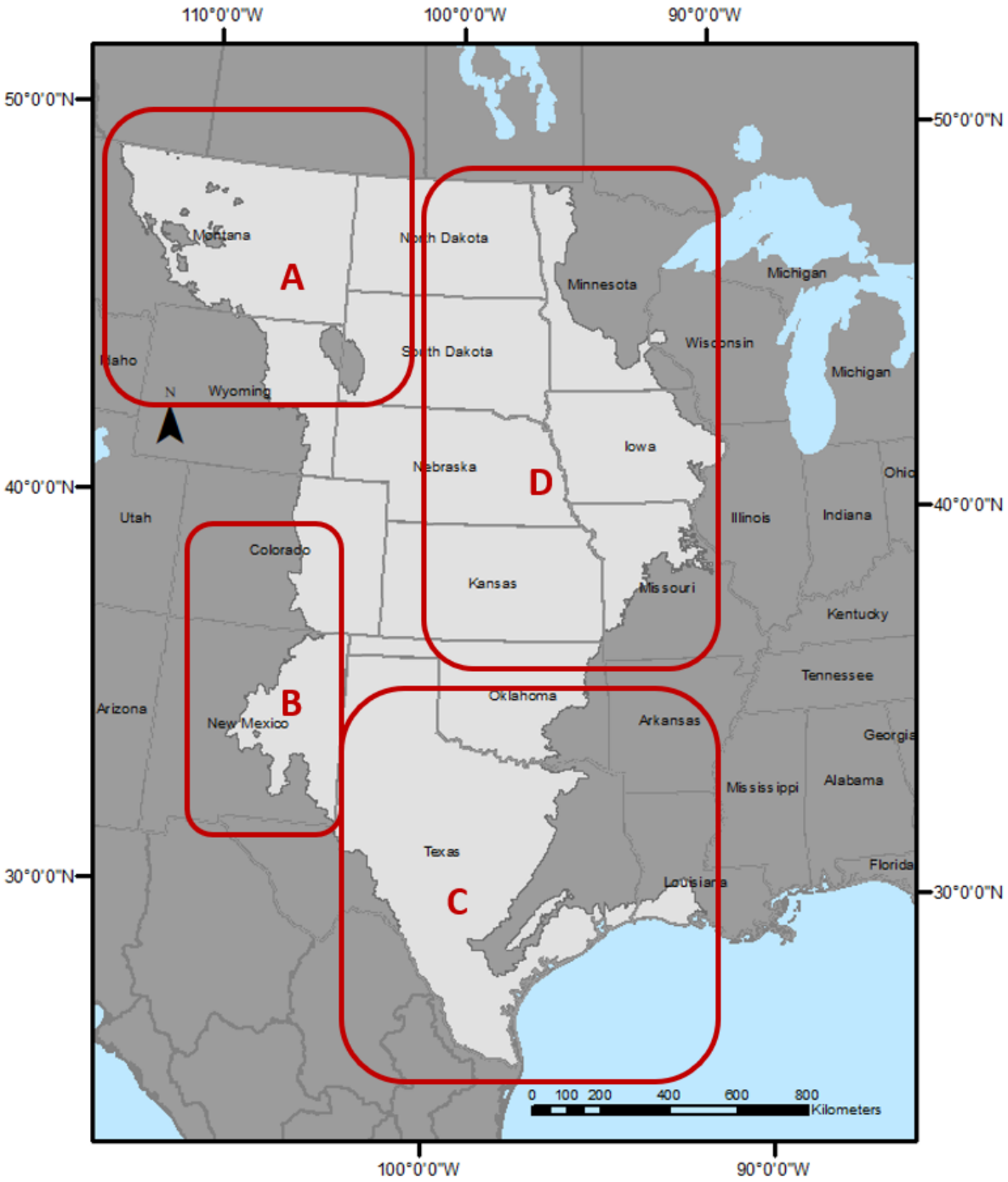

Figure 4.5: Observed regions of distinct spatial patterns for the 2001 to 2017 phenometrics in the Great Plains

In region A, the Northeastern corner of the ecoregion (Montana, Wyoming, the west of North Dakota, and west of South Dakota), the start of growing season ranges from day 60 to day 100 (March to

April), the middle of the growing season ranges from day 150 to 210 (June to July), there is a lot of variation in the end of growing season in this region, with values as low as 210 (July) to values as high as 350 (December). The region has one of the shortest growing season lengths in the entire Great Plains ecoregion, with season length values ranging from 100 to 200 days. For the VI-based phenometrics, there are generally lower values of maximum EVI, green-up rate, senescence rate, and relative amount of grassland biomass in this region compared to the rest of the Great Plains. The temporal trend for grassland phenometrics between 2001 and 2017 in this region includes a predominant move to an earlier start of growing season, an earlier middle of growing season, a predominant move to a later end of growing season, and an increased growing season length. Overall, there were increasing green-up rates, decreasing senescence rates, and increasing vegetation productivity (Max EVI and small integral).

In region B (New Mexico, Northwest Texas, and Colorado), the time-based phenometrics have overall later dates than region A. The start of growing season dates goes up to day 200 (July), the middle of the growing season ranges from day 200 to day 270, and the end of growing season ranges from day 300 to a few pixels of day 365. The growing season length is like that of region A, except for some areas (in the south of region B) that have longer growing season lengths up to 270 days. The VI-based phenometrics are not very different from region A. A general east-west gradient is obvious, with higher values in the east. The temporal trend of phenometrics from 2001 to 2017 in the region showed a predominant move to a later start of growing season, an earlier move to an earlier middle of growing season, an earlier end of growing season, and a decreased growing season length. There was an overall increasing green-up rate, senescence rate, and productivity in this region.

In region C (Most of Texas except the northwest area and southern Oklahoma), the time-based phenometrics have overall earlier dates for the start and middle of growing season and later dates for the end of growing season than other regions. The earlier start/middle of growing season and later end of growing season makes it the region with the longest growing season length (between 270 to 350 days). For the VI-based phenometrics, the green-up and senescence rates are not very different from regions A and B, but the productivity phenometrics (maximum EVI and small integral) show an east gradient with higher values in the east. The temporal trend of phenometrics from 2001 to 2017 in the region showed a predominant move to a later start of growing season except for the east end of the region (east Texas and Oklahoma). Also, a predominant move to an earlier middle of growing

season and end of growing season, and a decreased growing season length. There was an overall decreasing green-up rate, senescence rate, and productivity in this region.

In region D (Eastern parts of North Dakota and South Dakota, Minnesota, Iowa, Nebraska, Kansas, northern Texas, and northern Oklahoma), the start of growing season dates is more varied than other regions, with the day of the year ranging from 20 to 180. The middle of growing season dates are earlier than regions A and C but later than region B, and the end of growing season dates are very close to the end of the season (day 300 to day 365) like regions B and C. The growing season length in this region is also varied but generally longer than regions A and B but shorter than region C. The VI-based phenometrics show a general east-west gradient is apparent with higher values in the east. This means that this region has the highest green-up rate, senescence rate, and productivity values. The temporal trend of phenometrics from 2001 to 2017 in the region showed a predominant move to an earlier start of growing season, and a move to an earlier middle of growing season, a later end of growing season, and a decreased growing season length. The region shows the most decreasing growing season length compared to other regions. There was an overall increasing green-up rate, senescence rate, and productivity in this region.

We compared our findings of phenology and phenology trends in the Great Plains to other phenology studies carried out in a similar area and time. Wang et al. (2016) studied the spatial variability and temporal trends of vegetation phenology in the Northern hemisphere between 1982 and 2012, focusing on time-based phenometrics (start, middle, end, and length of growing season). Liang et al. (2021) analyzed the temporal trends of vegetation phenology across the contiguous U.S. between 1982 and 2016, focusing on time-based phenometrics (start, end, and length of growing season). Their results show that the start of growing season became predominantly earlier, the end of growing season became later, and the season length was shorter in the Great Plains region. These trends (start, middle, and end of growing season) disagree with our findings, but a shortening season length is similar to our results. There are some disparities in comparison that can be attributed to the study period difference. Liebmann et al. (2010) developed a method to determine the appropriate time frame where trend results are robust and representative of a long-term trend. Results of the study suggest a 20-years period. So, the longer time series you used in this study (2001-2017) compared to Wang's (2002-2012) should impact the difference in findings. Comparing Wang et al. (2016) results that coincide with the spatial (latitudinal) and period (2002-2012) of ours to our findings, there was an

overall shift towards a later start and middle of growing season, a shift toward an earlier end of growing season and shift to a shorter growing season length. These trends are similar to the findings reported here.

To understand the spatio-temporal patterns of vegetation phenology in the region, we drew connections between our results and key climate variables temperature, precipitation, and soil moisture. Other factors like land-cover changes and sea surface temperature may also contribute to changes in vegetation phenology (Jeong et al., 2011). In addition to latitudinal variation, other geographic factors like elevation and the proximity to water bodies contribute to the climatic variability in the Great Plains. But the Great Plains has a distinct north-south gradient and average temperature patterns with higher temperatures in the south and lower temperature in the north. On the other hand, the Great Plains has a distinct east-west gradient of average precipitation, with a wetter east and a drier west (Shafer et al., 2014).

The spatial patterns of the time-based phenometrics (SOS, EOS, MOS, and growing season length) reflect the influence of temperature. There is an overall north-south gradient with earlier SOS and later EOS days in the south, resulting in a longer growing season length in the south than in the north. According to the 2018 National Climate Assessment for the northern and southern Great Plains, the average temperature trends in the Great Plains indicate increasing temperatures since the 1900s (especially in the northern Great Plains), with the most recent years being the warmest (Conant et al., 2018). Temperatures in the Great Plains are projected to continually increase by 3.5^0F to 9.5^0F by 2085, even with low emission scenarios, with the greatest warming expected in the northern states of the region (Kunkel et al., 2013). The number of maximum/extreme temperature days exceeding the current hottest days is expected to increase, and the number of minimum ($>10^0$F) temperature days is expected to reduce (Kunkel et al., 2013; Shafer et al., 2014).

The spatio-temporal patterns of the VI-based phenometrics (green-up rate, senescence rate, maximum EVI, and small integral) reflect the influence of precipitation. They all show a west-east gradient with lower values in the west and higher values in the east. The Great Plains Ecoregion has experienced increasing precipitation in the last two decades, and the increased precipitation has been more prominent in the northern Great Plains (Conant et al., 2018; Kloesel et al., 2018). Precipitation is projected to increase (by 3% at the end of the century) during the winter and spring in the northern

and central Great Plains. Heavy rainfalls and snowfalls are also projected in the north and central Great Plains. Winter and spring precipitation is projected to decrease in the southern Great Plains. A lesser amount of summer rainfall is projected throughout the region, but it will be worse in the south with longer periods without rainfall (Walsh et al., 2014).

McDonough et al. (2020) studied near-surface soil moisture trends in the Great Plains ecoregion from 1987 to 2016, and the trends in soil moisture showed an overall north-south gradient with significant negative or drying trends in the southern parts of the ecoregion. The study factored in elevation and soil texture, temperature and precipitation, but temperature had the most influence on soil moisture trends within the time studied. The influence of temperature is also evident in our time-based phenometrics and phenology trends. Therefore, it is concerning data projected increase in temperature might severely change the growing patterns of grasslands in the region and impact the ecosystem. Even though precipitation is projected to increase, rising temperatures will lead to increased evapotranspiration and reduce water availability for vegetation growth. Based on the increasing temperature and precipitation trends (coupled with increasing atmospheric carbon dioxide concentrations), Conant et al. (2018) forecasted an increase in soil water availability during the primary growing season in the north and a decrease in the south. These forecasted conditions will alter vegetation phenology and increase the amount and competitiveness of invasive species for the ecoregion. The impact of climatic variables like temperature and precipitation on grasslands can be evaluated or assessed by analyzing the services provided by grassland ecosystems to humans, thereby known as ecosystem services. A temporal analysis of ecosystem value can highlight the impact of changing grasslands conditions.

4.5 Conclusions

Understanding long-term seasonal patterns of vegetation activity is critical to studying inter-annual variability, monitoring land degradation, and the impact of climate change in biomes like grasslands. The use of a high temporal and adequately spatial resolution remotely sensed VI data is a reliable and valuable method to characterize long-term trends in grasslands and other vegetation biomes. The characterization and evaluation of changes in vegetation grassland in the Great Plains ecoregions over the period of 16 growing seasons is presented in this study. The results show variation in vegetation phenology and productivity across the Great Plains over the last two decades. There was generally a

later or delayed start of season dates, a later middle growing season, and earlier end of season dates, resulting in shorter growing season lengths; vegetation productivity was usually increasing during the period. This is similar to Hufkens et al.'s (2016) findings.

Changing climate alters vegetation phenology. The impact of climate on the grassland phenology and phenology trends was obvious from the comparison of our results to climate variables such as temperature, precipitation, and soil moisture. There was an overall rising temperature and increasing precipitation in the time studied. The time-based phenometrics showed patterns that indicate a dominant temperature influence, and the VI-based phenometrics showed patterns that imply a dominant precipitation influence. Overall, temperature had the most significant impact on phenology patterns and trends in the ecoregion. Even though the growing season periods in the Great Plains are becoming shorter from increasing temperatures, the combination of the trends of the climatic variables examined resulted in improving or increasing greenness. Temperature is projected to keep rising in the ecoregion as well as precipitation. But in most parts of the study region, precipitation is projected to decrease in the summer, which is the peak of the growing season. It would be interesting to see how these climatic variables come into play to impact grassland conditions in the ecoregion in the future.

The results presented in this study provide important baseline information on the dynamics of grasslands in the Great Plains that will provide a benchmark for assessing future change in the region. Such information is important in aiding decision making in conservation, biodiversity, and sustainability-related policies for land managers because the result of this study has significant implications of long-term changes in vegetation phenology, gross primary production and affect the carbon cycle, water cycle, and energy fluxes through photosynthesis and evapotranspiration (Xiao et al., 2009). These impacts may subsequently influence food security, water resource availability, and climate (Suepa et al., 2016).

To further assess the long-term condition of grassland in the U.S. Great Plains, follow-on studies will look at how the spatial patterns and trends of grassland phenology reported in this work impact the provision of selected grassland-related ecosystem services within the U.S. Great Plains. Future

analyses to complement this work would be to understand the role of land-use change, climate change, and soils, along with other regional anthropogenic factors such as fire, on shaping long-term vegetation dynamics in the region.

Acknowledgment

This research was funded by the Kansas State University Department of Geography and Geospatial Sciences' Graduate Research Grant (GGRG) and the Phi Kappa Phi's 2020 Love of Learning Award. Also, special thanks to the Geographic Information Systems Spatial Analysis Laboratory (GISSAL) at Kansas State University for providing the computational capacity for processing the large volume of data used for this analysis.

4.6 References

Archer, S. R., Andersen, E. M., Predick, K. I., Schwinning, S., Steidl, R. J., & Woods, S. R. (2017). Woody Plant Encroachment: Causes and Consequences. In D. D. Briske (Ed.), *Rangeland systems: Processes, management, and challenges* (pp. 25–85). Springer.

Beck, H. E., Zimmermann, N. E., McVicar, T. R., Vergopolan, N., Berg, A., & Wood, E. F. (2018). Present and future Köppen-Geiger climate classification maps at 1-km resolution. *Scientific Data*, 5, 180214. https://doi.org/10.1038/sdata.2018.214

Blair, J., Nippert, J., & Briggs, J. (2014). Grassland Ecology. In R. K. Monson (Ed.), *Ecology and the environment* (pp. 389–423). Springer New York. https://doi.org/10.1007/978-1-4614-7501-9_14

Braget, R. B. (2017, Spring). *Time series analysis of phenometrics and long-term vegetation trends for the Flint Hills ecoregion using moderate resolution satellite imagery* [Master's thesis, Kansas State University]. https://krex.k-state.edu/dspace/handle/2097/35553

Briggs, J. M., Knapp, A. K., Blair, J. M., Heisler, J. L., Hoch, G. A., Lett, M. S., & McCarron, J. K. (2005). An ecosystem in transition: Causes and consequences of the conversion of mesic grassland to shrubland. *BioScience*, 55(3), 243–254.

Cerdan, O., Govers, G., Le Bissonnais, Y., Van Oost, K., Poesen, J., Saby, N., Gobin, A., Vacca, A., Quinton, J., Auerswald, K., Klik, A., Kwaad, F. J. P. M., Raclot, D., Ionita, I., Rejman, J., Rousseva, S., Muxart, T., Roxo, M. J., & Dostal, T. (2010). Rates and spatial variations of soil erosion in Europe: A study based on erosion plot data. *Geomorphology*, 122(1–2), 167–177. https://doi.org/10.1016/j.geomorph.2010.06.011

Cleland, E. E., Chuine, I., Menzel, A., Mooney, H. A., & Schwartz, M. D. (2007). Shifting plant phenology in response to global change. *Trends in Ecology & Evolution*, 22(7), 357–365. https://doi.org/10.1016/j.tree.2007.04.003

Comer, P. J., Hak, J. C., Kindscher, K., Muldavin, E., & Singhurst, J. (2018). Continent-Scale landscape conservation design for temperate grasslands of the Great Plains and Chihuahuan desert. *Natural Areas Journal*, 38(2), 196–211. https://doi.org/10.3375/043.038.0209

Conant, R. T., Kluck, D., Anderson, M., Badger, A., Boustead, B. M., Derner, J. D., Farris, L., Hayes, M. J., Livneh, B., McNeeley, S., Peck, D., Shulski, M. D., & Small, V. A. (2018). *Chapter 22: northern great plains. impacts, risks, and adaptation in the United States:*

the fourth national climate assessment, volume II. U.S. Global Change Research Program. https://doi.org/10.7930/NCA4.2018.CH22

Cui, T., Martz, L., & Guo, X. (2017). Grassland phenology response to drought in the Canadian prairies. *Remote Sensing*, 9(12), 1258. https://doi.org/10.3390/rs9121258

Davis, C. L., Hoffman, M. T., & Roberts, W. (2017). Long-term trends in vegetation phenology and productivity over Namaqualand using the GIMMS AVHRR NDVI3g data from 1982 to 2011. *South African Journal of Botany*, 111, 76–85. https://doi.org/10.1016/j.sajb.2017.03.007

DeAngelis, A., Dominguez, F., Fan, Y., Robock, A., Kustu, M. D., & Robinson, D. (2010). Evidence of enhanced precipitation due to irrigation over the Great Plains of the United States. *Journal of Geophysical Research*, 115, D15115. https://doi.org/10.1029/2010JD013892

De Beurs, K. M., & Henebry, G. M. (2005). A statistical framework for the analysis of long image time series. *International Journal of Remote Sensing*, 26(8), 1551–1573. https://doi.org/10.1080/01431160512331326657

De Castro, A., Six, J., Plant, R., & Peña, J. (2018). Mapping crop calendar events and phenology-related metrics at the parcel level by Object-Based Image Analysis (OBIA) of MODIS-NDVI Time-Series: A case study in central California. *Remote Sensing*, 10(11), 1745. https://doi.org/10.3390/rs10111745

Drummond, M. A., & Auch, R. F. (2015). Land-cover trends in the Great Plains of the United States—1973 to 2000. In J. L. Taylor, W. Acevedo, R. F. Auch, & M. A. Drummond (Eds.), *Status and trends of land change in the Great Plains of the United States—1973 to 2000* (pp. 3–19). US Geological Survey.

Dunnell, K. L., & Travers, S. E. (2011). Shifts in the flowering phenology of the northern Great Plains: patterns over 100 years. *American journal of botany*, 98(6), 935–945. https://doi.org/10.3732/ajb.1000363

Eklundh, L., & Jönsson, P. (2017). *TIMESAT 3.3 with seasonal trend decomposition and parallel processing - Software Manual*. Lund University. http://web.nateko.lu.se/timesat/timesat.asp?cat=6

Finch, D. M., & Dahms, C. W. (2004). Purpose and Need for a Grassland Assessment. In D. M. Finch (Ed*.), Assessment of grassland ecosystem conditions in the southwestern United States*: Vol. GTR-135 (pp. 1–11). US Dept. of Agriculture, Forest Service, Rocky Mountain Research Station.

Gauthier, D. A., Lafon, A., Toombs, T., & Wiken, E. (2003). *Grasslands: Towards a North American conservation strategy* (p. 127). Commission for Environmental Cooperation University of Regina. Canadian Plains Research Center.

Gibson, D. J. (2009). *Grasses and grassland ecology* (1st ed., p. 320). Oxford University Press.

Helsel, D., & Hirsch, R. (2002). *Statistical methods in water resources techniques of water resources investigations*, Book 4, chapter A3 (first (eBook), p. 522). United States Geological Survey.

Henebry, G. M. (2003). Grasslands of the North American Great Plains. In: Schwartz M.D. (eds) *Phenology: An integrative environmental science*. Tasks for Vegetation Science, vol 39. Springer, Dordrecht. https://doi.org/10.1007/978-94-007-0632-3_11

Homer, C., Dewitz, J., Yang, L., Jin, S., Danielson, P., Xian, G., Coulston, J., Herold, N., Wickham, J., & Megown, K. (2015). Completion of the 2011 National Land Cover Database for the conterminous United States – Representing a decade of land cover change information. *Photogrammetric Engineering & Remote Sensing*, 81(5), 345–354.

Hufkens, K., Keenan, T. F., Flanagan, L. B., Scott, R. L. Bernacchi, C. J., Joo, E., Brunsell, N. A., Verfaillie, J. & Richardson, A. D. (2016). Productivity of North American grasslands is increased under future climate scenarios despite rising aridity. *Nature Climate Change* 6, 710–714. https://doi.org/10.1038/nclimate2942

Inoue, M. (2017). Change of landscape and ecosystem services of semi-natural grassland in Mt. Sanbe, Shimane Prefecture, Japan. In S. K. Hong & N. Nakagoshi (Eds.), *Landscape ecology for sustainable society* (pp. 111–122). Springer International Publishing. https://doi.org/10.1007/978-3-319-74328-8_7

Jeong, S. J., Ho, C. H., Gim, H. J., & Brown, M. E. (2011). Phenology shifts at start vs. end of growing season in temperate vegetation over the Northern Hemisphere for the period 1982-2008. *Global Change Biology*, 17(7), 2385–2399. https://doi.org/10.1111/j.1365-2486.2011.02397.x

Jönsson, P., & Eklundh, L. (2004). *TIMESAT—a program for analyzing time-series of satellite sensor data*. Computers & Geosciences, 30(8), 833–845. https://doi.org/10.1016/j.cageo.2004.05.006

Kloesel, K., Bartush, B., Banner, J., Brown, D., Lemery, J., Lin, X., Loeffler, C., McManus, G., Mullens, E., Nielsen-Gammon, J., Shafer, M., Sorenson, C., Sperry, S. K., Wildcat, D. R., & Ziolkowska, J. R. (2018). *Chapter 23: southern great plains. impacts, risks, and adaptation in*

the United States: the fourth national climate assessment, volume II. U.S. Global Change Research Program. https://doi.org/10.7930/NCA4.2018.CH23

Kunkel, K. E., Stevens, L. E., Stevens, S. E., Sun, L., Janssen, E., Wuebbles, D., Kruk, M. C., Thomas, D., Shulski, M., Umphlett, N. A., Hubbard, K. G., Robbins, K., Romolo, L., Akyuz, A., Pathak, T. B., Bergantino, T. R., & Dobson, J. G. (2013). *Regional Climate Trends and Scenarios for the US National Climate Assessment Part 4. Climate of the US Great Plains*, NOAA Technical Report NESDIS 142-4, 82 pp.

Liang, L., Henebry, G. M., Liu, L., Zhang, X., & Hsu, L. C. (2021). Trends in land surface phenology across the conterminous United States (1982-2016) analyzed by NEON domains. Ecological Applications, 31(5), e02323. https://doi.org/10.1002/eap.2323

Liebmann, B., Dole, R. M., Jones, C., Bladé, I., & Allured, D. (2010) Influence of choice of time period on global surface temperature trend estimates. Bulletin of the American Meteorological Society, 91(11), 1485–1492. https://doi.org/10.1175/2010BAMS3030.1.

Machovina, B., & Feeley, K. J. (2017). Restoring low-input high-diversity grasslands as a potential global resource for biofuels. *The Science of the Total Environment*, 609, 205–214. https://doi.org/10.1016/j.scitotenv.2017.07.109

Mark, A. F., & McLennan, B. (2005). The conservation status of New Zealand's indigenous grasslands. *New Zealand Journal of Botany*, 43(1), 245–270. https://doi.org/10.1080/0028825X.2005.9512953

McDonough, K. R., Hutchinson, S. L., & Hutchinson, J. M. S. (2020). Declining soil moisture threatens water availability in the US Great Plains. *Transactions of the ASABE*, 63(5): 1147-1156. https://doi.org/10.13031/trans.13773

McManus, K. M., Morton, D. C., Masek, J. G., Wang, D., Sexton, J. O., Nagol, J. R., Ropars, P., & Boudreau, S. (2012). Satellite-based evidence for shrub and graminoid tundra expansion in northern Quebec from 1986 to 2010. *Global Change Biology*, 18(7), 2313–2323. https://doi.org/10.1111/j.1365-2486.2012.02708.x

Moulin, S., Kergoat, L., Viovy, N., & Dedieu, G. (1997). Global-scale assessment of vegetation phenology using NOAA/AVHRR satellite measurements. *Journal of Climate*, 10(6), 1154–1170. https://doi.org/10.1175/1520-0442(1997)010<1154:GSAOVP>2.0.CO;2

Oakleaf, J. R., Kennedy, C. M., Baruch-Mordo, S., West, P. C., Gerber, J. S., Jarvis, L., & Kiesecker, J. (2015). A world at risk: aggregating development trends to forecast global habitat conversion. *Plos One*, 10(10). https://doi.org/10.1371/journal.pone.0138334

O'Mara, F. P. (2012). The role of grasslands in food security and climate change. Annals of Botany, 110(6), 1263–1270. https://doi.org/10.1093/aob/mcs209

Omernik, J. M. (1987). Ecoregions of the conterminous United States. *Annals of the Association of American Geographers*, 77(1), 118–125. https://doi.org/10.1111/j.1467-8306.1987.tb00149.x

Omernik, J. M., & Griffith, G. E. (2014). Ecoregions of the conterminous United States: evolution of a hierarchical spatial framework. *Environmental Management*, 54(6), 1249–1266. https://doi.org/10.1007/s00267-014-0364-1

PRISM Climate Group. (2019). *PRISM Climate Data*. Oregon State University. http://prism.oregonstate.edu

Ratajczak, Z., Briggs, J. M., Goodin, D. G., Luo, L., Mohler, R. L., Nippert, J. B., & Obermeyer, B. (2016). Assessing the potential for transitions from tallgrass prairie to woodlands: Are we operating beyond critical fire thresholds? *Rangeland Ecology & Management*, 69(4), 280–287. https://doi.org/10.1016/j.rama.2016.03.004

Reed, B. C., White, M., & Brown, J. F. (2003). Remote Sensing Phenology. In M. D. Schwartz (Ed.), Phenology: an integrative environmental science (Vol. 39, pp. 365–381). *Springer Netherlands*. https://doi.org/10.1007/978-94-007-0632-3_23

Ricketts, T. H., Dinerstein, E., Olson, D. M., Loucks, C. J., Eichbaum, W., DellaSala, D. A., Kavanagh, K., Hedao, P., Hurley, P., Carney, K., Abell, R., & Walters, S. (1999). *Terrestrial ecoregions of North America: A conservation assessment* (1st ed.). Island Press.

Rossum, S., & Lavin, S. (2000). Where are the Great Plains? A cartographic analysis. *The Professional Geographer*, 52(3), 543–552. https://doi.org/10.1111/0033-0124.00245

Rumpel, C. (2011). Carbon storage and organic matter. In G. Lemaire, J. Hodgson, & A. Chabbi (Eds*.), Grassland productivity and ecosystem services* (pp. 65–72). CABI Publishing.

Schwartz, M. D. (1994). Monitoring global change with phenology: The case of the spring green wave. *International Journal of Biometeorology*, 38(1), 18–22. https://doi.org/10.1007/BF01241799

Seager, R., Lis, N., Feldman, J., Ting, M., Williams, A. P., Nakamura, J., Liu, H., & Henderson, N. (2018). Whither the 100th meridian? The once and future physical and human geography of

America's arid–humid divide. Part I: The story so far, *Earth Interactions*, *22*(5), 1-22. https://doi.org/10.1175/EI-D-17-0011.1

Shafer, M., Ojima, D., Antle, J. M., Kluck, D., McPherson, R. A., Petersen, S., Scanlon, B., & Sherman, K. (2014). Ch. 19: Great Plains. Climate change impacts in the United States: the third national climate assessment. U.S. Global Change Research Program. https://doi.org/10.7930/J0D798BC

Suepa, T., Qi, J., Lawawirojwong, S., & Messina, J. P. (2016). Understanding spatio-temporal variation of vegetation phenology and rainfall seasonality in the monsoon Southeast Asia. Environmental Research, 147, 621–629. https://doi.org/10.1016/j.envres.2016.02.005

Tan, B., Morisette, J. T., Wolfe, R. E., Gao, F., Ederer, G. A., Nightingale, J., & Pedelty, J. A. (2011). An Enhanced TIMESAT algorithm for estimating vegetation phenology metrics from MODIS data. *IEEE Journal of Selected Topics in Applied Earth Observations and Remote Sensing*, 4(2), 361–371. https://doi.org/10.1109/JSTARS.2010.2075916

Taylor, J. L., Acevedo, W., Auch, R. F., & Drummond, M. A. (2015). *Status and trends of land change in the Great Plains of the United States—1973 to 2000*: US Geological Survey Professional Paper 1794–B. United States: US Geological Survey. http://dx.doi.org/10.3133/ pp1794B

Tollerud, H., Brown, J., Loveland, T., Mahmood, R., & Bliss, N. (2018). Drought and land-cover conditions in the Great Plains. *Earth Interactions*, 22(17), 1–25. https://doi.org/10.1175/ EI-D-17-0025.1

US Geological Survey. (2017). *1 Arc-second Digital Elevation Models (DEMs)* - USGS National Map 3DEP Downloadable Data Collection. https://www.usgs.gov/core-science-systems/ ngp/tnm-delivery/gis-data-download

Walsh, J., Wuebbles, D., Hayhoe, K., Kossin, J., Kunkel, K., Stephens, G., Thorne, P., Vose, R., Wehner, M., Willis, J., Anderson, D., Doney, S., Feely, R., Hennon, P., Kharin, V., Knutson, T., Landerer, F., Lenton, T., Kennedy, J., & Somerville, R. (2014). *Ch. 2: our changing climate. climate change impacts in the United States: the third national climate assessment*. U.S. Global Change Research Program. https://doi.org/10.7930/J0KW5CXT

Wang, S., Lu, X., Cheng, X., Li, X., Peichl, M., & Mammarella, I. (2018). Limitations and challenges of MODIS-Derived phenological metrics across different landscapes in Pan-Arctic regions. *Remote Sensing*, 10(11), 1784. https://doi.org/10.3390/rs10111784

Wang, S., Yang, B., Yang, Q., Lu, L., Wang, X., & Peng, Y. (2016). Temporal trends and spatial variability of vegetation phenology over the Northern Hemisphere during 1982-2012. *Plos One*, 11(6), e0157134. https://doi.org/10.1371/journal.pone.0157134

West, P. C., & Nelson, C. J. (2017). Managing Grassland Ecosystems. In R. F. Barnes, C. J. Nelson, M. Collins, & K. J. Moore (Eds.), *Forages, Volume 1: An introduction to grassland agriculture* (7th ed., pp. 357–373). Wiley-Blackwell.

White, R., Murray, S., Rohweder, M., & Prince, S. D. (2000). Pilot Analysis of Global Ecosystems: Grassland Ecosystems (Illustrated, p. 94). World Resources Institute.

Willis, K. S. (2015). Remote sensing change detection for ecological monitoring in United States protected areas. *Biological Conservation*, 182, 233–242. https://doi.org/10.1016/j.biocon.2014.12.006

Xiao, X., Zhang, J., Yan, H., Wu, W., & Biradar, C. (2009). Land surface phenology: Convergence of satellite and CO_2 eddy flux observation. In: A., Noormets, (Ed.), *Phenology of ecosystem processes*. Springer, New York, pp. 247–270.

Yue, S., Pilon, P., & Cavadias, G. (2002). Power of the Mann–Kendall and Spearman's rho tests for detecting monotonic trends in hydrological series. *Journal of Hydrology*, 259(1), 254–271.

Zhang, X., Friedl, M. A., Schaaf, C. B., Strahler, A. H., Hodges, J. C. F., Gao, F., Reed, B. C., & Huete, A. (2003). Monitoring vegetation phenology using MODIS. *Remote Sensing of Environment*, 84(3), 471–475. https://doi.org/10.1016/S0034-4257(02)00135-9

Chapter 5 - Spatio-temporal valuation of grassland ecosystem services in the U.S. Great Plains

Abstract

Grasslands are well known for their high biodiversity, environmental regulation, social and cultural values. However, their capacity to deliver multiple ecosystem services (ES) and how changes in grasslands impact the provision of ES is surprisingly understudied compared to other biomes. Some existing studies have estimated total ES value of global grasslands and spatially explicit ES values at discrete times. This paper focuses on developing improved ES estimation methods using remote sensing data to capture the spatio-temporal dynamics of vegetation (grasslands specifically) while highlighting the impact of environmental factors/anthropogenic activities on the provision of grassland ES in the U.S. Great Plains. A selected set of grassland ecosystem services within the Great Plains was quantified (economic and biophysical values) for the period between 2001 and 2017 (time is based on data availability). Climate change (past, present, and future) influences grassland productivity and phenology with consequences on ecosystems and their value. Results from this study show the impact of changing grassland conditions based on greenness on the Great Plains ecoregion and how these changes might be manifested as variable levels of ES provision. An analysis of the carbon stock value over the period studied showed and overall positive trend. This agrees with findings from other previous work on increased productivity of grasslands in the time studied. Future work is suggested to analyze the specific factors that contribute to the increasing productivity of grasslands in the Great Plains ecoregion and its implications for the ecoregion.

KEYWORDS: Grasslands, Ecosystem Services, NDVI, Great Plains Ecoregion, and InVEST.

5.1 Introduction

5.1.1 Background and purpose

Grasslands are one of the most biodiverse and productive terrestrial biomes. They do provide many benefits that include environmental regulation, social and cultural values, yet grasslands receive very low levels of protection. The temperate grasslands in the United States are one of the most threatened grassland ecosystems, with almost 62% of the historical extent lost (Comer et al., 2018; Oakleaf et al., 2015). Many factors, including fire frequency, fragmentation, and conversion to other land use, come to play. The most significant is the conversion of grasslands to croplands. The conversion of grasslands to croplands have reaccelerated in the past decade; the rates of conversion of grassland to cropland have quadrupled after 2008 compared to 15 years ago in the U.S. Midwest (Lark et al., 2019). In 2019 alone, approximately 10,500 square kilometers of grasslands in the Great Plains were lost to crop cultivation (Plowprint report, 2021).

Long-term studies on a major ecosystem are critical to achieving an integrated understanding of how components of ecosystems interact. However, relatively little is known about the long-term conditions of grasslands in the Great Plains and how any change in the conditions long-term conditions (productivity) of the grassland biome impacts the provision of ecosystem services. The U.S. Great Plains hold the largest expanse of grasslands in the U.S. that are still intact (Lark, 2020). Reduction in grassland biomass by climate impact or conversion to cropland has negative ramifications. Negative environmental impacts include increased risks of soil erosion decrease in soil organic carbon, and an increase in atmospheric carbon (Zhang et al. 2021). Zhang et al. (2021) highlight the dire need to estimate the impact of changing grassland conditions in the U.S. to enable proper environmental monitoring and determining the extent of the consequences.

There are several definitions of ecosystem services (ES), but the general idea or theme is that they are benefits people obtain from ecosystems either directly or indirectly (Daily et al., 1997; MEA, 2005; TEEB, 2010). While the concept of ecosystem services has become prominent as a decision-making supporting tool over the last 20 years, there is little emphasis on grassland ES and how changes due to anthropogenic activities and resulting climate change impacts the provision of ES compared to other biomes; especially in the Great Plains where most of the U.S.'s grasslands occur. Some existing studies include the estimation of the total ES value of global grasslands and spatially-

explicit ES values of a single time period on some regional level (Costanza et al., 1997; Sala & Paruelo, 1997; Costanza et al., 2014; Xia et al., 2014). Costanza et al. (1997) estimation of the total ES value of global grasslands in 1997 was 302 (1994) U.S. dollars per hectare; also, Costanza et al.'s (2014) re-estimation of the total ES value of global grasslands in 2011 was 4,166 (2007) U.S. dollars per hectare. Sala and Paruelo (1997) demonstrated the provision of ES by grasslands through carbon sequestration and conservation of soil. They estimated the economic value carbon lost by converting native grasslands to cropland in eastern Colorado (U.S.) to $200 per hectare. Xia et al. (2014) also modeled the carbon density of grasslands but in North America (including the Great Plains on Canada) between 1982 and 2006; there was an overall positive trend in total C and an estimated value of 207.72 Tg/C of total carbon stock. This research will address this knowledge gap by quantifying a select set of grassland ecosystem services within the Great Plains using remotely sensed data for ES modeling to capture the spatio-temporal dynamics of grasslands.

Due to the vast coverage of grasslands, remote sensing is a popular method of data acquisition for mapping and valuation of grasslands ES. Remotely sensed data is used to produce spatially explicit assessments and quantification of ecosystem services (De Araujo Barbosa et al., 2015; Liquete et al., 2016). They also provide adequate temporal scale data or even real-time data for monitoring ES (Ayanu et al., 2012). Remotely sensed data are usually used as a proxy for a variable or indicator, which is then used as a proxy for an ES; that is, a proxy of a proxy (Ayanu et al., 2012). In this case, Vegetation indices as a proxy for a service like carbon sequestration because they provide an approximate measure of relative vegetation amount (Wang et al., 2018). The normalized difference vegetation index (NDVI) has shown a consistent correlation with vegetation dynamics in various scales of land area, and the ratio concept reduces many sources of noise (Huete, 1988; Wang et al., 2018). A wide range of ES modeling tools that usually require remote sensing data input exist. A detailed review of ecosystem services models was carried out by Dunford et al. (2017) and Kienast & Helfenstein (2016). Widely used and well-tested examples of the modeling software packages include the Integrated Valuation of Ecosystem Services and Tradeoffs (InVEST), Artificial Intelligence for ES (ARIES), Multiscale Integrated Model of ES (MIMES), Land Utilization and Capability Indicator (LUCI), Social Values for ES (SoLVE) (Bagstad et al., 2013; Dunford et al., 2017; Kienast & Helfenstein, 2016).

Bagstad et al. (2013) reviewed and carried out a performance rating for seventeen modeling tools

against criteria that include data requirement, level of development, scale application and capacity of the independent application. Seven of the seventeen tools (including InVEST, ARIES, and EcoAIM) were tested on the San Pedro watershed in Arizona, USA. They all had their specific strengths (e.g., LUCI is more site-specific), but InVEST was utilized because it has been well tested, open source, generalizable, suitable for the spatial scale of the study area and the availability of required data (Bagstad et al., 2013; Dunford et al., 2017; Kienast & Helfenstein, 2016; Nelson et al., 2009).

To sum this up, this project focuses on the use of remotely sensed data for ES modeling in InVEST to highlight the relative change in grasslands and its impact in the U.S. Great Plains. The study will use remotely sensed data which will be input into a geographic information system software and analyzed. While this project focuses on addressing the knowledge gap grassland ES quantification in the (especially in the Great Plains), improved methods were developed to better utilize the increasing remote sensing data qualities. These improved methods can be applied to vegetation monitoring not just in the United States but globally.

5.2. Study area

The Great Plains region is the vast interior of North America running from Canada in the North to Mexico in the south and lies between east of the Rocky Mountains and west of the eastern temperate forests and the Appalachian Mountains (Rossum & Lavin, 2000). The Great Plains Ecoregion used for this study is defined by the United States Environmental Protection Agency (EPA) based on Omernik (1987) and Omernik and Griffith's (2014) classifications. The ecoregion classifications are based on patterns of geology, physiography, vegetation, climate, soils, land use, wildlife, and hydrology affecting ecosystem quality (Omernik, 1987). The US EPA categorizes the area as a Level I ecoregion of the 15 coarsest level ecosystems in North America. In this ecosystem classification, the Great Plains has four level-II divisions and 16 Level-III subdivisions (Omernik & Griffith, 2014). The EPA Great plains cover approximately 2.8 million square kilometers, with more than 80 percent of this area in the U.S. (about 2.2 square kilometers). Grasslands followed by agricultural lands dominate the ecoregion, then other land uses (Drummond & Auch, 2015). This study, however, focuses only on grasslands in the Great Plains Ecoregion within the United States. The grassland area was defined by the grassland/herbaceous class of the United States Geological Survey's National Land Cover Dataset (NLCD) for 2011 (Homer et al., 2015). As defined for this study, the grassland

area is approximately 825,000 square kilometers and covers 13 U.S. states (Figure 5.1). It contains a mixture of tallgrass prairie (east), mixed-grass prairie (north central), and short grass prairie (west).

Climate is also diverse in this region, influenced by latitudes from north to south and elevation from east to west (Tollerud et al., 2018). The Koppen-Geiger climate classifications within the Great Plains show the range from the cold (snow) climate in northwestern North Dakota, with warm, humid summers and long, cold, snowy winters, to the arid climate of Texas (Beck et al., 2018). Precipitation in the Great Plains is highly variable from year to year. Based on 30-year normal (1981-2010), precipitation ranges from 1500 mm in the southeastern portions of the Great Plains to 250 mm in the west, and annual mean temperature ranges from 0^0C in the north to 22^0C in the south (PRISM Climate Group, 2019).

The Great Plains' elevation is generally described as low lying, but it decreases from the foot of the Rocky Mountains in the west to the east in meters above sea level. The west edge with a maximum of 3610 meters above sea level in Colorado to more than 18230 meters in New Mexico, but on the eastern edge, it reduces to an average of 200 meters from east Oklahoma to mid-Texas (U.S. Geological Survey, 2017). The hydrology of the Great Plains ecoregion is subjugated by the Missouri River basin in the northern areas; Arkansas and the Red Rivers basins in the southern portion with tributaries flowing into the Mississippi River (Galat et al., 2005; Matthews et al., 2005). Besides the Prairie Pothole Region in the upper Midwest parts of the ecoregion, most enclosed water bodies in the Great Plains region are manmade (Zhu et al., 2011).

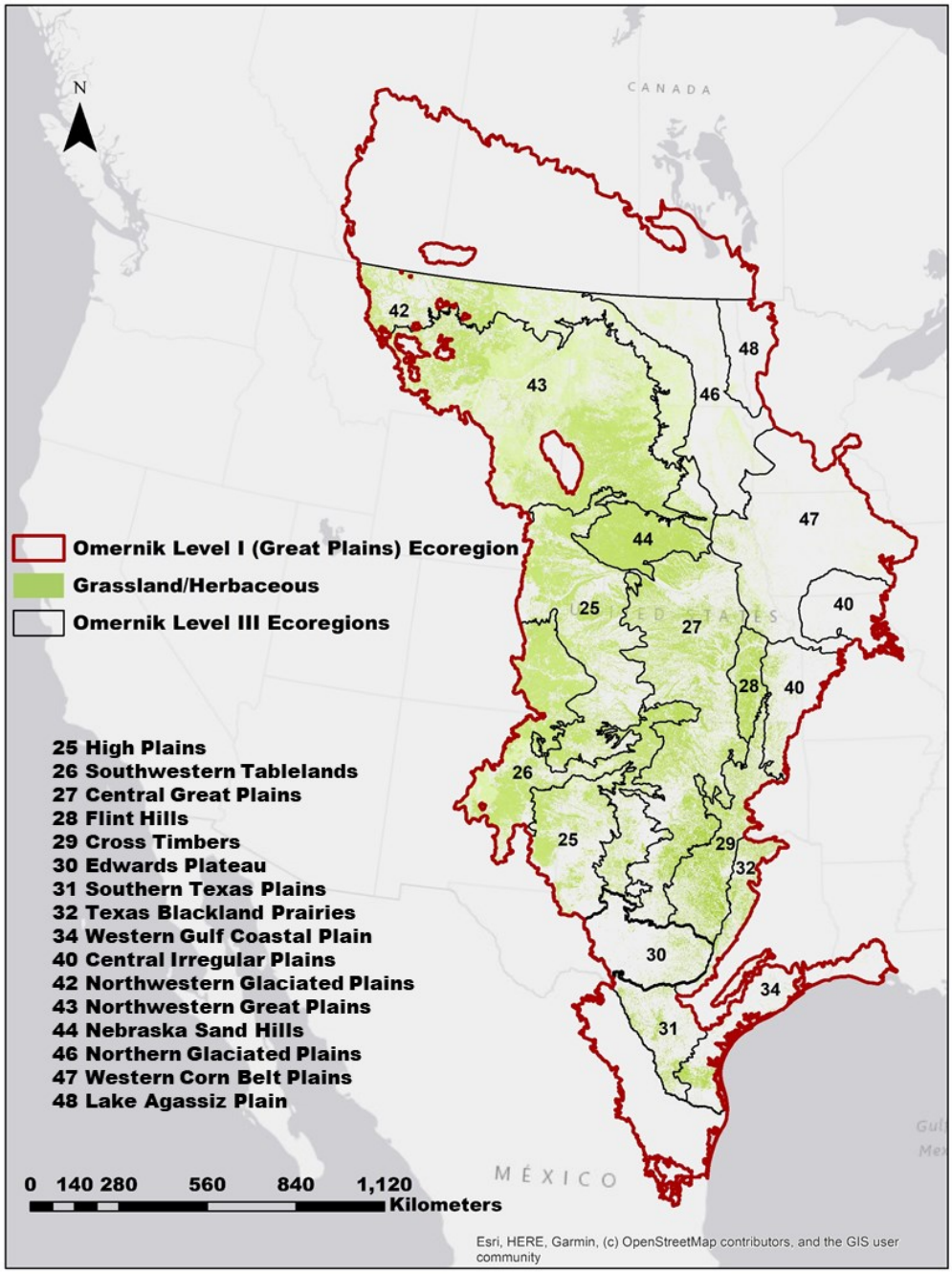

Figure 5.1: U.S. Great Plains study area showing Omernik level III ecoregions and grassland pixels extracted from the 2011 NLCD.

5.3. Data and methods

5.3.1 Modeling important ecosystem services

With the list of ecosystem services grasslands provide, it can be challenging to decide which ES to quantify and value that will best impact policy decisions. The choice of services to estimate was determined by the availability of data considering the large extent of the study area. The ES modeling tool used (InVEST) can be run at different levels of complexity, making it sensitive to data availability (Nelson et al., 2009). Based on the TEEB classification system, the following ecosystem services were estimated: climate regulation (carbon sequestration) and Erosion prevention (soil conservation) using the InVEST carbon and sediment retention models, respectively.

Due to the vast coverage of grasslands, remote sensing is a popular method of data acquisition for mapping and valuation of grasslands ES. Remotely sensed data is used to produce spatially explicit assessments and quantification of ecosystem services (De Araujo Barbosa, et al., 2015; Liquete et al., 2016). They also provide adequate temporal scale data or even real-time data for monitoring ES (Ayanu et al., 2012). A detailed review of remote sensing data, techniques suitability was described by several studies (Ayanu et al., 2012; De Araujo Barbosa, et al., 2015; Liquete et al., 2016). Ramirez-Reyes et al. (2019) discussed the important role remote sensing could play in ES valuation and assessment; they highlighted the potential of remotely sensed data in improving the modeling of ES demand, being a more direct indicator of ES supply and better and more accurate modeling of the temporal dynamics of ES.

The (version 3.9.0) model suite was used to quantify ecosystem services. InVEST is a suite of GIS-based models developed by Natural Capital Project (a partnership of Stanford University, University of Minnesota, Chinese Academy of Sciences, Stockholm Resilience Centre, the Nature Conservancy, and the World Wildlife Fund). InVEST comprises a suite of GIS-based models. It is the top choice tool for most ES valuation studies because it is open-source, highly generalizable, well documented, and independently applicable (Bagstad et al., 2013).

The InVEST models are based on land use and land cover (LULC) maps, converting them to production functions and ecosystem service supply (Nelson et al., 2009). Besides the common limitation of classification accuracy of LULC maps, another limitation is the lack of variability in

production functions tied to the LULC classes. That is, all pixels in a "forest" class are assigned one value: limiting the characteristic explicit spatial variability in this class. It is well known that the vegetation land cover specifically is very dynamic, so if the focus is on one land cover class like this study, there will be no explicit spatial distribution in the resulting ecosystem service supply using the existing data input method. Muche et al. (2019) used MODIS NDVI to account for spatiotemporal differences in grassland land cover conditions in the calculation of surface runoff using the curve number approach. In this study, the normalized difference vegetation index (NDVI) for grasslands was used in place of LULC maps for this study. The NDVI has shown a reliable correlation with vegetation dynamics in varying spatial scales and the available data for carbon and erosion modelling were NDVI based (Wang et al., 2018).

To prepare the NDVI for both models, the MODIS (MOD13Q1 Collection 6), a 16-day maximum composite NDVI product for the period of 2001 to 2017, was used (Table 5.1). Images were downloaded from NASA's Earth Observation Data website using the "MODIStsp" package (version 1.3.3) in R; as a 16-bit signed integer grid. The MODIStsp package was used to download MODIS HDF files automatically. The MOD13Q1 has a 250-meter spatial resolution. The various scenes of the downloaded images that make up the EPA Great Plains were mosaiced and reprojected from their original sinusoidal projection to a more useful projection: the USA Contiguous Albers Equal Area Conic projection. To extract the area of interest, pixels belonging to the "grassland/herbaceous" class of the 2011 NLCD data produced from a 30-meter spatial resolution were resampled to match the spatial resolution of the MOD13Q1 image. To address the potential for misidentifying a grassland pixel, resampled pixels included an 80% minimum of the original NLCD grassland/herbaceous class. This grassland mask was then used to extract the grassland pixels from the NDVI data.

5.3.2 Carbon model

The natural carbon stock that acts as a climate regulator is modeled in this study benefits according to four main carbon pools: aboveground (living plant) biomass, belowground (root) biomass, soil organic component, and dead organic matter (litter). The InVEST carbon stock and sequestration model aggregates the amount of carbon stored in the above-mentioned pools with values that are based on LULC maps. The model uses the LULC classes, and the amount of carbon stored in carbon pools (in a lookup table) to estimate the total amount of carbon stored in a landscape or the amount of carbon sequestered over a given time. Valuation is then applied to sequestration (change in carbon

stock/storage in an ecosystem over time; annually in this case) to estimate the economic value. See https://invest-userguide.readthedocs.io/en/latest/carbonstorage.html for more details on the general InVEST method. A new method of data input was adapted for this study. Grassland VI-based classes and VI-related values for the carbon stored in carbon pools for the lookup table are discussed below (Appendix C1).

The details of the data used to estimate the values of each carbon pool for each pixel in the study are presented in Table 1, and all carbon stock values are MgC/ha (megagrams of carbon per hectare). The aboveground and belowground biomass carbon values were estimated using the Oak Ridge National Laboratory's global aboveground and belowground biomass carbon density images for the year 2010 (Spawn & Gibbs, 2019). Aboveground and belowground carbon biomass correlate to several VI's, including NDVI (Kelsey & Neff, 2014; Vicharnakorn et al., 2014; Xia et al., 2014). Therefore, the best-fit regression model between the aboveground and belowground carbon biomass density (AGB, BLG; MgC/ha) for each pixel and its average annual growing season NDVI ($NDVI_g$) are given below (Equations 1 and 2). The growing season is defined as the period from May to October based on the majority start and end of growing season for the ecoregion.

$$\text{Log AGB} = -1.047895 + 2.307363 * NDVI_g \quad (R^2 = 0.48, \text{RSME}= 0.29, P < 0.0001) \quad [1]$$

$$\text{Log BLG} = 0.2476662 + 2.5910314 * NDVI_g \quad (R^2 = 0.59, \text{RSME}= 0.24, P < 0.0001) \quad [2]$$

The dead organic matter pool values were estimated from the range for grassland in North America available in the literature. Values are summarized in the 2006 IPCC Guidelines for National Greenhouse Gas Inventories based on Kauffman et al. (1997) and Naeth et al.'s (1991) carbon estimates for grasslands (as cited in Verchort et al., 2006). For the soil organic component, we used average values of the Global Soil Organic Carbon Map (GSOC map) covering the study area (Food and Agriculture Organization [FAO] & Intergovernmental Technical Panel on Soils [ITPS], 2020). The GSOC map was acquired from the Food and Agricultural Organization of the United Nations.

Table 5.1: The details of datasets used for the carbon model.

Data	**Spatial Resolution**	**Source**
NDVI layers of the MODIS (MOD13Q1 Collection 6)	250m	NASA (https://urs.earthdata.nasa.gov/)
Global aboveground and belowground biomass carbon density images for the Year 2010	300m	Oak Ridge National Laboratory (ORNL DAAC) (https://doi.org/10.3334/ORNLDAAC/1388)
IPCC's (2006) dead litter carbon estimates for grasslands	N/A	IPCC, Kauffman, et al., 1997 and Naeth, et al., 1991 https://www.ipcc-nggip.iges.or.jp/public/2006gl/pdf/4_Volume4/V4_06_Ch6_Grassland.pdf
GLOSIS - Global Soil Organic Carbon Map (GSOC map) (v1.5.0)	800m	Food and Agriculture Organization [FAO] of the UN http://54.229.242.119/GSOCmap/
Social Cost of CO_2, 2015-2050 (in 2007 dollars per metric ton CO_2)	N/A	EPA https://19january2017snapshot.epa.gov/climatechange/social-cost-carbon_.html

5.3.2.1 Economic valuation of carbon

Data for modeling economic values of carbon was acquired from the EPA's Social Cost of CO_2 (SCC) values for 2015-2050 in 2007 U.S. dollars per metric ton of carbon (Table 5.1). The data includes the price/metric ton of carbon, market discount in the price of carbon (an integer percentage value that reflects society's preference for immediate benefits over future benefits), and the annual rate of change in the price of carbon used for valuation. A 3% market discount rate was used as suggested by EPA, and the SCC price (per ton of carbon) values for the 3% discount rate were in increments of 5 years from 2015 to 2050. A simple linear interpolation used was used to estimate price (per ton of carbon) for the preceding and interval years in the study period. The annual rate of change in carbon price was calculated to be approximately 0.04% every year. The SCC values alongside a lookup table comprised of aboveground biomass, belowground biomass, soil organic component, and dead organic

matter carbon values with their corresponding NDVI values in increments of 0.04 were input for the carbon model. (Appendix C2). The InVEST carbon sequestration model calculates the net economic value over time, in this case, the difference between the economic values for a year and the preceding year.

5.3.3 Sediment delivery model

Controlling erosion naturally can benefit humans by improving water quality, reducing flooding, reducing pollutant transport, and increasing agricultural productivity (Duarte et al., 2016). Erosion control and sediment retention estimation in InVEST requires modeling the impact of land cover on on-site soil erosion using a set of landscape variables. Those variables include precipitation, land cover, topography, and soil properties. Then the sediments retained by the presence of a vegetative cover using the values of potential soil erosion for each watershed in the study area is estimated (Yoo et al., 2014).

The InVEST Sediment Delivery Ratio model uses the Universal Soil Loss Equation-USLE (Wischmeier & Smith, 1978):

$$ASL = R * K * LS * C * P \quad [3]$$

where ASL expresses annual soil loss (tons ha^{-1} yr^{-1}); R is rainfall erosivity (MJ mm $(ha . hr . yr)^{-1}$); K is a measure of soil erodibility (tons. ha . hr/$(ha . MJ . mm)^{-1}$), LS is a combined factor for slope length and steepness; C is the land cover management; and P represents conservation practices (LS, C, and P are dimensionless; but L (slope length) is measured in cm, and S (slope steepness) is measured in percentages). The data used to derive the variables for the soil loss estimation are listed in Table 5.2.

The model computes the amount of annual soil loss for each pixel then computes the sediment delivery ratio (SDR) for that pixel. The data required are listed and described below, mostly in raster format. The C and P factors are values that are based on LULC classes and are inputted as values that correspond to LULC classes in a lookup table. See https://investuserguide.readthedocs.io/en/latest/sdr.html for more details on the existing method. The C factor is a key component of

soil erosion analysis. Coupled with the fact that we are focused on one LULC category (grassland), there is a need to include spatially explicit and temporally variable values for the C factors for a more accurate estimation of soil loss. In this study, we used a modified C factor value input method was adapted for this study-VI-based classes and VI-related values instead of the generalized static value from literature. C factor values estimation is discussed in detail below, and a modified lookup table can be found in Appendix C3.

Table 5.2: The details of datasets used for the sediment delivery model.

Variable	**Data**	**Spatial Resolution**	**Source**	**Unit**
R	PRISM annual normal precipitation	4 km	PRISM Climate Group (https://prism.oregonstate.edu/recent/)	MJ mm (ha . hr . yr)$^{-1}$
K	The Soil Survey Geographic Database (SSURGO)	1:250,000-scale	USDA: NCRS, UC DAVIS, and UC-ANR (https://websoilsurvey.sc.egov.usda.gov/App/HomePage.htm)	ton. ha . hr(MJ. ha . mm)$^{-1}$
LS	The 3D Elevation Program (3D EP)	30 m	USGS (https://viewer.nationalmap.gov/basic/)	unitless
C	NDVI layers of the MODIS (MOD13Q1 Collection 6)	250 m	NASA (https://urs.earthdata.nasa.gov/)	unitless
P	Literature	N/A	Wischmeier and Smith. (1978). Predicting rainfall erosion losses (Vol. 537). U.S. Dep. of Agriculture.	unitless

The rainfall erosivity factor indicates how much erosive force a typical storm has on surface soils. The spatially distributed rain erosivity index for the study area was determined from rainfall data, a 4km mean monthly precipitation raster for the period between 2001 to 2017 (PRISM Climate Group, 2019). The rainfall erosivity factor was then estimated using the power function developed by Renard and Freimund (1994) for the conterminous U.S.:

$$R = 0.04830 \times P^{1.610} \quad [4]$$

where:
P = annual mean precipitation (mm)

The soil erodibility factor K value is the rate of soil loss per rainfall erosion index unit as measured on a standard plot and often determined using inherent soil properties (texture, grain size, permeability, and organic matter content (Parysow et al., 2003; Pan & Wen, 2013). The spatially distributed soil erodibility values were from the 1:250,000-scale U.S. Soil Survey Geographic Database. The soil erodibility raster covering the study area was aggregated by the California Soil Resource Lab at UC Davis (University of California, Davis) and UC-ANR (University of California, Agriculture, and Natural Resources) in collaboration with the USDA Natural Resources Conservation Service.

The length-slope factor computes the effect of slope length (L) and the slope steepness (S) on erosion. The length-slope values were obtained from the 30-meter USGS 3D EP data Digital Elevation Model (DEM). The InVEST Sediment Delivery Ratio model estimates the LS factor values from DEM using the method developed by Desmet and Govers (1996) for a two-dimensional surface. Prior to estimating the erosivity, erodibility, and length-slope values, the datasets were resampled to a 250-meter spatial resolution and reprojected to match the MODIS VI datasets.

The cover management factor is a major component of soil erosion analysis. It indicates how crop management and land cover affect soil erodibility. The C factor is an index that ranges from 0 to 1(forested to bare soil) is estimated using on-site field experiments, lookup tables based on land cover maps, soil-physical models, or land cover maps from regression models (Tsai et al., 2016). Erencin (2000) compared obtaining C factors using land cover maps backed by some field measurements, VI-derived, and transformation indexes. The accuracy was in the order the methods were listed. The NDVI-derived method was the most accurate method that did not require field measurement, which

is favorable for large areas like the Great Plains. Ayalew et al. (2020) also compared NDVI-derived C factors with C factors from existing literature, and the result shows the NDVI-derived factors were more sensitive to actual soil erosion conditions. This study, therefore, uses the NDVI-derived C factor for the erosion model. This method is also spatially explicit compared to using a single literature-derived value for all pixels in on LULC category. As discussed previously, another study used MODIS NDVI to account for spatiotemporal differences in grassland conditions in the calculation of surface runoff using the curve number approach (Muche et al., 2019).

The equation below by Van der Knijff et al. (2000) used for the C-factor estimation has been used in several studies (Ayalew et al., 2020; Balabathina et al., 2020; Durigon et al., 2014). According to Van der Knijff et al. (2000), values 2 and 1 are the best representatives of equation parameters α and β for temperate regions.

$$C = \exp\{-\alpha \times NDVI \div (\beta - NDVI)\} \quad [5]$$

where:
α=2
β=1
α and β are (dimensionless) empirical fitting parameters

The soil conservation practices represent the level of erosion control practices such as contour planting, terracing, and strip cropping, put in place relative to straight row farming up and down the slope. Since the study area is covered by grassland and not crops, it was assumed none of the practices were applied; therefore, the value of P = 1 was assigned for all pixels in the study area (Kuok et al., 2013; Yoo et al., 2014). A biophysical lookup table was created with C and P values corresponding to NDVI values in increments of 0.05, an input for the model (Appendix C3). The spatial distribution of annual soil loss or erosion obtained for grasslands in the Great Plains ecoregion by applying equation 3.

The other component of the InVEST sedimentary delivery model is the estimation of annual sediment retention from annual soil loss. Sediment retention values from the InVEST model represent how much sediment is retained by the natural vegetative cover (grasslands in this situation) compared to an alternative scenario where the current natural vegetative cover was "removed." Basically, sediment retention means how much soil sediment was retained because of the presence of grasslands. This provides a way to present an economic valuation related to soil erosion that is not soil loss. Even

though these values are presented with annual soil loss, there is no established correlation between the two measures. The sediment retention is used for valuation, and it was estimated in 3 steps; 1. the *sediment delivery ratio* (based on Borselli et al.'s (2008) method), 2. the *sediment export* given by the summation of the soil loss values multiplied by the sediment delivery ratio for each pixel, 3. the *sediment downslope deposition* estimates the amount of sediment that was deposited on a landscape downstream from the source that does not reach the stream (Sharp et al., 2020). The watershed boundaries of the study required for the sediment retention estimation were delineated from the DEM (same used to calculate the length-slope factor) using ArcGIS (10.7.1). The default for required parameters (threshold flow accumulation, at Borselli's K and IC_0 calibration parameters, and the maximum SDR value) were used to run the model.

5.3.3.1 Economic valuation of soil retention

The InVEST sediment delivery model does not model the economic value of sediment retained. Data for modeling economic values of soil retained was acquired from the Economic Research Service of the U.S. Department of Agriculture's estimates of soil conservation benefits (LeRoy & Ribaudo, 2008). The benefit estimates are in 2000 U.S. dollars per metric ton of soil (LeRoy & Ribaudo, 2008). The average of the regional values covering the Great Plains ecoregion (Northern Plains, Southern Plains, Mountain, Corn belt, Delta States, and Lake States); and the averages values were adjusted to 2007 U.S. dollars per metric ton of soil using the U.S. Bureau of Labor Statistic's CPI Inflation Calculator to match the unit of the carbon sequestration economic values. The estimated value for each ton of soil retained was $4.46 (2007 U.S. dollars).

To validate the resulting ecosystem service values estimated with the modified valuation method for the carbon model, the value transfer method of ES valuation where values were compared to existing studies in the area was estimated with a different method (Brander & Crossman, 2017).

5.4 Results

5.3.1 Carbon model

The spatial patterns of selected results from the InVEST carbon model analysis are shown in figure 4. The selected maps include years that show a representative variation in spatial patterns and total

value (high and low) of average annual carbon stock values and net economic values of sequestered grassland carbon in the U.S. Great Plains. See Appendix C4 for other maps.

Carbon stock

Figure 2 shows the total and average annual carbon stock values in MgC per hectare for the grasslands in the U.S. Great Plains for the study period (2001 to 2017). The average carbon stock values of grasslands in the ecoregion increases from west to east. This implies that carbon storage is highest in the tallgrass prairies (an average of 220 MgC per ha) and lowest in shortgrass prairies (with an average of 180 MgC per ha). Average carbon stock values in the south are slightly higher than in the north (Figure 5.2). The total annual carbon stock of grasslands in the ecoregion; the years 2002, 2006, and 2012 had the least total value with approximately 2.95, 2.96, and 2.93 B MgC/ha respectively, and 2007, 2010, and 2015 had the highest total values with approximately 3.03, 3.04 and 3.05 B MgC/ha respectively (Figure 5.3).

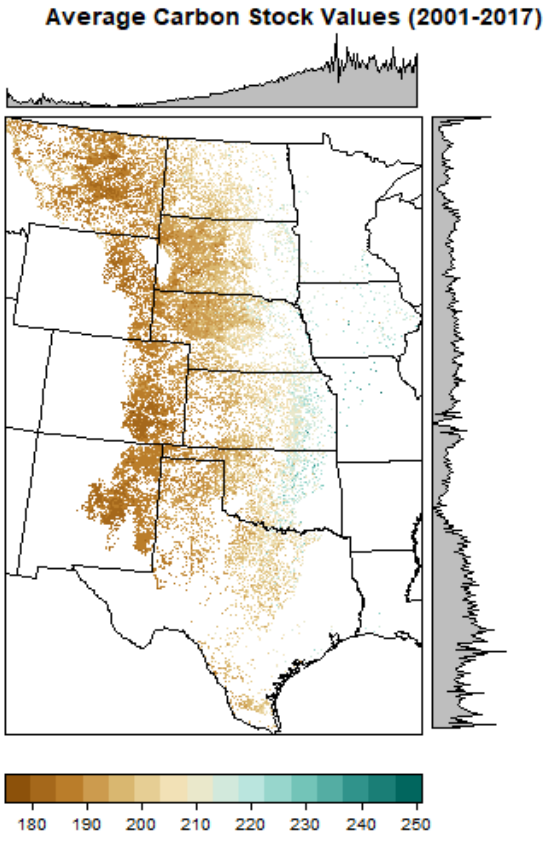

Figure 5.2: Average annual carbon stock (in Mg C/pixel) for the grasslands in the U.S. Great Plains

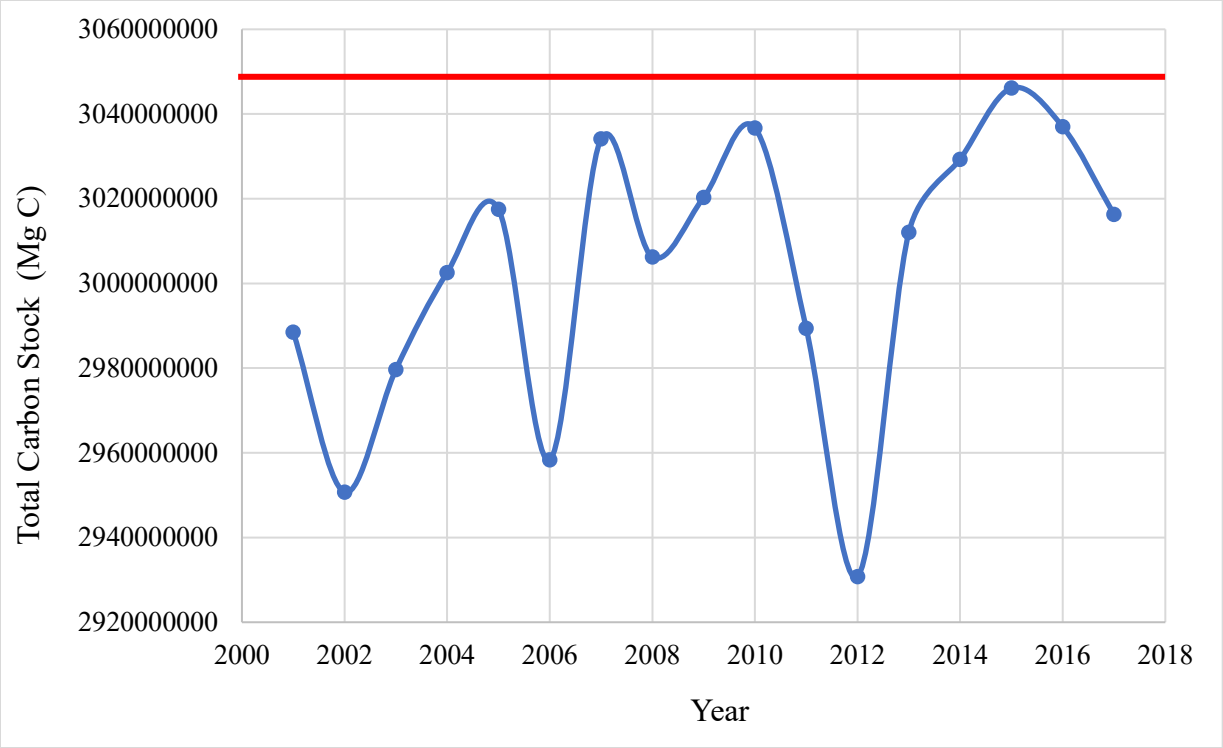

Figure 5.3: Total annual carbon stock (in MgC) for the grasslands in the U.S. Great Plains.

The spatial patterns of annual carbon stock for grasslands the U.S. Great Plains are like the overall average (increasing from west to east) and slightly higher carbon stock values in the south than the north (Figure 5.4).

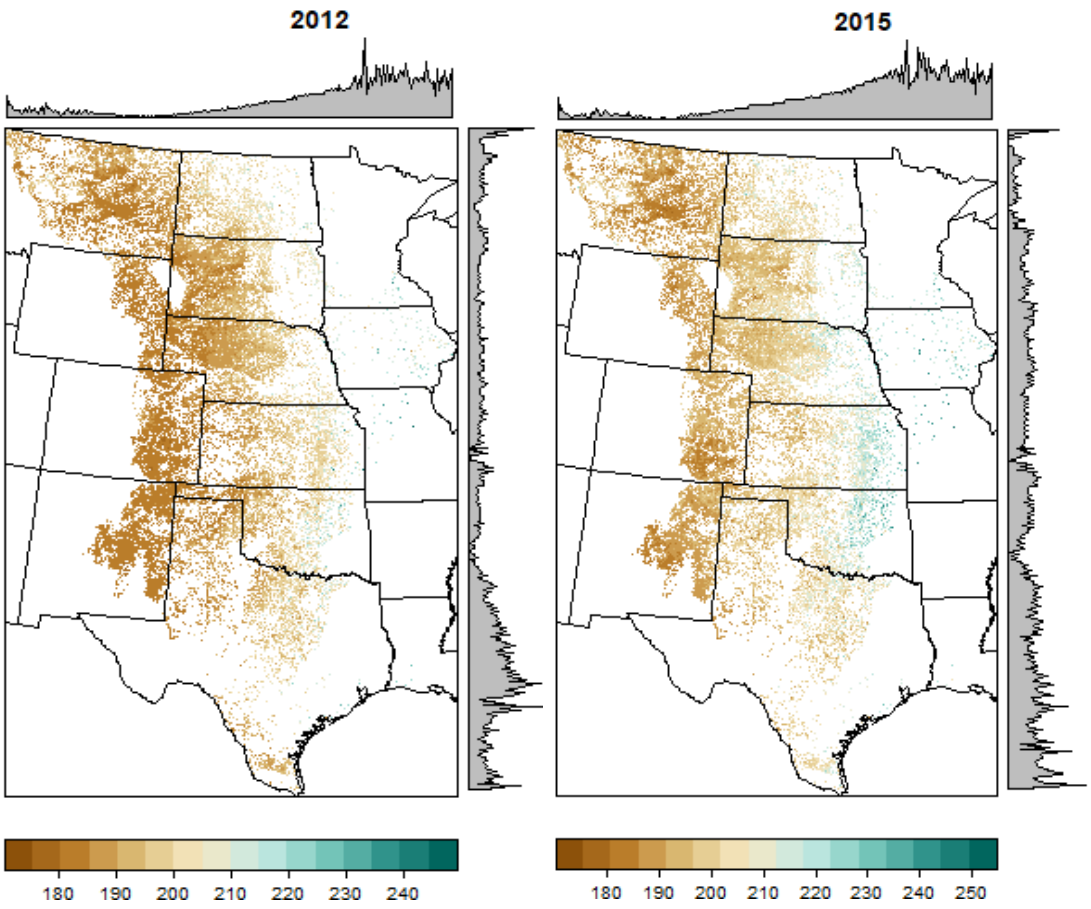

Figure 5.4: Spatial distribution of total carbon stock (in MgC) of grassland in the U.S. Great Plains for 2012 and 2015.

Net economic ES value of sequestered grassland carbon:

The net economic values of carbon sequestered by grasslands in the study area for the years 2001 to 2017 are shown in Table 5.3 and Figure 5.5. The values are in the 2007 U.S. dollars, and values reflect the annual change in carbon storage in the ecoregion. The net economic values between the years 2005 to 2006 and 2011 to 2012 were the least with approximately -1.6 and -1.9 billion 2007 U.S. dollars. On the other hand, the net economic values between the years 2006 to 2007 and 2012 to 2013 were the most, with approximately +2.1 and +2.7 billion 2007 U.S. dollars, respectively. The total net value from 2001 to 2017 was positive.

Table 5.3: Total annual net economic values of carbon sequestered by grasslands in the U.S. Great Plains

Time Period	The net economic value of carbon sequestered in 2007 U.S. Dollars
2001 to 2002	-869016908.7
2002 to 2003	693812686.9
2003 to 2004	573069435.9
2004 to 2005	389209754.1
2005 to 2006	-1598977703
2006 to 2007	2122456861
2007 to 2008	-808974007.6
2008 to 2009	422218704.3
2009 to 2010	509134417
2010 to 2011	-1491038612
2011 to 2012	-1875330605
2012 to 2013	2681820284
2013 to 2014	587028467.4
2014 to 2015	588145413.1
2015 to 2016	-328539203.8
2016 to 2017	-765942371.2

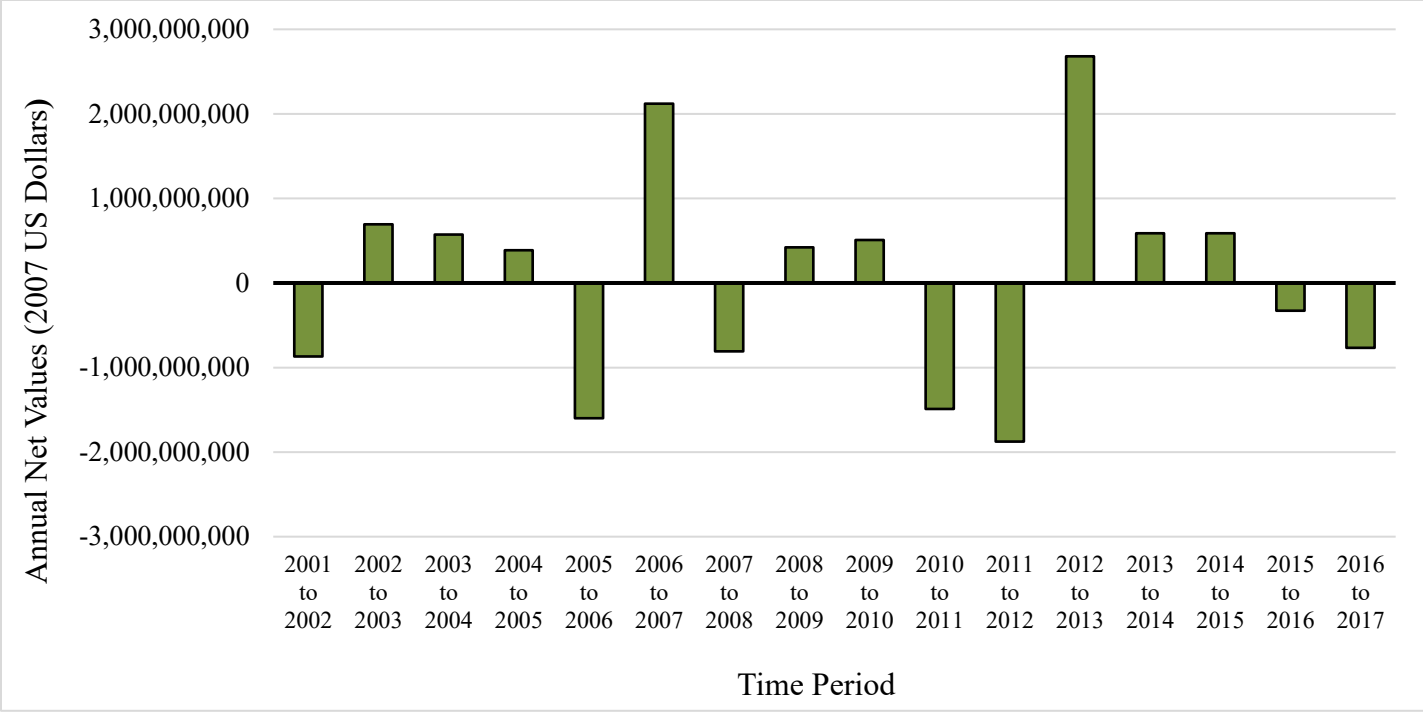

Figure 5.5: Total net economic values of carbon sequestered by grasslands in the U.S. Great Plains.

The spatial distribution of the net economic value of sequestered carbon (in 2007 dollars) for grasslands in the U.S. Great Plains is varied (figure 5.6). The net ES value of carbon between 2005 and 2006 saw an overall decrease with eastern parts of the study area (southern North Dakota, Mid Nebraska and South Dakota, east Kansas, Oklahoma, and Northern Texas) with the most decrease (less than 400 2007-dollars per hectare). Between 2006 and 2007, there was a turnaround with mostly increasing ES value in the southern parts of the study area. Another sharp decline in ES value happens between 2011 and 2012 (Figure 5.8), with the central to Northern region of the study having average of $700 decline per hectare.

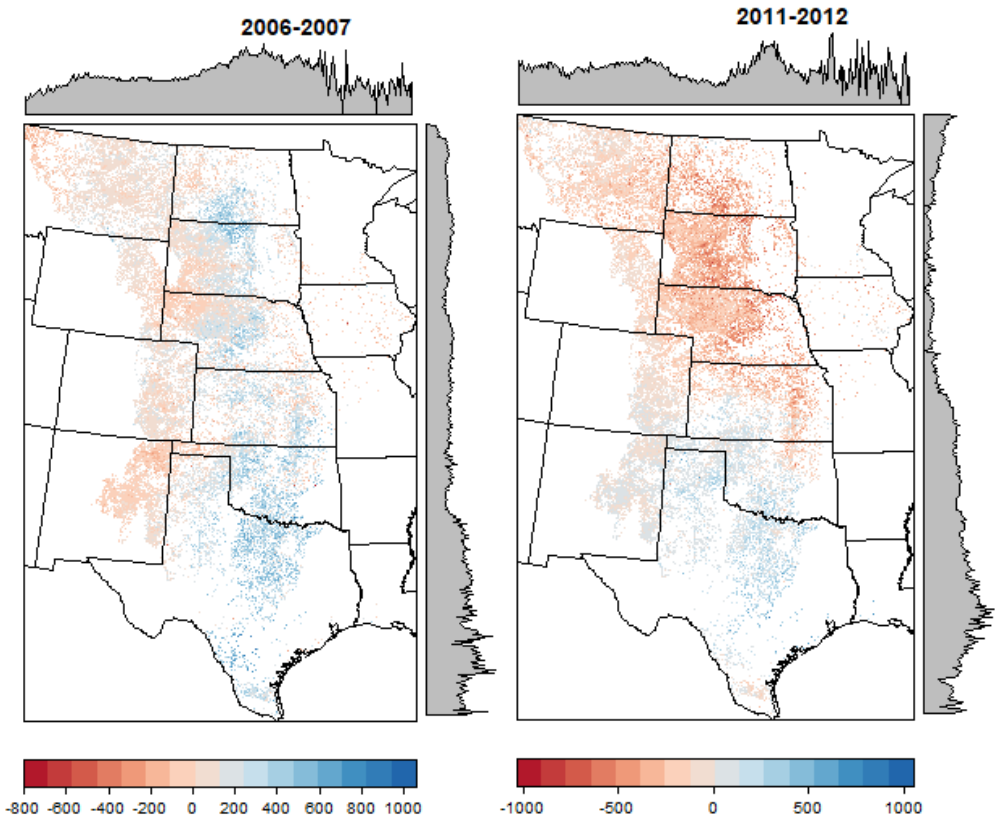

Figure 5.6: Spatial distribution of the net economic value of sequestered grassland carbon in the U.S. Great Plains in 2007 U.S. dollars per pixel (2006-2007, 2001-2012).

5.3.2 Sediment delivery model

The spatial patterns of selected results from the InVEST sediment delivery model analysis are shown in figures 5.7, 5.9, and 5.10. The selected maps include years that show a representative variation in spatial patterns of total annual potential soil loss and soil retention values (high and low) for the grassland areas in the U.S. Great Plains. See Appendix C5 for other maps.

Annual soil loss

The total annual soil loss in the study area for the years 2001 to 2017 is shown in figures 7 and 8. The estimated soil loss for the study period averaged 131 million tons per hectare. The total annual soil loss in the years 2003 and 2012 were the lowest, with approximately 92 and 83 million tons per hectare per year, respectively. On the other hand, the total annual soil loss in 2008, 2010, and 2011 were the most, with approximately 160, 180, and 167 million tons per hectare per year, respectively.

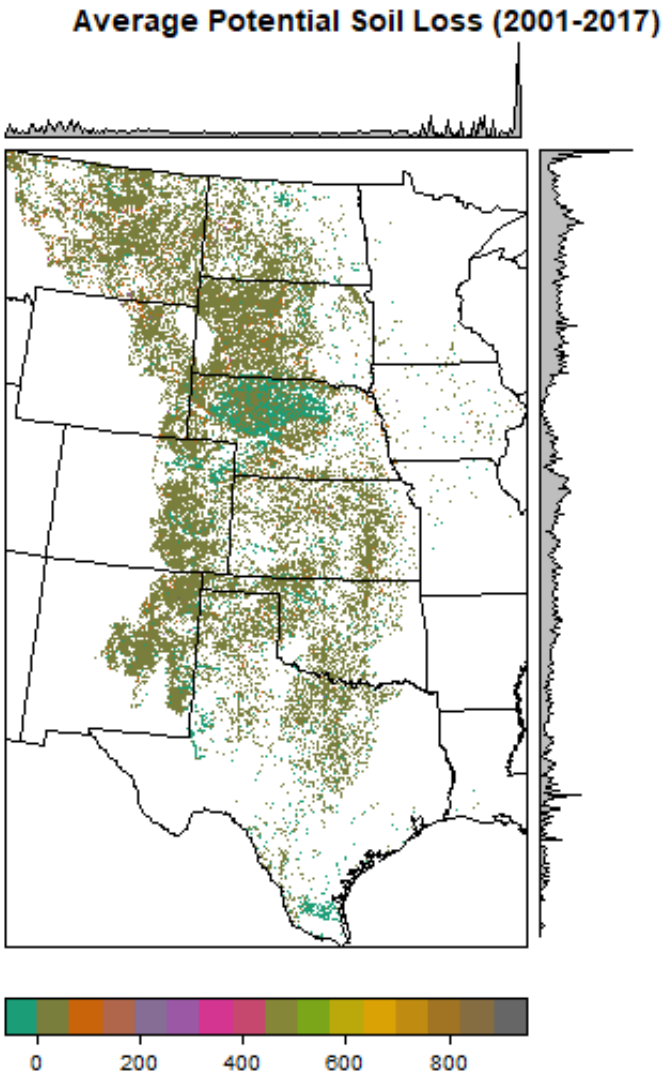

Figure 5.7: Average soil loss values (in tons per hectare) for the grassland area in the U.S. Great Plains

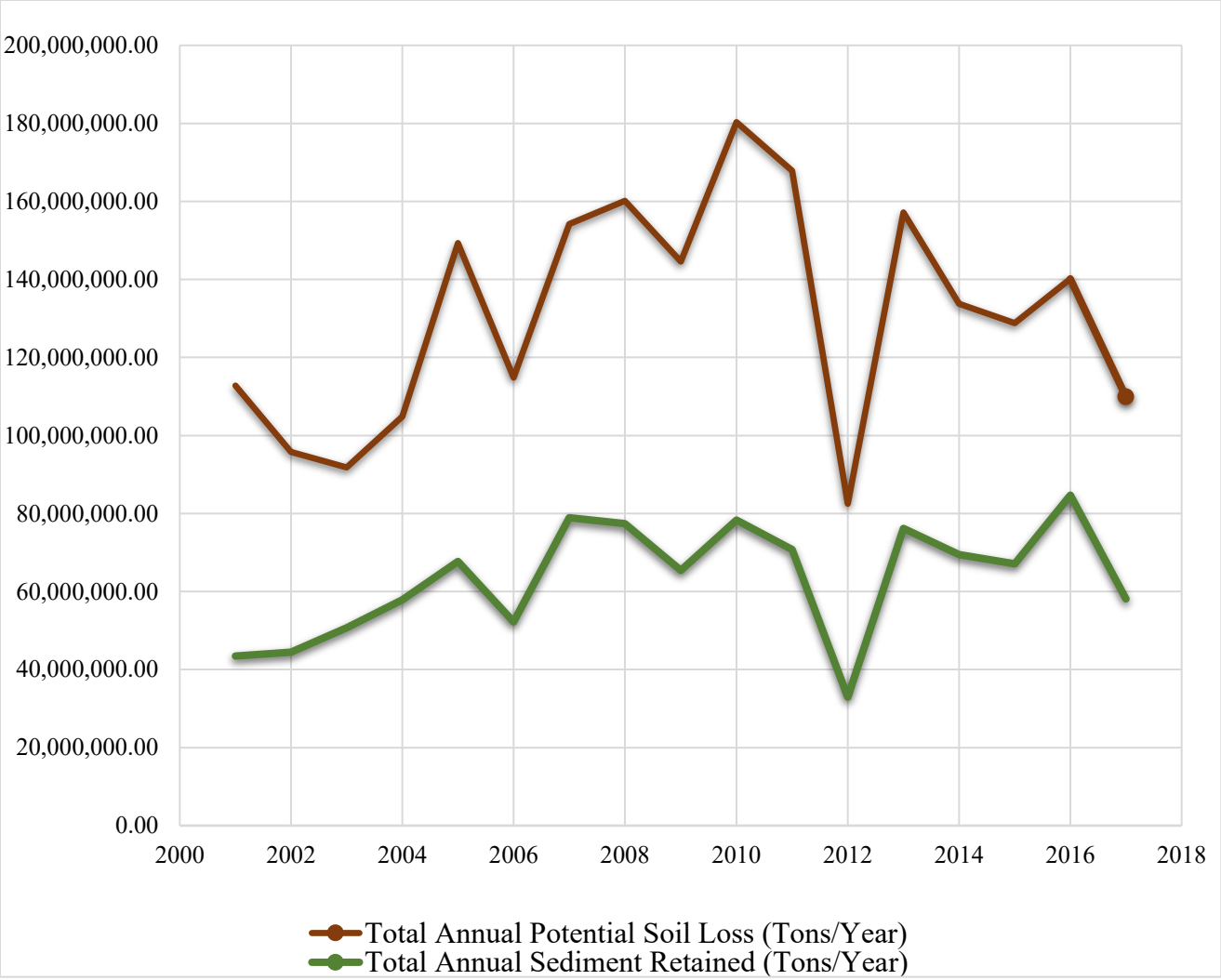

Figure 5.8: Total annual soil loss and sediment retention for the grassland areas in the U.S. Great Plains for 2001 to 2017.

The annual soil loss maps of grassland in the Great Plains Ecoregion show pixel-based biophysical measures of erosion prevention ES. The maps were derived using the USLE equation (Equation 3). Most of the ecoregion grassland areas had an annual soil loss value of 0 to 5 tons per hectare (Figure 5.9). These low values occur in northwest Nebraska, eastern parts of South Dakota, New Mexico, Colorado, and southern Texas. Higher values that range from 40 to 2000 tons/hectare occurs in varying parts of the study area, especially in Montana and the western part of South Dakota.

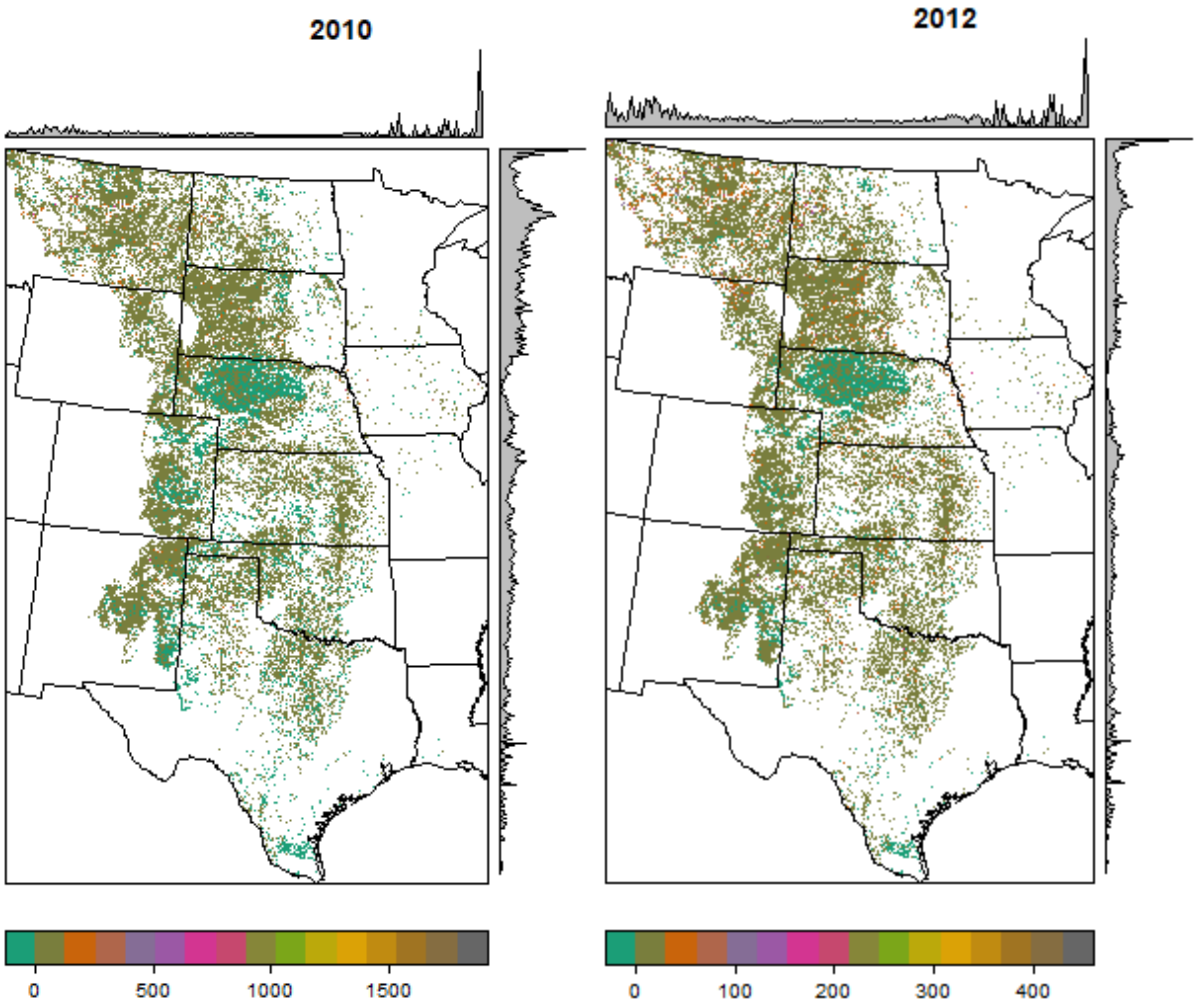

Figure 5.9: Spatial distribution of soil loss for the grassland areas in the U.S. Great Plains for the years 2010 and 2012.

Annual sediment retention

The spatial distribution of annual sediment retention for the grassland areas in the U.S. Great Plains is shown in Figure 5.10. The maps of annual sediment retention represent how much sediment is retained by the natural vegetative cover (grasslands in this situation) compared to an alternative scenario where the current natural vegetative cover was "removed." That is, how much soil sediment was retained because of the presence of grasslands. This was used to estimate the economic value related to soil erosion.

The total annual sediment retention in the study area for the years 2001 to 2017 is shown in figure 8. The estimated annual sediment retention for the study period averaged 63 million tons per hectare. The total annual sediment retained in the years 2001 and 2012 were the lowest, with approximately 44 and 33 million tons per hectare per year, respectively. On the other hand, the total annual sediment retained in 2007 and 2016 were the most, with approximately 79 and 85 million tons per hectare per year, respectively.

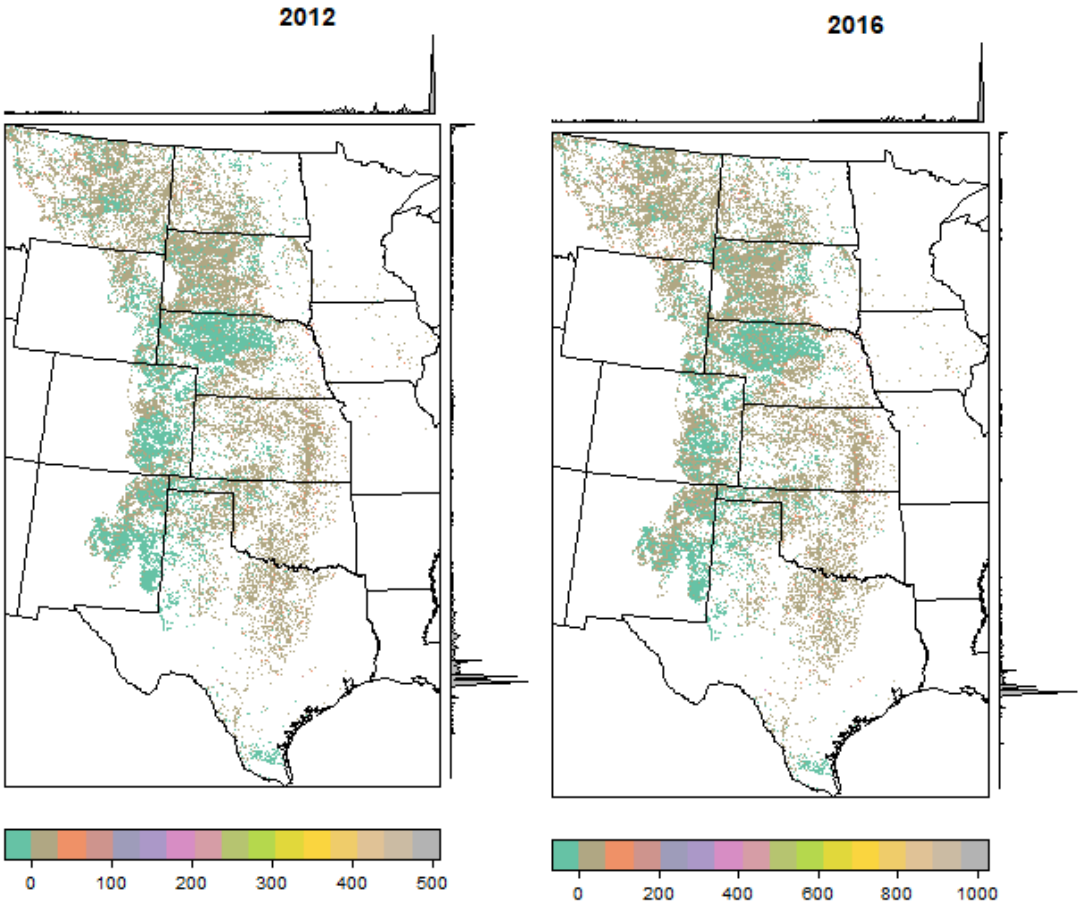

Figure 5.10: Spatial distribution of sediment retention for the grassland areas in the U.S. Great Plains for the years 2012 and 2016

.

There is generally increasing sediment retention from west to east in the study area (Figure 10). The western axis has values ranging from 0 to 5 tons per hectare per year to values over 40 tons per hectare per year on the eastern axis.

5.3.3 Validation

To validate the modified valuation method, ecosystem services values estimated from the carbon InVEST model were compared to estimation from another study that used a different method. The annual carbon stock in MgC was compared to estimation modeled by Zhu et al. (2011) for the grasslands in the Great Plains ecoregion. The Zhu et al. study is considered the "gold standard" comparison to this study because it was conducted by top-tier researchers from a reputable government organization. They carried out a detailed study of grasslands in the Great Plains in a similar study area and overlap of the period studied. Zhu et al. (2011) estimated a baseline (the average 2001 to 2005) carbon stock for grasslands in the Great Plains region in TgC. LULC data, climatic data, soil properties data including soil organic carbon (SOC) content were used to model baseline carbon storage. The values converted to MgC alongside values from the general inVEST method and the modified method of ES valuation for the same period are shown in Table 5.4.

Table 5.4: A comparison of approximate carbon stock estimates (2001-2005) produced for grasslands in the Great Plains ecoregion.

	Zhu et al. (2011)	**General InVEST Method**	**Modified Method**
C (TgC)	2,614	3,219	2,988
% Difference with Zhu et al. (2011)	--------	+18.8%	+12.5%

5.4. Discussion

The InVEST carbon storage and sequestration and sediment delivery models were applied to evaluate two important grassland-related ecosystem services in the U.S. Great Plains: carbon sequestration and erosion control. The temporal and spatial changes in ES values can be obtained from these aspects in response to changing conditions of grasslands in the study area. The method of quantifying ES using InVEST is highly generalizable and well documented; however, some limitations exist. The InVEST models used do not account for variability in carbon stock and sediment retention within specific LULC types (Duarte et al., 2016). This study uses improved methods that harness the

potential of remote sensing data to optimize spatial and temporal variability. Therefore, this research contributes to a literature that quantifies the value of multiple ecosystem services at a broad scale (Great Plains ecoregion as a whole) both spatially and temporally. It highlights the services provided by grasslands and how they are impacted by the changing state of grasslands (declination and degradation) while updating methods for biophysical and economic valuation.

5.4.1 Carbon model

The average carbon stock values for grasslands in the U.S. Great Plains from 2001 to 2017 varied in a west-east gradient, with values increasing from west to the east in the ecoregion. Values ranged from 180 MgC in the west to 220 MgC in the east (Figure 5.2). This distribution pattern of carbon stock is like the spatial distribution of prairie types that ranges from shortgrass prairies in the western part of the Great Plains to tallgrass prairies in the east. The main drivers of this pattern are the usual elevation and precipitation patterns in the Great Plains, which are also similar (Kunkel et al., 2013; Shafer et al., 2014). The regional precipitation has a west-east gradient, with a wetter east and a much drier West. The elevation gradient also runs west to east, with a higher elevation in the west that gets lower towards the east (Shafer et al., 2014). According to Pendall et al. (2018), grassland carbon balance is very sensitive to precipitation. On the other hand, there was little variation in the carbon stock value in the north-south axis of the ecoregion. The southern part had slightly higher carbon stock values than the north due to the temperature difference in these regions (Kunkel et al., 2013; Shafer et al., 2014).

The spatial patterns of annual carbon stock for grasslands in the U.S. Great Plains are like the overall average (increasing from west to east) and slightly higher carbon stock values in the south than the east (Figure 5.4). The temporal patterns of total annual grassland carbon stock also varied across the U.S. Great Plains. With reference to the mean total annual value (3 billion MgC), values decrease from 2001 to 2002, then continually increase and exceed the average total value in 2005, values the decreases drastically in 2006, overall increasing between 2006 and 2011 then the most decrease in the period in 2012. 2013 to 2015 saw the most increasing carbon storage with a slightly decreasing trend in 2016 and 2017 (Figure 5.3). Fitting a linear regression line of best fit through your yearly averages of carbon stock values for the grasslands in the U.S. Great Plains, the slope was significantly positive. A significant positive slope means that while the carbon uptake by grasslands in the U.S.

Great Plains was lower in the dry years (2002, 2012), it remained a net carbon sink in the 17 years studied.

Valuation of ES has many potential uses at various time and space scales, including the use in policy choices/scenarios, land use planning, raising awareness, payment for ES, etc. (Costanza et al., 2014). Just like the carbon stock estimation, the valuation of carbon sequestration by grassland in the U.S. Great Plains in the time studied showed some spatio-temporal variation. The average economic value of grassland carbon stock in the U.S. Great Plains between 2001 and 2017 was 93 billion 2007 U.S. dollars. The temporal economic values of carbon are like the values of carbon stock described in the preceding paragraph and presented in table 5. With a focus on carbon sequestration, the net values of carbon (the difference of the calculated economic value of a pixel in year one and the preceding year) were calculated (Table 5.3).

The net annual values of carbon decreased from 2001 to 2002, and it increased the period between 2002 and 2005 and then there is a sharp decline in net values between 2005 to 2006. Between 2006 to 2007, there was an increase in net values and an overall decrease in net value between 2007 to 2012. The biggest contrasts in annual net values of carbon in the Great Plains are between 2012 in 2013, and then we see a slight increase in value from 2014 to 2015 and the last two years decrease in value. The most significant temporal changes are in periods between 2005 to 2006 with a decrease, and then 2006 to 2007 is also show a sharp increase in net value (Figure 5.5). Another significant temporal change in the economic value of carbon in the Great Plains is between 2011 to 2012. This extreme shift in value can be observed in the carbon stock estimation, where 2012 was not a good year for grasslands (lowest value in the study period). These patterns are like precipitation patterns in the Great Plains during this time. In the Great Plains ecoregion. An example, 2012 was a drought year, and precipitation increased in 2013 hence that contrast. The spatial patterns of the net value vary from year to year (Figure 5.6), but temporally, the most increase occurred between 2012 and 2013 and the most loss in value between 2011 and 2012. Spatially, the net economic value of carbon within each period varies, but the Northern axis witnessed more decline than the south overall.

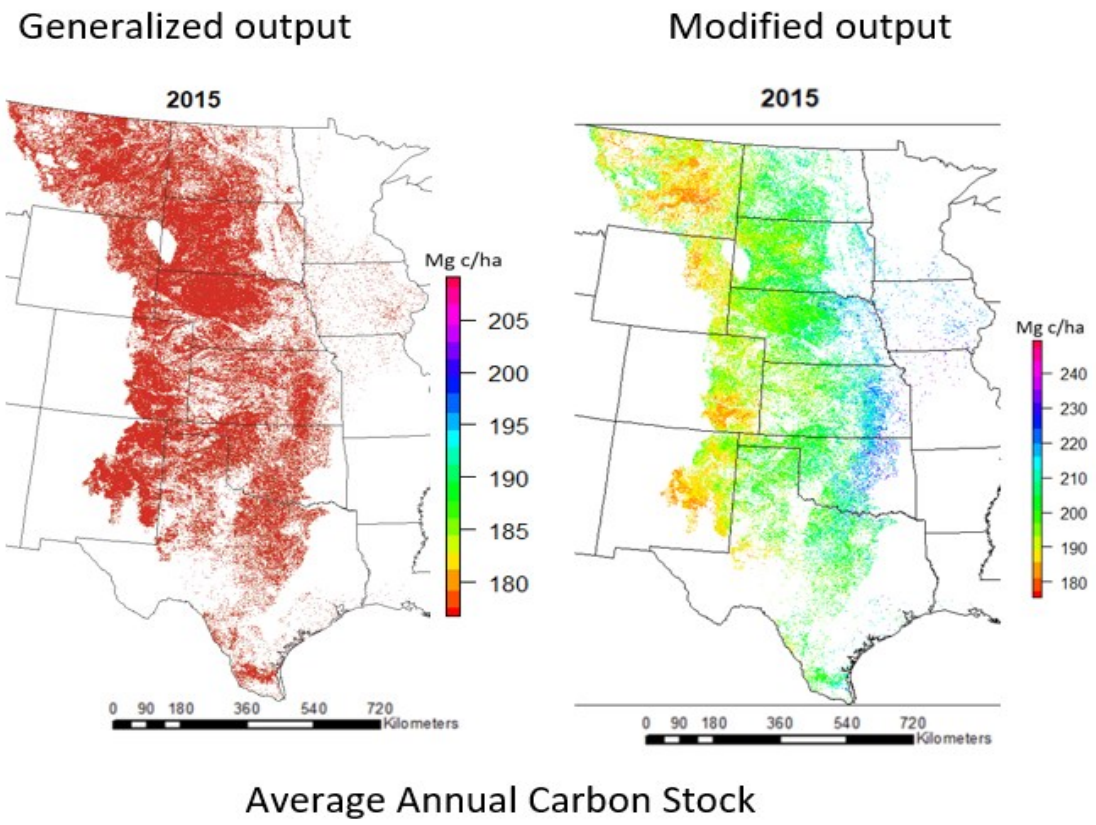

Figure 5.11: A comparison of the spatial distribution of total carbon stock of grassland in the U.S. Great Plains for 2015 using the generalized and modified InVEST methods.

Comparing Zhu et al. (2011) estimates to our estimates from the general InVEST and modified InVEST methods (Table 5.4), There is an 18.8% difference between the estimates of Zhu et al. (2011) and the general InVEST method, whereas there is a 12.5% difference between the Zhu et al. (2011) and the modified InVEST method. This means that there would be an overestimation of the value of ES using the general method. Thanks to the incorporation of remote sensing methods. Overestimation of C values might be detrimental to various areas that need and utilize ES values; environmental planning, environmental monitoring, policymaking, skewed or inaccurate contribution to the research area, etc. Zhang et al. (2019) study demonstrated how spatially homogenous global atmospheric CO_2 concentration values lead to overestimation, including the implications.

5.4.2 Sediment delivery model

Soil Loss: The patterns of annual soil loss varied across the U.S. Great Plains. Generally, there was

more soil loss in the northwestern parts of the ecoregion. Several factors impact soil erosion rates (precipitation, soil properties, topography), but the land cover and climate variability have the most impact (Joshi et al., 2020). Since our research was carried out on one landcover class (grasslands), the influence of climate will likely supersede the variation of grassland productivity (represented by the C factor in the sediment delivery analysis). Soil erosion might be more severe in other regions of the world, and there is still a huge impact on an ecosystem when soil loss rates exceed the rates of soil formation-soil degradation (Sala & Paruelo, 1997; Joshi et al., 2020).

The total annual soil loss value for the grassland area in the U.S. Great Plains ranged from 0 to 5 tons per hectare in the time studied (Figure 5.7), but the total annual value was averaged at 131 million tons per hectares. According to the U.S. Department of Agriculture's (USDA) 2017 National Resources Inventory (2020), soil erosion rates in the U.S. have constantly decreased since the 1980s but have remained constant in the past decade. The USDA's USLE database includes soil loss measurements from selected sites in the U.S. Midwest, and values fall between the range from our results, on average 0.2 tons per hectare a year (USDA, 2016). Soil loss values, especially for grasslands in the U.S., usually fall in this low range (less than 1), and soil loss in grassland areas is generally lower than in areas with other land covers (Salls et al., 2018; USDA, 2020). For example, as of 2017, the average soil erosion rate for croplands was 11.4 tons per hectare in the U.S. (USDA, 2020).

The spatial patterns of soil loss in the study area did not have a lot of variation. Distinct spatial patterns include very low values in the northwest areas of Nebraska (the Nebraska Sandhills ecoregion) and the southernmost of Texas (Figure 5.7). The Nebraska Sandhills ecoregion has the largest and most homogenous grassland expanse in North America, and it lies in the part of the region with the close to median temperature and precipitation values in the Great Plains (Conant et al., 2018). The southern part of Texas also has very high temperature and median precipitation values (Kloesel et al., 2018). Both regions are extremely dry regarding surface soil moisture, and they have mostly sand and sandy loam soil textures hence more precipitation infiltration and less runoff that leads to erosion (McDonough et al., 2020). Also, in the northwestern part of the Great Plains (Montana, Wyoming, and the Dakotas), several areas have high soil loss values; this region has the lowest precipitation rate in the study area and the lowest temperatures (Conant et al., 2018). The region also has mostly clay and clay loamy soils textures (McDonough et al., 2020). Hence, even though there is low precipitation

in this region, there is a high chance of mechanical weathering from the expansion and shrinking of clay soil, which temperature changes, and a lower rate of precipitation infiltration that may lead to increased surface runoff with time. So, contrary to our initial hypothesis that climate may play a considerable role in soil loss values in the Great Plains ecoregion, the spatial patterns also indicate a huge influence of land cover (in this case, grasslands), as evident from dense grasslands regions having lower soil loss values and soil texture.

The temporal patterns of annual soil loss are also varied across the U.S. Great Plains. 2003 and 2012 include years with the lowest amount of annual soil loss; these years are associated with lower than usual precipitation. On the other hand, 2008, 2010, and 2011 had the highest annual soil loss; these years also coincide with the years that had higher than normal precipitation (EPA, n.d.). On this broad scale, the influence of climate and soil erosion rates is most apparent. Fitting a linear regression line of best fit through the annual soil loss values slope was significantly positive, meaning increasing soil loss in the period studied.

Most analyses of soil loss rates in the U.S. Great Plains ecoregion were focused on croplands (Van Oost et al., 2006; Joshi et al., 2020). Therefore, the possibility of validating our annual soil loss values was minimal. Earlier, we compared our estimates to the USDA's 2017 National Resources Inventory values, and they were similar. We used an improved method to estimate annual soil loss values for grassland in the Great Plains as described in the methods section. As with the carbon stock estimation, soil loss estimations showed improved results using themodified methods compared to the generalized InVEST approach. Because we focused on one landcover class which is very variable and dynamic, the modified method highlights the variation in grasslands and yields more realistic, spatially explicit results. Figure 5.12 compares results from the generalized methods versus the modified method.

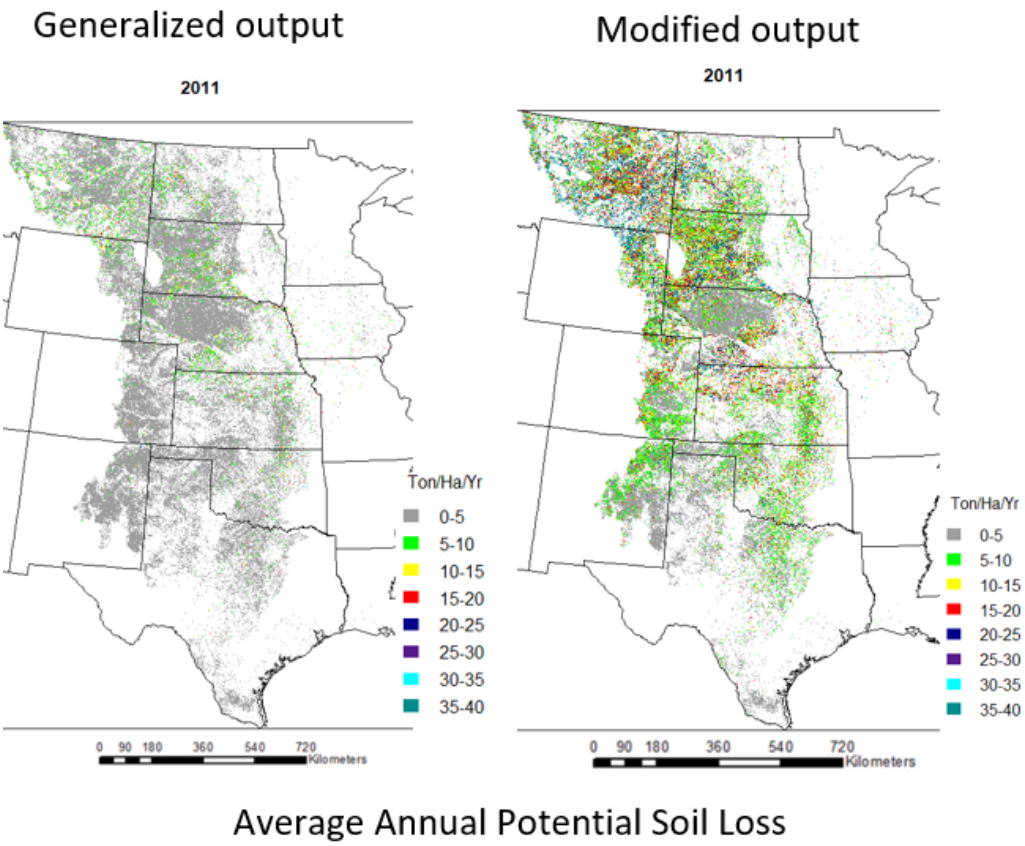

Figure 5.12: A comparison of the spatial distribution of the average annual soil loss in the grassland areas of the U.S. Great Plains for 2011 using the generalized and modified InVEST methods.

Sediment Retention: The annual sediment retention values for grassland areas in the U.S. great plains is how much soil sediment was retained because of the presence of a particular land cover, in this case, grasslands. This measure is used to estimate the economic value related to soil erosion. Spatially, sediment retention in the Great Plains ecoregion increases from west to east (Figure 5.10). This pattern is similar to precipitation and topographic patterns in the region. Surprisingly, the areas in the east with more sediment retention have more precipitation and lower elevation. The less steep topography could be why more sediments are retained in the west, but on the other hand, the type of grasslands could play a considerable role ask sediment retention is a factor of the land cover. The western region of the Great Plains is mostly covered by tallgrass prairies characterized by more biomass and longer roots hence, more sediment retention. The spatial patterns of sediment retention indicate a huge influence of landcover type and mirror the precipitation patterns in the ecoregion.

One will expect the opposite for correlation, but areas with higher precipitation experienced more sediment retention because of the presence of tallgrass prairie. However, the temporal analysis of sediment retention that considers total annual sediment retained in the study area shows similar patterns to the temporal patterns of soil loss (Figure 5.8). So, the years with drier than usual precipitation (2006 and 2012) have fewer sediments retained. We estimated the economic value for sediment retention in the ecoregion; since it was a direct estimation, the figures are very similar to the total annual sediment retained values.

One limitation that comes with the valuation of more the one ES is the possibility of overlapping. One ecosystem service correlating with another begs the question of overlapping estimation of their value. For example, Soil erosion is tied to carbon sequestration because the process of soil erosion-detachment and transportation can lead to the release of soil carbon (Joshi et al., 2020). This paper combined the estimated economic value of the carbon sequestration and soil erosion ESs (Table 5.5 and Figure 5.13 bottom). In the time studied, the average combined economic value is 93.43 billion (2007) U.S. dollars. The years 2002, 2006, and 2012 had the lowest combined economic value, and that he is 2007, 2010, and 2015 had the highest combined economic value in the 17 years studied. Again, fitting a linear regression line of best fit through the combined economic values slope was significantly positive, meaning increasing grassland ES values in the period studied.

Table 5.5: The combined economic values of carbon sequestration and soil erosion ESs for grasslands in the Great Plains ecoregion from 2001 to 2017.

Year	The economic value of carbon storage (2007$)	The economic value of soil retained (2007$)	Combined economic value (2007$)
2001	92686379098	193,785,419.06	92,880,164,516.78
2002	91514705640	198,382,236.12	91,713,087,876.39
2003	92411350916	226,295,360.47	92,637,646,276.10
2004	93122246432	258,257,762.84	93,380,504,194.43
2005	93586439101	302,084,204.29	93,888,523,304.99
2006	91749823376	232,896,809.04	91,982,720,184.59
2007	94100758155	352,050,362.78	94,452,808,517.61
2008	93235656231	345,229,018.77	93,580,885,249.80
2009	93672096782	291,713,016.27	93,963,809,798.34
2010	94181442918	349,290,437.63	94,530,733,355.27
2011	92713349887	315,625,330.49	93,028,975,217.94
2012	90895716838	146,867,933.67	91,042,584,771.59
2013	93416213812	339,826,724.56	93,756,040,536.28
2014	93951683214	309,700,690.97	94,261,383,905.45
2015	94472805825	299,171,667.30	94,771,977,492.73
2016	94189620744	377,810,327.94	94,567,431,071.70
2017	93547704355	259,289,834.53	93,806,994,189.30

We also compared the combined economic values of the ESs to the major climate variables in the U.S. (the EPA's precipitation and temperature anomalies). Figure 13 shows the side-by-side comparison, and the curve pattern shows that precipitation had more influence than temperature on ecosystem services in the Great Plains in the 17 years studied. In general, climate, soil texture, and land cover are major factors that influence the provision of carbon sequestration and soil erosion ecosystem services in the grassland areas of the U.S. Great Plains ecoregion.

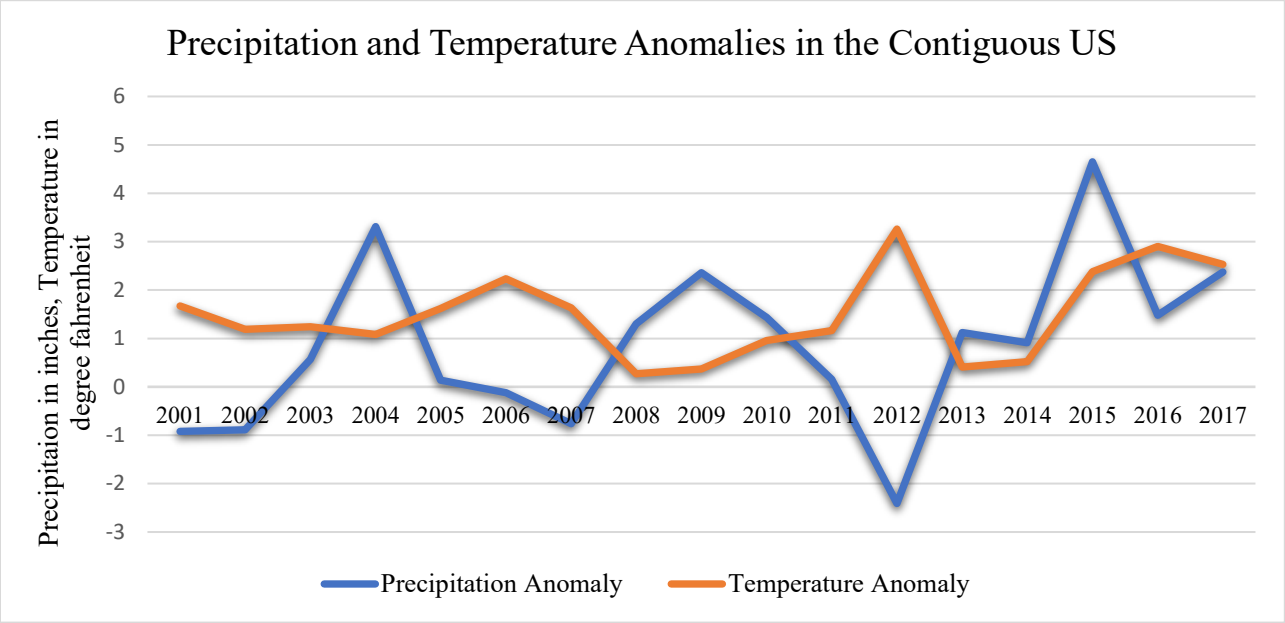

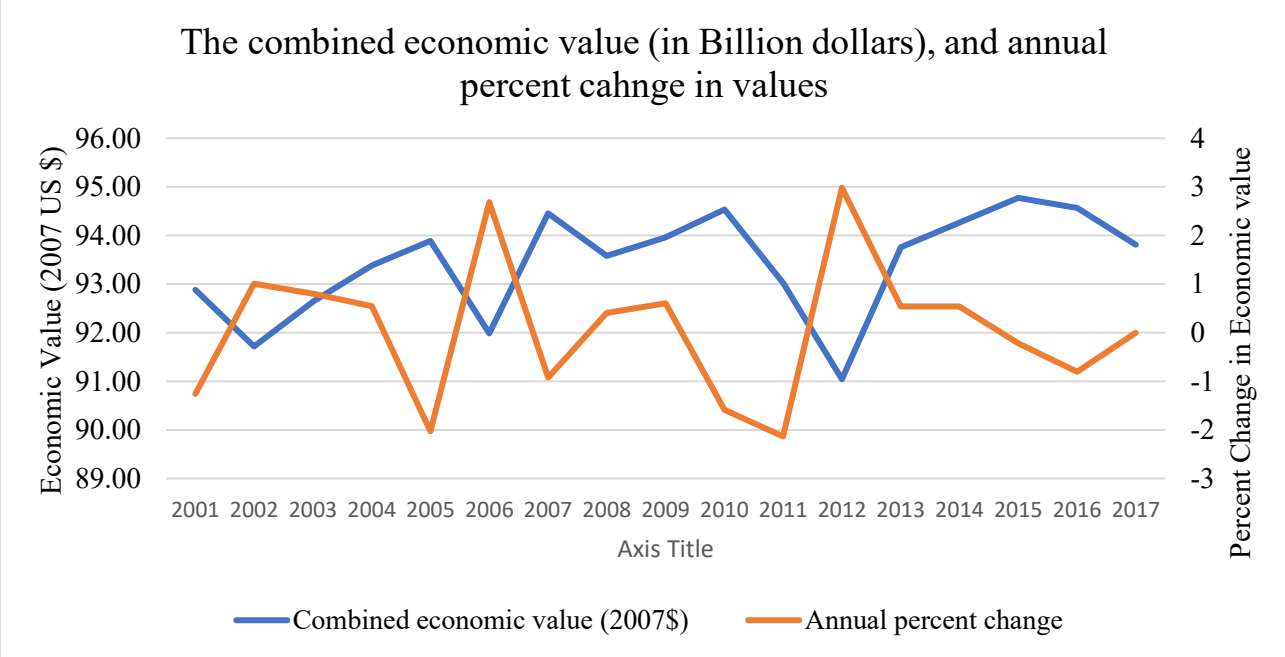

Figure 5.13: Top: Precipitation and earth surface temperature anomalies in the Contiguous 48 States, 2001-2017. Source: EPA's Climate Change Indicators in the United States. Bottom: The combined economic values of carbon sequestration and soil erosion ES for grasslands in the Great Plains ecoregion from 2001 to 2017.

Impact of the improved assessment of carbon and soil loss/retention:

Despite the constant evolution of the ecosystem services concept, there are still limitations regarding nomenclature, classification, and, most importantly, quantification and valuation. The use of earth observation in ecosystem services modeling has become the holy grail for ecosystem services quantification and valuation. As advances are made in remote sensing and GIS, it is expected that these advances will transfer into ecosystem services modeling. However, the use of earth observation data is yet in ES modeling is yet to see the necessary advancement. The many existing modeling/decision support tools that exist still have room to utilize the opportunities presented by earth observation data to overcome some of the limitations (Bagstad et al., 2013). Ramirez-Reyes et al. (2019) describe some challenges of integrating earth observation data into ecosystem services assessments to make it more optimal; one of the major technical challenges is moving from categorical to continuous conceptualizations. This means that many ecosystem modeling tools rely on the categorical representation of land use land cover data which is the basis of most models. A categorical conceptualization like this ignores the spatial heterogeneity of the ecosystem function being modeled, leading to inaccurate estimations and valuation. This is where our improved method comes in. The use of our improved methods harnesses the potential of remote sensing data to optimize spatial and temporal variability. As discussed in previous sections, our methods yielded results comparable to other studies and are more spatially heterogeneous, in essence, more realistic. So, the impact in our improved assessment of ecosystem services translates to more accurate estimates, improved valuation, and a better understanding of the provision of grassland ecosystem services in the Great Plains ecoregion (and likely other grassland regions).

5.5. Conclusions

Given the essential role of grasslands in the provision of several ES and the mitigation of several negative environmental processes like soil erosion and carbon sequestration, their monitoring and conservation still have some work to do. There is an urgent need to estimate the impact of grassland conditions in response to the changing climate and other anthropogenic activities through long-term studies. This paper estimated the biophysical and economic values of two grassland-related regulating ES in the U.S. Great Plains: the control of soil erosion and carbon sequestration. In addition to the estimation of grasslands, we developed and used an improved method that captures the spatial

heterogeneity of grasslands ecosystem function leading to more accurate quantification and valuation. Using the highly generalizable InVEST ES modeling tool, we incorporated spatially explicit and temporally available earth observation data to replace the categorical and static land use/land cover-based modeling of ES. Then we used the modeled biophysical measure to costs estimation methods to calculate the economic value of both ES.

The results show both spatial and temporal variation, and they indicate a significant influence of precipitation, soil texture, and land cover (in this case, grassland biomass). Our results were also validated using an existing study that is considered the "gold standard" because of its similarity in the study area, study period, and the reputation of the researchers, and our results using the improved methods compare to deaths. The comparison of this existing study to the generalized methods shows overestimation and possibly inaccuracy in results. ES quantification and valuation accuracy are crucial because they impact environmental planning and monitoring policymaking and contribute to research in related fields.

Ecosystem services are increasingly being considered in policymaking, decision making, interdisciplinary research, environmental management, and conservation, and there is still room for a wider application (Ramirez-Reyes et al., 2019). There is a potential to improve ecosystem services valuation in terms of accuracy, data availability, and generalizability by harnessing the very many advancements of earth observation or remotely sensed data. While the incorporation of remote sensing methods or data dos not the perfect solution for the limitations in ES modeling, it can improve the representation of the spatial heterogeneity that exists in reality and better capture the temporal dynamics after the supply and demand of ecosystem services.

Climate change (past, present, and future) influences grassland productivity and phenology with consequences on ecosystems and their value. Results from this study show the impact of changing grassland conditions based on greenness on the Great Plains ecoregion. An analysis of the carbon stock value over the period studied showed and overall positive trend. This agrees with findings from our previous work (Chapter 4) and Hufkens et al. (2016) on increased productivity of grasslands in the time studied. Future work is suggested to analyze the specific factors that contribute to the increasing productivity of grasslands in the Great Plains ecoregion and its implications on the ecoregion as a whole.

Acknowledgment

This research was funded by the Kansas State University Department of Geography and Geospatial Sciences' 2020 Steven Kale fellowship and the American Geographical Society's 2021 fellowship.

5.6 References

Ayalew, D. A., Deumlich, D., Šarapatka, B., & Doktor, D. (2020). Quantifying the Sensitivity of NDVI-Based C Factor Estimation and Potential Soil Erosion Prediction using Spaceborne Earth Observation Data. *Remote Sensing*, 12(7), 1136. https://doi.org/10.3390/rs12071136

Ayanu, Y. Z., Conrad, C., Nauss, T., Wegmann, M., & Koellner, T. (2012). Quantifying and mapping ecosystem services supplies and demands: a review of remote sensing applications. *Environmental Science & Technology*, 46(16), 8529–8541. https://doi.org/10.1021/es300157u

Bagstad, K. J., Semmens, D. J., Waage, S., & Winthrop, R. (2013). A comparative assessment of decision-support tools for ecosystem services quantification and valuation. *Ecosystem Services*, 5, 27–39. https://doi.org/10.1016/j.ecoser.2013.07.004

Balabathina, V. N., Raju, R. P., Mulualem, W., & Tadele, G. (2020). Estimation of soil loss using remote sensing and GIS-based universal soil loss equation in northern catchment of Lake Tana Sub-basin, Upper Blue Nile Basin, Northwest Ethiopia. *Environmental Systems Research*, 9(1). https://doi.org/10.1186/s40068-020-00203-3

Beck, H. E., Zimmermann, N. E., McVicar, T. R., Vergopolan, N., Berg, A., & Wood, E. F. (2018). Present and future Köppen-Geiger climate classification maps at 1-km resolution. *Scientific Data*, 5, 180214. https://doi.org/10.1038/sdata.2018.214

Borselli, L., Cassi, P., & Torri, D. (2008). Prolegomena to sediment and flow connectivity in the landscape: a GIS and field numerical assessment. *Catena*, 75(3), 268-277. https://doi.org/10.1016/j.catena.2008.07.006

Brander, L. M., & Crossman, N. (2017). *Economic quantification*. In B Burkhard & J. Maes (Eds.), Mapping Ecosystem Services (pp. 113–123). Pensoft Publishers.

Cerdan, O., Govers, G., Le Bissonnais, Y., Van Oost, K., Poesen, J., Saby, N., Gobin, A., Vacca, A., Quinton, J., Auerswald, K., Klik, A., Kwaad, F. J. P. M., Raclot, D., Ionita, I., Rejman, J., Rousseva, S., Muxart, T., Roxo, M. J., & Dostal, T. (2010). Rates and spatial variations of soil erosion in Europe: A study based on erosion plot data. *Geomorphology*, 122(1–2), 167–177. https://doi.org/10.1016/j.geomorph.2010.06.011

Comer, P. J., Hak, J. C., Kindscher, K., Muldavin, E., & Singhurst, J. (2018). Continent-Scale Landscape Conservation Design for Temperate Grasslands of the Great Plains and Chihuahuan Desert. Natural Areas Journal, 38(2), 196–211. https://doi.org/10.3375/043.038.0209

Costanza, R., d'Arge, R., de Groot, R., Farber, S., Grasso, M., Hannon, B., Limburg, K., Naeem, S., O'Neill, R. V., Paruelo, J., Raskin, R. G., Sutton, P., & van den Belt, M. (1997). The value of the world's ecosystem services and natural capital. *Nature*, 387(6630), 253–260. https://doi.org/10.1038/387253a0

Costanza, R., de Groot, R., Braat, L., Kubiszewski, I., Fioramonti, L., Sutton, P., Farber, S., & Grasso, M. (2017). Twenty years of ecosystem services: How far have we come and how far do we still need to go? *Ecosystem Services*, 28, 1–16. https://doi.org/10.1016/j.ecoser.2017.09.008

Costanza, R., de Groot, R., Sutton, P., van der Ploeg, S., Anderson, S. J., Kubiszewski, I., Farber, S., & Turner, R. K. (2014). Changes in the global value of ecosystem services. *Global Environmental Change*, 26, 152–158. https://doi.org/10.1016/j.gloenvcha.2014.04.002

Daily, G. C., Myers, J. P., & Reichert, J. (1997). *Nature's services: Societal dependence on natural ecosystems* (2nd ed., p. 412). Island Press

De Araujo Barbosa, C. C., Atkinson, P. M., & Dearing, J. A. (2015). Remote sensing of ecosystem services: A systematic review. *Ecological Indicators*, 52(52), 430–443. https://doi.org/10.1016/j.ecolind.2015.01.007

Desmet, P. J. J. & Govers, G. (1996). A GIS Procedure for automatically calculating the USLE LS factor on topographically complex landscape units. *Journal of Soil and Water Conservation,* 51, 427-433.

Drummond, M. A., & Auch, R. F. (2015). Land-Cover Trends in the Great Plains of the United States—1973 to 2000. In J. L. Taylor, W. Acevedo, R. F. Auch, & M. A. Drummond (Eds.), Status and Trends of Land Change in the Great Plains of the United States—1973 to 2000 (pp. 3–19). U.S. Geological Survey.

Duarte, G. T., Ribeiro, M. C., Paglia, A. P. (2016). Ecosystem Services Modeling as a tool for defining priority areas for conservation. *PLoS ONE* 11(5). https://doi.org/10.1371/journal.pone.0154573

Dunford, R. W., Harrison, P. A., & Bagstad, K. J. (2017). Computer modelling for ecosystem service assessment-4.4. In B. Burkhard, & J. Maes, J (Eds). *Mapping Ecosystem Services*. Advanced Books. https://doi.org/10.3897/ab.e12837

Durigon, V. L., Carvalho, D. F., Antunes, M. A. H., Oliveira, P. T. S., & Fernandes, M. M. (2014). NDVI time series for monitoring RUSLE cover management factor in a tropical watershed.

International Journal of Remote Sensing, 35(2), 441–453. https://doi.org/10.1080/01431161.2013.871081

EPA's Climate Change Indicators in the United States. (2021). *Precipitation in the Contiguous 48 States, 1901-2020*. https://www.epa.gov/climate-indicators/climate-change-indicators-us-and-global-temperature#ref1

EPA's Climate Change Indicators in the United States. (2021). *Temperature in the Contiguous 48 States, 1901-2020*. https://www.epa.gov/climate-indicators/climate-change-indicators-us-and-global-precipitation

Erencin, Z. (2000, August). *C-factor Mapping Using Remote Sensing and GIS, A Case Study of Lom Sak/Lom Kao, Thailand* [Master's thesis, Geographisches Institut, Justus Liebig Universität, Giessen Soil Science Division International Institute for Aerospace Survey and Earth Sciences Enschede, The Netherlands]. https://core.ac.uk/download/pdf/56347214.pdf

Food and Agriculture Organization [FAO] & Intergovernmental Technical Panel on Soils [ITPS]. (2020). *Global Soil Organic map V1.5: Technical Report*. Rome, FAO. https://doi.org/10.4060/ca7597en

Galat, D. L., Berry, C. R., Jr., Peters, E. J., & White, R. G. (2005). *Missouri River basin, in Benke*, A.C., and Cushing, C.E., eds., Rivers of North America: Burlington, Mass., Elsevier Academic Press, p. 427–479.

Homer, C., Dewitz, J., Yang, L., Jin, S., Danielson, P., Xian, G., Coulston, J., Herold, N., Wickham, J., & Megown, K. (2015). Completion of the 2011 National Land Cover Database for the Conterminous United States – Representing a Decade of Land Cover Change Information. Photogrammetric Engineering & Remote Sensing, 81(5), 345–354.

Huete, A. R. (1988). A soil-adjusted vegetation index (SAVI). *Remote Sensing of Environment*, 25(3), 295–309. https://doi.org/10.1016/0034-4257(88)90106-X

Hufkens, K., Keenan, T. F., Flanagan, L. B., Scott, R. L. Bernacchi, C. J., Joo, E., Brunsell, N. A., Verfaillie, J. & Richardson, A. D. (2016). Productivity of North American grasslands is increased under future climate scenarios despite rising aridity. *Nature Climate Change* 6, 710–714. https://doi.org/10.1038/nclimate2942

Joshi, D. R., Clay, D. E., Smart, A., Clay, S. A., Tulsi P. Kharel, T. P., & Mishra, U. (2020). *Soil and Land-Use Change Sustainability in the Northern Great Plains of the USA*. In S. Appiah-

Opoku (Eds.). Land Use Change and Sustainability. *Intech Open*. https://doi.org/10.5772/intechopen.84781

Kelsey, K. C., & Neff, J. C. (2014). Estimates of aboveground biomass from texture analysis of Landsat imagery. *Remote sensing*, 6, 6407-6422. https://doi.org/10.3390/rs6076407

Kienast, F., & Helfenstein, J. (2016). Modelling ecosystem services. In M Potschin, R. Haines-Young, R. Fish, & R. K. Turner (Eds.), Routledge handbook of ecosystem services (pp. 144–156). Routledge.

Kloesel, K., Bartush, B., Banner, J., Brown, D., Lemery, J., Lin, X., Loeffler, C., McManus, G., Mullens, E., Nielsen-Gammon, J., Shafer, M., Sorenson, C., Sperry, S. K., Wildcat, D. R., & Ziolkowska, J. R. (2018). *Chapter 23: southern great plains. impacts, risks, and adaptation in the United States: the fourth national climate assessment, volume II*. U.S. Global Change Research Program. https://doi.org/10.7930/NCA4.2018.CH23

Kunkel, K. E., Stevens, L. E., Stevens, S. E., Sun, L., Janssen, E., Wuebbles, D., Kruk, M. C., Thomas, D., Shulski, M., Umphlett, N. A., Hubbard, K. G., Robbins, K., Romolo, L., Akyuz, A., Pathak, T. B., Bergantino, T. R., & Dobson, J. G. (2013). *Regional Climate Trends and Scenarios for the US National Climate Assessment Part 4. Climate of the US Great Plains*, NOAA Technical Report NESDIS 142-4, 82 pp.

Kuok, K. K., Mah, D. & Chiu, P. (2013). Evaluation of C and P Factors in Universal Soil Loss Equation on Trapping Sediment: Case Study of Santubong River. Journal of Water Resource and Protection, 5 (12),1149-1154. https://doi.org/10.4236/jwarp.2013.512121

LeRoy, H., & Ribaudo, M. (2008). *Economic Measures of Soil Conservation Benefits: Regional Values for Policy Assessment, TB-1922*. U.S. Dept. of Agriculture, Economic Research Service.

Lark, T. J. (2020). Protecting our prairies: Research and policy actions for conserving America's grasslands. Land Use Policy, 97, 104727. https://doi.org/10.1016/j.landusepol.2020.104727

Lark, T., Larson, B., Schelly, I., Batish, S., & Gibbs, H. (2019). Accelerated Conversion of Native Prairie to Cropland in Minnesota. *Environmental Conservation*, 46(2), 155-162. doi:10.1017/S0376892918000437

Liquete, C., Haas, E., Bondo, T., Hirzinger, C., Schnelle, M., Reisinger, D., Lyon, D., Finisdore, J., & Ledwith, M. (2016). *A practical approach to mapping of ecosystems and ecosystem services using remote sensing*. In Marion Potschin, R. Haines-Young, R. Fish, & R. K. Turner (Eds.),

Routledge handbook of ecosystem services (pp. 205–212). Routledge. https://doi.org/10.4324/9781315775302-18

Matthews, W. J., Vaughn, C. C., Gido, K. B., & Marsh-Matthews, E. (2005). *Southern Plains rivers*. In Benke, A. C., & Cushing, C. E. (Eds.), Rivers of North America (pp. 283–311). Elsevier Academic Press.

McDonough, K., Hutchinson, S., Moore, T., & Hutchinson, J. M. S. (2017). Analysis of publication trends in ecosystem services research. *Ecosystem Services*, 25, 82–88. https://doi.org/10.1016/j.ecoser.2017.03.022

MEA (Millennium Ecosystem Assessment). (2005). Ecosystems and Human Well-being: Synthesis (2nd ed., p. 160). Island Press.

Muche, M. E., Hutchinson, S. L., Hutchinson, J. S., & Johnston, J. M. (2019). Phenology-adjusted dynamic curve number for improved hydrologic modeling. *Journal of Environmental Management*, 235, 403–413. https://doi.org/10.1016/j.jenvman.2018.12.115

Naeth, M. A., Bailey, A. W., Pluth, D. J., Chanasyk, D., & Hardin, R. T. (1991). Grazing impacts on litter and soil organic matter in mixed prairie and fescue grassland ecosystems of Alberta. *Journal of Range Management*, 44(1), 7-12. https://doi.org/10.2307/4002629

Nelson, E., Mendoza, G., Regetz, J., Polasky, S., Tallis, H., Cameron, Dr., Chan, K. M., Daily, G. C., Goldstein, J., Kareiva, P. M., Lonsdorf, E., Naidoo, R., Ricketts, T. H., & Shaw, M. (2009). Modeling multiple ecosystem services, biodiversity conservation, commodity production, and tradeoffs at landscape scales. Frontiers in Ecology and the Environment, 7(1), 4–11. https://doi.org/10.1890/080023

Oakleaf, J. R., Kennedy, C. M., Baruch-Mordo, S., West, P. C., Gerber, J. S., Jarvis, L., & Kiesecker, J. (2015). A world at risk: aggregating development trends to forecast global habitat conversion. *Plos One*, 10(10): e0138334. https://doi.org/10.1371/journal.pone. 0138334

Omernik, J. M. (1987). Ecoregions of the Conterminous United States. Annals of the Association of American Geographers, 77(1), 118–125. https://doi.org/10.1111/j.1467-8306.1987.tb00149.x

Omernik, J. M., & Griffith, G. E. (2014). Ecoregions of the conterminous United States: evolution of a hierarchical spatial framework. *Environmental Management*, 54(6), 1249–1266. https://doi.org/10.1007/s00267-014-0364-1

Pan, J. & Wen, Y. (2014). Estimation of soil erosion using RUSLE in Caijiamiao watershed, China. *Natural Hazards*, 71, 2187–2205. https://doi.org/10.1007/s11069-013-1006-2

Parysow, P., Wang, G., Gertner, G., & Anderson, A. B. (2003). Spatial uncertainty analysis for mapping soil erodibility based on joint sequential simulation. *Catena*, 53(1), 65–78. https://doi.org/10.1016/S0341-8162(02)00198-4

Plowprint annual report (2021). *World Wildlife Fund*. Retrieved from https://files.worldwildlife.org/wwfcmsprod/files/Publication/file/5yrd3g00ig_PlowprintReport_2021_Final_HiRes_b.pdf?_ga=2.206397267.119456530.1640946732-1705276999.1640946731

PRISM Climate Group. (2019). *PRISM Climate Data*. Oregon State University. http://prism.oregonstate.edu

Ramirez-Reyes, C., Brauman, K. A., Chaplin-Kramer, R., Galford, G. L., Adamo, S. B., Anderson, C. B., Anderson, C., Allington, G., Bagstad, K. J., Coe, M. T., Cord, A. F., Dee, L. E., Gould, R. K., Jain, M., Kowal, V. A., Muller-Karger, F. E., Norriss, J., Potapov, P., Qiu, J., Rieb, J. T., … Wright, T. M. (2019). Reimagining the potential of Earth observations for ecosystem service assessments. *The Science of the total environment*, 665, 1053–1063. https://doi.org/10.1016/j.scitotenv.2019.02.150

Renard, K. G. & Freimund, J. R. (1994). Using monthly precipitation data to estimate the R-Factor in the revised USLE. *Journal of Hydrology*, 157, 287–306. https://doi.org/10.1016/0022-1694(94)90110-4

Rossum, S., & Lavin, S. (2000). Where are the great plains? A cartographic analysis. *The Professional Geographer*, 52(3), 543–552. https://doi.org/10.1111/0033-0124.00245

Sala, O. E., & Paruelo, J. M. (1997). *Ecosystem services in grasslands*. In G. C. Daily (Ed.), Nature's Services: Societal Dependence on Natural Ecosystems (pp. 237–252). Island Press.

Salls, W., Larsen, R., Lewis, D., Roche, L., Eastburn, D., Hollander, A., Walkinshaw, M., Kaffka, S., Tate, K., & O'geen, A. (2018). Modeled soil erosion potential is low across California's annual rangelands. *California Agriculture* 72(3),179-191. https://doi.org/10.3733/ca.2018a0021.

Shafer, M., Ojima, D., Antle, J. M., Kluck, D., McPherson, R. A., Petersen, S., Scanlon, B., & Sherman, K. (2014). *Ch. 19: Great Plains*. Climate change impacts in the United States: the third national climate assessment. U.S. Global Change Research Program. https://doi.org/10.7930/J0D798BC

Sharp, R., Douglass, J., Wolny, S., Arkema, K., Bernhardt, J., Bierbower, W., Chaumont, N., Denu, D., Fisher, D., Glowinski, K., Griffin, R., Guannel, G., Guerry, A., Johnson, J., Hamel, P.,

Kennedy, C., Kim, C.K., Lacayo, M., Lonsdorf, E., Mandle, L., Rogers, L., Silver, J., Toft, J., Verutes, G., Vogl, A. L., Wood, S., & Wyatt, K. (2020). *InVEST 3.9.0.post77+ug.g875ac02 User's Guide*. The Natural Capital Project, Stanford University, University of Minnesota, The Nature Conservancy, and World Wildlife Fund.

Sollenberger, L. E., Kohmann, M. M., Dubeux, J. C. B., & Silveira, M. L. (2019). Grassland management affects delivery of regulating and supporting ecosystem services. Crop Science, 59(2), 441-459. https://doi.org/10.2135/cropsci2018.09.0594

Spawn, S. A., & Gibbs, H. K. (2019). Global Aboveground and Belowground Biomass Carbon Density Maps for the Year 2010. ORNL DAAC, Oak Ridge, Tennessee, USA. https://doi.org/10.3334/ORNLDAAC/1763

TEEB. (2010). *The Economics of Ecosystems and Biodiversity: Mainstreaming the Economics of Nature: A synthesis of the approach, conclusions and recommendations of TEEB*. Progress Press.

Tollerud, H., Brown, J., Loveland, T., Mahmood, R., & Bliss, N. (2018). Drought and Land-Cover Conditions in the Great Plains. Earth Interactions, 22(17), 1–25. https://doi.org/10.1175/ EI-D-17-0025.1

Tsai, F., Lin, T. C., Chiang, S. H., & Chen, W. W. (2016). *Spatial data mining for estimating cover management factor of Universal Soil Loss Equation*. AGU Fall Meeting Abstracts. American Geophysical Union. https://ui.adsabs.harvard.edu/abs/2016AGUFMIN23B1777T

United States Environmental Protection Agency, [USEPA]. (2015). National Ecosystem Services Classification System (NESCS): Framework Design and Policy Application. EPA-800-R-15-002. United States Environmental Protection Agency.

U.S. Department of Agriculture. (2016). *National Soil Erosion Research: West Lafayette, IN.* https://www.ars.usda.gov/midwest-area/west-lafayette-in/national-soil-erosion-research/docs/usle-database/usle-data/

U.S. Department of Agriculture. (2020). Summary Report: 2017 National Resources Inventory, Natural Resources Conservation Service, Washington, DC, and Center for Survey Statistics and Methodology, Iowa State University, Ames, Iowa. https://www.nrcs.usda.gov/wps/portal/nrcs/main/national/technical/nra/nri/results/

U.S. Geological Survey. (2017). 1 Arc-second Digital Elevation Models (DEMs) - USGS National Map 3DEP Downloadable Data Collection. https://www.usgs.gov/core-science-systems/ngp/tnm-delivery/gis-data-download

Van der Knijff, J. M., Jones, R. J. A., & Montanarella, L. (2000). *Soil Erosion Risk Assessment in Italy*. Space Applications Institute, European Soil Bureau, and Joint Research Centre of the European Commission, EUR 19044 EN. https://www.unisdr.org/files/1581_ereurnew2.pdf

Van Oost, K., Quine, T. A., Govers, G., De Gryze, S., Six, J., Harden, J. W., Ritchie, J. C., McCarty, G. W., Heckrath, G., Kosmas, C., Giraldez, J. V., da Silva, J. R. M., & Merckx, R. (2007). The impact of agricultural soil erosion on the global carbon cycle. Science, 318(5850), 626–629. https://doi.org/10.1126/science.1145724

Verchort, L., Krug, T., Lasco, R. D., Ogle, S., Raison, J., Li, Y., Martino, D. L., McConkey, B. G., Smith, P., & Karunditu, M. W. (2006). Chapter 6: Grassland. In H. S. Eggleston, L. Buendia, K. Miwa, T. Ngara, & K. Tanabe (Eds.), & T. Krug (Trans.), *2006 IPCC Guidelines for National Greenhouse Gas Inventories* (Vol. 4, pp. 6.1-6.49). IPCC.

Vicharnakorn, P., Shrestha, R., Nagai, M., Salam, A., & Kiratiprayoon, S. (2014). Carbon Stock Assessment Using Remote Sensing and Forest Inventory Data in Savannakhet, Lao PDR. Remote Sensing, 6(6), 5452–5479. http://dx.doi.org/10.3390/rs6065452

Wang, S., Lu, X., Cheng, X., Li, X., Peichl, M., & Mammarella, I. (2018). Limitations and Challenges of MODIS-Derived Phenological Metrics Across Different Landscapes in Pan-Arctic Regions. Remote Sensing, 10(11), 1784. https://doi.org/10.3390/rs10111784

Wang, S., Yang, B., Yang, Q., Lu, L., Wang, X., & Peng, Y. (2016). Temporal Trends and Spatial Variability of Vegetation Phenology over the Northern Hemisphere during 1982-2012. Plos One, 11(6), e0157134. https://doi.org/10.1371/journal.pone.0157134

Wischmeier, W. H., & Smith, D. D. (1978). Predicting rainfall erosion losses (Vol. 537). US Dep. of Agriculture.

Xia, J., Liu, S., Liang, S., Chen, Y., Xu, W., & Yuan, W. (2014). Spatio-temporal patterns and climate variables controlling of biomass carbon stock of global grassland ecosystems from 1982 to 2006. *Remote Sensing, 6*, 1783-1802. https://doi.org/10.3390/rs6031783

Yoo, J., Simonit, S., Connors, J. P., Kinzig, A. P., & Perrings, A. (2014). The valuation of off-site ecosystem service flows: Deforestation, erosion, and the amenity value of lakes in Prescott, Arizona. Ecological Economics, 97, 74–83. http://dx.doi.org/10.1016/j.ecolecon. 2013.11.001

Yue, S., Pilon, P., & Cavadias, G. (2002). Power of the Mann–Kendall and Spearman's rho tests for detecting monotonic trends in hydrological series. Journal of Hydrology, 259(1), 254–271.

Zhang, X., Lark, T. J., Clark, C. M., Yuan, Y., & LeDuc, S. D. (2021). Grassland-to-cropland conversion increased soil, nutrient, and carbon losses in the US Midwest between 2008 and 2016. *Environmental Research Letters*, 16(5), 054018. https://doi.org/10.1088/1748-9326/abecbe

Zhang, X., Li, X., Chen, D., Cui, H. & Ge, Q. (2019). Overestimated climate warming and climate variability due to spatially homogeneous CO_2 in climate modeling over the Northern Hemisphere since the mid-19th century. *Scientific Report* 9, 17426. https://doi.org/10.1038/s41598-019-53513-7

Zhu, Z. (Ed.), Bouchard, M., Butman, D., Hawbaker, T., Li, Z., Liu, J., Liu, S., McDonald, C., Reker, R., Sayler, K., Sleeter, B., Sohl, T., Stackpoole, S., Wein, A., & Zhu, Z. (2011). *Baseline and projected future carbon storage and greenhouse-gas fluxes in the Great Plains region of the United States*. U.S. Geological Survey Professional Paper 1787. http://pubs.usgs.gov/pp/1787/.

Chapter 6 – Summary and conclusions

6.1 Introduction

Grasslands show significant variability in vegetation structure, including the density, percentage of trees, and spatial patterns. These variations result from varying factors, including but not limited to climate, soils, topography, fire regimes, woody encroachment, etc. They cover a substantial portion of the earth's surface and provide many benefits, yet they are not adequately protected. There is a rapid conversion to other land cover and degradation, especially in temperate prairies in North America (Comer et al., 2018; Plowprint report, 2021).

The is the need to advance our understanding of the dynamics of grasslands in the Great Plains ecoregion, their relationship to the global decline in ecosystem services (MEA, 2005; Comer et al., 2018; Plowprint report, 2021), and highlight the need for the best practices for grasslands conservation/restoration by showing the potential impact on essential benefits grasslands provide. The comprehensive goal of this research was to **investigate long-term grassland vegetation conditions using a well-known indicator (greenness) within the U.S. Great Plains for the period 2001-2017 and assess the impact on the provision of related grasslands benefits.** The following objectives were laid out and carried out to accomplish the research goal:

1. Assess the long-term trends in grassland based on vegetation greenness within the U.S. Great Plains grasslands from 2001 to 2017.

   The temporal decomposition of a time series of vegetation indices (NDVI and EVI) data and the statistical analysis of the trend within the period 2001 to 2017.

2. Assess the spatial patterns and trends of grassland phenology in the U.S. Great Plains within the period between 2001 to 2017.

   Filtering of a time series of vegetation indices (EVI) data, the extraction of phenology metrics, and the use of summary statistics to assess temporal and spatial patterns over the period 2001-2017.

3. Estimate the spatio-temporal changes in grassland-related ecosystem services within the U.S. Great Plains.

Improve existing ecosystem valuation methods by highlighting the spatially explicit and temporal elements of ecosystem services. Estimate the values (biophysical and economic) of two grassland-related ecosystem services to assess the impact of changing grassland conditions on the provision of these ecosystem services.

6.2 Summary of results and key findings

The primary results of the research are summarized below from chapters 3, 4, and 5:

Chapter 3: Detection of Long-Term Grassland Vegetation Trends for the Great Plains Ecoregion using Temporal Decomposition and Satellite-derived Vegetation Indices

- Most of the grasslands in the U.S. Great Plains (approximately 71%) experienced greening (a positive trend), and a minority (an average of 7.2%) experienced browning (a negative trend) between 2001 and 2017.
- The greening areas are in the midwestern to the northern part of the study region Great Plains (East Colorado, Nebraska, Montana, and western South Dakota). So, there is a generalized north to a south gradient with greening in the northwest to the middle and more browning in the southeast axis of the Great Plains.
- Comparing the NDVI and the EVI for trend analysis using BFAST results from the initial statistical (chi-square analysis) comparison of the two VI shows that there is a significant difference, and the trend results are dependent on the VI used.
- Further pixel-difference comparison showed clusters of pixels with a shift to a more negative class from the NDVI to the EVI trends results in the northwestern part of the study area; there are clusters of pixels with a shift to a more positive class in the eastern part of the study area with tallgrass prairies. This distribution indicates the ability of the EVI to make up for the limitation of saturation of high values with NDVI.
- The cross-tabulation and examination of the difference components (quantity, exchange, and shift) indicate the most difference between the trend results of the two VI's are in the stable class and that most pixels are interchanged between the stable class and positive class.

- The trend results were validated by comparing them to trend analysis using higher spatial resolution data, and they were similar.

Chapter 4: Time Series Analysis of Phenometrics for the U.S. Great Plains Ecoregion using Satellite-derived Vegetation Indices

- The average start of growing season was day 105 and the start of season trend of grasslands in the Great Plains between 2001 and 2017 showed a predominant move to a later start of growing season.
- The average middle of growing season was day 189 and the middle of season trend of grasslands in the Great Plains between 2001 and 2017 showed a predominant move to a later middle of growing season.
- The average end of growing season was day 313 and the end of season trend of grasslands in the Great Plains between 2001 and 2017 showed a predominant move to an earlier end of growing season.
- The average growing season length was 204 days and the growing season length trend of grasslands in the Great Plains between 2001 and 2017 showed a predominant move to a shorter growing season.
- The average green-up rate was 0.04, and the green-up trend of grasslands in the Great Plains between 2001 and 2017 showed predominantly increasing green-up rates.
- The average senescence was 0.03, and the senescence trend of grasslands in the Great Plains between 2001 and 2017 also showed predominantly increasing green-up rates.
- The average maximum EVI value was 0.34, and the EVI trend of grasslands in the Great Plains between 2001 and 2017 showed a predominant increasing trend.
- The average small integral was 1.75, and the small integral trend of grasslands in the Great Plains between 2001 and 2017 showed a predominant increasing trend.
- The spatial patterns of the time-based phenometrics (SOS, EOS, MOS, and growing season length) reflect the influence of temperature; with an overall north-south gradient (higher temperature in the south- earlier SOS and later EOS days in the south, and longer growing season length in the south than in the north).

- The spatio-temporal patterns of the VI-based phenometrics (green-up rate, senescence rate, maximum EVI, and small integral) reflect the influence of precipitation. They all show a west-east gradient with lower values in the west and higher values in the east.

Chapter 5: Spatio-temporal Valuation of Grassland Ecosystem Services in the U.S. Great Plains

- The average carbon stock values for grasslands in the U.S. Great Plains from 2001 to 2017 varied in a west-east gradient, with higher carbon stock values in the east than the west. Values ranged from 180 MgC in the west to 220 MgC in the east.
- The total annual carbon stock of grasslands in the ecoregion; the years 2002, 2006, and 2012 had the least total value with approximately 2.95, 2.96, and 2.93 B MgC/ha respectively, and 2007, 2010, and 2015 had the highest total values with approximately 3.03, 3.04 and 3.05 B MgC/ha respectively.
- The average economic value of grassland carbon stock in the U.S. Great Plains between 2001 and 2017 was 93 billion 2007 U.S. dollars.
- The net economic values between the years 2005 to 2006 and 2011 to 2012 were the least with approximately -1.6 and -1.9 billion 2007 U.S. dollars. On the other hand, the net economic values between the years 2006 to 2007 and 2012 to 2013 were the most, with approximately +2.1 and +2.7 billion 2007 U.S. dollars, respectively.
- The estimated soil loss for the study period averaged 131 million tons per hectare. The total annual soil loss in the years 2003 and 2012 were the lowest, with approximately 92 and 83 million tons per hectare per year, respectively. On the other hand, the total annual soil loss in 2008, 2010, and 2011 were the most, with approximately 160, 180, and 167 million tons per hectare per year, respectively.
- Most of the ecoregion grassland areas had an annual soil loss value of 0 to 5 tons per hectare, occurring in northwest Nebraska, eastern parts of South Dakota, New Mexico, Colorado, and southern Texas. Higher values that range from 40 to 2000 tons/hectare occurs in varying parts of the study area, especially in Montana and the western part of South Dakota.
- The estimated annual sediment retention for the study period averaged 63 million tons per hectare, and the average economic value of sediment retained was 282 million (2007) U.S.

dollars. The total annual sediment retained in the years 2001 and 2012 were the lowest, with approximately 44 and 33 million tons per hectare per year, respectively. On the other hand, the total annual sediment retained in 2007 and 2016 were the most, with approximately 79 and 85 million tons per hectare per year, respectively.

- In the time studied, the average combined economic value is 93.43 billion (2007) U.S. dollars. The years 2002, 2006, and 2012 had the lowest combined economic value, and that he is 2007, 2010, and 2015 had the highest combined economic value in the 17 years studied.
- There is an 18.8% difference between the estimates of Zhu et al. (2011) (a comparative, standard study) and the general InVEST method of carbon stock estimation, whereas there is a 12.5% difference between the Zhu et al. (2011) and the modified InVEST method. This means that there would be an overestimation of the value of ES using the general method.

6.3 Conclusions

6.3.1 Detection of long-term grassland vegetation trends for the Great Plains Ecoregion using temporal decomposition and satellite-derived vegetation indices

Long-term studies on a major ecosystem are critical to achieving an integrated understanding of how components of ecosystems interact. The use of remotely sensed VI time series for trend analysis using BFAST is a reliable and valuable method to characterize long-term trends in grasslands and other vegetation biomes. This study uses the MOD13Q1(C5) NDVI and EVI data to determine grassland vegetation greenness in the Great Plains over a 17-year interval. The description of both the overall and area-specific trends in the U.S. Great Plains can provide important information to aid decision-making in conservation, biodiversity, and stainability-related policies.

Overall, our results show a prevalent greening trend within the time studied, indicating that vegetation greenness or productivity, as implied, increased over the study period. Our study also found, by comparing our results to climate patterns in the region, that this period was associated with the increasing precipitation and temperature trends. There is a north-south temperature gradient with higher temperatures and the south and east-west precipitation gradient with higher precipitation in the east after Great Plains. The gradients of these climatic variables influence the distinct trend patterns in various regions after the study area, with more browning trends in the southern and

southeastern parts of the study area. This leads us to conclude that even though there was increasing precipitation, overall high temperatures in the south have more influence on vegetation patterns than precipitation.

Comparing our results to similar studies conducted within the same region and within a similar time, there were some findings that were not similar to ours and a few that were similar to ours too, but the validation using higher resolution images provides confidence in interpreting the interannual trend results confirming the overall greening in the Great Plains (2001-2017). The comparison of our results to other studies with dissimilar findings can be attributed to a difference in the period of the time series that was analyzed. Meaning an additional or excluded couple of years can highly impact our trend results given that the major driver of vegetation trends – climate, is highly variable. This has led us to infer that climate change impacts are unpredictable; therefore, there is a need for continuous trend monitoring analysis (Lamchin et al., 2020).

We also explored the impact of using difference VI data for the trend analysis in this region. The difference between the NDVI and EVI results shows the prominent limitation of the NDVI: the saturation of values in areas with high biomass making pixels to be classified as stable, whereas in the EVI trend, they were classified as positive. The impact of saturation and less variation in high biomass areas can affect the classification and the overall trend analysis. The EVI is thereby strongly recommended for long-term trend analysis in the Great Plains, especially in the tallgrass prairies.

The findings of this study suggest the need for additional analyses to quantify the influence of climate and soils, along with critical regional anthropogenic factors such as fire, on shaping long-term vegetation dynamics and estimate the impact on the values or services we acquire from grasslands in the ecoregion. To further assess the long-term condition of grassland in the U.S. Great Plains, this dissertation also looks at the spatial patterns and trends of grassland phenology and how the trends reported in this work impact the provision of selected grassland-related ecosystem services within the U.S. Great Plains.

6.3.2 Time series analysis of phenometrics for the U.S. Great Plains Ecoregion using satellite-derived vegetation indices

Understanding long-term seasonal patterns of vegetation activity are critical to studying inter-annual variability, monitoring land degradation, and the impact of climate change in biomes like grasslands. The use of a high temporal and adequately spatial resolution remotely sensed VI data is a reliable and valuable method to characterize long-term trends in grasslands and other vegetation biomes. The characterization and evaluation of changes in vegetation grassland in the Great Plains ecoregions over the period of 16 growing seasons is presented in this study. The results show variation in vegetation phenology and productivity across the Great Plains over the last two decades. There was generally a start of season dates, a later middle growing season, an earlier later, or delayed end of season dates, resulting in shorter growing season lengths; vegetation productivity was usually increasing during the period. This is similar to Hufkens et al.'s (2016) findings.

Changing climate alters vegetation phenology. The impact of climate on the grassland phenology and phenology trends was obvious from the comparison of our results to climate variables such as temperature, precipitation, and soil moisture. There was an overall rising temperature and increasing precipitation in the time studied. The time-based phenometrics showed patterns that indicate a dominant temperature influence, and the VI-based phenometrics showed patterns that imply a dominant precipitation influence. Overall, temperature had the most significant impact on phenology patterns and trends in the ecoregion. Even though the growing season periods in the Great Plains are becoming shorter from increasing temperatures, the combination of the trends of the climatic variables examined resulted in improving or increasing greeness. Temperature is projected to keep rising in the ecoregion as well as precipitation. But in most parts of the study region, precipitation is projected to decrease in the summer, which is the peak of the growing season. It would be interesting to see how these climatic variables come into play to impact grassland conditions in the ecoregion in the future.

The results presented in this study provide important baseline information on the dynamics of grasslands in the Great Plains that will provide a benchmark for assessing future change in the region. Such information is important in aiding decision making in conservation, biodiversity, and sustainability-related policies for land managers; because the result of this study has significant

implications of long-term changes in vegetation phenology, in gross primary production and affect the carbon cycle, water cycle, and energy fluxes through photosynthesis and evapotranspiration (Xiao et al., 2009). These impacts may subsequently influence food security, water resource availability, and climate (Suepa et al., 2016).

To further assess the long-term condition of grassland in the US Great Plains, this dissertation also looks at how the spatial patterns and trends of grassland phenology reported in this work impact the provision of selected grassland-related ecosystem services within the U.S. Great Plains. Future analyses to complement this work would be to understand the role of land-use change, climate change, and soils, along with other regional anthropogenic factors such as fire, in shaping long-term vegetation dynamics in the region.

6.3.3 Spatio-temporal valuation of grassland ecosystem services in the U.S. Great Plains

Given the essential role of grasslands in the provision of several ES and the mitigation of several negative environmental processes like soil erosion and carbon sequestration, their monitoring and conservation still have some work to do. There is an urgent need to estimate the impact of grassland conditions in response to the changing climate and other anthropogenic activities through long-term studies. This paper estimated the biophysical and economic values of two grassland-related regulating ES in the U.S. Great Plains: the control of soil erosion and carbon sequestration. In addition to the estimation of grasslands, we developed and used an improved method that captures the spatial heterogeneity of grasslands ecosystem function leading to more accurate quantification and valuation. Using the highly generalizable InVEST ES modeling tool, we incorporated spatially explicit and temporally available earth observation data to replace the categorical and static land use/land cover-based modeling of ES. Then we used the modeled biophysical measure to costs estimation methods to calculate the economic value of both ES.

The results show both spatial and temporal variation, and they indicate a significant influence of precipitation, soil texture, and land cover (in this case, grassland biomass). Our results were also validated using an existing study that is considered the "gold standard" because of its similarity in the study area, study period, and the reputation of the researchers, and our results using the improved methods compare two deaths. The comparison of this existing study to the generalized methods shows

overestimation and possibly inaccuracy in results. ES quantification and valuation accuracy is crucial because it impacts environmental planning and environmental monitoring policymaking and contribution to research in related fields.

Ecosystem services are increasingly being considered in policymaking, decision making, interdisciplinary research, environmental management, and conservation, and there is still room for a wider application (Ramirez-Reyes et al., 2019). There is a potential to improve ecosystem services valuation in terms of accuracy, data availability, and generalizability by harnessing the very many advancements of earth observation or remotely sensed data. While the incorporation of remote sensing methods or data dos not the perfect solution for the limitations in ES modeling, it can improve the representation of the spatial heterogeneity that exists in reality, and better capture the temporal dynamics after the supply and demand of ecosystem services.

Climate change (past, present, and future) influences grassland productivity and phenology with consequences on ecosystems and their value. Results from this study show the impact of changing grassland conditions based on greenness on the Great Plains ecoregion. An analysis of the carbon stock value over the period studied showed and overall positive trend. This agrees with findings from our previous work (Chapter 4) and Hufkens et al. (2016) on increased productivity of grasslands in the time studied. Future work is suggested to analyze the specific factors that contribute to the increasing productivity of grasslands in the Great Plains ecoregion and its implications on the ecoregion.

6.4 Contributions and future research

With the goal of understanding investigate long-term grassland vegetation conditions within the U.S. Great Plains, this research yielded several important contributions. First, it highlights the impact of climate change and land management on ecosystem structure on a very large spatial scale. Related literature identifies a lack of broad-scale studies on the temporal condition of grasslands in the U.S. The Great Plains in the U.S. is the location of most of the U.S. grasslands, which is a hotspot for biodiversity, aid in carbon sequestration, provides aesthetically pleasant scenery for people, and provides food to support livestock farming in the region. With variation in land management practices in this region, providing a general picture of trends that adds to scientific knowledge in this field and provides a base reference for land management decisions for policymakers in this region. The

utilization of freely available remotely sensed data to analyze long-term regional trends provides detailed trend patterns of the ecoregion over the past two decades.

This research also highlights the relationship between phenological changes and climate patterns/variability to understand the influence of climate change on biophysical characteristics and provides essential information to understand and model the effects of climate variability on grassland vegetation dynamics. This research highlights the influence of temperature on the timed-based phenology metrics and the influence of precipitation on the productivity-based phenology metrics. Finally, this study is relevant to global climate change studies. Grasslands are an essential component of the earth's biosphere that is critical to regulating ecosystems and maintaining biodiversity. The literature review reveals the scarcity of studies in the valuation of grassland ecosystem services and the dearth of studies assessing the condition of the Great Plains ecoregion. The Great Plains is one of the very important ecoregions in the U.S. and the world with its impact on climate regulation, livestock production, and biodiversity, to name a few. This research adds to the number of studies estimating grassland ecosystem value, especially in the Great Plains. In addition to this, an improved method to highlight the spatially explicit and temporally dynamic nature of grasslands was used by harnessing the improving availability and properties of remotely sensed data to achieve more accurate ecosystem valuation results.

Future work is needed to determine the explanatory factors responsible for the spatio-temporal pattern in the grassland vegetation conditions within the U.S. Great Plains. In this research, results were compared to some climate variables like presentation and temperature, but an extensive analysis of the explanatory factors is required. Also, in the future, the need for the valuation of grassland ecosystem services should be extended beyond the analysis of results. There is a need to transfer results into policy and decision making. So, based on the value of grassland ES, future work should suggest the form and magnitude of payment mechanisms to secure private beneficiaries' interest and policymaking decisions.

6.5 References:

Comer, P. J., Hak, J. C., Kindscher, K., Muldavin, E., & Singhurst, J. (2018). Continent-Scale Landscape Conservation Design for Temperate Grasslands of the Great Plains and Chihuahuan Desert. *Natural Areas Journal, 38*(2), 196–211. https://doi.org/10.3375/043.038.0209

Conant, R. T., Kluck, D., Anderson, M., Badger, A., Boustead, B. M., Derner, J. D., Farris, L., Hayes, M. J., Livneh, B., McNeeley, S., Peck, D., Shulski, M. D., & Small, V. A. (2018). *Chapter 22: northern great plains. impacts, risks, and adaptation in the United States: the fourth national climate assessment, volume II*. US Global Change Research Program. https://doi.org/10.7930/NCA4.2018.CH22

Lamchin, M., Wang, S. W., Lim, C.-H., Ochir, A., Pavel, U., Gebru, B. M., Choi, Y., Jeon, S. W., & Lee, W.-K. (2020). Understanding global spatio-temporal trends and the relationship between vegetation greenness and climate factors by land cover during 1982–2014. *Global Ecology and Conservation*, 24, e01299. https://doi.org/10.1016/j.gecco.2020.e01299

Millennium Ecosystem Assessment [MEA]. (2005*). Ecosystems and human well-being: Synthesis* (2nd ed., p. 160). Island Press.

Plowprint annual report (2021). World Wildlife Fund. Retrieved from https://files.worldwildlife.org/wwfcmsprod/files/Publication/file/5yrd3g00ig_PlowprintReport_2021_Final_HiRes_b.pdf?_ga=2.206397267.119456530.1640946732-1705276999.1640946731

Ramirez-Reyes, C., Brauman, K. A., Chaplin-Kramer, R., Galford, G. L., Adamo, S. B., Anderson, C. B., Anderson, C., Allington, G., Bagstad, K. J., Coe, M. T., Cord, A. F., Dee, L. E., Gould, R. K., Jain, M., Kowal, V. A., Muller-Karger, F. E., Norriss, J., Potapov, P., Qiu, J., Rieb, J. T., … Wright, T. M. (2019). Reimagining the potential of Earth observations for ecosystem service assessments. *The Science of the total environment*, 665, 1053–1063. https://doi.org/10.1016/j.scitotenv.2019.02.150

Suepa, T., Qi, J., Lawawirojwong, S., & Messina, J. P. (2016). Understanding spatio-temporal variation of vegetation phenology and rainfall seasonality in the monsoon Southeast Asia. Environmental Research, 147, 621–629. https://doi.org/10.1016/j.envres.2016.02.005

Xia, J., Liu, S., Liang, S., Chen, Y., Xu, W., & Yuan, W. (2014). Spatio-temporal patterns and climate variables controlling of biomass carbon stock of global grassland ecosystems from 1982 to 2006. *Remote Sensing, 6*, 1783-1802. https://doi.org/10.3390/rs6031783

Zhu, Z. (Ed.), Bouchard, M., Butman, D., Hawbaker, T., Li, Z., Liu, J., Liu, S., McDonald, C., Reker, R., Sayler, K., Sleeter, B., Sohl, T., Stackpoole, S., Wein, A., & Zhu, Z. (2011). *Baseline and projected future carbon storage and greenhouse-gas fluxes in the Great Plains region of the United States*. US Geological Survey Professional Paper 1787. http://pubs.usgs.gov/pp/1787/.

Appendices

Appendix A: Additional materials for Chapter 3

Appendix A1: BFAST Script:

```
library("zoo")
library("sandwich")
library("MASS")
library("quadprog")
library("tseries")
library("strucchange")
library("fracdiff")
library("forecast")
library("iterators")
library("codetools")
library("foreach")
library("bfast")

setwd("C:/Users/honuoha/Desktop")
filename <- "tile_097_ndvi_fill.csv"

inidata<-read.table(filename, header=FALSE, sep = ",", dec = ".") #use only with small files; modify if no
labels are in the input
mdata<-as.matrix(inidata)
tpdata<-mdata
vmax<-dim(mdata)
vmax[1]
vmax[2]
for(count in 1:vmax[1]){
poly_id<-tpdata[count,1]  #highlighted number identifies field that will used to ID pixel
ndvi<-tpdata[count,2:vmax[2]]  #highlighted number identifies first column with NDVI data
plot(ndvi)
tsdata<-ts(ndvi,frequency=23,start=c(2001,1))
dim(tsdata)<-NULL
#rdist<-23/length(tsdata)
fits<-bfast(tsdata,h=0.1,season="harmonic",max.iter=1)
plot(fits)
```

```
fits2<-fits$Time
ts_trend_break_time<-t(fits2[1])
fits3<-fits$Magnitude
ts_trend_break_magnitude<-t(fits3[1])
fits4<-fits$output
fits4a<-fits4[[1]]$Vt.bp
fits4adata<-as.matrix(fits4a)
fits4amax<-dim(fits4adata)
ts_trend_nbbreak<-t(fits4amax[1])
results1<-ts_trend_break_time
aLine<-t(c(poly_id,results1))
write.table(aLine, file=paste0(filename, "_trend_breaks_time.txt"), append=TRUE,quote=FALSE,sep=",",
eol="\n",na="NA", dec=".",row.names=FALSE,col.names=FALSE,qmethod=c("escape","double"))
results2<-ts_trend_break_magnitude
aLine<-t(c(poly_id,results2))
write.table(aLine,file=paste0(filename, "_trend_breaks_magnitude.txt"), append=TRUE,quote=FALSE,
sep=",",eol="\n", na="NA", dec=".",row.names=FALSE,col.names=FALSE,qmethod=c("escape","double"))
results3<-ts_trend_nbbreak
aLine<-t(c(poly_id,results3))
write.table(aLine,file=paste0(filename, "_trend_nbbreaks.txt"),append=TRUE,quote=FALSE,sep=",",
eol="\n",na="NA", de=".", ,row.names=FALSE,col.names=FALSE,qmethod=c("escape","double"))
fits4b<-fits4[[1]]$Tt
results4<-fits4b
aLine<-t(c(poly_id,results4))
write.table(aLine,file=paste0(filename, "_trend_bfast.txt"),append=TRUE,quote=FALSE,
sep=",",eol="\n",na="NA",dec=".", row.names=FALSE,col.names=FALSE,qmethod=c("escape","double"))
fits4c<-fits4[[1]]$Wt.bp
fits4cdata<-as.matrix(fits4c)
fits4cmax<-dim(fits4cdata)
ts_season_nbbreak<-t(fits4cmax[1])
results5<-ts_season_nbbreak
aLine<-t(c(poly_id,results5))
write.table(aLine,file=paste0(filename, "_season_nbbreaks.txt"),append=TRUE,quote=FALSE,
sep=",",eol="\n", na="NA", de=".", row.names=FALSE,col.names=FALSE,qmethod=c("escape","double"))
ts_season_breaks_time<-t(fits4cdata)
results6<- ts_season_breaks_time
aLine<- t(c(poly_id,results6))
```

```
write.table(aLine,file=paste0(filename, "_season_breaks_time.txt"),append=TRUE,quote=FALSE,sep=",",
eol="\n",na="NA", de=".",row.names=FALSE,col.names=FALSE,qmethod=c("escape","double"))
fits4d<-fits4[[1]]$St
results7<-fits4d
aLine<-t(c(poly_id,results7))
write.table(aLine,file=paste0(filename, "_season_bfast.txt"),append=TRUE,quote=FALSE,sep=",",eol="\n",
na="NA",dec=".", row.names=FALSE,col.names=FALSE,qmethod=c("escape","double"))}

rm(list=ls())
```

Appendix B: Additional materials for Chapter 4

Appendix B-1: A portion of TIMESAT input File list

```
391
Z:\Projects\Onuoha_Hilda\Timesat\71_NdviImagesDat\MOD13Q1.A2001001_NDVI.dat
Z:\Projects\Onuoha_Hilda\Timesat\71_NdviImagesDat\MOD13Q1.A2001017_NDVI.dat
Z:\Projects\Onuoha_Hilda\Timesat\71_NdviImagesDat\MOD13Q1.A2001033_NDVI.dat
Z:\Projects\Onuoha_Hilda\Timesat\71_NdviImagesDat\MOD13Q1.A2001049_NDVI.dat
Z:\Projects\Onuoha_Hilda\Timesat\71_NdviImagesDat\MOD13Q1.A2001065_NDVI.dat
Z:\Projects\Onuoha_Hilda\Timesat\71_NdviImagesDat\MOD13Q1.A2001081_NDVI.dat
Z:\Projects\Onuoha_Hilda\Timesat\71_NdviImagesDat\MOD13Q1.A2001097_NDVI.dat
Z:\Projects\Onuoha_Hilda\Timesat\71_NdviImagesDat\MOD13Q1.A2001113_NDVI.dat
Z:\Projects\Onuoha_Hilda\Timesat\71_NdviImagesDat\MOD13Q1.A2001129_NDVI.dat
Z:\Projects\Onuoha_Hilda\Timesat\71_NdviImagesDat\MOD13Q1.A2001145_NDVI.dat
Z:\Projects\Onuoha_Hilda\Timesat\71_NdviImagesDat\MOD13Q1.A2001161_NDVI.dat
Z:\Projects\Onuoha_Hilda\Timesat\71_NdviImagesDat\MOD13Q1.A2001177_NDVI.dat
Z:\Projects\Onuoha_Hilda\Timesat\71_NdviImagesDat\MOD13Q1.A2001193_NDVI.dat
Z:\Projects\Onuoha_Hilda\Timesat\71_NdviImagesDat\MOD13Q1.A2001209_NDVI.dat
Z:\Projects\Onuoha_Hilda\Timesat\71_NdviImagesDat\MOD13Q1.A2001225_NDVI.dat
Z:\Projects\Onuoha_Hilda\Timesat\71_NdviImagesDat\MOD13Q1.A2001241_NDVI.dat
Z:\Projects\Onuoha_Hilda\Timesat\71_NdviImagesDat\MOD13Q1.A2001257_NDVI.dat
Z:\Projects\Onuoha_Hilda\Timesat\71_NdviImagesDat\MOD13Q1.A2001273_NDVI.dat
Z:\Projects\Onuoha_Hilda\Timesat\71_NdviImagesDat\MOD13Q1.A2001289_NDVI.dat
```

Appendix B-2: A portion of the TIMESAT TSF convert to images script

```
M:\timesat33\timesat_fortran\tools\TSF_seas2img.exe NDVIwithQuality_TS.tpa 1 1 23 -99 -99 sos01 3
M:\timesat33\timesat_fortran\tools\TSF_seas2img.exe NDVIwithQuality_TS.tpa 1 24 46 -99 -99 sos02 3
M:\timesat33\timesat_fortran\tools\TSF_seas2img.exe NDVIwithQuality_TS.tpa 1 47 69 -99 -99 sos03 3
M:\timesat33\timesat_fortran\tools\TSF_seas2img.exe NDVIwithQuality_TS.tpa 1 70 92 -99 -99 sos04 3
M:\timesat33\timesat_fortran\tools\TSF_seas2img.exe NDVIwithQuality_TS.tpa 1 93 115 -99 -99 sos05 3
M:\timesat33\timesat_fortran\tools\TSF_seas2img.exe NDVIwithQuality_TS.tpa 1 116 138 -99 -99 sos06 3
M:\timesat33\timesat_fortran\tools\TSF_seas2img.exe NDVIwithQuality_TS.tpa 1 139 161 -99 -99 sos07 3
M:\timesat33\timesat_fortran\tools\TSF_seas2img.exe NDVIwithQuality_TS.tpa 1 162 184 -99 -99 sos08 3
M:\timesat33\timesat_fortran\tools\TSF_seas2img.exe NDVIwithQuality_TS.tpa 1 185 207 -99 -99 sos09 3
M:\timesat33\timesat_fortran\tools\TSF_seas2img.exe NDVIwithQuality_TS.tpa 1 208 230 -99 -99 sos10 3
M:\timesat33\timesat_fortran\tools\TSF_seas2img.exe NDVIwithQuality_TS.tpa 1 231 253 -99 -99 sos11 3
M:\timesat33\timesat_fortran\tools\TSF_seas2img.exe NDVIwithQuality_TS.tpa 1 254 276 -99 -99 sos12 3
M:\timesat33\timesat_fortran\tools\TSF_seas2img.exe NDVIwithQuality_TS.tpa 1 277 299 -99 -99 sos13 3
M:\timesat33\timesat_fortran\tools\TSF_seas2img.exe NDVIwithQuality_TS.tpa 1 300 322 -99 -99 sos14 3
M:\timesat33\timesat_fortran\tools\TSF_seas2img.exe NDVIwithQuality_TS.tpa 1 323 345 -99 -99 sos15 3
M:\timesat33\timesat_fortran\tools\TSF_seas2img.exe NDVIwithQuality_TS.tpa 1 346 368 -99 -99 sos16 3

M:\timesat33\timesat_fortran\tools\TSF_seas2img.exe NDVIwithQuality_TS.tpa 2 1 23 -99 -99 eos01 3
M:\timesat33\timesat_fortran\tools\TSF_seas2img.exe NDVIwithQuality_TS.tpa 2 24 46 -99 -99 eos02 3
M:\timesat33\timesat_fortran\tools\TSF_seas2img.exe NDVIwithQuality_TS.tpa 2 47 69 -99 -99 eos03 3
M:\timesat33\timesat_fortran\tools\TSF_seas2img.exe NDVIwithQuality_TS.tpa 2 70 92 -99 -99 eos04 3
M:\timesat33\timesat_fortran\tools\TSF_seas2img.exe NDVIwithQuality_TS.tpa 2 93 115 -99 -99 eos05 3
M:\timesat33\timesat_fortran\tools\TSF_seas2img.exe NDVIwithQuality_TS.tpa 2 116 138 -99 -99 eos06 3
M:\timesat33\timesat_fortran\tools\TSF_seas2img.exe NDVIwithQuality_TS.tpa 2 139 161 -99 -99 eos07 3
M:\timesat33\timesat_fortran\tools\TSF_seas2img.exe NDVIwithQuality_TS.tpa 2 162 184 -99 -99 eos08 3
M:\timesat33\timesat_fortran\tools\TSF_seas2img.exe NDVIwithQuality_TS.tpa 2 185 207 -99 -99 eos09 3
M:\timesat33\timesat_fortran\tools\TSF_seas2img.exe NDVIwithQuality_TS.tpa 2 208 230 -99 -99 eos10 3
M:\timesat33\timesat_fortran\tools\TSF_seas2img.exe NDVIwithQuality_TS.tpa 2 231 253 -99 -99 eos11 3
M:\timesat33\timesat_fortran\tools\TSF_seas2img.exe NDVIwithQuality_TS.tpa 2 254 276 -99 -99 eos12 3
M:\timesat33\timesat_fortran\tools\TSF_seas2img.exe NDVIwithQuality_TS.tpa 2 277 299 -99 -99 eos13 3
M:\timesat33\timesat_fortran\tools\TSF_seas2img.exe NDVIwithQuality_TS.tpa 2 300 322 -99 -99 eos14 3
M:\timesat33\timesat_fortran\tools\TSF_seas2img.exe NDVIwithQuality_TS.tpa 2 323 345 -99 -99 eos15 3
M:\timesat33\timesat_fortran\tools\TSF_seas2img.exe NDVIwithQuality_TS.tpa 2 346 368 -99 -99 eos16 3

M:\timesat33\timesat_fortran\tools\TSF_seas2img.exe NDVIwithQuality_TS.tpa 3 1 23 -99 -99 gsl01 3
```

```
M:\timesat33\timesat_fortran\tools\TSF_seas2img.exe NDVIwithQuality_TS.tpa 3 24 46 -99 -99 gsl02 3
M:\timesat33\timesat_fortran\tools\TSF_seas2img.exe NDVIwithQuality_TS.tpa 3 47 69 -99 -99 gsl03 3
M:\timesat33\timesat_fortran\tools\TSF_seas2img.exe NDVIwithQuality_TS.tpa 3 70 92 -99 -99 gsl04 3
M:\timesat33\timesat_fortran\tools\TSF_seas2img.exe NDVIwithQuality_TS.tpa 3 93 115 -99 -99 gsl05 3
M:\timesat33\timesat_fortran\tools\TSF_seas2img.exe NDVIwithQuality_TS.tpa 3 116 138 -99 -99 gsl06 3
M:\timesat33\timesat_fortran\tools\TSF_seas2img.exe NDVIwithQuality_TS.tpa 3 139 161 -99 -99 gsl07 3
M:\timesat33\timesat_fortran\tools\TSF_seas2img.exe NDVIwithQuality_TS.tpa 3 162 184 -99 -99 gsl08 3
M:\timesat33\timesat_fortran\tools\TSF_seas2img.exe NDVIwithQuality_TS.tpa 3 185 207 -99 -99 gsl09 3
M:\timesat33\timesat_fortran\tools\TSF_seas2img.exe NDVIwithQuality_TS.tpa 3 208 230 -99 -99 gsl10 3
M:\timesat33\timesat_fortran\tools\TSF_seas2img.exe NDVIwithQuality_TS.tpa 3 231 253 -99 -99 gsl11 3
M:\timesat33\timesat_fortran\tools\TSF_seas2img.exe NDVIwithQuality_TS.tpa 3 254 276 -99 -99 gsl12 3
M:\timesat33\timesat_fortran\tools\TSF_seas2img.exe NDVIwithQuality_TS.tpa 3 277 299 -99 -99 gsl13 3
M:\timesat33\timesat_fortran\tools\TSF_seas2img.exe NDVIwithQuality_TS.tpa 3 300 322 -99 -99 gsl14 3
M:\timesat33\timesat_fortran\tools\TSF_seas2img.exe NDVIwithQuality_TS.tpa 3 323 345 -99 -99 gsl15 3
M:\timesat33\timesat_fortran\tools\TSF_seas2img.exe NDVIwithQuality_TS.tpa 3 346 368 -99 -99 gsl16 3
```

Appendix B-3: Script to calculate TIMESAT phenometric summaries (standard deviation and mean using arcGIS and Python)

```
# Import required modules/classes:
import arcpy
from arcpy import env

# Define input and output workspaces
env.workspace = "Z:/Projects/Onuoha_Hilda/Timesat/71_NdviResults/PhenoSummaries/Adjusted/"
env.snapRaster = "Z:/Projects/Onuoha_Hilda/Timesat/NdviImages/MOD13Q1_A2001001_NDVI.tif"
outFolder = "Z:/Projects/Onuoha_Hilda/Timesat/71_NdviResults/PhenoSummaries/"

# Define local variables - only section that requires editing
phenoCode = "sos*"          # other valid values include max, gsl, lder, sint, etc
summaryStat = "MEAN"        # other valid values include MEAN, MEDIAN, STD
outName = "SOS_0116_"

# Check out required licenses
arcpy.CheckOutExtension("Spatial")
```

```
# Create a list of all rasters
gridList = arcpy.ListRasters(phenoCode)

# Compute summary statistic and save result
outCellStats = arcpy.sa.CellStatistics(gridList, summaryStat, "DATA")
outCellStats.save(outFolder + outName + summaryStat + ".tif")
arcpy.CheckInExtension("Spatial")
```

Appendix B-4: ANOVA and Tukey HSD R Script

```
library(data.table)
setwd("Extract")
filename <- "PhenomeansCounty1.csv"
data <- fread(filename)

data2 <- data[,c(-2, -3, -4, -6)]
remove(data)
data <- data2[ MAX_0116_M > -9999 ]
pheno <- data$MAX_0116_M

output1 <- lm(pheno ~ data$NAME)
#summary(output1)
capture.output(summary(output1), file="MAX_0116_Summary.txt")
#anova(output1)
capture.output(anova(output1), file="MAX_0116_ANOVA.txt")

rm(list=ls())

##Run ANOVA and assess whether differences exist between phenometrics and counties
#
#attach(mtcars)
#
#var1 <- "mpg"
#var2 <- "wt"
#
#output1 <- lm(var1~var2)
#summary(output1)
```

```
#
#capture.output(summary(output1), file=paste0("Summary", pheno))
#
#output1 <- lm(pheno ~ data$NAME)
#summary(output1)
#anova(output1)
#
##Run the Tukey's HSD test to see where differences lie
#a1 <- aov(pheno ~ data$County)
#posthoc <- TukeyHSD(x=a1, "data$NAME", conf.level=0.95)
#posthoc
```

Appendix B-5: Script to calculate phenometric (Mann-Kendall) trends

```
#important note: Always move the mkTrend(x) and the second return (NA) code lines one space on the rstudio interface

#use devtools to install the older version of fume package (needed once), install devtools first
require(devtools)
install_version("fume", version = "1.0", repos ="https://cran.us.r-project.org")

#import libraries
library(fume)
library(trend)
library(raster)
#dir <- setwd ("F:\\Research\\Timesat\\Phenometrics\\EVI\\LDER")

#import rasters, stack them and create brick
#r_path <-list.files(path="F:\\Research\\Timesat\\Phenometrics\\EVI\\EOS", pattern = ".tif$", full.names = TRUE)
r_path <-list.files(path="F:\\Research\\Timesat\\Phenometrics\\EVI\\GSL", pattern = ".dat$", full.names = TRUE)
s <- stack(r_path)
all_brick <- brick(s)

#perfom MK trentest: tau, sen slope and p_value
p_value <- function(x) {
   if (any(is.na(x))) {
      return(NA)
   }  else if (any(x != x[1])) {
```

```
        mkTrend(x)$`Corrected p.value`
    }  else{
        return(NA)
    }
}
sen <- function(x) {
    if (any(is.na(x))) {
        return(NA)
    }  else if (any(x != x[1])) {
        mkTrend(x)$`Sen's Slope`
    }  else{
        return(NA)
    }
}
tau <- function(x) {
    if (any(is.na(x))) {
        return(NA)
    }  else if (any(x != x[1])) {
        mkTrend(x)$tau
    }  else{
        return(NA)
    }
}

trend_pvalue <- calc(all_brick, p_value)
trend_sen <- calc(all_brick, sen)
trend_tau<- calc(all_brick, tau)

#Save raster to tiff
writeRaster(trend_pvalue, filename = "F:\\Research\\Timesat\\Phenometrics\\EVI\\GSL\\p-value.tif", format="GTiff",
overwrite=TRUE)
writeRaster(trend_sen, filename = "F:\\Research\\Timesat\\Phenometrics\\EVI\\GSL\\sen_slope.tif", format="GTiff",
overwrite=TRUE)
writeRaster(trend_tau, filename = "F:\\Research\\Timesat\\Phenometrics\\EVI\\GSL\\tau.tif", format="GTiff",
overwrite=TRUE)
```

Appendix C: Additional materials for Chapter 5

Appendix C-1: Lookup table for the updated method using InVEST carbon model.

lucode	LULC_Name	C_above	C_below	C_soil	C_dead
1	Mean GS NDVI <0	0.3506751	1.281032	31	0.0625
2	Mean GS NDVI 0-0.025	0.3714983	1.366759	31	0.075
3	Mean GS NDVI 0.025-0.05	0.393558	1.458222	31	0.0875
4	Mean GS NDVI 0.05-0.075	0.4169276	1.555806	31	0.1
5	Mean GS NDVI 0.075-0.1	0.4416848	1.65992	31	0.1125
6	Mean GS NDVI 0.1-0.125	0.4679122	1.771001	31	0.125
7	Mean GS NDVI 0.125-0.15	0.4956969	1.889516	31	0.1375
8	Mean GS NDVI 0.15-0.175	0.5251316	2.015962	31	0.15
9	Mean GS NDVI 0.175-0.2	0.556314	2.15087	31	0.1625
10	Mean GS NDVI 0.2-0.225	0.5893481	2.294806	31	0.175
11	Mean GS NDVI 0.225-0.25	0.6243437	2.448374	31	0.1875
12	Mean GS NDVI 0.25-0.275	0.6614174	2.612218	31	0.2
13	Mean GS NDVI 0.275-0.3	0.7006925	2.787028	31	0.2125
14	Mean GS NDVI 0.3-0.325	0.7422998	2.973535	31	0.225
15	Mean GS NDVI 0.325-0.35	0.7863778	3.172523	31	0.2375
16	Mean GS NDVI 0.35-0.375	0.8330731	3.384828	31	0.25
17	Mean GS NDVI 0.375-0.4	0.8825412	3.61134	31	0.2625
18	Mean GS NDVI 0.4-0.425	0.9349467	3.85301	31	0.275
19	Mean GS NDVI 0.425-0.45	0.9904641	4.110852	31	0.2875
20	Mean GS NDVI 0.45-0.475	1.0492781	4.385949	31	0.3
21	Mean GS NDVI 0.475-0.5	1.1115845	4.679456	31	0.3125
22	Mean GS NDVI 0.5-0.525	1.1775907	4.992604	31	0.325
23	Mean GS NDVI 0.525-0.55	1.2475163	5.326708	31	0.3375
24	Mean GS NDVI 0.55-0.575	1.3215942	5.68317	31	0.35
25	Mean GS NDVI 0.575-0.6	1.4000708	6.063487	31	0.3625
26	Mean GS NDVI 0.6-0.625	1.4832074	6.469254	31	0.375
27	Mean GS NDVI 0.625-0.65	1.5712806	6.902175	31	0.3875
28	Mean GS NDVI 0.65-0.675	1.6645836	7.364067	31	0.4
29	Mean GS NDVI 0.675-0.7	1.763427	7.856869	31	0.4125
30	Mean GS NDVI 0.7-0.725	1.8681398	8.382649	31	0.425
31	Mean GS NDVI 0.725-0.75	1.9790704	8.943614	31	0.4375
32	Mean GS NDVI 0.75-0.775	2.0965881	9.542119	31	0.45
33	Mean GS NDVI 0.775-0.8	2.2210841	10.18068	31	0.4625
34	Mean GS NDVI 0.8-0.825	2.3529726	10.86196	31	0.475
35	Mean GS NDVI 0.825-0.85	2.4926927	11.58884	31	0.4875
36	Mean GS NDVI 0.85-0.875	2.6407095	12.36437	31	0.5
37	Mean GS NDVI 0.875-0.9	2.7975155	13.19179	31	0.5
38	Mean GS NDVI 0.9-0.925	2.9636327	14.07458	31	0.5
39	Mean GS NDVI 0.925-0.95	3.139614	15.01645	31	0.5
40	Mean GS NDVI 0.95-0.975	3.326045	16.02134	31	0.5
41	Mean GS NDVI 0.975-1.0	3.5235465	17.09349	31	0.5

Appendix C-2: Estimation of SCC per year

2001	23.2238
2002	24.1476
2003	25.0714
2004	25.9952
2005	26.919
2006	27.8428
2007	28.7666
2008	29.6904
2009	30.6142
2010	31.538
2011	32.4618
2012	33.3856
2013	34.3094
2014	35.2332
2015	36.157
2016	37.0808
2017	38.0046

Social Cost of CO_2, 2015-2050 [a] (in 2007 dollars per metric ton CO_2)

Source: Technical Support Document: Technical Update of the Social Cost of Carbon for Regulatory Impact Analysis Under Executive Order 12866 (May 2013, Revised August 2016)

	Discount Rate and Statistic			
Year	5% Average	**3% Average**	2.5% Average	High Impact (3% 95th percentile)
2015	$11	**$36**	$56	$105
2020	$12	**$42**	$62	$123
2025	$14	**$46**	$68	$138
2030	$16	**$50**	$73	$152
2035	$18	**$55**	$78	$168
2040	$21	**$60**	$84	$183
2045	$23	**$64**	$89	$197
2050	$26	**$69**	$95	$212

[a] The SC-CO_2 values are dollar-year and emissions-year specific.

Approximately 0.2 % every 5 years = approximately 0.04% every year

used a simple linear interpolation

Appendix C-3: Lookup table for the updated method using InVEST sediment delivery ratio model.

LUCODE	usle_c	usle_p	description
1	1	1	Mean NDVI <0
2	0.950011	1	Mean NDVI 0-0.025
3	0.900088	1	Mean NDVI 0.025-0.05
4	0.850303	1	Mean NDVI 0.05-0.075
5	0.800737	1	Mean NDVI 0.075-0.1
6	0.751477	1	Mean NDVI 0.1-0.125
7	0.702619	1	Mean NDVI 0.125-0.15
8	0.654265	1	Mean NDVI 0.15-0.175
9	0.606531	1	Mean NDVI 0.175-0.2
10	0.559537	1	Mean NDVI 0.2-0.225
11	0.513417	1	Mean NDVI 0.225-0.25
12	0.468312	1	Mean NDVI 0.25-0.275
13	0.424373	1	Mean NDVI 0.275-0.3
14	0.38176	1	Mean NDVI 0.3-0.325
15	0.340642	1	Mean NDVI 0.325-0.35
16	0.301194	1	Mean NDVI 0.35-0.375
17	0.263597	1	Mean NDVI 0.375-0.4
18	0.228034	1	Mean NDVI 0.4-0.425
19	0.194687	1	Mean NDVI 0.425-0.45
20	0.163732	1	Mean NDVI 0.45-0.475
21	0.135335	1	Mean NDVI 0.475-0.5
22	0.109643	1	Mean NDVI 0.5-0.525
23	0.086774	1	Mean NDVI 0.525-0.55
24	0.066811	1	Mean NDVI 0.55-0.575
25	0.049787	1	Mean NDVI 0.575-0.6
26	0.035674	1	Mean NDVI 0.6-0.625
27	0.024373	1	Mean NDVI 0.625-0.65
28	0.015704	1	Mean NDVI 0.65-0.675
29	0.009404	1	Mean NDVI 0.675-0.7
30	0.00513	1	Mean NDVI 0.7-0.725
31	0.002479	1	Mean NDVI 0.725-0.75
32	0.001019	1	Mean NDVI 0.75-0.775
33	0.000335	1	Mean NDVI 0.775-0.8
34	8.04E-05	1	Mean NDVI 0.8-0.825
35	1.20E-05	1	Mean NDVI 0.825-0.85
36	8.32E-07	1	Mean NDVI 0.85-0.875
37	1.52E-08	1	Mean NDVI 0.875-0.9
38	1.94E-11	1	Mean NDVI 0.9-0.925
39	3.14E-17	1	Mean NDVI 0.925-0.95
40	1.33E-34	1	Mean NDVI 0.95-0.975
41	0	1	Mean NDVI 0.975-1.0

Appendix C-4: Maps showing the spatial of total carbon stock (in MgC) of grassland in the U.S. Great Plains for 2001 to 2017.

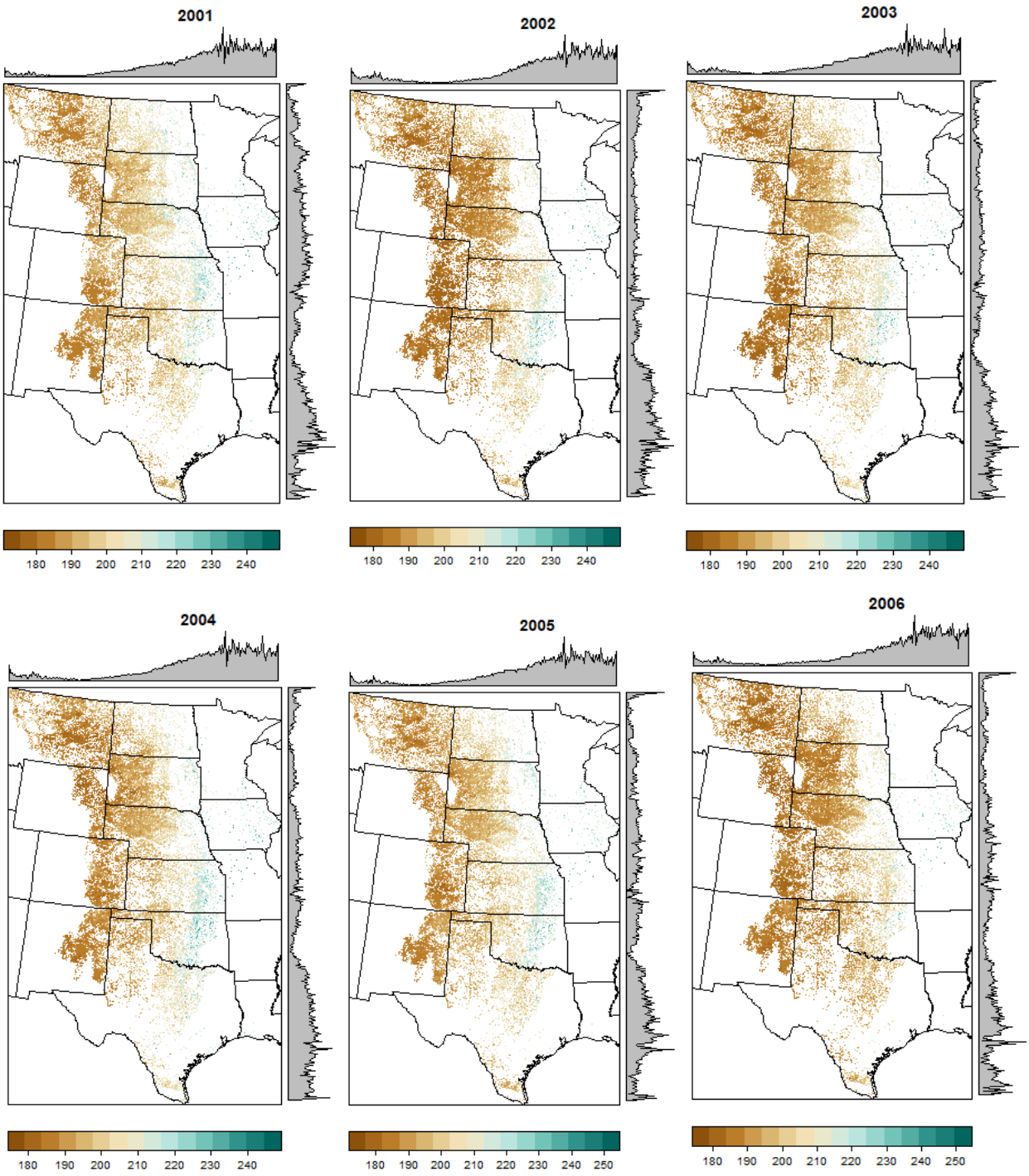

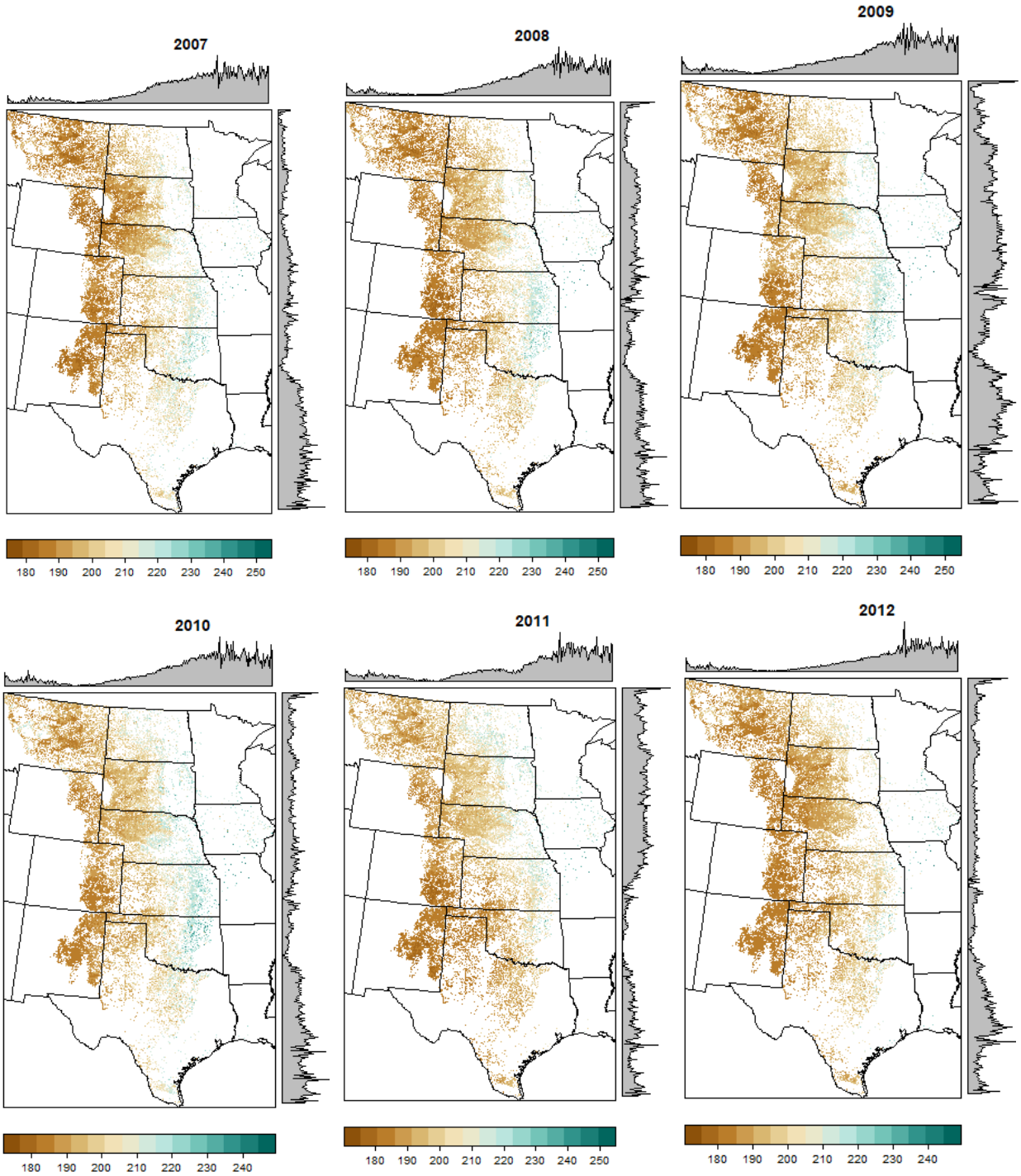
2007
2008
2009
2010
2011
2012
180 190 200 210 220 230 240 250
180 190 200 210 220 230 240 250
180 190 200 210 220 230 240 250
180 190 200 210 220 230 240
180 190 200 210 220 230 240 250
180 190 200 210 220 230 240

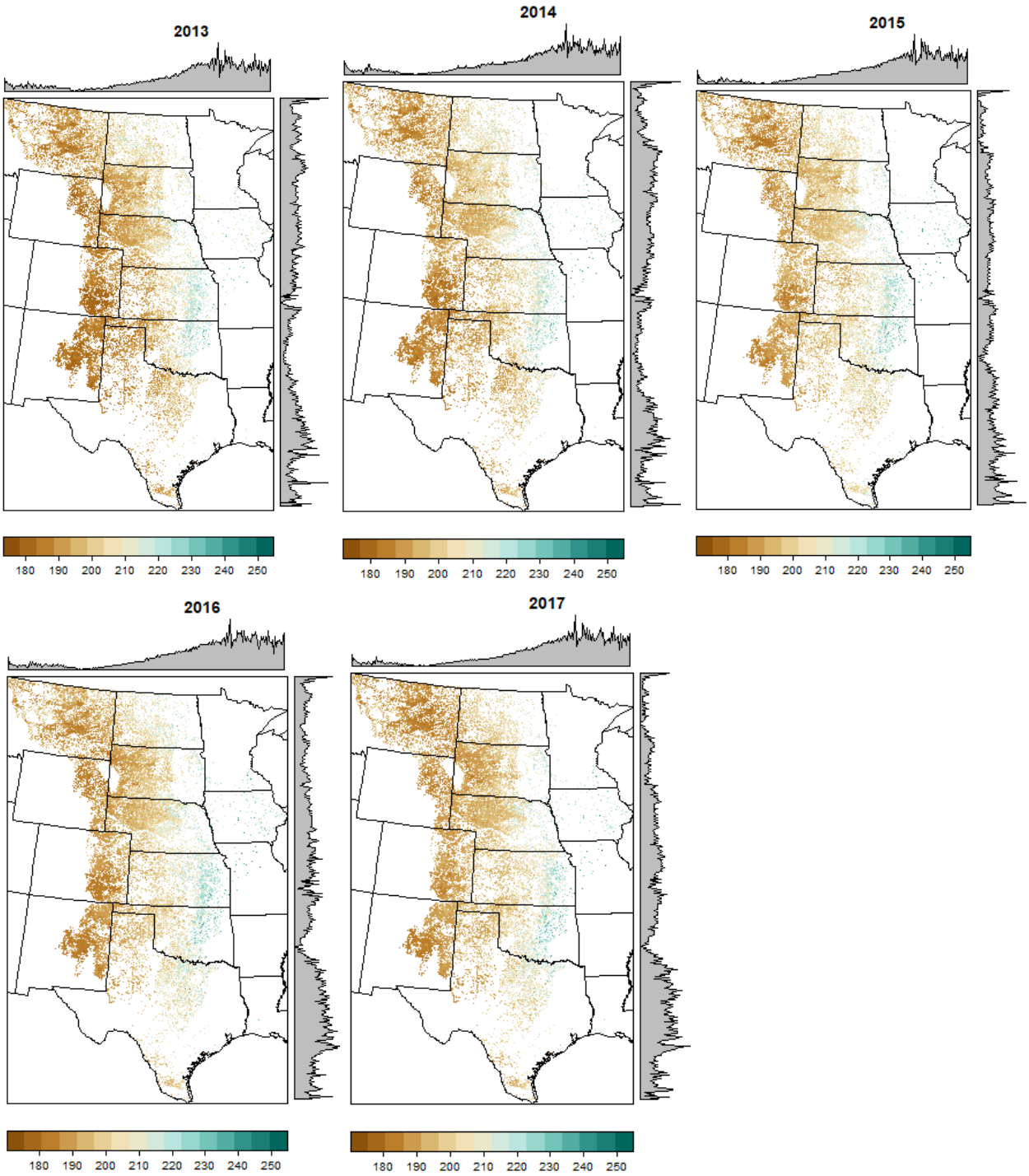
2013
2014
2015
2016
2017
180 190 200 210 220 230 240 250

Appendix C-5: Maps showing the spatial distribution of the net economic value of sequestered grassland carbon in the U.S. Great Plains (2007 U.S. dollars per pixel) for 2001 to 2017.

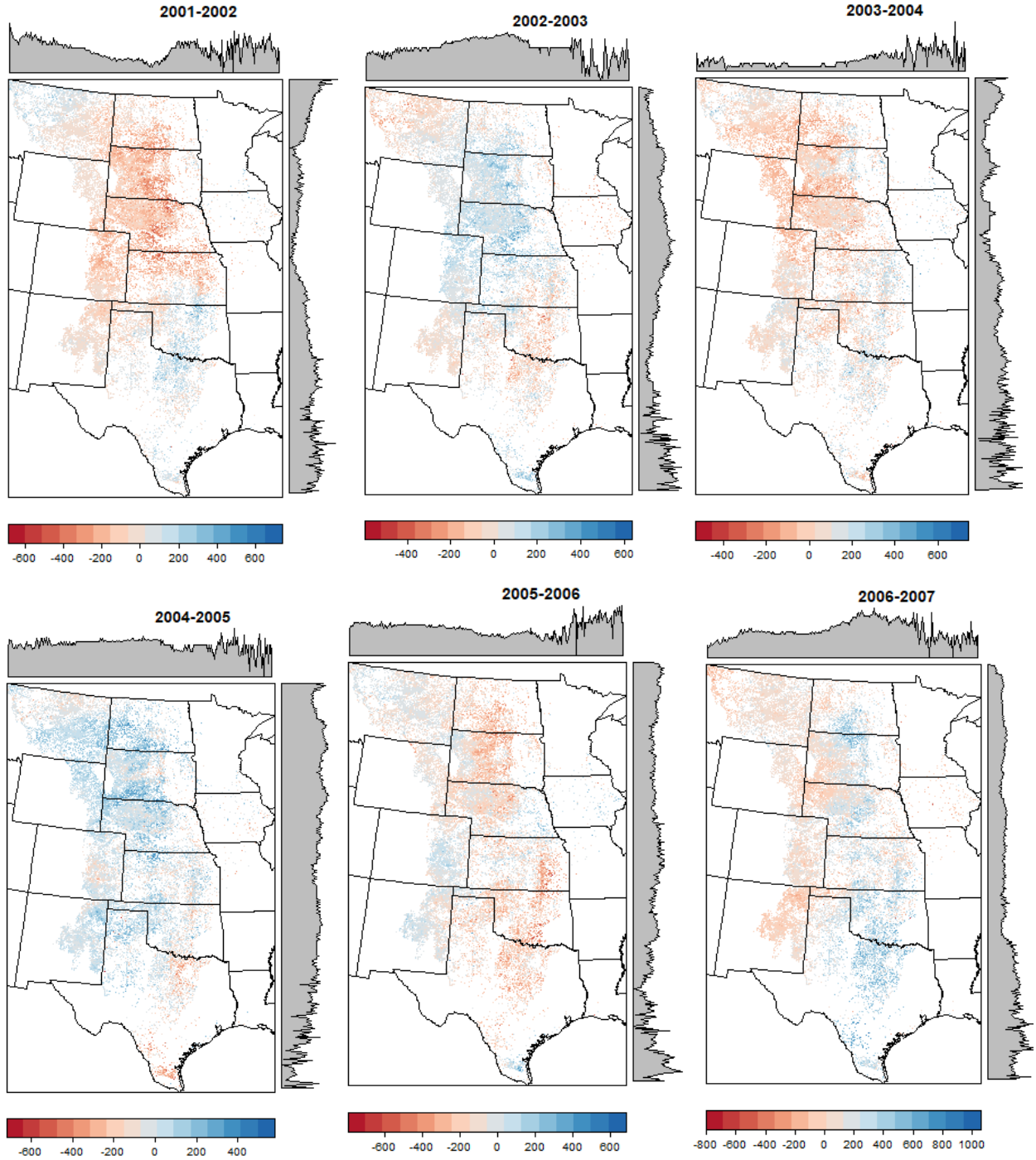

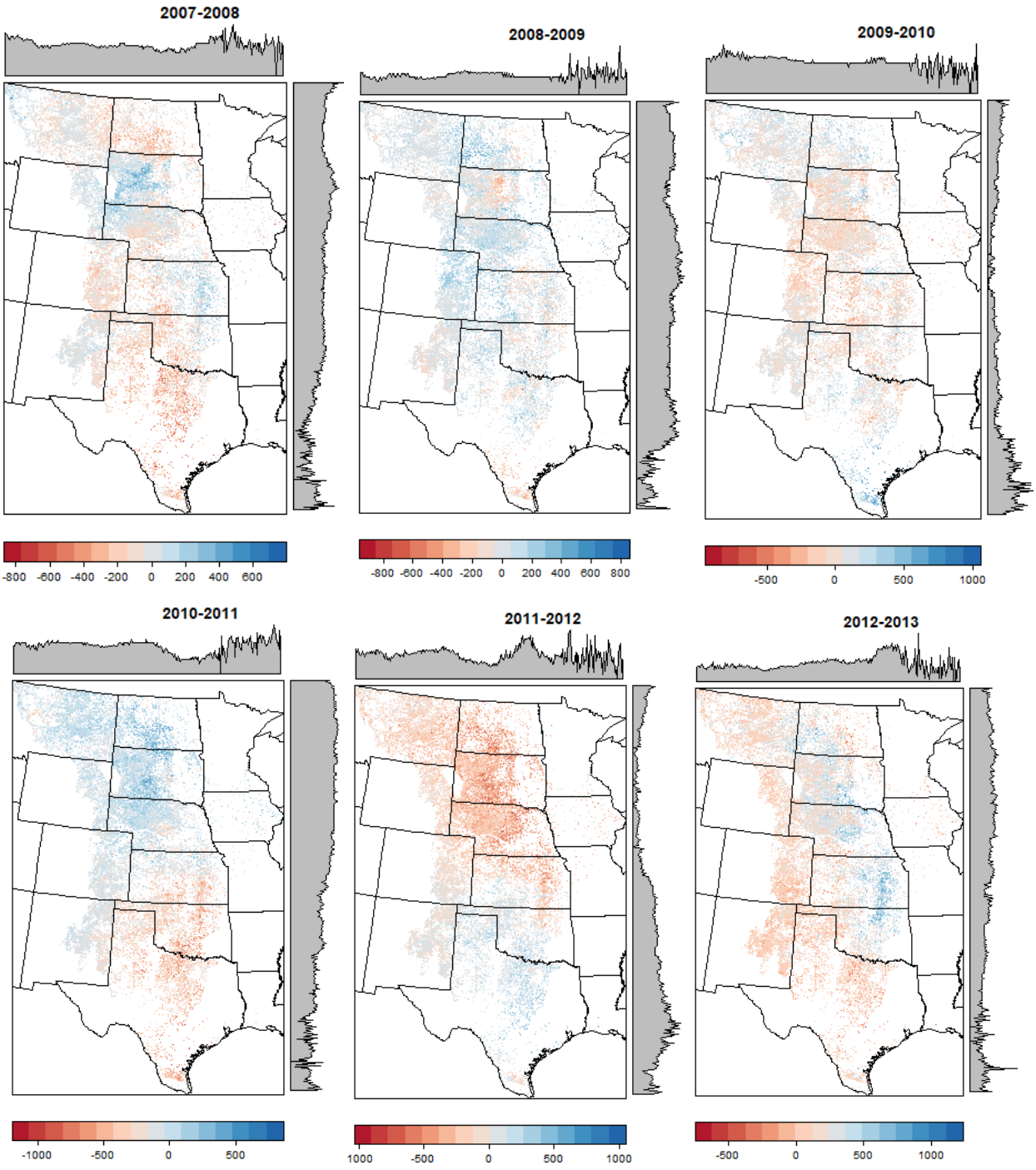
2007-2008
-800 -600 -400 -200 0 200 400 600
2008-2009
-800 -600 -400 -200 0 200 400 600 800
2009-2010
-500 0 500 1000
2010-2011
-1000 -500 0 500
2011-2012
1000 -500 0 500 1000
2012-2013
-500 0 500 1000

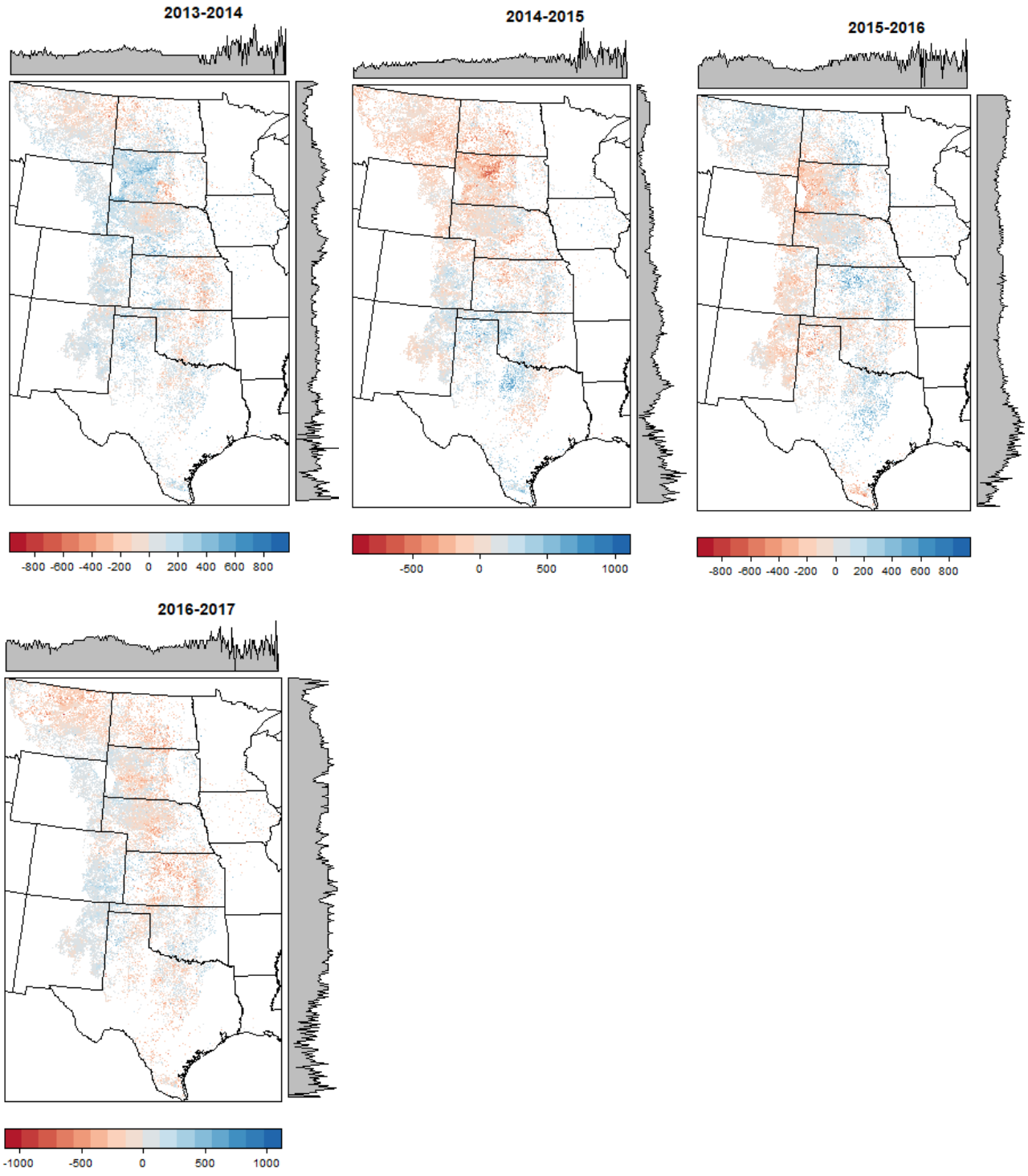
2013-2014
-800 -600 -400 -200 0 200 400 600 800
2014-2015
-500 0 500 1000
2015-2016
-800 -600 -400 -200 0 200 400 600 800
2016-2017
-1000 -500 0 500 1000

Appendix C-6: Maps showing the spatial distribution of soil loss for the grassland areas in the U.S. Great Plains for the years 2001 to 2017.

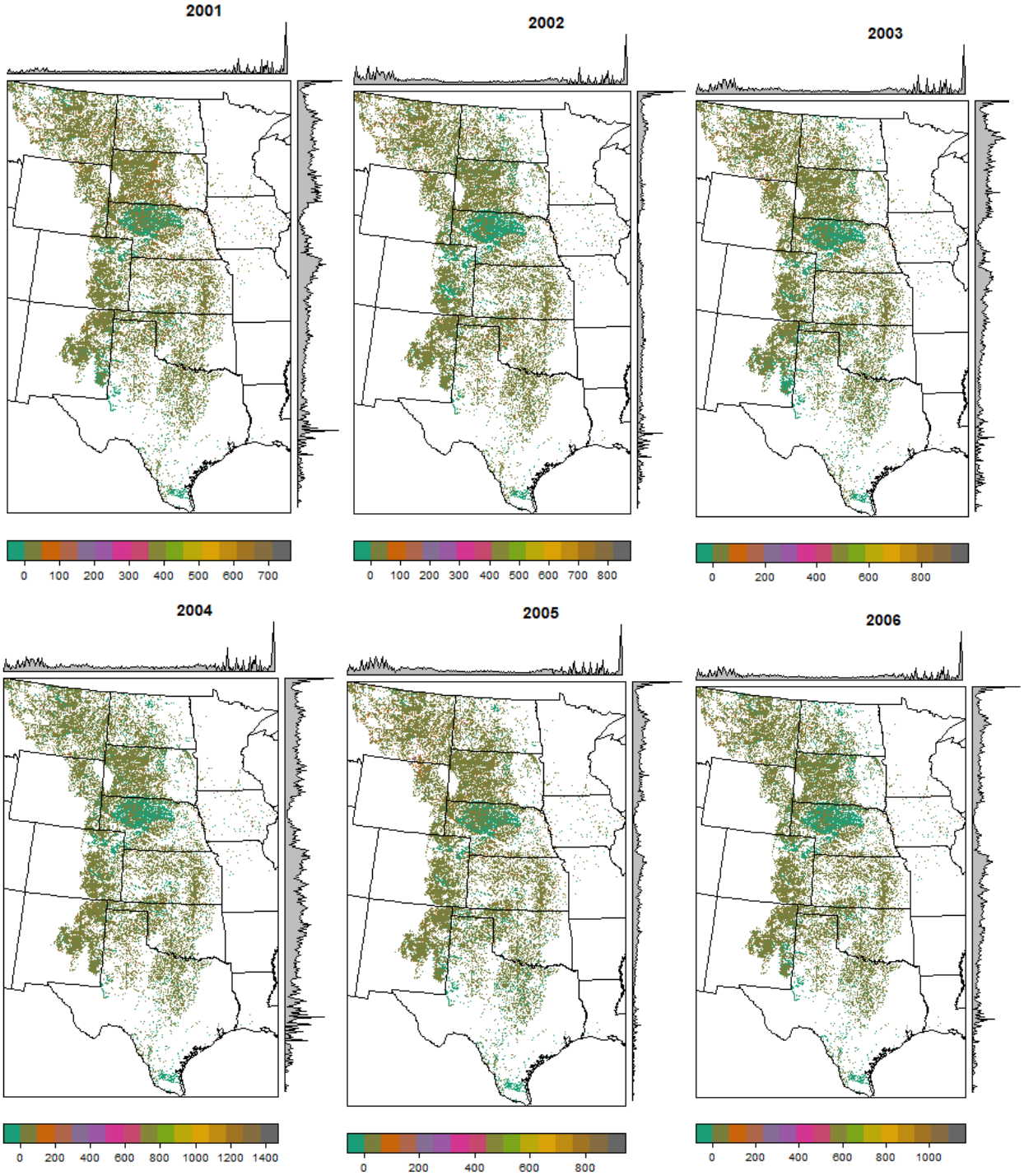

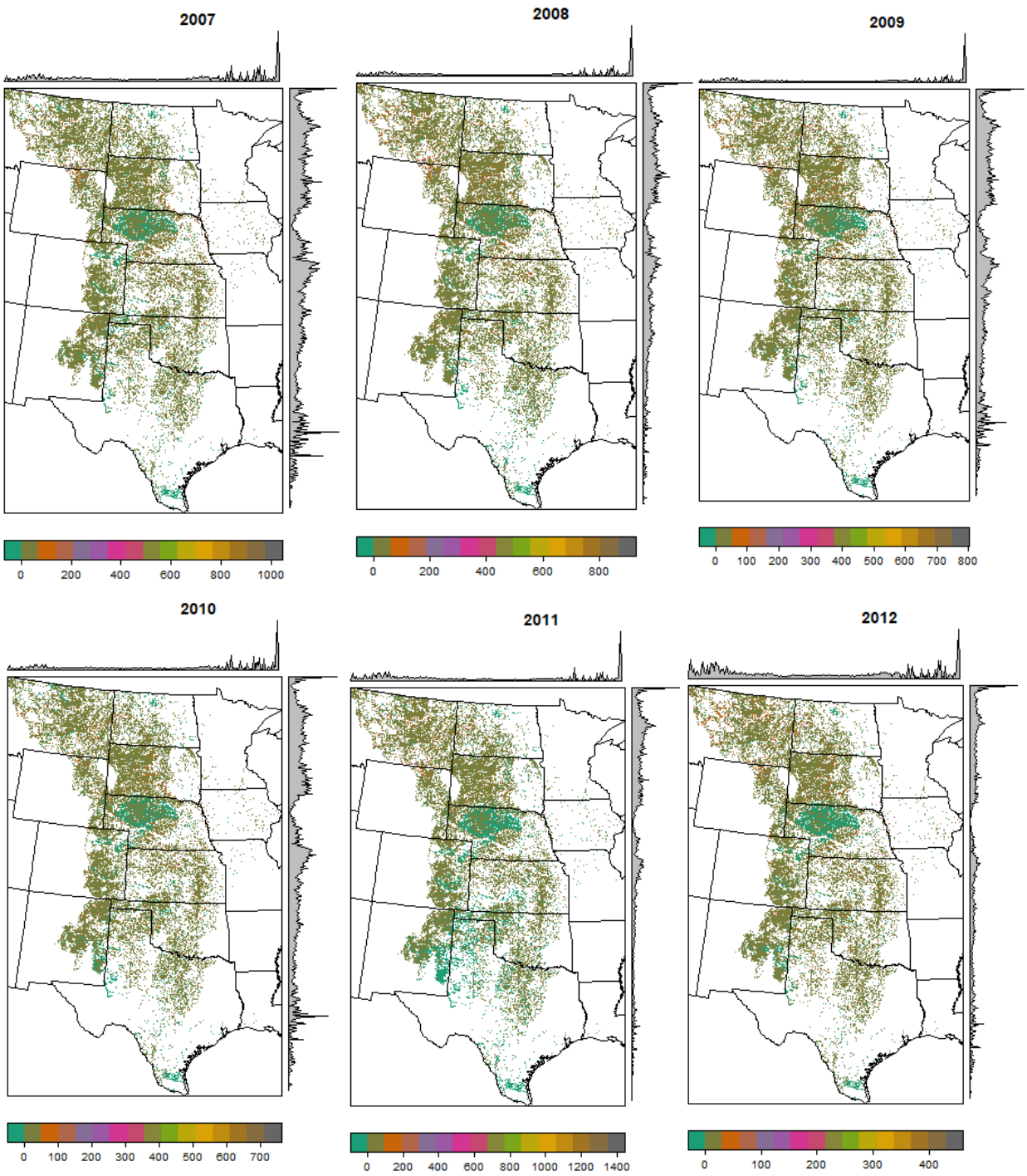
2007
0 200 400 600 800 1000
2008
0 200 400 600 800
2009
0 100 200 300 400 500 600 700 800
2010
0 100 200 300 400 500 600 700
2011
0 200 400 600 800 1000 1200 1400
2012
0 100 200 300 400

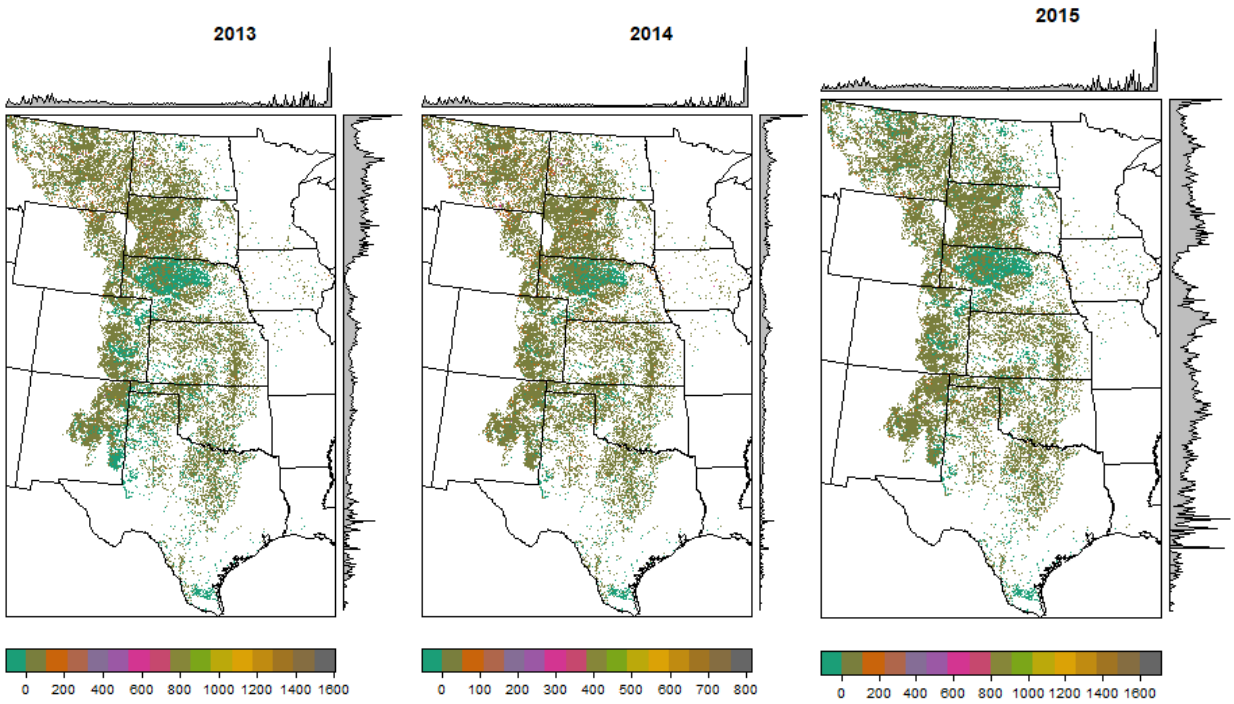
2013
2014
2015
0 200 400 600 800 1000 1200 1400 1600
0 100 200 300 400 500 600 700 800
0 200 400 600 800 1000 1200 1400 1600

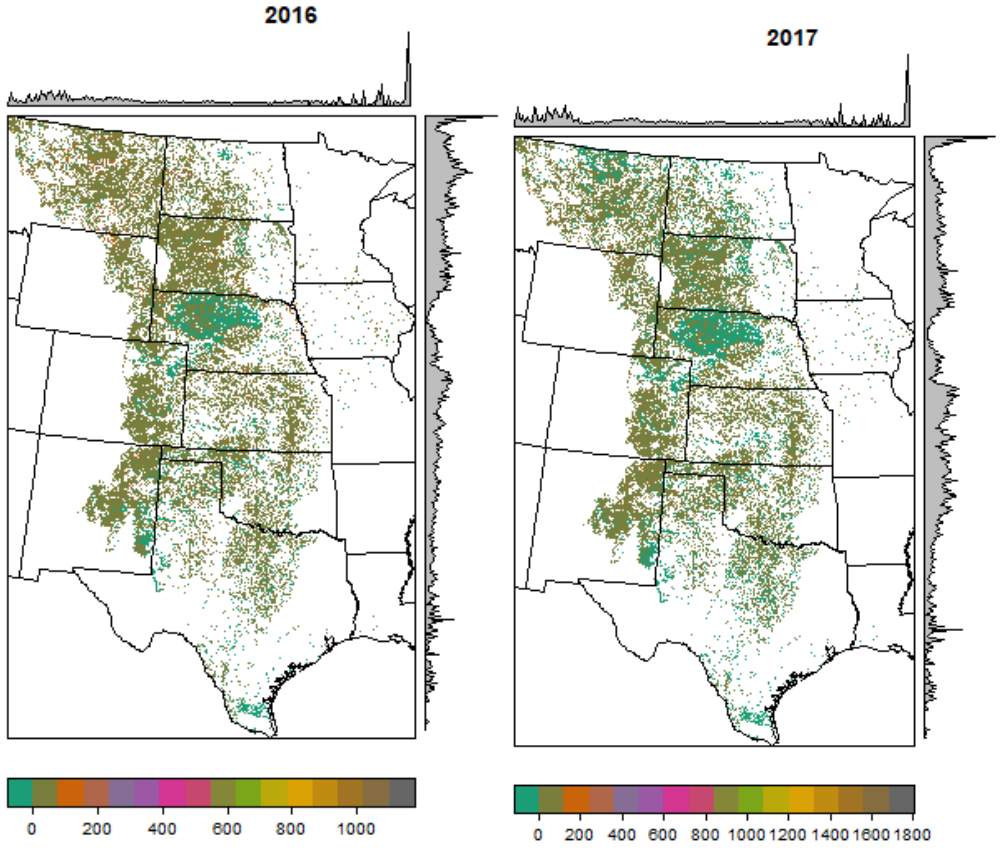
2016
2017
0 200 400 600 800 1000
0 200 400 600 800 1000 1200 1400 1600 1800

Appendix C-7: Maps showing the spatial distribution of sediment retention for the grassland areas in the U.S. Great Plains for the years 2001 to 2017

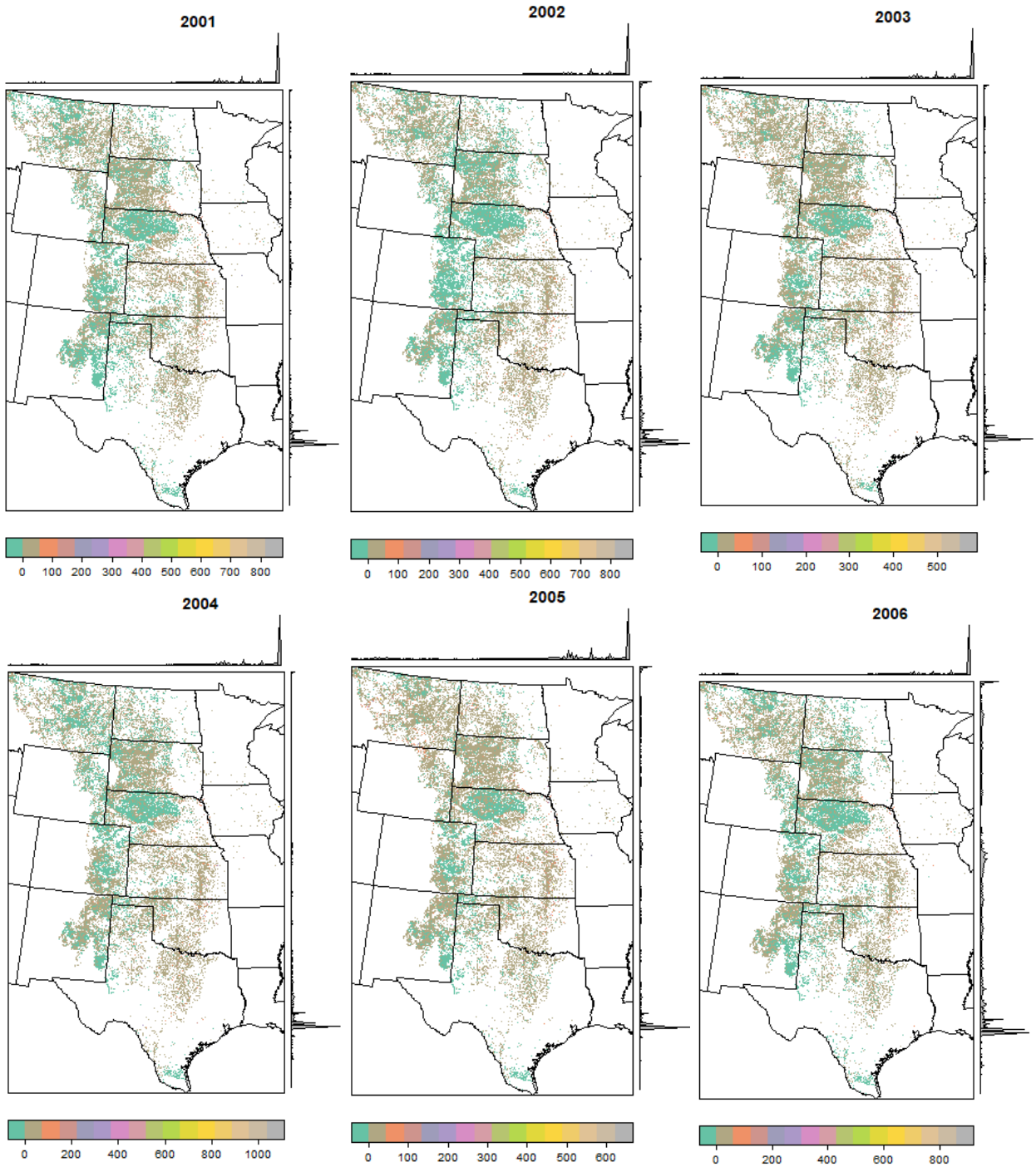

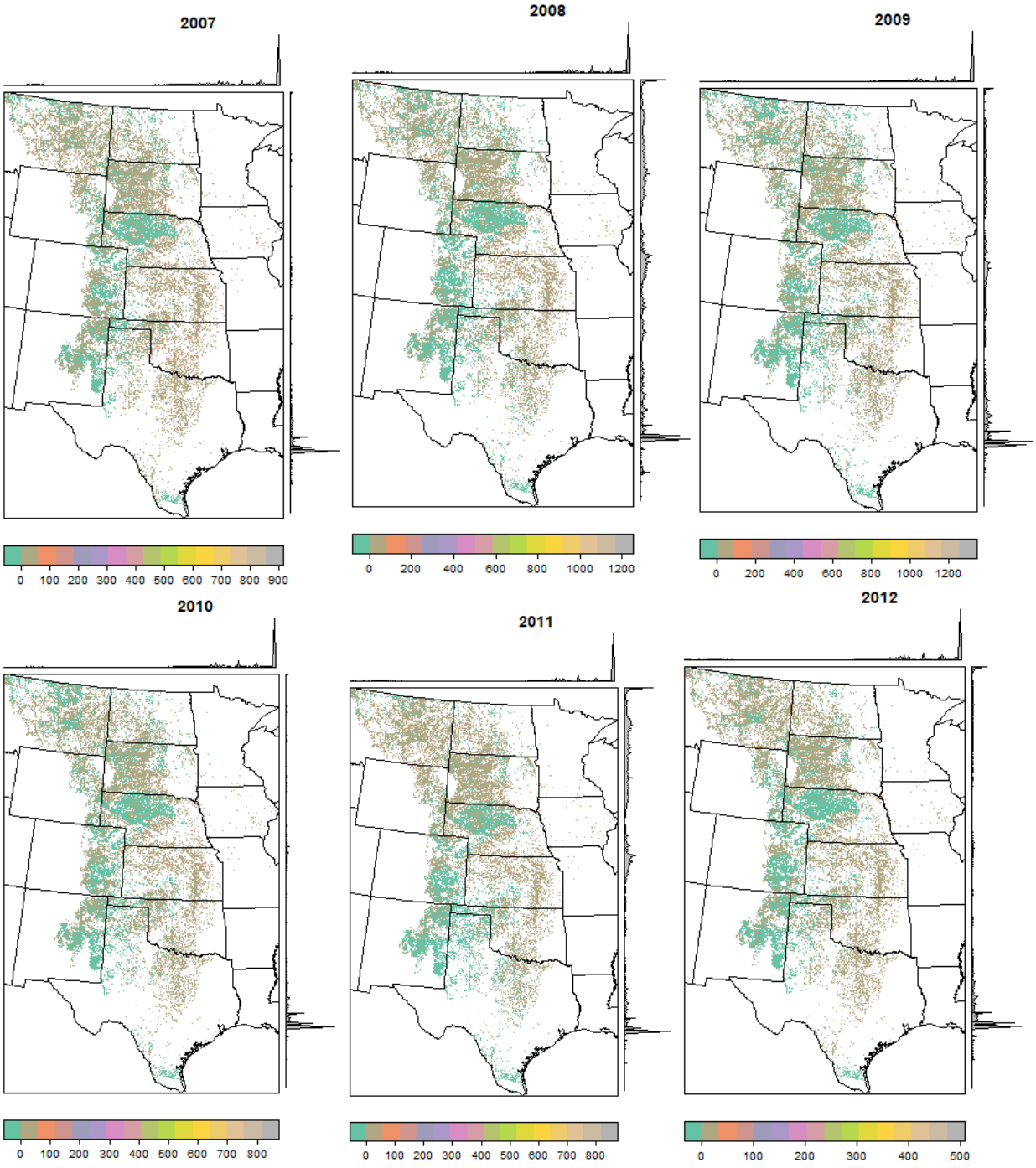
2007
0 100 200 300 400 500 600 700 800 900
2008
0 200 400 600 800 1000 1200
2009
0 200 400 600 800 1000 1200
2010
0 100 200 300 400 500 600 700 800
2011
0 100 200 300 400 500 600 700 800
2012
0 100 200 300 400 500

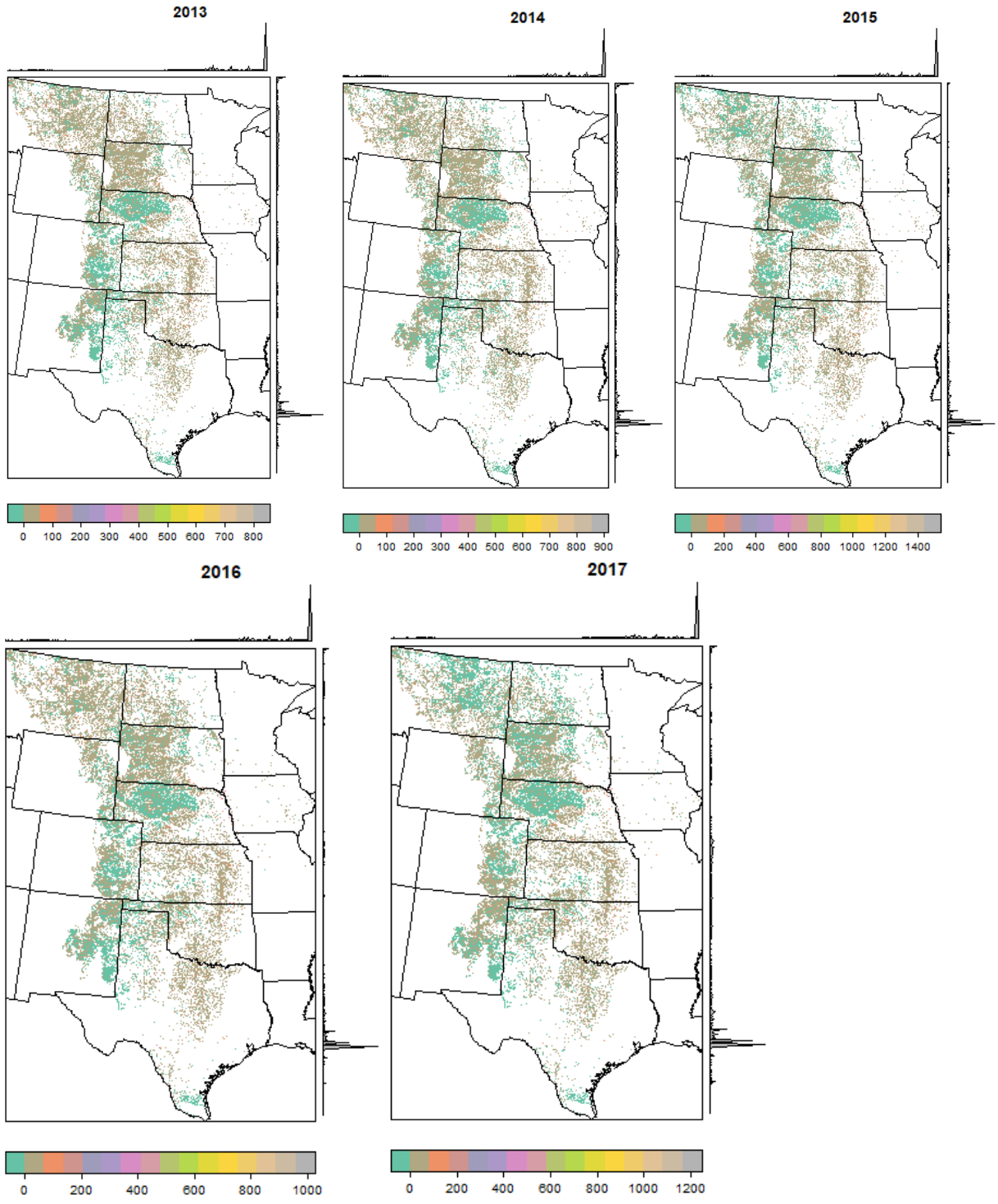
2013
0 100 200 300 400 500 600 700 800
2014
0 100 200 300 400 500 600 700 800 900
2015
0 200 400 600 800 1000 1200 1400
2016
0 200 400 600 800 1000
2017
0 200 400 600 800 1000 1200